Injection of Progenitor Cells from Adipose and Muscle Tissue for Therapy of Urethral Sphincter Insufficiency in a Large Animal Model

Dissertation

der Mathematisch-Naturwissenschaftlichen Fakultät
der Eberhard Karls Universität Tübingen
zur Erlangung des Grades eines
Doktors der Naturwissenschaften
(Dr. rer. nat.)

vorgelegt von
Jasmin Sabrina Knoll
aus Nürtingen

Tübingen
2023

Gedruckt mit Genehmigung der Mathematisch-Naturwissenschaftlichen Fakultät der Eberhard Karls Universität Tübingen.

Tag der mündlichen Qualifikation:	13.07.2023
Dekan:	Prof. Dr. Thilo Stehle
1. Berichterstatter:	Prof. Dr. Wilhelm K. Aicher
2. Berichterstatter:	Prof. Dr. Stefan A. Laufer

“Who says that my dreams have to stay just my dreams?”

Ariel in The Little Mermaid (1989)

Clements, R. & Musker, J; Walt Disney Studio Motion Pictures

Table of contents

I. Summary

Urinary incontinence (UI) is a significant medical challenge affecting more than 200 million people worldwide. It will become even more significant due to the improved life expectancy in modern populations. Stress urinary incontinence (SUI) is the overall most common form of UI, defined as a "complaint of involuntary loss of urine on effort or physical exertion including sporting activities, or on sneezing or coughing". The major problem with this condition is that the quality of life of those affected deteriorates. Current treatment options of conservative treatments or surgical procedures often fail to result in permanent healing because they do not address the underlying pathology of urethral sphincter deficiency. Therefore, cell therapy emerged as a new treatment option for SUI, with adipose-derived mesenchymal stromal cells (ADSCs) and myogenic progenitor cells (MPCs) being the most investigated cell types.

In the first project, a novel cell injection technology, the waterjet technology, was investigated and compared to the state-of-art technology of needle injections. Two different experiments were conducted. Publication 1 analyzed the influence of the waterjet technique on several cell characteristics. It demonstrated that injection via waterjet did not affect the cells' viability, surface markers, differentiation, and attachment capabilities. However, the biomechanical properties were significantly reduced after injection, possibly requiring further development. Publication 2 focused on injecting MPCs into the urethra of porcine cadaveric tissue and living healthy pigs. This study showed that viable MPCs were delivered more precisely, rapidly, and with a wider distribution by waterjet than needle injections.

The second project focused on comparing well-characterized MPCs to ADSCs injected into a urethral sphincter insufficiency in large animal models. For this purpose, MPC isolation, production, and characterization were optimized in Publication 3. Furthermore, in Publication 4, the urethral sphincter insufficiency in the large animal model pig was validated over a follow-up period of five weeks in landrace pigs. The transfer of the incontinence induction via balloon dilatation and electrocautery to Göttingen minipigs failed due to their rapid recovery after incontinence induction. In Publication 5, the regeneration potential of the improved MPCs and ADSCs was investigated by needle injection into incontinent landrace pigs. After five weeks, MPCs improved the sphincter function, while ADSCs fully recovered the defect.

Taken together, new data for the approval of the waterjet technology were provided and displayed its feasibility as an improved cell injection method. Furthermore, the promising therapeutical aspects of cell therapy were demonstrated, indicating its potential for the treatment of UI.

II. Zusammenfassung

Harninkontinenz ist eine große medizinische Herausforderung, von der weltweit mehr als 200 Millionen Menschen betroffen sind. Aufgrund der gestiegenen Lebenserwartung der Bevölkerung wird sie sogar noch an Bedeutung gewinnen. Belastungsharninkontinenz (SUI) ist die insgesamt häufigste Form der Harninkontinenz und wird definiert als "Beschwerden über unfreiwilligen Urinverlust bei Anstrengung oder körperlicher Belastung, einschließlich sportlicher Aktivitäten, oder beim Niesen oder Husten". Das Hauptproblem bei dieser Erkrankung ist, dass sich die Lebensqualität der Betroffenen verschlechtert. Die derzeitigen konservativen oder chirurgischen Behandlungsmöglichkeiten führen häufig nicht zu einer dauerhaften Heilung, da sie die zugrunde liegende Pathologie der Harnröhrenschließmuskelschwäche nicht angehen. Daher hat sich die Zelltherapie als neue Behandlungsoption für SUI herauskristallisiert, wobei aus Fettgewebe stammende mesenchymale Stromazellen (ADSCs) und myogene Vorläuferzellen (MPCs) die am meisten untersuchten Zelltypen sind.

Im ersten Projekt wurde eine neuartige Technologie zur Zellinjektion, die Wasserstrahl-Technologie, untersucht und mit dem Stand der Technik, der Nadelinjektion, verglichen. Es wurden zwei verschiedene Studien durchgeführt. Publikation 1 analysierte den Einfluss der Wasserstrahltechnik auf verschiedene Zelleigenschaften. Es zeigte sich, dass die Injektion mit dem Wasserstrahl keinen Einfluss auf die Lebensfähigkeit, die Oberflächenmarker, die Differenzierung und die Anheftungsfähigkeit der Zellen hatte. Allerdings waren die biomechanischen Eigenschaften nach der Injektion deutlich reduziert, was möglicherweise eine weitere Entwicklung erfordert. Publikation 2 befasste sich mit der Injektion von MPCs in die Harnröhre von Schweinekadavern und lebenden gesunden Schweinen. Diese Studie zeigte, dass lebensfähige MPCs mit dem Wasserstrahl präziser, schneller und mit einer breiteren Verteilung als mit einer Nadelinjektion eingebracht werden konnten.

Das zweite Projekt konzentrierte sich auf den Vergleich von gut charakterisierten MPCs mit ADSCs, die bei einer Harnröhrenschließmuskelinsuffizienz in Großtiermodellen injiziert wurden. Zu diesem Zweck wurden in Publikation 3 die Isolierung, Produktion und Charakterisierung von MPCs optimiert. Darüber hinaus wurde in Publikation 4 die Harnröhrenschließmuskelinsuffizienz im Großtiermodell Schwein über einen Nachbeobachtungszeitraum von fünf Wochen an Landschweinen validiert. Die

Übertragung der Inkontinenzinduktion mittels Ballondilatation und Elektrokauterisation auf Göttinger Minischweine scheiterte an der schnellen Erholung dieser Tiere nach Inkontinenzinduktion. In Publikation 5 wurde das Regenerationspotenzial der verbesserten MPCs und ADSCs durch Nadelinjektion in inkontinente Landschweine untersucht. Nach fünf Wochen verbesserten die MPCs die Schließmuskelfunktion, während die ADSCs den Defekt vollständig wiederherstellten.

Insgesamt wurden neue Daten für die Zulassung der Wasserstrahltechnik vorgelegt, die ihre Machbarkeit als verbesserte Zellinjektionsmethode belegen. Darüber hinaus wurden die vielversprechenden therapeutischen Aspekte der Zelltherapie aufgezeigt, die auf ihr Potenzial für die Behandlung von Harninkontinenz hinweisen.

III. List of Publications and Conference Contributions

i. Accepted Peer-Review Publications

Geng, R., **Knoll, J.**, Harland, N., Amend, B., Enderle, M. D., Linzenbold, W., Abruzzese, T., Kalbe, C., Kemter, E., Wolf, E., Schenk, M., Stenzl, A., & Aicher, W. K. (2022). Replacing Needle Injection by a Novel Waterjet Technology Grants Improved Muscle Cell Delivery in Target Tissues. Cell transplantation, 31, 9636897221080943. https://doi.org/10.1177/09636897221080943 *

Knoll, J.†, Danalache, M.†, Linzenbold, W., Enderle, M., Abruzzese, T., Stenzl, A., & Aicher, W. K. (2021). Injection of Porcine Adipose Tissue-Derived Stroma Cells via Waterjet Technology. *Journal of visualized experiments: JoVE*, (177), 10.3791/63132. https://doi.org/10.3791/63132

†The authors J.K. and M.D. share first authorship as they contributed equally.

Amend, B., Harland, N., **Knoll, J.**, Stenzl, A., Aicher, W. K. (2021). Large Animal Models for Investigating Cell Therapies of Stress Urinary Incontinence. *International journal of molecular sciences*, 22(11), 6092. https://doi.org/10.3390/ijms22116092

Danalache, M.†, **Knoll, J.**†, Linzenbold, W., Enderle, M., Abruzzese, T., Stenzl, A., Aicher, W. K. (2021). Injection of Porcine Adipose Tissue-Derived Stromal Cells by a Novel Waterjet Technology. *International Journal of Molecular Sciences*, 22(8), 3958. https://doi.org/10.3390/ijms22083958 *

†The authors M.D. and J.K. share first authorship as they contributed equally.

*These publications are presented in this thesis.

ii. Submitted Manuscripts

Knoll, J., Amend, B., Abruzzese, T., Stenzl, A., Aicher, W. K. (2023). Improved production of proliferation- and differentiation-competent porcine striated muscle-derived myoblasts. *Tissue engineering and regenerative medicine* (submitted)*

Knoll, J.[#], Harland, N.[#], Amend, B., Abruzzese, T., Stenzl, A., Aicher, W. K. (2023). Göttingen minipigs present with significant regeneration kinetics after sphincter injury compared to German landrace gilts. *BMC veterinary research* (submitted)*
[#]Both, J.K. and N.H., contributed equally to the study and therefore deserve shared first authorship.

Knoll, J., Amend, B., Harland, N., Freisinger, S., Bézière, N., Kraushaar, U., Stenzl, A., Aicher, W. K. (2023) Cell therapy by mesenchymal stromal cells versus myoblasts in a pig model of urinary incontinence. *Tissue engineering. Part A* (submitted)*

*These manuscripts are part of this thesis, hereafter referred to as Publication 3-5.

iii. Conference Contributions

Tissue Engineering and Regenerative Medicine International Society (TERMIS) – AM (Americas) 2023, Boston, United States, April 11th–14th

Oral presentation: Abstract #378

Regeneration of urethral sphincter deficiency by injection of cells in a pig large animal model of stress urinary incontinence

Knoll, J., Harland, N., Amend, B., Stenzl, A., Aicher, W. K

Tissue Engineering and Regenerative Medicine International Society (TERMIS) – EU-Chapter 2023, Manchester, United Kingdom, March 28th–31st

Oral presentation: Abstract #523

Investigating the regenerative potential of porcine mesenchymal stromal cells versus myoblasts in a large animal model of stress urinary incontinence

Knoll, J., Harland, N., Amend, B., Abruzzese, T., Stenzl, A., Aicher, W. K

Tissue Engineering and Regenerative Medicine International Society (TERMIS) – 6th World Congress 2021, Maastricht, Netherlands, November 15th–19th

Poster presentation: Abstract #73

Waterjet: a novel technology to inject cells in predetermined regions of the urethral sphincter for improved cell therapy of urinary incontinence

Geng, R., **Knoll, J.**, Linzenbold, W., Jäger, L., Enderle, M., Abruzzese, T., Aicher, W. K.

Tissue Engineering and Regenerative Medicine International Society (TERMIS) – EU-Chapter 2022, Krakow, Poland, June 28th–July 1st

Poster presentation: Abstract # 31412706966

A novel needle−free technology waterjet by improved delivery to transport muscle−derived cells to the urethral sphincter of living pigs

Geng, R., **Knoll, J.**, Harland, N., Amend, B., Enderle, M. D., Linzenbold, W., Abruzzese, T., Stenzl, A., Aicher, W. K

73. Kongress der Deutschen Gesellschaft für Urologie e.V. (DGU) 2021, Stuttgart, Germany, September 15th–18th

Oral presentation: Abstract: Der Urologe, Ausgabe Sonderheft 1/2021, V1 1.8

WaterJet: A novel needle-free injection technique for cell therapy of stress urinary incontinence

Geng, R., **Knoll, J.**, Harland, N., Abruzzese, T., Stenzl, A., Linzenbold, W., Enderle, M., Aicher, W. K

IV. Author Contributions of presented publications

i. Publication 1

Injection of Porcine Adipose Tissue-Derived Stromal Cells by a Novel Waterjet Technology

Jasmin Knoll and Marina Danalache contributed equally to this publication. Jasmin Knoll planned and conducted all cell culture experiments, including cell characterization, tissue sample preparation, cell injections, and attachment assays. She also analyzed the data obtained from these experiments. Additionally, she was involved in the evaluation of the AFM data. Jasmin Knoll created the figures together with Marina Danalache and Wilhelm K. Aicher. She also proofread the manuscript. For further information, refer to the "Author Contributions" section of the publication in Chapter VI.

ii. Publication 2

Replacing Needle Injection by a Novel Waterjet Technology Grants Improved Muscle Cell Delivery in Target Tissues

Jasmin Knoll is the co-author of this publication. She assisted Ruizhi Geng in the planning and execution of cell culture experiments, especially in cell production and characterization. Furthermore, she was involved in the animal surgeries in which she was responsible for the urodynamic measurements and aided in urethral sample preparation after the scarification of the pigs. Afterward, she produced the cryosections together with Tanja Abruzzese, which were further analyzed by Ruizhi Geng. Jasmin Knoll also participated in the preparation of the manuscript and proofread it. For further information, refer to the "Author Contributions" section of the publication in Chapter VI.

iii. Publication 3

Improved production of proliferation- and differentiation-competent porcine striated muscle-derived myoblasts

Jasmin Knoll was involved in the study design, planned, and performed all experiments, and analyzed the respective data. She created the figures and drafted the manuscript with Wilhelm K. Aicher. Tanja Abruzzese assisted in cell culture experiments. Bastian Amend, Arnulf Stenzl, and Wilhelm K. Aicher were involved in the study design and funding. Wilhelm K. Aicher supervised all experiments. All authors critically proofread the manuscript.

iv. Publication 4

Göttingen minipigs present with significant regeneration kinetics after sphincter injury compared to German landrace gilts

Jasmin Knoll and Niklas Harland contributed equally to this study. Jasmin Knoll was involved in the animal experiments, mainly responsible for the urodynamic measurements and preparation of the urethra after the scarification of the pigs. Together with Niklas Harland, she analyzed the urodynamic data. Jasmin Knoll calculated the statistics of these data. Additionally, Jasmin Knoll performed the cryosection, conducted the histological analyses, and evaluated the data obtained. Furthermore, she prepared the figures and manuscript with Wilhelm K. Aicher. For further information, refer to the “Author Contributions” section of the publication in Chapter VI.

v. Publication 5

Cell therapy by mesenchymal stromal cells versus myoblasts in a pig model of urinary incontinence

Jasmin Knoll was involved in all experiments. During animal surgeries, she was mainly responsible for urodynamic measurements, and after the scarification of the pigs, she prepared the urethras. Moreover, she produced the cells for animal surgeries and conducted cell culture and characterization experiments. She assisted Udo Kraushaar with the experiments and analyses of the physiological measurements of the myogenic cells. Together with Simon Freisinger and Nicolas Bézière, she performed the IVIS measurements. She prepared the cryosections and conducted the stainings. Furthermore, she created the figures and drafted the manuscript with Wilhelm K. Aicher. For further information, refer to the “Author Contributions” section of the publication in Chapter VI.

V. Introduction

1. Urinary System

The urinary system consists of the upper urinary tract, comprising the kidneys and ureters, and the lower urinary tract, comprising the bladder and urethra. As one of its primary functions, the urinary system produces urine and excretes toxic substances and metabolites [1]. The urine with its waste products is built by the kidneys in the upper urinary tract [1,2]. The ureters, which connect the kidneys with the bladder in the lower urinary tract, are responsible for transporting urine between these two organs [2]. The bladder, a hollow organ, primarily stores urine (continence) coming from the ureters until it gets excreted (micturition) through the urethra. The length of the urethra differs significantly between the sexes [1,2]. While the male urethra measures 20–25 cm with an average of 22.3 cm [2,3], the female urethra only ranges from 2 cm to 5 cm with an average of 3.1 cm [4] (Figure 1). The male urethra can be classified into the prostatic, membranous, and spongy urethra (Figure 1A). The prostatic urethra originates at the bladder neck and runs approximately 3 cm through the center of the prostate gland. At the end of the prostate gland, the membranous urethra proceeds for approximately 2–2.5 cm through the pelvic floor muscles. When the urethra enters the urethral corpus cavernosum, it is called the spongy urethra. The spongy urethra ends at the external urethral orifice [1,2,5]. The female urethra originates at the bladder neck as well, runs directly through the pelvic floor muscles, proceeds diagonally along the anterior vaginal wall, and ends at the external urethral orifice above the vaginal opening (Figure 1B) [1,2,5].

The musculature of the organs of the lower urinary tract has a key function in micturition and maintaining continence (Figure 1). The detrusor muscle which surrounds the bladder consists of smooth muscle cells. At the transition of the bladder to the urethra, the detrusor muscle continues to form longitudinal and circular muscle layers of smooth muscle cells. These muscle layers build the internal urethral sphincter [2,5,6]. The external urethral sphincter, also known as the rhabdosphincter, is located in the region where the urethra passes through the pelvic floor muscles. It is formed by skeletal striated muscle fibers that split off from the pelvic floor muscles [1,6]. Especially the two urethral sphincters build the fundament of urinary continence in the urethra [5]. Pelvic floor muscles also contribute to continence [7,8]. Especially in women, the supportive layers of pelvic floor muscles provide

additional compression of the urethra against these layers, ensuring complete continence, particularly with increased intra-abdominal pressures (e.g., by coughing) [7,9,10]. The levator ani muscle, which belongs to this supportive layer of pelvic floor muscles, plays an essential role because of its connection to the external urethral sphincter [7,8]. However, this anatomical fixation to the levator ani muscle is absent in men, suggesting that only the external urethral sphincter provides continence [8].

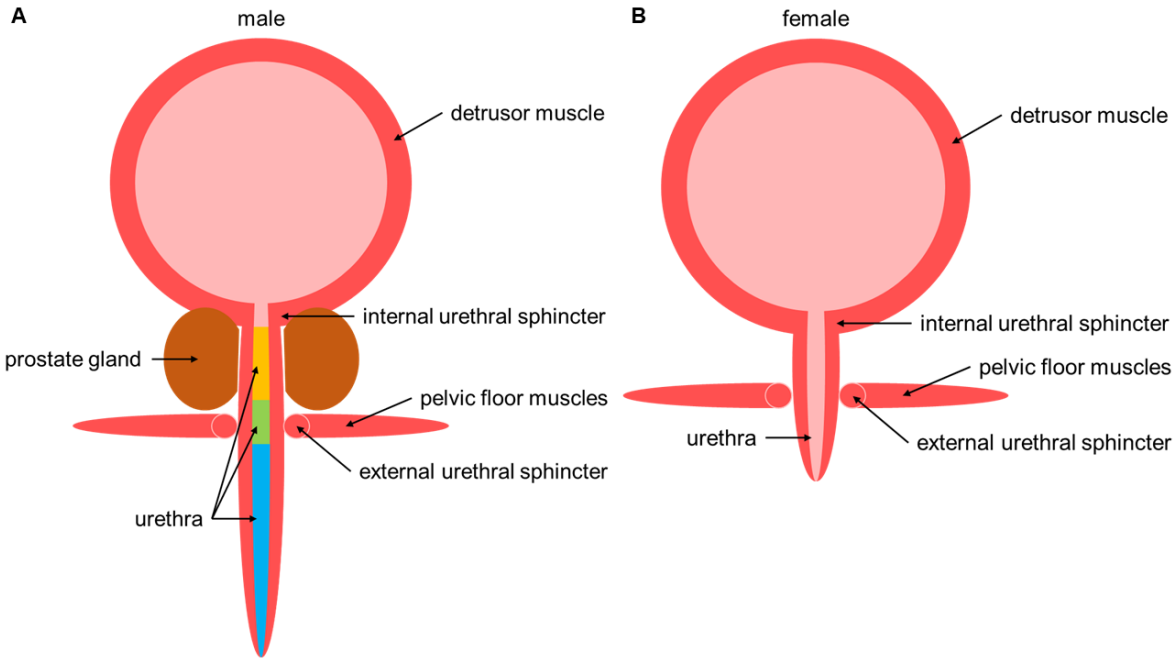

Figure 1: Urethral sphincter muscles of the bladder and urethra by sex. (A) The male bladder and urethra with the detrusor muscle, the internal urethral sphincter, the external urethral sphincter, and the pelvic floor muscles are schematically displayed. Alongside the male urethra, the prostate gland is located. The three parts of the urethra are marked in color: prostatic urethra (yellow), membranous urethra (green), and spongy urethra (blue). (B) The female bladder and urethra are schematically displayed with the same muscles. The female urethra is about one-seventh of the length of the male urethra. Figure adapted with modifications[2].

The bladder is filled with approximately 50 ml urine per hour [11]. In the filling state, the detrusor muscle of the bladder is relaxed, while the internal urethral sphincter is contracted, especially the circular muscle layers. This is regulated by the autonomous vegetative nervous system, which cannot be voluntarily controlled. The sympathetic innervation is responsible for maintaining continence [2,5,6,11]. The voiding typically starts when the bladder contains 350–500 ml of urine [7,11]. The fullness of the bladder activates the parasympathetic nervous system via the pelvic splanchnic nerves and inactivates the sympathetic one. This leads to detrusor muscle contraction and internal urethral sphincter relaxation by shortening the longitudinal muscle layers [5,6,11]. The somatic nervous system

controls the external urethral sphincter through the pudendal nerve. Therefore, it maintains the continence or allows micturition voluntarily [5,11].

Overall, for the urinary system to function correctly and to control the flow of urine, all components, including innervation and muscles, need to work correctly so that all mechanisms can interact with each other [5,6].

2. Urinary Incontinence (UI)

Urinary incontinence (UI) is defined as a "complaint of involuntary loss of urine" [12,13]. It poses a significant problem in the population because it can worsen the quality of life of each individual [5]. More than 200 million people worldwide are affected by UI [7]. Depressions, anxiety, decrease in physical activity, and social isolation are more common in people affected by UI than in nonaffected individuals [14,15]. Additionally, UI economically impacts society and, particularly, health services [16,17]. The economic aspects of UI include self-management (e.g., pads, laundry), treatment (e.g., doctor's appointment, performed tests), and consequence-related costs (resulting illness, e.g., urinary tract infections) [18]. A study in the United States estimated the annual cost for UI at 16.3 billion US dollars (in 1995 dollars) [19]. UI also is associated with urinary tract infections, pressure ulcers, lower work productivity, and admission to long-term residential care [20].

The prevalence of UI is reported by several population studies and ranges between 5–70%, with a mostly reported prevalence of 25–45% regarding occasional leakage [17,18]. The overall prevalence of UI for women with leakage at least weekly is about 10% [17,18]. In Germany, about 41% of women report uncontrolled urine leakage [21]. In men, the prevalence is reported to be half of the prevalence in women (Figure 2) and studies state prevalences for men from 1–39% [18]. The UI of men is often caused by radical prostatectomy as a main complication leading to a reported UI prevalence of 2–60% after the procedure [18]. Overall, for both sexes, the prevalence increases with age (Figure 2) [12,21]. Different study samples or participation rates and definitions of significant UI can explain the discrepancies among the prevalence rates [17,18].

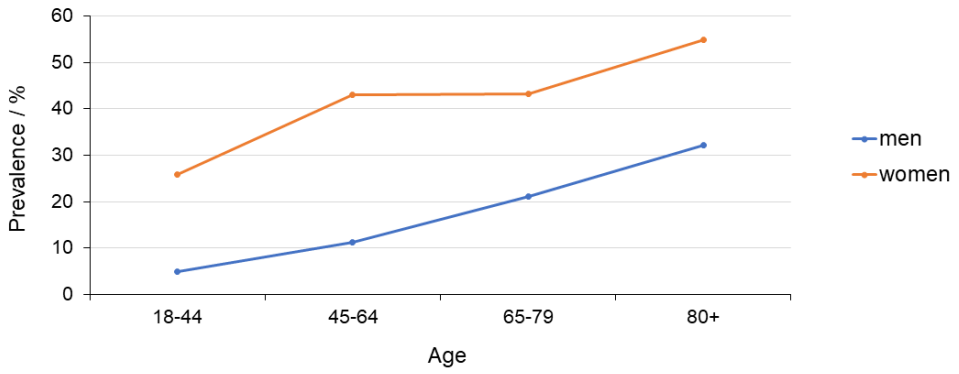

Figure 2: Prevalence of UI distinguished by sex. The prevalence of UI increases in both, women and men, with age. However, the prevalence of UI in women is at least twice that of men in almost all age groups. The prevalence of women displays a plateau between the ages of 50 to 79 years. Data for the UI prevalence of women were obtained from Hunskaar et al. 2004 [21]; data for the UI prevalence of men were obtained from D'Ancona et al. 2019 [12].

The International Continence Society (ICS) differentiates between three prevalent subtypes of UI: urgency urinary incontinence (UUI), stress urinary incontinence (SUI), and mixed urinary incontinence (MUI) which is a combination of UUI and SUI (Table 1) [12,13]. Other variants are also mentioned, but due to their low prevalence, they are not considered further [21]. The three main subtypes generally differ in prevalence (Table 1) and age-dependent by sex [18].

Table 1: Subtypes of urinary incontinence

Subtype of UI	Definition by ICS	Prevalence
Urgency urinary incontinence (UUI)	"complaint of involuntary loss of urine associated with urgency" [12,13]	Women: 1–7% [18] Men: 40–80% [18]
Stress urinary incontinence (SUI)	"complaint of involuntary loss of urine on effort or physical exertion including sporting activities, or on sneezing or coughing" [12,13]	Women: 10–39% [18] Men: <10% [18]
Mixed urinary incontinence (MUI)	"complaint of involuntary loss of urine associated with urgency and also with effort or physical exertion or on sneezing or coughing" [12,13]	Women: 7.5–25% [18] Men: 10–30% [18]

In men, the prevalence of UI increases over age, with UUI being the dominant type in all age groups [18,22]. In women, the overall predominantly reported subtype is SUI [18,21]. Nevertheless, looking closer at the age groups, the predominant subtype shifts from SUI in women under 60 years to MUI in women 60 years and older, with UUI also increasing (Figure 3). In Germany, the prevalence of SUI was 47% in the 18–44 year-olds and decreased to 31% in those over 60 years of age [21].

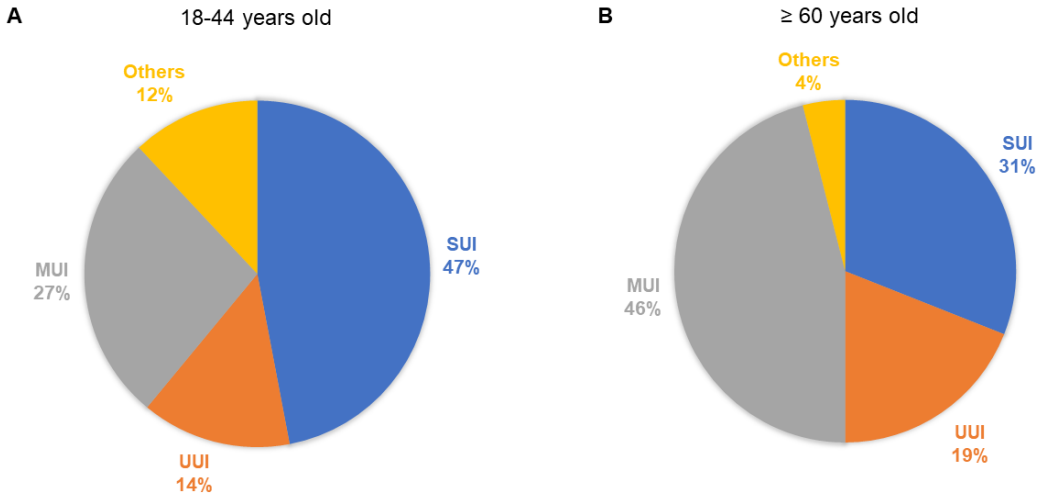

Figure 3: The prevalences of the subtypes of UI in women compared between two age groups. (A) The prevalence of the different subtypes of UI, especially SUI, MUI, and UUI, in women aged 18–44. (B) The prevalence of the different subtypes of UI, especially SUI, MUI, and UUI, in women over 60 years old. Data were obtained from Hunskaar et al. 2004 [21]

The pathophysiology of UI involves that one component (storage function or emptying function) of the urinary tract is not working properly anymore [6,7]. This involves impairment or damage to the nervous system or direct mechanical injuries on the involved muscles [5,20]. Since different subtypes predominate in men and women, it can be assumed that the underlying pathophysiologies are also different [23]. The overall predominant subtypes are UUI in men and SUI in women [18,21,22]. UUI can be attributed to the overactivity of the detrusor muscle, whereas SUI is related to dysfunction of urethral sphincter or pelvic floor muscles [20,23].

Risk factors for both sexes causing these pathophysiologies include aging and obesity[17,20]. Genetic factors and other diseases such as neurological disorders (e.g., stroke), diabetes, and urinary tract infections can also contribute to UI [17,18]. Additionally, there are sex-specific risk factors. In women, these include high parity, mode of delivery, pregnancy, birth weight of the infant, and menopause [18,20]. A rising number of parities is related to an increased risk of UI, while already one delivery is associated with UI [17,18].

The vaginal delivery causes stretching of the muscles leading to tissue damage or affected nerves [5,6]. During pregnancy, the prevalence of UI also increases. The related physiological changes tend to produce a predisposition for UI later in the life of women [17,18,24]. The infant's birth weight is also associated with UI, with the maximum weight of the infant being the risk factor [17,18]. Further studies also report a peak in UI prevalence during menopause [5]. The lack of estrogen during menopause [6] could explain the plateau (Figure 2) seen in ages 50–79 [21]. However, also the replacement therapy of estrogen does not improve UI. In contrast, it also correlates with increasing UI since it weakens the periurethral connective tissue, decreasing urethral closure pressure [6,18]. These UI risk factors, especially for women, correlate mostly to SUI [18]. In men, a particular risk factor poses a radical prostatectomy as prostate surgery after prostate cancer [6,20,22]. The risk for UI after this therapy increased fourfold compared to the control group [25] and is caused by the loss of sphincter function [6].

Overall, the significance of UI will increase due to the increasing life expectancy [17]. The number of women affected by UI and, therefore, the prevalence of UI is estimated to increase by 55% from 2010 to 2050 (18.3 million to 28.4 million women) [26].

2.1 Stress Urinary Incontinence (SUI)

Stress urinary incontinence (SUI) is defined as a "complaint of involuntary loss of urine on effort or physical exertion including sporting activities, or on sneezing or coughing" (Table 1) [12,13]. Its prevalence differs in women and men. The overall reported prevalence for women is 10–39%, while for men, it is below 10% [18]. Despite the low prevalence of SUI in men, SUI is the most common form of UI in humans [27,28]. SUI also shows age-dependent differences. As stated above, it is the predominant subtype in younger women, while in older ones, MUI dominates (Figure 3) [17,21]. Several studies report a prevalence of SUI in women under 65 of 50% [20,28]. Over the ages, a peak is visible for SUI's prevalence between 45–59 years old [21,28]. However, the prevalence rates for SUI should be considered cautiously, as the numbers for SUI are usually under-reported.

The underlying pathophysiology of SUI is, on the one hand, the weakened urethral sphincter muscle, also known as intrinsic urinary sphincter deficiency, [10,20] and, on the other hand, the hypermobility of the urethra caused by the loss of compression of the urethra and bladder neck by the supportive layer of pelvic floor muscles, especially in women [9,10]. An enfeebled levator ani muscle may contribute to the second mechanism.

Fewer muscle fibers, less skeletal muscle content, and instead more connective tissue in the levator ani muscle lead to a weaker and thinner muscle and, thus, resulting in dysfunction of the external urethral sphincter and hypermobility [8,10,27]. Overall, both pathophysiologies lead to problems in the closing mechanism [5]. However, it is reported that the impaired function of the urethral sphincter muscle is the predominant factor leading to SUI [29]. If there is a sudden increase in intra-abdominal forces as it happens, e.g., with sporting activities, sneezing, or coughing, the bladder pressure can exceed the urethral pressure [7]. Several risk factors can contribute to these underlying pathomechanisms.

The risk factor of age leads to decreased muscle mass in the rhabdosphincter by apoptosis [6,30] and, therefore, weakens the urethral sphincter directly [10]. In contrast, obesity mostly correlates to hypermobility of the urethra because it damages the pelvic floor muscles due to excess loading, reducing the anatomical support [10]. Obesity is also suggested to increase the intra-abdominal pressure on the bladder resulting in rising bladder pressure and, thus, SUI [31].

The sex-dependent risk factors described in Chapter 2 also contribute to the SUI subtype. In women, these are pregnancy, frequent pregnancy, mode of delivery, birth weight of the infant, and menopause. Vaginal delivery may involve both pathomechanisms. On the one hand, it might be responsible for direct muscle injuries and the reduction of urethral nerves [6]. On the other hand, damage to the levator ani muscle and other supportive tissue layers can lead to reduced pelvic floor muscles resulting in hypermobility of the urethra [5,6,32]. Pregnancy is also associated with hypermobility of the urethra due to reduced pelvic floor muscle strength. This reduction can be explained by the weight gain during pregnancy and the weight of the fetus, which lays on the pelvic floor muscles and results in chronic stress [33]. Additionally, the growing fetus might change the bladder neck position and increase the pressure on the bladder resulting in increased bladder pressure [33]. Furthermore, menopause is also correlated to the hypermobility of the urethra [10].

In men, the most considerable risk factor for SUI is radical prostatectomy as prostate surgery after prostate cancer [6,20,22]. Prostate cancer is the third most common cancer with a rising incidence [34]. With radical prostatectomy being the primary treatment, the prevalence of SUI as a side-effect will likely increase [34]. The underlying pathophysiology is the loss of sphincter function [6]. During a radical prostatectomy, the prostate is removed, which surrounds the prostatic urethra. Therefore, this part of the urethra is not covered anymore, resulting in missing compression in this area and, thus, a weakened urethral sphincter [35].

Additionally, the procedure damages the internal urinary sphincter [36]. Furthermore, the external urethral sphincter and several nerves are close to the prostate and, therefore, are at high risk of damage during the procedure [35]. Both pathophysiologies could be possible for SUI in men after radical prostatectomy [12,35,36], but the sphincter deficiency is more common [12].

2.2 Diagnosis and Current Therapeutical Approaches for SUI

The diagnosis of SUI includes, as a first step, an initial general assessment. This covers the medical history, bladder diaries, and urine analyses [10,18]. Reversible causes such as excess fluid intake, pharmaceuticals, infections, and restricted mobility have to be excluded [10]. Then, the type of UI is determined by the clinical history, symptom assessment, and physical examination (e.g., cough test, post-void residual volume) [10,18]. If there are complex symptoms, e.g., bladder pain, pelvic organ prolapse, haematuria, and urogenital malignancies, a specialist has to be consulted [10]. In addition to the initial examination, urodynamic tests or pelvic floor imaging can be performed [10].

After the diagnosis of SUI, the treatment primarily aims to optimize the patient's quality of life [20]. This can be achieved by controlling incontinence [37], mainly accomplished by conservative treatment [18]. The conservative treatment methods include lifestyle changes (e.g., weight reduction, fluid uptake management) and pelvic floor muscle training [18]. Weight reduction is especially indicated in individuals who are obese since obesity is one of the risk factors leading to SUI [10]. With weight loss, the excess loading on the pelvic floor muscles and the increased pressure on the bladder is minimized, thereby ameliorating incontinence. A study reported a reduction of 58% of SUI events in a group of patients that participated in a 6-month weight loss program (8% weight loss in the observed time period) compared to a reduction of 33% in the control group (1.6% weight loss in the observed time period). This study supports the benefits of weight loss on SUI [31]. Pelvic floor muscle training aims to improve the pelvic floor muscles [10]. Several studies report the effectiveness of the training on SUI. The improvement of pelvic floor muscle training was reported to be 56% in patients with SUI compared to 6% in control groups [38]. The efficacy of this training can be attributed to conscious contractions of the pelvic floor muscles before and during events of increased intra-abdominal pressures, permanently built muscle volumes that provide anatomical support to the urethra, or indirectly strengthened pelvic floor muscles [39]. Nevertheless, the duration of the treatment effect remains unclear due to

the lack of long-term follow-ups [38,40]. Further treatment options are electrophysiological stimulation [18] and regular toileting (bladder training), which prevents urine leakage events and is mostly performed in nursery homes [37]. Despite the discussions about the effectiveness of these methods, they are still recommended [40]. Vaginal continence pessaries can also be used as treatments for women. They do not need the amount of individual motivation as behavioral therapies [41]. The underlying mechanism of the pessaries is the compression of the urethra during intra-abdominal pressures leading to higher urethral closure pressure and resistance [41]. This treatment method shows the same effectiveness compared to behavioral therapies after one year [41]. Nevertheless, controlled incontinence, as it may be achieved by the mentioned approaches, does not imply that the incontinence is cured. Instead, the incontinence returns if the treatment methods are discontinued [37]. Therefore, the patient's compliance is an essential factor in treating SUI with conservative methods [37].

If the initial attempts fail, SUI can be treated with minimally invasive therapy or surgery [18,40]. This includes bulking agents, tapes and slings, and colposuspension for women [18]. Bulking agents comprise natural or synthetic substances injected into the urethra using a minimally invasive procedure [40,42]. Nevertheless, the durability of this treatment is not sufficient and further complications such as degradation, tissue migration, bladder outlet obstruction, and allergic reactions are reported [42]. However, this method is indicated mainly in SUI based on intrinsic urinary sphincter deficiency and in patients unable or unwilling to undergo more invasive surgical interventions [43]. Due to their low morbidity rate and minimally invasive approach, bulking agents are often used as an alternative in old or frail women [7]. The surgeries of sling implantation or bladder neck colposuspension are reported to be quite effective [42]. The bladder neck colposuspension was the primary treatment up to the mid-1990s until it got replaced by the mid-urethral slings [40,44]. The latest used procedure is the Burch procedure [40]. It aims to elevate the bladder neck enabling intra-abdominal pressure to be reapplied to the urethra, resulting in increased urethral closure pressure [45]. The procedure is a form of retropubic colposuspension and can be performed as open or laparoscopic surgery. The bladder is moved to the other side before the paravaginal fascia is sewed to Cooper's ligament, which is attached to the pubic bone [7,45]. Two to four sutures are placed on both sides of the bladder neck [45]. The long-term efficacy of this treatment was reported to be 68.9–88% [44]. After one year of follow-up, the reported efficacy increased to 85–90% but declined to about 70% after

five years of follow-up [46]. However, one complication reported with open colposuspension is the higher risk of pelvic organ prolapse than sling surgeries. For laparoscopic surgery, long-term data for effectiveness and safety are missing [46]. Complications resulting from the procedure are voiding dysfunction, de novo detrusor instability, and small bowel prolapses [7]. Colposuspension is still recommended when mid-urethral slings are not suitable [40]. The current primarily used surgical method is the synthetic mid-urethral sling placement. As the name suggests, the sling consisting of permanent mesh is placed at the mid-urethra to replace the function of pubourethral ligaments [7,40]. The treatment is considered less invasive than colposuspension or pubovaginal slings. Additionally, the operating and recovery times are shorter than the more invasive methods [40]. The improvement of both mid-urethral sling types, retropubic tapes, also known as tension-free vaginal tapes, and transobturator tapes, is reported to range between 71% to 97% (retropubic tapes) and 62% to 98% (transobturator tapes) after one year of follow-up. These rates declined to 51–88% (retropubic tapes) and 43–92% (transobturator tapes) after five years of follow-up [47]. However, complications can occur with urine retention or voiding difficulties. Additionally, the urgency symptoms can worsen, the implanted mesh may erode, or de novo urgency incontinence can be observed [40,42]. Among the intra-operative complications reported, bladder perforation is the most common one [40]. In women, the artificial sphincter is mostly used as the last treatment option when lesser invasive therapies fail, while, in men, it is used much more frequently as a "gold-standard" [18,40,48]. An artificial sphincter consists of three main components: a ballon regulating the pressure, a cuff placed around the urethra to open or close it mechanically, and a pump in the labia, which is needed to inflate the cuff [40]. This therapy option shows a success rate of 76–89% and is quite long-lasting [40,48]. However, complications like device failure, erosion of the device components, or infections can occur [40]. Additionally, urethral atrophy can be developed, resulting in the recurrence of urine leakage. These complications then lead to the explantation of the artificial sphincter in at least 30% of implantates[48].

Despite the high success rate, all surgical procedures provide the risks of bleeding, infection, pain, anesthetic problems, and visceral injury. Persisting SUI after primary surgery is also a concern of up to 20% of patients [10,49,50]. Additionally, these therapy options do not treat the predominant underlying cause of SUI, the urethral sphincter deficiency, but only alleviate the symptoms of urine leakage by strengthening the pelvic

floor muscles to address the cause of urethral hypermobility [29,50,51]. Therefore, the research for minimally invasive therapies that treat the underlying cause is ongoing [49,51].

3. Cell Therapy in SUI Research

Cell therapy offers the possibility of treating the dominant underlying cause of SUI, the weakened urethral sphincter [52]. As described above, the current therapies do not address this cause. Therefore, the aim of cell therapy in the context of SUI includes the regeneration of the external and internal urethral sphincter as well as the repair of peripheral nerve tissues [52,53].

Stem cells are characterized by their ability of self-renewal, formation of clonal populations, and differentiation into multiple cell types [49]. They are involved in several repair mechanisms after injuries to regain normal tissue function [51]. Depending on environmental conditions, stem cells can contribute to healing by differentiating into the desired cell type and integrating into the defective tissue or by producing secretory bioactive factors that impact the affected tissue [49,51,53]. There are two main types of stem cells, embryonic and adult stem cells (Table 2) [49]. Embryonic stem cells originate from the blastocyst's inner cell mass and are truly pluripotent. This pluripotency is the main advantage of these cells because they can differentiate into every cell and tissue type of all three lineages [54]. However, several concerns exist regarding the risk of tumors, genetic instability, and transplant rejection associated with cell therapy using embryonic stem cells [55]. Besides a few exceptions, the research and use of embryonic stem cells are strictly forbidden in Germany by the Embryo Protection Act [56]. In contrast to embryonic stem cells, adult stem cells are considered multipotent, originate in specific tissues and organs, and can differentiate into multiple cells of a specific lineage or tissue [49,57]. However, there are also adult stem cells that are considered unipotent, which means that they are capable of developing into only one specific cell type. The limitation of adult stem cells compared to embryonic stem cells is that their application should be tissue-specific. However, apart from this limitation, their therapeutic ability is not limited, in fact, adult stem cells are preferable [57]. Different sources of adult stem cells for cell therapy of SUI were investigated, including bone marrow, peripheral blood, skeletal muscle, adipose tissue, skin, urine, etc., leading the focus on multipotent mesenchymal stromal cells (Chapter 3.1) and myoblasts derived from unipotent satellite cells (Chapter 3.2) (Table 2) [49,51].

Table 2: Definitions, types, and examples of cell potency

Potency [57]	**Definition** [57]	**Type** [57]	**Example** [57]
Pluripotent	Differentiation into all three lineages	Embryonic stem cell	
Multipotent	Differentiation into various cell types of one lineage	Adult stem cell	Mesenchymal stromal cell
Unipotent	Differentiation into one cell type of one lineage	Adult stem cell	Satellite cell

Autologous stem cell transplantation is the current treatment of choice as it excludes the risks of immunological reactions [51]. To isolate and produce stem cells, three stages are usually distinguished [58]. In the first stage, a biopsy of the tissue desired is taken (e.g., muscle, bone marrow, fat). The cells are isolated from the tissue during the second stage and expanded. As soon as enough cells have been produced, they are injected locally into the desired area in the patient [58,59]. However, the aim would be to use allogeneic cells to avoid this time-consuming three-stage procedure [59] and to provide an alternative source of stem cells for elderly patients since the regenerative potential of stem cells is influenced by age [60].

Several clinical studies were conducted to analyze the safety and efficacy of stem cell therapy for SUI [59,61]. Minimal adverse effects were reported, and the results were promising. Improvement rates of 88% for adipose-derived mesenchymal stromal cells in four clinical trials and 77% for muscle-derived cells in eleven clinical trials were recorded. Nevertheless, the follow-up in these studies was mostly below 12 months requiring further investigation of long-term safety and efficacy [51,61]. Further details regarding the clinical studies of adipose-derived stem cells and muscle-derived cells are described in Chapters 3.1 and 3.2.

Despite promising results, several challenges remain regarding the cell therapy of SUI [51,59]. The optimal dose still has to be determined, as well as the optimal delivery route of the cells. Additionally, it is unclear how the cells' proliferation, differentiation, and distribution after implantation could be maintained, promoted, and directed [51]. The poor

cell retention and engraftment into the defective tissue of injected cells is a limitation that is part of this challenge [52,53]. Even if they are considered safer than embryonic stem cells, some papers discussed a risk of tumor growth upon adult stem cell therapy [62]. This, however, is controversial, as several other studies have highlighted the safety of adult stem cells, e.g., in hematopoietic stem cell transplantation, commonly referred to as bone marrow transplantation, even in young children [63], in the application of mesenchymal stromal cells in the context of graft-versus-host-disease or muscle regeneration [64,65], or in ocular stem cells to restore a damaged cornea [66]. Therefore, long-term follow-ups are still required. Furthermore, the need for representative animal models to investigate the treatment efficacy and underlying mechanisms remains [51]. In terms of cell culture, the long preparation time and the risk of losing the regenerative potential in vitro are challenging [67]. Moreover, the number of clinical trials and patients included is small and results must therefore be viewed critically [61,68].

In conclusion, further research is needed to establish cell therapy as a realistic treatment option [69]. The future aim of cell therapy for SUI would be to have cells ready to use for minimally invasive allogeneic transplantation for single and systematic administration [59].

3.1 Mesenchymal Stromal Cells (MSC)

Mesenchymal stromal cells (MSCs) are adult stem cells that demonstrate multipotency (Table 2) [70]. They are derived from the mesenchyme, which forms from the mesoderm during embryonic development [68,71]. The cell culture of MSCs is not complicated because they are easily isolated and expanded in vitro. Isolation of cells can be conducted from various tissue sources such as bone marrow, adipose tissue, placenta, and several more [70,71]. During expansion, the characterization of MSCs will be performed according to the three minimal criteria defined by the International Society for Cellular Therapy (ISCT) [69,72]. The first criterion states that MSCs must demonstrate plastic-adherence under in vitro cell culture conditions. The second criterion relates to the expression of several cell surface markers. In particular, CD73, CD90, and CD105 must be expressed, while CD45, CD34, CD14 or CD11b, CD79α or CD19, and HLA-DR should not be expressed. The third and last criterion describes their ability to differentiate in vitro into osteoblasts, adipocytes, and chondroblasts [72]. MSCs can differentiate into cells of mesodermal origin, such as bone, fat, and cartilage cells [70]. Additionally, they were claimed to differentiate into muscle cells and were reportedly involved in ecto- and endodermal tissue formation,

angiogenesis, and peripheral nerve regeneration [70]. This wide MSC differentiation spectrum is considered nowadays as an in vitro artifact [73].

Several features of MSCs lead to their success. MSCs provide the possibility of allogeneic transplantation, possibly due to their reduced expression of major histocompatibility complex class I and class II antigens or costimulatory molecules and their suppressive action on pro-inflammatory cells [59]. Furthermore, the regeneration potential of MSCs can be mediated by the differentiation and engraftment, MSC cell fusion, paracrine activity, the transfer of mitochondria by tunneling nanotubes, or by the transfer of molecules from exosomes or microvesicles (Figure 4) [53,74]. Current concepts of MSC action favor rather the release of factors over differentiation processes in tissue regeneration or wound healing as mediated by MSCs [75]. When considering cell therapy for SUI, the focus is also less on the differentiation and long-term engraftment of MSCs (Figure 4A) but mainly on their paracrine activity (Figure 4C) [68,69,74]. This may include mechanisms of cell communication by cytokines and growth factors, nanotubes, exosomes, or microvesicles (Figure 4C, D, E).

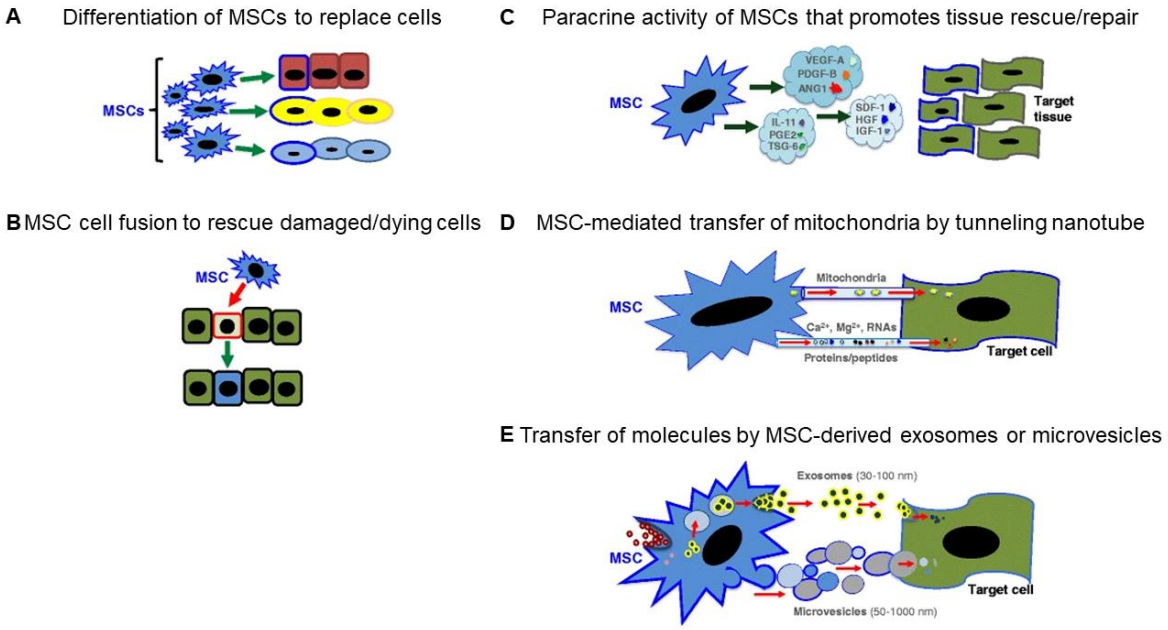

Figure 4: Regenerative potential of MSCs mediated by different mechanisms. (A) The differentiation and engraftment of MSCs into defective tissue to replace lacking cells. (B) MSC cell fusion with damaged or dying cells to provide a rescue mechanism. (C) Paracrine activity through secretion of growth factors, cytokines, chemokines, and hormones to promote tissue repair. (D) Transfer of mitochondria or other organelles/molecules by tunneling nanotubes. (E) Transfer of molecules (RNA, proteins, hormones, and chemicals) by extracellular vesicles such as exosomes or microvesicles. This figure was adapted with modifications from Spees, Lee et al. 2016 [74]

In terms of SUI, there is the MSCs' capability to support myogenic differentiation. Specific growth factors, matrix stimuli, or biomechanical stimulation can induce myogenic differentiation of the corresponding progenitor cells. Depending on the factors applied, MSCs themselves can build smooth or striated muscle cells [68,69]. However, differentiation into striated muscle cells in vitro is not efficient [76]. Moreover, smooth muscle cells show two different states, with only the contractile state being suitable for cell therapy, as only this type expresses the factors required for muscular function [69]. A study investigated the differentiation and engraftment of MSCs. It included 18 rats whose urethral sphincters were injured. After a follow-up of 13 weeks, analyses suggested that the injected MSCs contributed to the recovery of striated muscle cells and peripheral nerves. However, the experimental evidence to prove in vivo differentiation is not convincing, and improved leak point pressure was not recorded [77].

On the other hand, there is the MSCs' capability to secrete bioactive factors (Figure 4C) [69]. In general, the bioactive factors can enhance the efficacy of cell therapy by their interaction with the surrounding tissue modifying the microenvironment [53]. Bioactive factors secreted by MSCs contribute to healing by inducing anti-apoptotic, anti-scarring, and neovascularization effects [49,59,69]. Through these pathways, they can also influence systemic and local immunomodulatory characteristics [59]. Furthermore, cytokines and chemokines secreted contribute to the activation of endogenous stem and progenitor cells in the area of injury [59,69]. This mechanism might also be involved in the repair of the denervated urethral sphincters. MSCs can secrete neurotrophic factors such as brain-derived neurotrophic factor, nerve growth factor, hepatocyte growth factor, insulin-like growth factor, and vascular endothelial growth factor to induce the regrowth of axons controlling the sphincter muscles [69]. In other diseases, such as multiple sclerosis or ischemic brain injury, MSCs were studied more intensively [53,69]. In these contexts, the secretion of paracrine factors is considered the main factor contributing to the therapeutic effect [78,79].

Overall, numerous mechanisms of action of MSCs and the interactions of the different mechanisms are still not completely explored (Figure 4). However, based on the current state-of-the-art, the paracrine function plays a significant role [53,58,74].

Several preclinical studies showed the benefit of injecting MSCs. Rats and rabbits were primarily used to investigate the potential of bone marrow-MSCs [80-84]. To simulate the injury of SUI, either bilateral pudendal nerve dissection [80,84], cryo-injury of the internal

urethral sphincter [81], or dual injury of pudendal nerve crush and vaginal distension [82,83] were applied. The studies had follow-ups of two to four weeks. After the respective observation period, the influence of the injected bone marrow-MSCs was evaluated by measuring the leak point pressure. These studies reported significant improvements in animals treated with MSCs compared to control groups [80-84]. One study also showed that multiple doses enhance the treatment effect [82]. In two studies, pudendal nerve testing was also performed, and improvement was shown [82,83]. Furthermore, histological analyses conducted in two studies revealed that the proportions of skeletal and smooth muscles are higher in the cell-injected areas compared to the controls [80,81]. The mechanism leading to the proliferation of striated or smooth muscle fibers cannot be uniquely attributed to cell differentiation and engraftment alone because the influence of paracrine secretion of the injected cells has not been analyzed in those papers [80,81].

Notwithstanding these promising results in preclinical trials, no clinical studies have been conducted with bone-marrow MSCs to date. This might be due to the painful bone aspiration under general anesthesia required for producing bone marrow-MSCs [61]. Another factor contributing to these cells not being considered further is that bone marrow-MSCs show signs of spontaneous osteogenic differentiation, which is undesirable in cell therapy for SUI [68,69].

3.1.1 Adipose-derived Stromal Cells (ADSC)

Adipose-derived stromal cells (ADSCs) are MSC-like cells isolated from adipose tissue [67,71]. The advantages of ADSCs are their simple collection, i.e., via lipoaspiration and their large number when harvested [67]. Additionally, repeated sampling is tolerated well among patients [51]. Adipose tissue contains about 15 million ADSCs per gram adipose tissue [61]. This large number leads to the possibility of cell isolation from fat and direct injection into the desired area [85]. In breast augmentation, it was reported that there were only four hours between cell harvesting and injection [86]. As a subfraction of MSCs, ADSCs display almost the same characteristics as MSCs outlined above. Their specific multilineage characteristics and ability to secrete anti-apoptotic and angiogenic factors were proven [87,88].

In addition to the preclinical studies conducted with bone marrow-MSC, various preclinical and clinical studies investigated the specific safety and efficacy of ADSCs in the treatment of SUI.

The first preclinical study regarding this topic was performed in 2010. It used labeled ADSCs and injected them into rats. Urethral sphincter deficiency was induced by balloon dilatation and ovariectomy. Abnormal voiding was reported for 33.3% with injected ADSCs compared to 80% in the controls after four weeks of follow-up, displaying a significant improvement. Additionally, rare differentiation of injected cells toward smooth muscle fibers was detected, while the majority of the injected cells remained undifferentiated [85]. Another study used almost the same experimental settings (animal model, follow-up period). The measured leak point pressure after four weeks of animals injected with ADSCs was significantly increased compared to the control group (25.9% increase). Additionally, normal striated muscle appearance and significantly increased smooth muscle contents were reported. This study further investigated the expression of vascular endothelial growth factor and showed that in animals with injected ADSCs, this factor is secreted significantly higher than in controls. However, it remains unknown if the ADSCs secreted vascular endothelial growth factors or if they differentiated into cells that are able to produce it [89]. Three other studies also used ADSC injections in injured rats. All of them induced the injury via pudendal nerve transection. These studies supported the findings of the first two studies. After their respective follow-up of 2–8 weeks, they all reported increased leak point pressures [90-92]. Other factors such as enhanced urethral muscle layer distribution and neuronal density of the urethra [92], the decreased urethral lumen and expression of myogenic antigens in injected cells [90], or reconstituted urethral wall muscle layers, dense surrounding connective tissues, and improved ultrastructures [91] complemented the analyses of these studies. The study with the longest follow-up of twelve weeks was also conducted in rats. Rats were also injured by pudendal nerve transection. In contrast to the others, this study employed ADSCs that adhered to silk fibroin microspheres. The microspheres were used as a bulking agent. The results showed that the injection of ADSC-covered microspheres after twelve weeks enhanced muscle and nerve regeneration, but the injection with microspheres only did not. The microspheres alone were able to increase the leak point pressure in a short time, but after twelve weeks, their level was the same as the controls. Only the treatment with ADSC-covered microspheres could restore normal leak point pressures and urethral lumen area. The leak point pressures increased by 51.8% compared to controls, and the urethral lumen area decreased by 94% [93]. Only one preclinical animal study was not performed on rats. Instead, rabbits were used. The injury was induced by spraying liquid nitrogen to cryo-injure the urethral sphincters. Leak point pressures were measured after 14 days of

follow-up and revealed a significant increase of 33.7% in the animals with injected ADSCs compared with the control animals. Histological analyses showed that the skeletal and smooth muscle proportions were also significantly enhanced. The authors concluded that the injected cells differentiated toward striated or smooth muscle cells, nerve cells, or vascular endothelial cells due to their expression of specific markers. Furthermore, three other potential paracrine growth factors expressed by the injected cells were determined, suggesting support and promotion of tissue regeneration [94].

In contrast to bone marrow-MSCs, several clinical trials in men and women using ADSCs were conducted. The first clinical study regarding this topic was performed in 2012 [95]. In this feasibility study, three men, after radical prostatectomy, were treated by transurethral injections of ADSCs into the external urethral sphincter and the submucosal space of the urethra. The initial analyses reported were carried out up to six months after treatment. In all three cases, the leakage volume decreased by an average of 78.5%. One case even reported complete continence after the treatment. Urodynamic measurements and subjective symptom assessments supported these findings. Additionally, increased blood flow to the injection area and a bulking effect at the injection site were recorded. Moreover, no significant adverse side effects were registered [96]. The results of this preliminary study were supported and extended by three additional clinical trials conducted in men. These three studies used the same settings as the first one [97-99]. One of the studies showed that the first study could be replicated in terms of efficacy and safety [97]. The other two studies, conducted by the same group as the feasibility study mentioned above, extended the patient number to thirteen and the follow-up time to up to six years. The same findings were reported, except three out of the thirteen patients showed no improvement at one year and the final assessment [98,99]. Another study that had two arms was also conducted on treating SUI with ADSCS. The two arms included one male and one female cohort in the clinical trial. Eight men with SUI after radical prostatectomy were involved in the study. Three men showed an improvement in continence regarding the results from pad tests and urodynamic measurements (urethra profile, cough leakage, and urodynamics) [100]. Two studies were also conducted on women [100,101]. In one clinical trial, ten women with SUI were treated with transurethral injections of ADSCs. The follow-up was three months. Pad tests and questionnaires were used to investigate the efficacy of the treatment. All ten patients showed significant decreases in the pad tests and supported this improvement in continence in the subjective questionnaires [101]. The other study conducted on women is the

second arm of the above-mentioned clinical trial. Five out of ten women showed improvements in pad tests and urodynamic measurements (urethra profile, cough leakage, and urodynamics) [100].

Overall, all these studies suggest that ADSCs are a safe and suitable treatment option for SUI, demonstrating the regenerative potential of ADSCs with a success rate in clinical studies ranging from 30% to 100% [96-98,100-102]. Furthermore, this cell type meets all the treatment requirements of SUI, including the increase in smooth and striated musculature, vascularization, and innervation, because they can differentiate toward these cell types and produce various growth factors that could improve their efficacy in treatment [67,87,88].

3.2 Myogenic Progenitor Cell/Myoblasts (MPC)

Myogenic progenitor cells, also known as myoblasts (MPCs), are derived from satellite cells and differentiate toward striated muscle fibers. Satellite cells demonstrate unipotency (Table 2) and can only differentiate further into the striated muscle [57,103]. They have an essential role in repairing and maintaining skeletal muscles [70,103-105].

Muscle regeneration is initiated upon muscle injury (Figure 5) [106]. Quiescent satellite cells are activated in the first step to re-enter the cell cycle. They are located in their stem cell niche next to the basal lamina of mature skeletal muscle fibers and stay dormant in undamaged tissues [68,70,103,106]. About 2–10% of total myonuclei per muscle fiber are satellite cells. They have the ability to self-renew and express mainly the paired box protein 7 (Pax7) [70,105,106]. Myogenic factor 5 (Myf5) can also already be expressed in some satellite cells [105]. Activated satellite cells further proliferate into MPCs. During this process, the myoblast determination protein 1 (MyoD1) and Myf5 are critical for the regeneration to continue [104,106]. Both factors prime the cells' development toward the myogenic lineage [107]. It was demonstrated that the lack of one of these factors resulted in moderate difficulties in recovery, while the simultaneous absence of both factors led to complete failure of muscle regeneration [104]. MPCs start to differentiate toward myocytes. During this process, the specific factor of satellite cells, Pax7, declines [105]. Instead, myogenin (MyoG) increases during this differentiation and in the following fusion process [105]. MyoG and MyoD1 act together to further activate muscle-specific structural and contractile gene expression [105]. Myocytes can fuse with each other to form myotubes or with already existing muscle fibers [105]. This fusion is controlled by the factors MyoG and myogenic regulatory factor 4 (MRF4), also known as myogenic factor 6 (Myf6) [70,107].

The self-renewal capability of the satellite cells ensures that a constant pool of satellite cells is always maintained [70,105]. In conclusion, muscle regeneration is a highly complex process involving even more genes and factors contributing to the mechanism and regulation of proliferation and differentiation than are presented in this chapter [105].

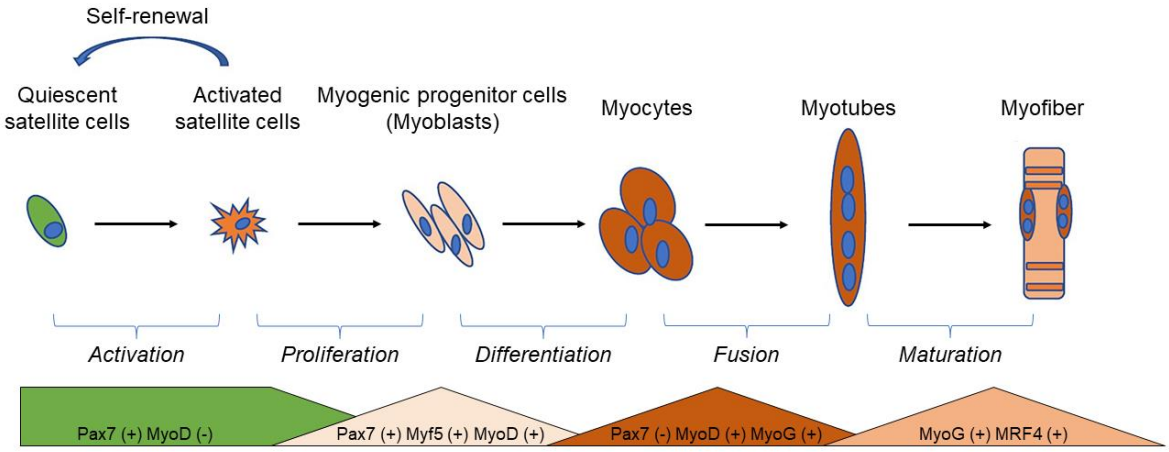

Figure 5: Differentiation of satellite cells toward myofibers. Satellite cells remain quiescent upon muscle injury. They are characterized by paired box protein 7 (Pax7) expression and their ability to self-renewal. After an injury, satellite cells get activated. They start to proliferate into myogenic progenitor cells/myoblasts (MPCs). The myoblast determination protein 1 (MyoD1) and myogenic factor 5 (Myf5) are expressed at this stage. MPCs further differentiate into myocytes. Myocytes fuse to myotubes. During this process, the expression of Pax7 declines and the expression of myogenin (MyoG) increases. Myotubes mature into myofibers expressing MyoG and myogenic regulatory factor 4 (MRF4), also known as myogenic factor 6 (Myf6). This figure was adapted with modifications from Isesele and Mazurak 2021 [106]

Since MPCs can form myotubes and myofibers and are limited to striated muscle differentiation, this is an advantage for their use in cell therapy for SUI [49,108]. Their natural role as precursors in this cell lineage makes them a suitable cell type for SUI cell therapy [76,107]. By this differentiation and possible engraftment after injection, MPCs can contribute to the contractility of the urethral sphincter [61,108]. This repair mechanism is basically the same as in MSCs (Figure 4A), just for striated muscles.

Several studies injecting MPCs in the defective urethral sphincter showed promising results. One of the first preclinical studies conducted in healthy rats displayed the possibility of cell injections into the urethra and was able to show that 88% of injected β-galactosidase-transduced muscle-derived cells persisted at the injection site for 30 days [109]. Another study supported these results. In this study, green fluorescent protein-transduced MPCs were injected in rats. After ten days of follow-up, the injected cells started to fuse with the striated myofibers. Ninety days after injection, green fluorescent myofibers were found all over the striated muscle layer but not in the smooth

muscle layer [110]. The first preclinical study using MPCs in a deficient urethral sphincter model was performed in 2002. A myotoxic substance induced injury in the striated urethral sphincter of mice. PKH 26 labeled MPCs were injected, and results after seven days showed significantly higher myofiber numbers and diameters than the control group. However, after a month, both control and MPC-treated mice fully recovered. These results suggest that MPCs have accelerated the regeneration and that an animal model with a more permanent injury is needed [111]. This problem was solved in studies with rats [112,113]. One study used electrocoagulation to injure the external urethral sphincter. It reported that leak point pressures reached 41% of normal after 30 days of follow-up. Additionally, they monitored motor units consisting of regenerated myotubes with acetylcholine receptors associated with nerves. These motor units also improved to 58.4% of normal levels within 30 days after injection [113]. In another study, rats were injured by bilateral sciatic nerve transection to simulate denervation before injection with muscle-derived cells. After two weeks, contractility tests identified an increase in the fast-twitch muscle contraction amplitude to 87% of normal levels compared to 8.8% in controls. Additionally, histological analyses showed new striated muscle fibers at injection sites [112]. The same group conducted three other studies with the same animal model and expanded the follow-up to four [114,115] and twelve weeks [116]. Furthermore, they measured the leak point pressure in these studies [114-116]. One of the four-week follow-up studies only compared the leak point pressures. It demonstrated a significant increase in the animals treated with cell injections after four weeks compared to the control group [115]. The other four-week follow-up study supported the findings by showing the same results regarding contractility testing and histological analyses. The leak point pressures also contributed to the result by proving a significant increase after four weeks. This study also added a dosage effect showing that the leak point pressures increase with injected cell numbers [114]. The twelve-week follow-up study also supported the histological findings regarding new striated muscle fibers. Regarding the leak point pressure measurements, they also showed a significant increase after twelve weeks suggesting that MPCs have a long-term effect on the function of the urethral sphincter [116]. Again, the same group performed another study. They used a different rat model of urethral sphincter insufficiency that is more consistent with the clinical picture. In this model, rats were injured by electrocauterization. β-galactosidase-transduced muscle-derived cells were injected, and leak point pressures were measured every two weeks. After four and six weeks, the leak point pressures displayed significant improvement of the sphincter function. As described in the previous

studies, histological analyses also demonstrated the integration of injected cells in the striated muscle layer [117]. All described models involved the denervation of the striated muscle sphincter [118]. Therefore, two other studies aimed to directly injure the external urethral sphincter [118,119]. The first of the two studies used longitudinal microsurgical sectioning of the external urethral sphincter. They injected MPCs and measured the closure pressure three weeks after injection. The closure pressure significantly increased by 62% in the animals with injected cells compared to 11.9% in the control group. This study also suggested that new myofibers were formed in the injected cell clusters [118]. The other study simulated radical prostatectomy's operative injuries by the removal of one-third of the external urethral sphincter. After four and twelve weeks, the recovery ratio of the injected muscle-derived cells was measured via urethral pressure profiles. The study showed that the recovery ratio was 72.9% after four weeks compared to 37.6% in the control group. After twelve weeks, almost the same values were reported (78.4% compared to 41.6%). This study again supported the findings that transplanted cells differentiate into muscle fibers. Moreover, this study also suggests that muscle-derived cells can contribute to nerve regeneration and innervation by intrinsic activation after myotube formation [119].

Clinical trials using MPCs as a treatment for SUI started in 2004. However, one of the first studies published was withdrawn due to the illegal conduct of the study and severe violation of ethical rules [67]. Nevertheless, various studies in this field of research followed.

Most of the studies were performed on women. The first, not withdrawn and lasting clinical study using MPCs as cell therapy assessed the efficacy of the treatment in 123 women. Urodynamic measurements were performed to evaluate the improvement. After one year of follow-up, 79% of the patients reached complete continence, while 13% were substantially and 8% slightly improved. Additionally, a significant increase in the thickness and contractility of the external urethral sphincter was reported for all women. However, in this study, not only MPCs were injected into the external urethral sphincter, but also fibroblasts were injected into the submucosa [120]. Therefore, the first pilot study with only injecting MPCs was performed in North America. Eight women with SUI were included in the study. However, three women dropped out of the study one month after the treatment because no positive effect was detectable by this time. Among the remaining five women, the continence level was assessed via pad tests after one year of follow-up. All of them reported improvements in their incontinence. One woman even experienced complete continence [121]. The subsequent study was conducted on twelve women with severe SUI

due to intrinsic urinary sphincter deficiency. This study aimed to determine the safety and efficacy of MPC injections depending on the dosage. Of the twelve patients, three were dry at the twelve-month follow-up, and seven more improved in the pad test independent of dosage. However, two women showed a worsening of their symptoms. Overall, no adverse effects were observed regarding the MPCs' safety [122]. The same patients were followed for up to six years. One patient was lost during the follow-up period. Of the remaining patients, the two who were completely dry remained dry after this extended follow-up. In the five patients who showed an improvement after one year, worsening and recurrence of SUI were recorded [123]. Nevertheless, the findings of the last three reported studies relied on pad tests and not functional measurements [121-123]. This also applies to several other studies [124-126]. Another study was also conducted on complicated SUI. After a follow-up of 36 months, 30% of the patients were classified as cured, 40% improved, and 30% had persistent SUI [127]. A specific study addressed the difference in therapy efficacy depending on the severity of SUI. Complicated and uncomplicated SUI were included in the study and analyzed separately for the number of leakages in a three-day diary. Women with uncomplicated SUI reported no leakage in 25% of cases, and 63% reported a decline in leakages. In contrast, only 7% of women with complicated SUI recorded no leakage. Nevertheless, 57% declared an improvement [126]. Four other studies also displayed improvements upon MPC injections [42,124,125]. Two of the studies added that the efficacy of the treatment increases with higher dosages [42,125]. There are only two studies that had a follow-up of two years [128,129]. In one study, 89% of patients were classified as cured, and 11% showed improvements. This study also displayed significant increases in the thickness of the external urethral sphincter and its contractility [128]. The other study reported a 75% success rate, including 50% cured and 25% improved conditions [129]. The observation time was also extended to four years with the same patients. The questionnaire scores significantly increased from 49 to 63 after four years. Even though the scores were slightly higher after two years (77), this symbolizes long-term efficacy on the subjective assessment level [130].

The newest study is a prospective phase I clinical trial. Nine women were treated with transurethral injections of MPCs into the external urethral sphincter. The study aimed to determine the safety and feasibility by investigating several functional measurements. Overall, this surgical and treatment method can be claimed safe due to the minimal number of reported adverse effects and feasible due to improvements in the urethral length,

questionnaire scores, and diameter of the external urethral sphincter [131]. Only one study was conducted as double-blind, randomized, placebo-controlled clinical trial. The aim of the study also was to investigate the safety and efficacy of MPC injection in women with SUI. It was planned to enroll 246 patients in this trial. However, the trial was stopped after 150 enrolled patients due to relevant and unexpectedly high placebo response rates in the primary outcome. Nevertheless, 141 patients completed the study at twelve months of follow-up. The primary outcome was a combination of measurements, including a reduction of over 50% in incontinence episode frequency or pad tests compared to the level before treatment. However, if more stringent endpoint measurements of over 75% were used in post-hoc analyses, the placebo group displayed greater reductions in incontinence episode frequency and pad tests. Despite these inconclusive primary results, the treatment can be considered safe [132].

Moreover, two studies also investigated the injections of MPCs into the urethra in men suffering from SUI. Both studies had a follow-up of one year [133,134]. To date, one of the studies was the largest study conducted to investigate cell therapy in SUI with 222 patients. 12% of the patients regained continence, and 42% experienced at least some improvement. However, 46% of the patients reported no effect. It is important to note, though, that the results of this study were obtained using a questionnaire only, and no functional tests were performed [133]. In the other study of 63 men suffering from SUI, functional tests were performed. These resulted in 65% continent men after treatment with MPCs, and 27% of patients with improved functionality. Only 8% of the patients displayed a persistent SUI. Additionally, the study demonstrated that the thickness and contractility of the external urethral sphincter were significantly increased [134].

Despite these promising clinical results, there are several challenges regarding cell therapies. In addition to the above-stated challenges, for MPCs, the variations in isolation techniques and administration routes also play a critical role [53]. The administration route is highly critical to MPCs due to their limited migration. This was reported, i.e., for donor cells injected for cell therapy purposes of dystrophic muscles [103]. MPCs are thought to act through the mechanism of differentiation and engraftment. However, since they only differentiate toward striated muscles, they seem unable to restore deficiencies in the smooth muscle fibers and to improve innervation and vascularization [67]. In contrast, preclinical studies demonstrated at least an involvement of MPC injections in the innervation and vascularization after injury. However, the exact mechanism is still

unknown [119]. Moreover, in a clinical context, muscle-derived cells are limited in number in humans due to the limited size of muscle biopsy, which leads to extended cell culture periods [49,51,67,69,108]. These extended cell culture periods give rise to risks such as cell transformation and sterility issues [49,51,67,69,135]. Additionally, the procedure of muscle biopsy is considered to be painful [51].

Overall, all presented studies display the potential of MPCs for treating SUI by improving the damaged sphincter function with a success rate in clinical studies ranging from 13% to 90% [61,102]. Furthermore, long-term follow-up showed evidence that a long-lasting positive effect was occurring [49,123,130].

4. Animal Models in SUI Research

Animal models are used to study SUI's pathomechanisms but are especially important to evaluate the safety, efficacy, and underlying mechanisms of action of cell therapy in SUI [53,136,137]. They are relevant because they can provide controlled environmental and experimental conditions, allowing standardized settings [53,137]. However, differences between humans and animals regarding anatomy, physiology, and disease mechanisms may contribute to translational problems [53]. An example of the differences in anatomy is the lower pelvic floor, which is considerably different in quadruped animals than in humans [138]. Since SUI is a rather complex disease, animal models face difficulties addressing all underlying mechanisms in humans [53,137]. Furthermore, ethical concerns regarding the use of animals can arise [53].

Various methods are applied to induce incontinence in animal models. These cover vaginal distension by balloon or bougie dilatation, ovariectomy, cryo-injury, pudendal nerve crush or transection, urethrolysis, myotoxic substances, electrocautery, or sectioning of the external urethral sphincter [77,80-85,89-94,111-119,139-147]. All these methods mainly aim to mimic injury to the urethral sphincters caused by vaginal delivery or prostatectomy. The different methods provide the opportunity to deepen the knowledge of each pathophysiology [53,136,137]. Also, combinations to induce a dual injury are applied [53,137]. However, the incontinence induction methods vary widely in their efficiency in generating a permanent incontinence model [53,136], i.e., as described above (Chapter 3.2), the myotoxic substances do not provide durable incontinence in mice [111]. Another possibility of an incontinence animal model, especially for female incontinence pathology, is that the incontinence is not induced. Instead, a model is used in which the pathology is caused by the mechanical stress of many births and age-related factors such as the loss of tissue elasticity and muscle strength. Multipari goats used in one study are an example of this model [138,148].

Determining incontinence in animals also faces some difficulties compared to humans. The assessment in humans often relies on subjective reports like questionnaires or on pad tests. However, in animals, this type of assessment is not possible [53,136]. Therefore, other objective measurement methods have to be applied. These include the sneeze test, discharge monitoring, or urinary leak point pressure measurement [137,138]. Nevertheless, the

results of these methods are inconsistent and might not be entirely transferable to the human situation [53,136,138,144].

Overall, animal models, in general, provide a useful way to analyze cell therapy for SUI and improve the clinical management of SUI [53,137]. Although clinical studies are already being conducted, studies in animal models are still required to investigate the mechanisms of injury and, subsequently, the mechanisms of therapies [137]. Moreover, animals inherit opportunities to develop novel therapeutic strategies that are not yet approved by the authorities, even at the lowest levels. In this thesis, a differentiation is made between small and large animal models, both of which have advantages and disadvantages. The focus of this thesis is a porcine large animal model.

4.1 Large Animal Models

Large animal models present several advantages and disadvantages. They are preferred because standard surgery equipment and standardized established procedures, such as minimally invasive surgical techniques, including transurethral administration, can be used similarly to humans, facilitating the transferability of results [138]. This also allows the development of novel surgical instruments without adjustments [138]. The transferability of the received findings of small animal models might also be questionable [149]. Additionally, as described, the methods for determining incontinence display inconsistent and, therefore, unreliable results, especially in small animal models [138,144]. On the one hand, this inconsistency could be better managed in large animals leading to more reliable results [149,150]. On the other hand, inconsistencies in animal models require large cohorts to provide robust results, which is more difficult to achieve with large animals [138]. Husbandry and resulting costs may limit the cohort size in large animal studies [149]. Further challenges with these large animals arise regarding the availability of specific antibodies, specific other reagents, and information on gene sequences or expression levels [138]. Despite these technical disadvantages, several studies were performed using large animal models to investigate the cell therapy of SUI.

As mentioned, there are differences in the anatomy of the lower pelvic floor of four-legged animals compared to humans, including lower pressure on the urinary bladder and pelvic floor muscles [138]. Some studies addressed this problem by using nonhuman primates [140,141,146,147]. The incontinence model was established by pudendal nerve electrocauterization and transection, leading to durable incontinence for at least twelve

months. Decreased amounts of skeletal and smooth muscle and nerve responses were also reported [140]. Three studies used this model to investigate cell therapy for SUI, and all studies injected MPCs into the muscle layer of the external urethral sphincter [141,146,147]. The first study injected the cells six weeks after incontinence induction. Cell injections improved the maximal urethral pressure in the twelve months of follow-up. No significant difference compared to untreated continent controls could be detected after twelve months, demonstrating long-term efficacy. Histological analyses regarding the muscle content in the sphincter area supported these results [141]. The second study injected cells six months after incontinence induction to mimic chronic intrinsic urinary sphincter deficiency. The follow-up was six months after cell injections. However, the maximal urethral pressure and muscle content of animals with cell injections remained significantly different from untreated continent controls indicating a difference between the acute and chronic disease state [147]. This difference was addressed in the third study together with the investigation of local compared to systemic administration of cells. For the acute intrinsic urinary sphincter deficiency MPCs were injected six weeks after incontinence induction, whereas for chronic deficiency, they were injected after six months. The local injection of cells into the external urethral sphincter showed significantly higher maximal urethral pressures than systemic injections. Additionally, this study supported the concept that improvement is greater in acute deficiency than in chronic deficiency [146]. Overall, the experiments with nonhuman primates supported the promising outcomes of preclinical and clinical trials by injecting MPCs. Nevertheless, the use of nonhuman primates in preclinical trials is part of severe ethical concerns. Additionally, breeding and husbandry of nonhuman primates are challenging [138].

Animals with social affection, such as dogs and cats, are another option for large animal models [138]. Dogs are suitable as SUI animal models due to their similar sphincter muscle function. Moreover, the rate of tissue growth in dogs is relatively constant throughout adulthood. However, dogs are also quadrupeds which is why the anatomical differences to humans also apply [151]. In addition, animals with social affection are also part of ethical concerns [138]. This is the reason why only some studies investigated the potential use of these animals for SUI. One study in cats cut several pelvic floor nerves resulting in UI. The study showed that innervation of the external urethral sphincter ensures urinary continence [142]. Three other studies tried to establish an incontinence model in dogs using urethrolysis, pudendal denervation, or removal of a part of the external urethral

sphincter [139,144,145]. The last method effectively showed long-term sphincter deficiency determined by urodynamics [144]. It was the only incontinence animal model using social affection animals in a cell therapy study for SUI. MPCs were injected one month after incontinence induction into twelve dogs. After six months of follow-up, the urodynamic results showed that animals with injected MPCs recovered to 75% of normal while the control group stayed at 18%. A significant increase was observed after one month and remained significant over the entire follow-up period. Additionally, histological analyses revealed that injected cells were able to form new muscle fibers in the defective region. So overall, this study also supported the findings of MPCs injections in the SUI context [143]. One further study investigated the safety profile of injected MPCs dose-dependent in the same incontinence model of dogs [152]. The same dosage shown to be effective ($5*10^7$ cells/ml) in the reported study [143] and two additional dosages (half and twice the reported effective dose) were tested. After nine months of follow-up, it was reported that the cells did not produce any local or systemic pathologies, regardless of dosage. Furthermore, it was shown that the originally used dosage resulted in improved sphincter function while the others did not. However, the reasons for this dose dependence remain to be elucidated [152].

Due to the ethical concerns regarding nonhuman primates and animals with social affection, other large animals are gaining more focus. These include especially agricultural animals sheep, goats, and pigs [138]. The breeding and husbandry of these animals are, in contrast to nonhuman primates, simple and well-established, resulting in a larger cohort and, thus, greater statistical robustness [138]. Several studies were performed using pigs. The next chapter outlines these in more detail (Chapter 4.1.1). Furthermore, one study for cell therapy in the SUI context was conducted in multipari goats. Autologous bone marrow-MSCs, MPCs, and a combination of both cell types were injected transurethrally close to the external urethral sphincter. After twelve weeks of follow-up, the maximum urethral closure pressure and the functional area significantly increased only in the animals treated with the combined cell therapy. The individual types of cells injected alone showed a slight improvement which was not significant. Histological analyses revealed that both cell types were involved in forming striated muscles when injected precisely into the external urethral sphincter. However, MSCs displayed lower rates of striated muscle formation. Therefore, this study concluded that the combination of cell types might enhance functional improvement [148].

Overall, large animal models used to investigate cell therapy for SUI supported the findings of the small animal models. Further investigations in large animal models should be considered because of the more representative pathology and the better translation to the clinical situation of humans, including long-term assessment of function, clinical outcomes, and urodynamic measurements [149].

4.1.1 Pigs

Pigs belong to agricultural animals that can be used as large animal models [138]. The physiology, anatomy, and diet of pigs are comparable to humans [153,154]. The genome of pigs is closer to that of humans than that of mice [155]. Their similar body and organ size to humans facilitate translating results to the clinic. As described, all advantages and challenges of large animals also apply to pigs. Additionally, their short generation intervals, large litter sizes, and standardized breeding techniques are advantageous compared to other large animals [154]. In particular, it was reported that the dimensions and principal anatomy of the rhabdosphincter of pigs are comparable to those of humans [156,157]. Therefore, they are a useful animal model to investigate cell therapy for SUI [158].

Several available breeds offer the possibility of selecting the most suitable race for specific research purposes [153]. Female landrace or female Göttingen minipigs are often used [138]. However, it was demonstrated that urodynamic curves differ among race, age, weight, and breeder status (virgin or multipari) [138]. Therefore, these parameters have to be kept constant throughout one study. The advantage of Göttingen minipigs is that their weight increase over time is limited, making them an optimal large animal model for long-term studies [138]. However, incontinence models up to date were established in landrace pigs [150,159].

Small feasibility studies were conducted using pigs. Several studies investigated the potential of cell injections in healthy pigs [156,158,160]. One study used different doses of MPCs to inject them transurethrally into the external urethral sphincter and evaluated them three weeks after injections. Urodynamic values revealed that the measured pressures varied depending on the dose. High cell concentrations ($2.26–7.8*10^7$) injected increased pressure values by more than 300%, and mid-range cell concentrations ($5.69–16*10^6$) increased the values by about 150%. However, low cell concentrations ($1.5–4.2*10^6$) resulted in decreased pressure values after injection. In histological analyses, the dose dependency was supported. The formation of new muscle fibers increased with increasing

cell numbers [156]. Another study also used MPCs to inject them into the middle of the urethra. About $6*10^7$ cells were injected, which is among the high cell concentrations of the previously reported one. In contrast to this previously reported study, no significant improvement could be detected in the maximal urethral closure pressure after four weeks compared to the control group. Moreover, it was observed that only cells injected into the muscle layer integrated with muscle fibers. Cells injected into the submucosa, lacked myogenic differentiation [158]. Another study investigated the possible appearance of unspecific bulking effects after cell injections. After injection of four times 250 µl aliquots, no bulking effect was recorded in a follow-up of twelve months [160]. Overall, despite inconclusive results regarding the effectiveness of cell injections, these studies showed that injecting cells transurethrally into the urethra of pigs is feasible [156,158,160].

Therefore, three further studies aimed to produce an incontinence model in pigs. One study used large white pigs[157], and the two other studies used landrace pigs [150,159]. Incontinence induction methods included electrocautery, urethral dilatation, or a combination of both [150,157,159]. The study using five large white pigs induced incontinence only by distal electrocautery. The maximum urethral closure pressure and the area under the curve were still significantly reduced one month after electrocautery, whereas the functional length of the urethra showed no significant changes. Interrupted sphincteric myofibers were also detected at the suspected electrocautery site [157]. One of the studies using landrace pigs used balloon dilatation to injure the sphincter by distension of the urethra. The balloon was inflated with 40 ml, held in the urethra for five minutes, and slowly pulled out of the urethra without draining the fluid. The area under the curve also displayed a significant reduction in this model one month after treatment. However, the maximum urethral closure pressure showed no significance. Instead, the functional urethral length decreased significantly. In contrast to the incontinence model induced by electrocautery, histological analyses revealed no interruption of the muscular layer but a significant increase in connective tissue [150]. One feasibility study was conducted to determine the optimal method of incontinence induction in landrace pigs. Proximal four-fold electrocautery, balloon dilatation (inflated to 20 ml), and a combination of distal four-fold electrocautery and balloon dilatation (inflated to 20 ml) were compared. All methods led to decreased maximum urethral closure pressures and area under the curves directly after treatment. However, the animals treated with balloon dilatation or electrocautery recovered after three

weeks. Only the animals treated with the combination remained below their baseline levels of maximum urethral closure pressure and area under the curve [159].

In conclusion, these studies provided different methods of incontinence induction. Urethral distention by balloon dilatation is intended to mimic vaginal delivery, whereas electrocautery mimics direct injury to the urethral sphincter as may occur during prostatectomy [136,159]. The recovery observed in the last reported study for incontinence induction by electrocautery or balloon dilatation alone could be due to differing procedures, i.e., balloon inflation or site of electrocautery [159]. Overall, the feasibility of cell injections into the porcine urethra and the possible incontinence models in pigs should be further investigated and combined in a cell therapy study.

5. Surgical Procedures

5.1 Urodynamics

Urodynamics involves measurements to assess the function and dysfunction of the lower urinary tract by physiological parameters [12,13,161]. Several tests are grouped under this term, including uroflowmetry, post void residual cystometry, pressure-flow studies, electromyography, and urethra pressure profiles [12,13]. This thesis focuses on the urethra pressure profile that measures the urethral pressure along the urethral length [162,163]. Urethral pressure profiles are the only urodynamic examination that provides quantitative information about the urethral closure mechanism [163]. In humans, measurements can be differentiated between at rest or during coughing and straining [162,163]. However, only the measurement at rest under anesthesia is manageable for animals, especially for pigs, because patient compliance is required for the stress profile [163].

Urodynamic measurements are performed with a catheter that is equipped with pressure sensors. This catheter is inserted into the urethra and bladder. During steady retraction, the pressure levels are recorded (Figure 6) [138]. The urethral pressure (Pura, Figure 6, red curve) and the bladder pressure (Pves, Figure 6, blue curve), also known as intravesical pressure, are measured simultaneously by two sensors. The urethral closure pressure (Pclo, Figure 6, green curve) is determined by subtracting urethral pressure minus vesical pressure [157,162]. The maximum urethral closure pressure, the functional urethral length, and the area under the curve (AUC) are often reported parameters (Figure 6) [13,163]. The maximum urethral closure pressure is the maximal difference between Pura and Pves [13,163]. It indicates the position of the highest density of mainly striated muscle fibers [138]. The functional urethral length corresponds to the length in which Pura exceeds Pves [13,163]. However, twitches might occur during measurements and must be excluded (Figure 6, twitches marked with *). The AUC is the calculated integral of the urethral pressure profile in a defined area (Figure 6, greenish shaded area with marked start and end lines) [138]. These measured and calculated parameters indicate urethral closure pressures and resulting continence or incontinence [163].

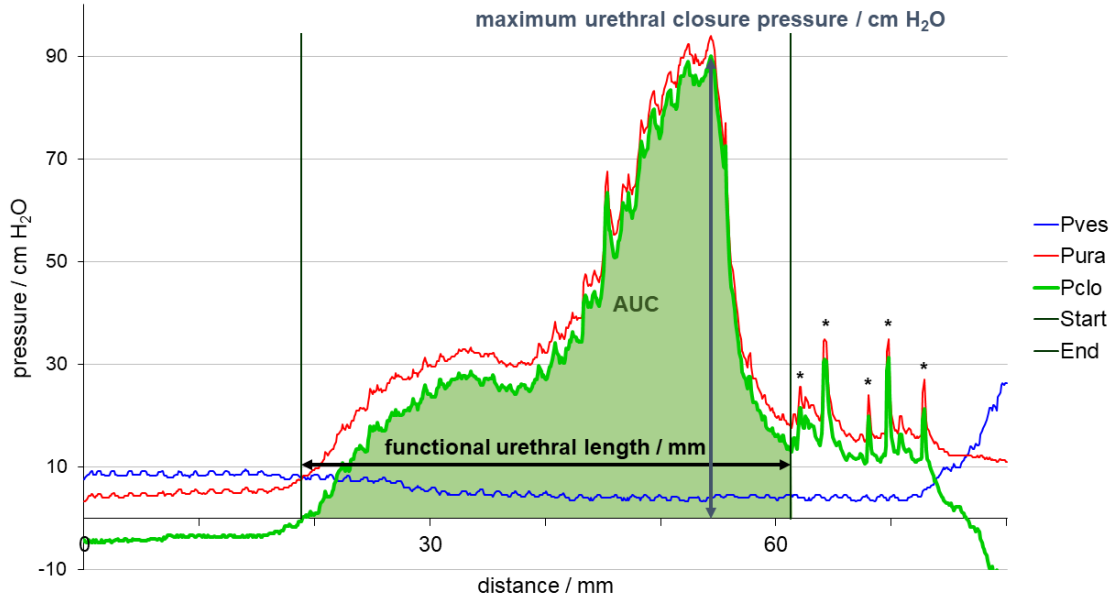

Figure 6: Urodynamic urethral pressure profile of porcine urethral sphincter. The urethral pressure profile was measured with two different sensors. The intravesical (Pves, blue) and the urethral (Pura, red) pressure were determined, and the urethral closure pressure (Pclo, green) was calculated (Pura-Pves). Twitching of the pig during measurement were marked with stars (*) and excluded from the functional urethral length. The functional urethral length in mm describes the length during which Pura exceeds Pves. The maximum urethral closure pressure is the highest point measure of Pclo in cm H_2O. The area under the curve (AUC, greenish shaded) is the calculated integral of the curve of Pclo between two distinct start and end lines corresponding to the functional urethral length.

Urodynamics, including the urethral pressure profile in humans, are still under debate regarding their clinical utility and reliability. However, their importance for scientific purposes is unquestionable [162,163]. Moreover, to address these problems, an alternative high-definition prototype for measuring urethral pressure profiles was established in several studies to provide better accuracy and sensitivity [164-167]. This prototype was already used with promising results in two studies with minipigs and landrace pigs compared to the standard technique [159,160]. It was also used to provide further data for the development compared to the standard technique in one of the presented studies (Publication 4).

5.2 Application of Cells via Needle Compared to Waterjet

Needle injections are currently state-of-the-art [168]. They provide the possibility for minimally invasive injections, either transurethral or periurethral [169]. The Williams cystoscopic injection needle is the most commonly used needle for placing bulking materials outside of the urethra. It has also been used for cell therapy studies and injections in the urethra of patients suffering from SUI [121,170]. Therefore, needle injections were also used in large animal studies investigating cell therapy in SUI [148,158,160]. These studies

reported that precise injection of the cells into the muscular layer, especially for MPCs, is crucial because these cells do not differentiate if injected into the submucosa [158]. One study optimized the injection depth by shortening the length of the needle tip. They showed that a shorter needle tip of about five millimeters leads to more injections of cells closer to the muscular layer [160]. However, in this study and another, the reported accuracy of cell injections into the muscular layer was less than 20% [160,171]. Even a well-trained surgeon is not expected to produce more reliable results due to the movement of the urethra during injection resulting in differing injection angles for each injection [171]. Neither periurethral nor transurethral injection provides improved accuracy [171]. The only improvement regarding precision was achieved by ultrasound-guided injections [169]. However, even with this application method, it is unclear if the injected needle fully penetrates the urethra or if it is placed correctly to deliver the cells to the muscular layer [168]. This low accuracy could be the reason for poor therapy effects after cell injections, especially with MPCs [168,171]. Moreover, needle injections can contribute to this poor efficiency, as cells can leak out after the needle is withdrawn from the injection site through the injection channel or due to possible bleeding [171]. Therefore, a novel approach using waterjet technology is currently under investigation [168].

Waterjet techniques have been used for surgical resections in various medical fields, such as orthopedics, neurology, gastroenterology, dermatology, and urology [172,173]. Advantages of this technology include the selective dissection and cutting parameters that can be applied to specific tissues leading to lower bleeding and leakage likelihood [172]. The waterjet is also able to elevate tissue layers by injecting fluid between the mucosa and submucosa to facilitate submucosal dissection [173]. It was hypothesized that instead of fluids, cells could be injected into specific depths of tissues [173]. The company Erbe Elektromedizin GmbH produced a prototype of a waterjet that is able to inject cells. This prototype is based on the ERBEJET®2 [168,172,173]. It generates pressures within a range from E5 to E80 – an equivalent of 5–80 bar – with the ability to quickly switch between different pressure levels for tissue penetration and cell injection. Depending on the tissue, these pressures can be adjusted. In contrast to needle injections, the waterjet nozzle does not penetrate the tissue directly. It uses fluid only under higher pressures to create small channels. In a following low pressure phase, the cells get gently injected. This two-phase application is preprogrammed, so that it provides simple handling for the surgeon [168].

In a first feasibility study, human MSCs were injected into cadaveric porcine samples with the waterjet device compared to needle injections. This study showed that the injections with waterjet were more precise and faster. Cell viability was not compromised [173]. A second study investigated the new application method by application of porcine ADSCs into the urethra of living pigs. This experiment supported the findings of the cadaveric injections. Waterjet injections were faster, more precise, and the handling was quite simple. Additionally, no leakage of cell suspension after injection was observed for waterjet injections [168]. However, further data are needed to establish the waterjet as a novel cell application method.

6. Aim of this Thesis

Urinary incontinence (UI) is mainly reported to have a prevalence of 25–45%, with stress urinary incontinence (SUI) being the most common form [17,27]. Due to the aging population, the importance of UI will increase in the future [17]. One of the leading underlying causes of SUI is intrinsic urinary sphincter deficiency [10,20]. However, current treatment options for patients suffering from SUI only aim to improve patients' quality of life, primarily with conservative treatments [18,20]. If these treatments fail, only surgical options remain, which are associated with several noticeable health risks. Additionally, the results are often not satisfactory [10,18,40,49,50]. These therapies also do not address the underlying cause, the weakened sphincter muscle function. Therefore, minimally invasive therapies that treat the underlying cause are being sought [51]. Thus, the option of cell therapy emerged, which offers the possibility of treating the leading cause of SUI [52]. As reported, various preclinical and clinical studies were conducted using MSCs or MPCs.

Preliminary data in the group of Prof. Dr. Aicher established an incontinence model in landrace pigs. It was shown that the combination of urethral dilatation and electrocautery resulted in significant urethral sphincter deficiency. However, the follow-up was only three weeks [159]. In addition, due to the frequent misplacement of cells via needle injections under visual control [160,171], preliminary data were gained on the functional, precise injection of cells using waterjet technology [168,172,173]. Nevertheless, only one study using ADSCs was performed in vivo in healthy pigs [168], so further data were required to prove the functional concept of this novel cell injection technology.

The overall aim of this thesis was to contribute to the knowledge about the clinical situation of SUI and to help improve the situation of the patients. Therefore, preclinical studies were performed regarding the promising treatment of cell therapy since the available data are still insufficient. This thesis addresses the following three main aspects.

The first objective was to further analyze the novel technology of waterjet injection to be used for cell delivery. To achieve this aim, two different attempts were carried out. On the one hand, the properties of ADSCs after injection with the waterjet compared to needle injections into fluids and porcine cadaveric tissue were tested. The observed properties included cell viability, cell surface markers, differentiation ability, attachment capabilities, and biomechanical features. On the other hand, the possibility of injecting viable muscle-derived cells into cadaveric and living animals using the waterjet device was

observed. The integrity and distribution of cells in the tissues were analyzed and compared to needle injections.

The second objective was to validate the established incontinence model in the large animal model using landrace pigs. Additionally, the possible transfer of this model to Göttingen minipigs was investigated due to their limited growth and, thus, easier handling for long-term follow-ups. Furthermore, this study aimed to extend the follow-up period of only three weeks.

The third objective was to comparatively investigate the potential of transurethrally injected MPCS and ADSCs to improve sphincter function in a clinically relevant large animal model of sphincter insufficiency. Cell characterizations and improvement of MPC production were established and performed. Urethral pressure profilometry served as a measurement technique to assess the regeneration of the urethral sphincter deficiency. Additionally, in vivo fluorimetry was used to determine the localization of the cell throughout the follow-up period. Histochemistry, immunofluorescence, and detection of male DNA were used to observe the effects on the tissue.

Overall, the results of the thesis provided experimental evidence that the novel technology of waterjet injection is a suitable, rapid injection procedure for viable cells. Furthermore, the incontinence model in landrace pigs was validated for up to five weeks of follow-up. However, the transfer to Göttingen minipigs was not successful. In the comparison of the regenerative potential of ADSCs versus MPCs, ADSC injections in the incontinent pig led to full recovery. MPC injections also improved the urethral closure pressure compared to controls, but the enhancement was not significant.

7. List of Figures

8. List of Tables

9. References

1 Hickling, D. R., Sun, T. T. & Wu, X. R. Anatomy and Physiology of the Urinary Tract: Relation to Host Defense and Microbial Infection. *Microbiol Spectr* **3** (2015). https://doi.org:10.1128/microbiolspec.UTI-0016-2012

2 Schünke, M. & Schünke, G. in *Der Körper des Menschen* (eds Michael Schünke & Adolf Faller) (Georg Thieme Verlag KG, 2020).

3 Kohler, T. S., Yadven, M., Manvar, A., Liu, N. & Monga, M. The length of the male urethra. *Int Braz J Urol* **34**, 451-454; discussion 455-456 (2008). https://doi.org:10.1590/s1677-55382008000400007

4 Pomian, A. *et al.* Demographic features of female urethra length. *Neurourol Urodyn* **37**, 1751-1756 (2018). https://doi.org:10.1002/nau.23509

5 Jung, J., Ahn, H. K. & Huh, Y. Clinical and functional anatomy of the urethral sphincter. *Int Neurourol J* **16**, 102-106 (2012). https://doi.org:10.5213/inj.2012.16.3.102

6 Fry, C. H. *et al.* Animal models and their use in understanding lower urinary tract dysfunction. *Neurourology and Urodynamics* **29**, 603-608 (2010). https://doi.org:https://doi.org/10.1002/nau.20903

7 Norton, P. & Brubaker, L. Urinary incontinence in women. *The Lancet* **367**, 57-67 (2006). https://doi.org:https://doi.org/10.1016/S0140-6736(06)67925-7

8 Wallner, C., Dabhoiwala, N. F., DeRuiter, M. C. & Lamers, W. H. The Anatomical Components of Urinary Continence. *European Urology* **55**, 932-944 (2009). https://doi.org:https://doi.org/10.1016/j.eururo.2008.08.032

9 DeLancey, J. O. L. Structural support of the urethra as it relates to stress urinary incontinence: The hammock hypothesis. *American Journal of Obstetrics and Gynecology* **170**, 1713-1723 (1994). https://doi.org:https://doi.org/10.1016/S0002-9378(94)70346-9

10 Aoki, Y. *et al.* Urinary incontinence in women. *Nat Rev Dis Primers* **3**, 17042 (2017). https://doi.org:10.1038/nrdp.2017.42

11 Schmidt, R. F., Lang, F. & Heckmann, M. *Physiologie des Menschen: mit Pathophysiologie*. 31., überarbeitete und aktualisierte Auflage edn, (Springer, 2010).

12 D'Ancona, C. *et al.* The International Continence Society (ICS) report on the terminology for adult male lower urinary tract and pelvic floor symptoms and dysfunction. *Neurourology and Urodynamics* **38**, 433-477 (2019). https://doi.org:https://doi.org/10.1002/nau.23897

13 Haylen, B. T. *et al.* An International Urogynecological Association (IUGA)/International Continence Society (ICS) joint report on the terminology for female pelvic floor dysfunction. *Int Urogynecol J* **21**, 5-26 (2010). https://doi.org:10.1007/s00192-009-0976-9

14 Melville, J. L., Fan, M.-Y., Rau, H., Nygaard, I. E. & Katon, W. J. Major depression and urinary incontinence in women: temporal associations in an epidemiologic sample. *American Journal of Obstetrics and Gynecology* **201**, 490.e491-490.e497 (2009). https://doi.org:https://doi.org/10.1016/j.ajog.2009.05.047

15 Pizzol, D. *et al.* Urinary incontinence and quality of life: a systematic review and meta-analysis. *Aging Clin Exp Res* **33**, 25-35 (2021). https://doi.org:10.1007/s40520-020-01712-y

16 Nitti, V. W. The prevalence of urinary incontinence. *Rev Urol* **3 Suppl 1**, S2-6 (2001).
17 Milsom, I. & Gyhagen, M. The prevalence of urinary incontinence. *Climacteric* **22**, 217-222 (2019). https://doi.org:10.1080/13697137.2018.1543263
18 Abrams, P., Cardozo, L., Wagg, A. & Wein, A. *Incontinence 6th Edition*. (ICI-ICS. International Continence Society 2017).
19 Wilson, L., Brown, J. S., Shin, G. P., Luc, K.-O. & Subak, L. L. Annual direct cost of urinary incontinence. *Obstetrics & Gynecology* **98**, 398-406 (2001). https://doi.org:https://doi.org/10.1016/S0029-7844(01)01464-8
20 Irwin, G. M. Urinary Incontinence. *Primary Care: Clinics in Office Practice* **46**, 233-242 (2019). https://doi.org:https://doi.org/10.1016/j.pop.2019.02.004
21 Hunskaar, S., Lose, G., Sykes, D. & Voss, S. The prevalence of urinary incontinence in women in four European countries. *BJU International* **93**, 324-330 (2004). https://doi.org:https://doi.org/10.1111/j.1464-410X.2003.04609.x
22 Shamliyan, T. A., Wyman, J. F., Ping, R., Wilt, T. J. & Kane, R. L. Male urinary incontinence: prevalence, risk factors, and preventive interventions. *Rev Urol* **11**, 145-165 (2009).
23 Diokno, A. C., Estanol, M. V. C., Ibrahim, I. A. & Balasubramaniam, M. Prevalence of urinary incontinence in community dwelling men: a cross sectional nationwide epidemiological survey. *International Urology and Nephrology* **39**, 129-136 (2007). https://doi.org:10.1007/s11255-006-9127-0
24 Foldspang, A., Hvidman, L., Mommsen, S. & Nielsen, J. B. Risk of postpartum urinary incontinence associated with pregnancy and mode of delivery. *Acta Obstetricia et Gynecologica Scandinavica* **83**, 923-927 (2004). https://doi.org:10.1080/j.0001-6349.2004.00353.x
25 Adolfsson, J., Helgason, Á. R., Dickman, P. & Steineck, G. Urinary and Bowel Symptoms in Men with and without Prostate Cancer: Results from an Observational Study in the Stockholm Area. *European Urology* **33**, 11-16 (1998). https://doi.org:10.1159/000019528
26 Wu, J. M., Hundley, A. F., Fulton, R. G. & Myers, E. R. Forecasting the prevalence of pelvic floor disorders in U.S. Women: 2010 to 2050. *Obstet Gynecol* **114**, 1278-1283 (2009). https://doi.org:10.1097/AOG.0b013e3181c2ce96
27 Falah-Hassani, K., Reeves, J., Shiri, R., Hickling, D. & McLean, L. The pathophysiology of stress urinary incontinence: a systematic review and meta-analysis. *Int Urogynecol J* **32**, 501-552 (2021). https://doi.org:10.1007/s00192-020-04622-9
28 Minassian, V. A., Drutz, H. P. & Al-Badr, A. Urinary incontinence as a worldwide problem. *International Journal of Gynecology & Obstetrics* **82**, 327-338 (2003). https://doi.org:https://doi.org/10.1016/S0020-7292(03)00220-0
29 DeLancey, J. O. L. *et al.* Stress urinary incontinence: relative importance of urethral support and urethral closure pressure. *The Journal of urology* **179**, 2286-2290; discussion 2290 (2008). https://doi.org:10.1016/j.juro.2008.01.098
30 Strasser, H. *et al.* Age dependent apoptosis and loss of rhabdosphincter cells. *Journal of Urology* **164**, 1781-1785 (2000). https://doi.org:doi:10.1016/S0022-5347(05)67106-6
31 Subak, L. L. *et al.* Weight Loss to Treat Urinary Incontinence in Overweight and Obese Women. *New England Journal of Medicine* **360**, 481-490 (2009). https://doi.org:10.1056/NEJMoa0806375
32 Fonti, Y., Giordano, R., Cacciatore, A., Romano, M. & La Rosa, B. Post partum pelvic floor changes. *J Prenat Med* **3**, 57-59 (2009).

33 Sangsawang, B. & Sangsawang, N. Stress urinary incontinence in pregnant women: a review of prevalence, pathophysiology, and treatment. *Int Urogynecol J* **24**, 901-912 (2013). https://doi.org:10.1007/s00192-013-2061-7

34 Parsons, B. A., Evans, S. & Wright, M. P. Prostate cancer and urinary incontinence. *Maturitas* **63**, 323-328 (2009). https://doi.org:https://doi.org/10.1016/j.maturitas.2009.06.005

35 Hoyland, K., Vasdev, N., Abrof, A. & Boustead, G. Post-radical prostatectomy incontinence: etiology and prevention. *Rev Urol* **16**, 181-188 (2014).

36 Rehder, P. *et al.* Hypothesis That Urethral Bulb (Corpus Spongiosum) Plays an Active Role in Male Urinary Continence. *Advances in Urology* **2016**, 6054730 (2016). https://doi.org:10.1155/2016/6054730

37 Fonda, D. & Abrams, P. Cure sometimes, help always—a "continence paradigm" for all ages and conditions. *Neurourology and Urodynamics* **25**, 290-292 (2006). https://doi.org:https://doi.org/10.1002/nau.20187

38 Dumoulin, C., Hay-Smith, J., Habée-Séguin, G. M. & Mercier, J. Pelvic floor muscle training versus no treatment, or inactive control treatments, for urinary incontinence in women: A short version Cochrane systematic review with meta-analysis. *Neurourology and Urodynamics* **34**, 300-308 (2015). https://doi.org:https://doi.org/10.1002/nau.22700

39 Bø, K. Pelvic floor muscle training is effective in treatment of female stress urinary incontinence, but how does it work? *International Urogynecology Journal* **15**, 76-84 (2004). https://doi.org:10.1007/s00192-004-1125-0

40 de Vries, A. M. & Heesakkers, J. Contemporary diagnostics and treatment options for female stress urinary incontinence. *Asian J Urol* **5**, 141-148 (2018). https://doi.org:10.1016/j.ajur.2017.09.001

41 Richter, H. E. *et al.* Continence Pessary Compared With Behavioral Therapy or Combined Therapy for Stress Incontinence: A Randomized Controlled Trial. *Obstetrics & Gynecology* **115** (2010).

42 Peters, K. M. *et al.* Autologous muscle derived cells for treatment of stress urinary incontinence in women. *J Urol* **192**, 469-476 (2014). https://doi.org:10.1016/j.juro.2014.02.047

43 de Vries, A. M., van Breda, H. M. K., Fernandes, J. G., Venema, P. L. & Heesakkers, J. P. F. A. Para-Urethral Injections with Urolastic® for Treatment of Female Stress Urinary Incontinence: Subjective Improvement and Safety. *Urologia Internationalis* **99**, 91-97 (2017). https://doi.org:10.1159/000452450

44 Karim, N. B., Lo, T.-S., Nawawi, E. A. b. & Wu, P.-Y. Review on midurethral sling procedures for stress urinary incontinence. *Gynecology and Minimally Invasive Therapy* **4**, 33-36 (2015). https://doi.org:https://doi.org/10.1016/j.gmit.2015.04.003

45 Veit-Rubin, N. *et al.* Burch colposuspension. *Neurourology and Urodynamics* **38**, 553-562 (2019). https://doi.org:https://doi.org/10.1002/nau.23905

46 Lapitan, M. C. M. & Cody, J. D. Open retropubic colposuspension for urinary incontinence in women. *Cochrane Database of Systematic Reviews* (2012). https://doi.org:10.1002/14651858.CD002912.pub5

47 Ford, A. A., Rogerson, L., Cody, J. D., Aluko, P. & Ogah, J. A. Mid-urethral sling operations for stress urinary incontinence in women. *Cochrane Database of Systematic Reviews* (2017). https://doi.org:10.1002/14651858.CD006375.pub4

48 Léon, P. *et al.* Long-term functional outcomes after artificial urinary sphincter implantation in men with stress urinary incontinence. *BJU International* **115**, 951-957 (2015). https://doi.org:https://doi.org/10.1111/bju.12848

49 Aragón, I. M., Imbroda, B. H. & Lara, M. F. Cell Therapy Clinical Trials for Stress Urinary Incontinence: Current Status and Perspectives. *Int J Med Sci* **15**, 195-204 (2018). https://doi.org:10.7150/ijms.22130

50 Vilsbøll, A. W. *et al.* Cell-based therapy for the treatment of female stress urinary incontinence: an early cost–effectiveness analysis. *Regenerative Medicine* **13**, 321-330 (2018). https://doi.org:10.2217/rme-2017-0124

51 Zhou, S. *et al.* Stem Cell Therapy for Treatment of Stress Urinary Incontinence: The Current Status and Challenges. *Stem Cells Int* **2016**, 7060975 (2016). https://doi.org:10.1155/2016/7060975

52 Hart, M. L., Izeta, A., Herrera-Imbroda, B., Amend, B. & Brinchmann, J. E. Cell Therapy for Stress Urinary Incontinence. *Tissue Engineering Part B: Reviews* **21**, 365-376 (2015). https://doi.org:10.1089/ten.teb.2014.0627

53 Shan, S., Li, Q., Criswell, T., Atala, A. & Zhang, Y. Stem cell therapy combined with controlled release of growth factors for the treatment of sphincter dysfunction. *Cell & Bioscience* **13**, 56 (2023). https://doi.org:10.1186/s13578-023-01009-3

54 Keller, G. Embryonic stem cell differentiation: emergence of a new era in biology and medicine. *Genes Dev* **19**, 1129-1155 (2005). https://doi.org:10.1101/gad.1303605

55 Deb, K. D. & Sarda, K. Human embryonic stem cells: preclinical perspectives. *Journal of Translational Medicine* **6**, 7 (2008). https://doi.org:10.1186/1479-5876-6-7

56 Engels, E.-M. Human embryonic stem cells — the German debate. *Nature Reviews Genetics* **3**, 636-641 (2002). https://doi.org:10.1038/nrg871

57 Dulak, J., Szade, K., Szade, A., Nowak, W. & Józkowicz, A. Adult stem cells: hopes and hypes of regenerative medicine. *Acta Biochim Pol* **62**, 329-337 (2015). https://doi.org:10.18388/abp.2015_1023

58 Tran, C. & Damaser, M. S. The potential role of stem cells in the treatment of urinary incontinence. *Ther Adv Urol* **7**, 22-40 (2015). https://doi.org:10.1177/1756287214553968

59 Vaegler, M. *et al.* Stem cell therapy for voiding and erectile dysfunction. *Nat Rev Urol* **9**, 435-447 (2012). https://doi.org:10.1038/nrurol.2012.111

60 Fan, M. *et al.* The effect of age on the efficacy of human mesenchymal stem cell transplantation after a myocardial infarction. *Rejuvenation Res* **13**, 429-438 (2010). https://doi.org:10.1089/rej.2009.0986

61 Barakat, B. *et al.* Stem cell applications in regenerative medicine for stress urinary incontinence: A review of effectiveness based on clinical trials. *Arab Journal of Urology* **18**, 194-205 (2020). https://doi.org:10.1080/2090598X.2020.1750864

62 Herberts, C. A., Kwa, M. S. & Hermsen, H. P. Risk factors in the development of stem cell therapy. *J Transl Med* **9**, 29 (2011). https://doi.org:10.1186/1479-5876-9-29

63 Dvorak, C. C. *et al.* Safety of hematopoietic stem cell transplantation in children less than three years of age. *Pediatr Hematol Oncol* **25**, 705-722 (2008). https://doi.org:10.1080/08880010802243524

64 Lalu, M. M. *et al.* Safety and Efficacy of Adult Stem Cell Therapy for Acute Myocardial Infarction and Ischemic Heart Failure (SafeCell Heart): A Systematic Review and Meta-Analysis. *Stem Cells Transl Med* **7**, 857-866 (2018). https://doi.org:10.1002/sctm.18-0120

65 Prasad, V. K. *et al.* Efficacy and safety of ex vivo cultured adult human mesenchymal stem cells (Prochymal™) in pediatric patients with severe refractory

acute graft-versus-host disease in a compassionate use study. *Biol Blood Marrow Transplant* **17**, 534-541 (2011). https://doi.org:10.1016/j.bbmt.2010.04.014

66 Sotiropulos, K., Kourkoutas, D., Almaliotis, D., Ploumidou, K. & Karampatakis, V. Ocular stem cells: a narrative review of current clinical trials. *Int J Ophthalmol* **15**, 1529-1537 (2022). https://doi.org:10.18240/ijo.2022.09.17

67 Roche, R., Festy, F. & Fritel, X. Stem cells for stress urinary incontinence: the adipose promise. *Journal of Cellular and Molecular Medicine* **14**, 135-142 (2010). https://doi.org:https://doi.org/10.1111/j.1582-4934.2009.00915.x

68 Klein, G. *et al.* Mesenchymal stromal cells for sphincter regeneration. *Advanced Drug Delivery Reviews* **82-83**, 123-136 (2015). https://doi.org:https://doi.org/10.1016/j.addr.2014.10.026

69 Hart, M. L. *et al.* Cell-Based Therapy for the Deficient Urinary Sphincter. *Current Urology Reports* **14**, 476-487 (2013). https://doi.org:10.1007/s11934-013-0352-7

70 Alarcin, E. *et al.* Current Strategies for the Regeneration of Skeletal Muscle Tissue. *Int J Mol Sci* **22** (2021). https://doi.org:10.3390/ijms22115929

71 Staack, A. & Rodríguez, L. V. Stem cells for the treatment of urinary incontinence. *Curr Urol Rep* **12**, 41-46 (2011). https://doi.org:10.1007/s11934-010-0155-z

72 Dominici, M. *et al.* Minimal criteria for defining multipotent mesenchymal stromal cells. The International Society for Cellular Therapy position statement. *Cytotherapy* **8**, 315-317 (2006). https://doi.org:10.1080/14653240600855905

73 Bianco, P. *et al.* The meaning, the sense and the significance: translating the science of mesenchymal stem cells into medicine. *Nat Med* **19**, 35-42 (2013). https://doi.org:10.1038/nm.3028

74 Spees, J. L., Lee, R. H. & Gregory, C. A. Mechanisms of mesenchymal stem/stromal cell function. *Stem Cell Research & Therapy* **7**, 125 (2016). https://doi.org:10.1186/s13287-016-0363-7

75 Caplan, A. I. Mesenchymal Stem Cells: Time to Change the Name! *Stem Cells Transl Med* **6**, 1445-1451 (2017). https://doi.org:10.1002/sctm.17-0051

76 Aicher, W. K. *et al.* Towards a Treatment of Stress Urinary Incontinence: Application of Mesenchymal Stromal Cells for Regeneration of the Sphincter Muscle. *J Clin Med* **3**, 197-215 (2014). https://doi.org:10.3390/jcm3010197

77 Kinebuchi, Y. *et al.* Autologous bone-marrow-derived mesenchymal stem cell transplantation into injured rat urethral sphincter. *International Journal of Urology* **17**, 359-368 (2010). https://doi.org:https://doi.org/10.1111/j.1442-2042.2010.02471.x

78 Ji, X. L., Ma, L., Zhou, W. H. & Xiong, M. Narrative review of stem cell therapy for ischemic brain injury. *Transl Pediatr* **10**, 435-445 (2021). https://doi.org:10.21037/tp-20-262

79 Smith, J. A. *et al.* Stem Cell Therapies for Progressive Multiple Sclerosis. *Frontiers in Cell and Developmental Biology* **9** (2021). https://doi.org:10.3389/fcell.2021.696434

80 Corcos, J. *et al.* Bone marrow mesenchymal stromal cell therapy for external urethral sphincter restoration in a rat model of stress urinary incontinence. *Neurourology and Urodynamics* **30**, 447-455 (2011). https://doi.org:https://doi.org/10.1002/nau.20998

81 Imamura, T. *et al.* Implantation of autologous bone-marrow-derived cells reconstructs functional urethral sphincters in rabbits. *Tissue Eng Part A* **17**, 1069-1081 (2011). https://doi.org:10.1089/ten.TEA.2010.0478

82 Janssen, K. *et al.* Multiple doses of stem cells maintain urethral function in a model of neuromuscular injury resulting in stress urinary incontinence. *American Journal*

of Physiology-Renal Physiology **317**, F1047-F1057 (2019). https://doi.org:10.1152/ajprenal.00173.2019

83 Deng, K. *et al.* Mesenchymal stem cells and their secretome partially restore nerve and urethral function in a dual muscle and nerve injury stress urinary incontinence model. *American Journal of Physiology-Renal Physiology* **308**, F92-F100 (2015). https://doi.org:10.1152/ajprenal.00510.2014

84 Kim, S. O. *et al.* Bone-Marrow-Derived Mesenchymal Stem Cell Transplantation Enhances Closing Pressure and Leak Point Pressure in a Female Urinary Incontinence Rat Model. *Urologia Internationalis* **86**, 110-116 (2011). https://doi.org:10.1159/000317322

85 Lin, G. *et al.* Treatment of stress urinary incontinence with adipose tissue-derived stem cells. *Cytotherapy* **12**, 88-95 (2010). https://doi.org:10.3109/14653240903350265

86 Yoshimura, K. *et al.* Cell-Assisted Lipotransfer for Cosmetic Breast Augmentation: Supportive Use of Adipose-Derived Stem/Stromal Cells. *Aesthetic Plastic Surgery* **44**, 1258-1265 (2020). https://doi.org:10.1007/s00266-020-01819-7

87 Rehman, J. *et al.* Secretion of Angiogenic and Antiapoptotic Factors by Human Adipose Stromal Cells. *Circulation* **109**, 1292-1298 (2004). https://doi.org:doi:10.1161/01.CIR.0000121425.42966.F1

88 Zuk, P. A. *et al.* Human Adipose Tissue Is a Source of Multipotent Stem Cells. *Molecular Biology of the Cell* **13**, 4279-4295 (2002). https://doi.org:10.1091/mbc.e02-02-0105

89 Li, G.-Y. *et al.* Activation of VEGF and ERK1/2 and Improvement of Urethral Function by Adipose-derived Stem Cells in a Rat Stress Urinary Incontinence Model. *Urology* **80**, 953.e951-953.e958 (2012). https://doi.org:https://doi.org/10.1016/j.urology.2012.05.030

90 Watanabe, T. *et al.* Increased urethral resistance by periurethral injection of low serum cultured adipose-derived mesenchymal stromal cells in rats. *International Journal of Urology* **18**, 659-666 (2011). https://doi.org:https://doi.org/10.1111/j.1442-2042.2011.02795.x

91 Wu, G., Song, Y., Zheng, X. & Jiang, Z. Adipose-derived stromal cell transplantation for treatment of stress urinary incontinence. *Tissue and Cell* **43**, 246-253 (2011). https://doi.org:https://doi.org/10.1016/j.tice.2011.04.003

92 Zhao, W. *et al.* Periurethral Injection of Autologous Adipose-Derived Stem Cells with Controlled-Release Nerve Growth Factor for the Treatment of Stress Urinary Incontinence in a Rat Model. *European Urology* **59**, 155-163 (2011). https://doi.org:https://doi.org/10.1016/j.eururo.2010.10.038

93 Shi, L. B. *et al.* Tissue engineered bulking agent with adipose-derived stem cells and silk fibroin microspheres for the treatment of intrinsic urethral sphincter deficiency. *Biomaterials* **35**, 1519-1530 (2014). https://doi.org:https://doi.org/10.1016/j.biomaterials.2013.11.025

94 Silwal Gautam, S. *et al.* Implantation of Autologous Adipose-Derived Cells Reconstructs Functional Urethral Sphincters in Rabbit Cryoinjured Urethra. *Tissue Engineering Part A* **20**, 1971-1979 (2014). https://doi.org:10.1089/ten.tea.2013.0491

95 Yamamoto, T. & Gotoh, M. Editorial comment to Regenerative medicine as a new therapeutic strategy for lower urinary tract dysfunction. *International Journal of Urology* **20**, 675-675 (2013). https://doi.org:https://doi.org/10.1111/iju.12173

96 Yamamoto, T. *et al.* Periurethral injection of autologous adipose-derived regenerative cells for the treatment of male stress urinary incontinence: Report of

three initial cases. *International Journal of Urology* **19**, 652-659 (2012). https://doi.org:https://doi.org/10.1111/j.1442-2042.2012.02999.x

97 Choi, J. Y., Kim, T. H., Yang, J. D., Suh, J. S. & Kwon, T. G. Adipose-Derived Regenerative Cell Injection Therapy for Postprostatectomy Incontinence: A Phase I Clinical Study. *Yonsei Med J* **57**, 1152-1158 (2016). https://doi.org:10.3349/ymj.2016.57.5.1152

98 Gotoh, M. *et al.* Regenerative treatment of male stress urinary incontinence by periurethral injection of autologous adipose-derived regenerative cells: 1-year outcomes in 11 patients. *International Journal of Urology* **21**, 294-300 (2014). https://doi.org:https://doi.org/10.1111/iju.12266

99 Gotoh, M. *et al.* Treatment of male stress urinary incontinence using autologous adipose-derived regenerative cells: Long-term efficacy and safety. *Int J Urol* **26**, 400-405 (2019). https://doi.org:10.1111/iju.13886

100 Garcia-Arranz, M. *et al.* Two phase I/II clinical trials for the treatment of urinary incontinence with autologous mesenchymal stem cells. *Stem Cells Translational Medicine* **9**, 1500-1508 (2020). https://doi.org:10.1002/sctm.19-0431

101 Arjmand, B. *et al.* Concomitant Transurethral and Transvaginal-Periurethral Injection of Autologous Adipose Derived Stem Cells for Treatment of Female Stress Urinary Incontinence: A Phase One Clinical Trial. *Acta Medica Iranica* **55** (2017).

102 Li, P.-C. & Ding, D.-C. Stem-cell therapy in stress urinary incontinence: A review. *Tzu Chi Medical Journal* **35** (2023).

103 Chen, J. C. & Goldhamer, D. J. Skeletal muscle stem cells. *Reprod Biol Endocrinol* **1**, 101 (2003). https://doi.org:10.1186/1477-7827-1-101

104 Yamamoto, M. *et al.* Loss of MyoD and Myf5 in Skeletal Muscle Stem Cells Results in Altered Myogenic Programming and Failed Regeneration. *Stem Cell Reports* **10**, 956-969 (2018). https://doi.org:https://doi.org/10.1016/j.stemcr.2018.01.027

105 Yin, H., Price, F. & Rudnicki, M. A. Satellite cells and the muscle stem cell niche. *Physiol Rev* **93**, 23-67 (2013). https://doi.org:10.1152/physrev.00043.2011

106 Isesele, P. O. & Mazurak, V. C. Regulation of Skeletal Muscle Satellite Cell Differentiation by Omega-3 Polyunsaturated Fatty Acids: A Critical Review. *Frontiers in Physiology* **12** (2021). https://doi.org:10.3389/fphys.2021.682091

107 Almeida, C. F., Fernandes, S. A., Ribeiro Junior, A. F., Keith Okamoto, O. & Vainzof, M. Muscle Satellite Cells: Exploring the Basic Biology to Rule Them. *Stem Cells Int* **2016**, 1078686 (2016). https://doi.org:10.1155/2016/1078686

108 Furuta, A., Carr, L. K., Yoshimura, N. & Chancellor, M. B. Advances in the understanding of sress urinary incontinence and the promise of stem-cell therapy. *Rev Urol* **9**, 106-112 (2007).

109 Yokoyama, T. *et al.* Persistence and survival of autologous muscle derived cells versus bovine collagen as potential treatment of stress urinary incontinence. *The Journal of Urology* **165**, 271-276 (2001). https://doi.org:https://doi.org/10.1097/00005392-200101000-00077

110 Peyromaure, M. *et al.* Fate of implanted syngenic muscle precursor cells in striated urethral sphincter of female rats: Perspectives for treatment of urinary incontinence. *Urology* **64**, 1037-1041 (2004). https://doi.org:https://doi.org/10.1016/j.urology.2004.06.058

111 Yiou, R., Dreyfus, P., Chopin, D. K., Abbou, C.-C. & Lefaucheur, J.-P. Muscle precursor cell autografting in a murine model of urethral sphincter injury. *BJU*

International **89**, 298-302 (2002). https://doi.org:https://doi.org/10.1046/j.1464-4096.2001.01618.x

112 Cannon, T. W. *et al.* Improved sphincter contractility after allogenic muscle-derived progenitor cell injection into the denervated rat urethra. *Urology* **62**, 958-963 (2003). https://doi.org:https://doi.org/10.1016/S0090-4295(03)00679-4

113 Yiou, R., Yoo, J. J. & Atala, A. Restoration of functional motor units in a rat model of sphincter injury by muscle precursor cell autografts1. *Transplantation* **76** (2003).

114 Kwon, D. *et al.* Periurethral cellular injection: Comparison of muscle-derived progenitor cells and fibroblasts with regard to efficacy and tissue contractility in an animal model of stress urinary incontinence. *Urology* **68**, 449-454 (2006). https://doi.org:https://doi.org/10.1016/j.urology.2006.03.040

115 Lee, J. Y. *et al.* The effects of periurethral muscle-derived stem cell injection on leak point pressure in a rat model of stress urinary incontinence. *International Urogynecology Journal* **14**, 31-37 (2003). https://doi.org:10.1007/s00192-002-1004-5

116 Lee, J. Y. *et al.* Long term effects of muscle-derived stem cells on leak point pressure and closing pressure in rats with transected pudendal nerves. *Mol Cells* **18**, 309-313 (2004).

117 Chermansky, C. J. *et al.* Intraurethral muscle-derived cell injections increase leak point pressure in a rat model of intrinsic sphincter deficiency. *Urology* **63**, 780-785 (2004). https://doi.org:https://doi.org/10.1016/j.urology.2003.10.035

118 Praud, C., Sebe, P., Biérinx, A. S. & Sebille, A. Improvement of urethral sphincter deficiency in female rats following autologous skeletal muscle myoblasts grafting. *Cell Transplant* **16**, 741-749 (2007). https://doi.org:10.3727/000000007783465118

119 Hoshi, A. *et al.* Reconstruction of Radical Prostatectomy-Induced Urethral Damage Using Skeletal Muscle-Derived Multipotent Stem Cells. *Transplantation* **85**, 1617-1624 (2008). https://doi.org:10.1097/TP.0b013e318170572b

120 Mitterberger, M. *et al.* Autologous myoblasts and fibroblasts for female stress incontinence: a 1-year follow-up in 123 patients. *BJU Int* **100**, 1081-1085 (2007). https://doi.org:10.1111/j.1464-410X.2007.07119.x

121 Carr, L. K. *et al.* 1-year follow-up of autologous muscle-derived stem cell injection pilot study to treat stress urinary incontinence. *International Urogynecology Journal* **19**, 881-883 (2008). https://doi.org:10.1007/s00192-007-0553-z

122 Sèbe, P. *et al.* Intrasphincteric injections of autologous muscular cells in women with refractory stress urinary incontinence: a prospective study. *International Urogynecology Journal* **22**, 183-189 (2011). https://doi.org:10.1007/s00192-010-1255-5

123 Cornu, J.-N., Lizée, D., Pinset, C. & Haab, F. Long-term Follow-up After Regenerative Therapy of the Urethral Sphincter for Female Stress Urinary Incontinence. *European Urology* **65**, 256-258 (2014). https://doi.org:https://doi.org/10.1016/j.eururo.2013.09.022

124 Blaganje, M. & Lukanović, A. Intrasphincteric autologous myoblast injections with electrical stimulation for stress urinary incontinence. *Int J Gynaecol Obstet* **117**, 164-167 (2012). https://doi.org:10.1016/j.ijgo.2011.11.029

125 Carr Lesley, K. *et al.* Autologous Muscle Derived Cell Therapy for Stress Urinary Incontinence: A Prospective, Dose Ranging Study. *Journal of Urology* **189**, 595-601 (2013). https://doi.org:10.1016/j.juro.2012.09.028

126 Gräs, S., Klarskov, N. & Lose, G. Intraurethral Injection of Autologous Minced Skeletal Muscle: A Simple Surgical Treatment for Stress Urinary Incontinence. *Journal of Urology* **192**, 850-855 (2014). https://doi.org:10.1016/j.juro.2014.04.005

127 Sharifiaghdas, F. *et al.* Effect of autologous muscle-derived cells in the treatment of urinary incontinence in female patients with intrinsic sphincter deficiency and epispadias: A prospective study. *Int J Urol* **23**, 581-586 (2016). https://doi.org:10.1111/iju.13097

128 Mitterberger, M. *et al.* Adult stem cell therapy of female stress urinary incontinence. *Eur Urol* **53**, 169-175 (2008). https://doi.org:10.1016/j.eururo.2007.07.026

129 Stangel-Wojcikiewicz, K. *et al.* Autologous muscle-derived cells for the treatment of female stress urinary incontinence: A 2-year follow-up of a polish investigation. *Neurourology and Urodynamics* **33**, 324-330 (2014). https://doi.org:https://doi.org/10.1002/nau.22404

130 Stangel-Wojcikiewicz, K., Piwowar, M., Jach, R., Majka, M. & Basta, A. Quality of life assessment in female patients 2 and 4 years after muscle-derived cell transplants for stress urinary incontinence treatment. *Ginekologia Polska* **87**, 183-189 (2016). https://doi.org:10.17772/gp/61330

131 Schmid, F. A. *et al.* Transurethral injection of autologous muscle precursor cells for treatment of female stress urinary incontinence: a prospective phase I clinical trial. *Int Urogynecol J* (2023). https://doi.org:10.1007/s00192-023-05514-4

132 Jankowski, R. J. *et al.* A double-blind, randomized, placebo-controlled clinical trial evaluating the safety and efficacy of autologous muscle derived cells in female subjects with stress urinary incontinence. *International Urology and Nephrology* **50**, 2153-2165 (2018). https://doi.org:10.1007/s11255-018-2005-8

133 Gerullis, H. *et al.* Muscle-derived cells for treatment of iatrogenic sphincter damage and urinary incontinence in men. *ScientificWorldJournal* **2012**, 898535 (2012). https://doi.org:10.1100/2012/898535

134 Mitterberger, M. *et al.* Myoblast and fibroblast therapy for post-prostatectomy urinary incontinence: 1-year followup of 63 patients. *J Urol* **179**, 226-231 (2008). https://doi.org:10.1016/j.juro.2007.08.154

135 Lecoeur, C. *et al.* Intraurethral transfer of satellite cells by myofiber implants results in the formation of innervated myotubes exerting tonic contractions. *J Urol* **178**, 332-337 (2007). https://doi.org:10.1016/j.juro.2007.02.044

136 Herrera-Imbroda, B., Lara, M. F., Izeta, A., Sievert, K.-D. & Hart, M. L. Stress urinary incontinence animal models as a tool to study cell-based regenerative therapies targeting the urethral sphincter. *Advanced Drug Delivery Reviews* **82-83**, 106-116 (2015). https://doi.org:https://doi.org/10.1016/j.addr.2014.10.018

137 Jiang, H. H. & Damaser, M. S. Animal models of stress urinary incontinence. *Handb Exp Pharmacol*, 45-67 (2011). https://doi.org:10.1007/978-3-642-16499-6_3

138 Amend, B., Harland, N., Knoll, J., Stenzl, A. & Aicher, W. K. Large Animal Models for Investigating Cell Therapies of Stress Urinary Incontinence. *Int J Mol Sci* **22** (2021). https://doi.org:10.3390/ijms22116092

139 Ali-El-Dein, B. & Ghoneim, M. A. Effects of selective autonomic and pudendal denervation on the urethral function and development of retention in female dogs. *J Urol* **166**, 1549-1554 (2001).

140 Badra, S., Andersson, K. E., Dean, A., Mourad, S. & Williams, J. K. A nonhuman primate model of stable urinary sphincter deficiency. *J Urol* **189**, 1967-1974 (2013). https://doi.org:10.1016/j.juro.2012.09.103

141 Badra, S., Andersson, K. E., Dean, A., Mourad, S. & Williams, J. K. Long-term structural and functional effects of autologous muscle precursor cell therapy in a

nonhuman primate model of urinary sphincter deficiency. *J Urol* **190**, 1938-1945 (2013). https://doi.org:10.1016/j.juro.2013.04.052

142 Bernabé, J. *et al.* Peripheral neural lesion-induced stress urinary incontinence in anaesthetized female cats. *BJU International* **102**, 1162-1167 (2008). https://doi.org:https://doi.org/10.1111/j.1464-410X.2008.07795.x

143 Eberli, D., Aboushwareb, T., Soker, S., Yoo, J. J. & Atala, A. Muscle Precursor Cells for the Restoration of Irreversibly Damaged Sphincter Function. *Cell Transplantation* **21**, 2089-2098 (2012). https://doi.org:10.3727/096368911x623835

144 Eberli, D., Andersson, K. E., Yoo, J. J. & Atala, A. A canine model of irreversible urethral sphincter insufficiency. *BJU Int* **103**, 248-253 (2009). https://doi.org:10.1111/j.1464-410X.2008.08001.x

145 Kato, H., Igawa, Y., Khaleque, M., Abdul & Nishizawa, O. Bladder dysfunction after proximal urethrolysis in female dogs. *International Journal of Urology* **6**, 33-37 (1999). https://doi.org:https://doi.org/10.1046/j.1442-2042.1999.06126.x

146 Williams, J. K. *et al.* Local versus intravenous injections of skeletal muscle precursor cells in nonhuman primates with acute or chronic intrinsic urinary sphincter deficiency. *Stem Cell Research & Therapy* **7**, 147 (2016). https://doi.org:10.1186/s13287-016-0411-3

147 Williams, J. K. *et al.* Cell versus Chemokine Therapy in a Nonhuman Primate Model of Chronic Intrinsic Urinary Sphincter Deficiency. *The Journal of Urology* **196**, 1809-1815 (2016). https://doi.org:https://doi.org/10.1016/j.juro.2016.05.106

148 Burdzinska, A. *et al.* Intraurethral co-transplantation of bone marrow mesenchymal stem cells and muscle-derived cells improves the urethral closure. *Stem Cell Research & Therapy* **9**, 239 (2018). https://doi.org:10.1186/s13287-018-0990-2

149 Williams, J. K., Dean, A., Badlani, G. & Andersson, K.-E. Regenerative Medicine Therapies for Stress Urinary Incontinence. *The Journal of Urology* **196**, 1619-1626 (2016). https://doi.org:https://doi.org/10.1016/j.juro.2016.05.136

150 Burdzińska, A. *et al.* Urethral distension as a novel method to simulate sphincter insufficiency in the porcine animal model. *International Journal of Urology* **19**, 676-682 (2012). https://doi.org:https://doi.org/10.1111/j.1442-2042.2012.02994.x

151 Stolzenburg, J.-U. *et al.* Histomorphology of canine urethral sphincter systems, including three-dimensional reconstruction and magnetic resonance imaging. *Urology* **67**, 624-630 (2006). https://doi.org:https://doi.org/10.1016/j.urology.2005.09.055

152 Williams, J. K. *et al.* The dose-effect safety profile of skeletal muscle precursor cell therapy in a dog model of intrinsic urinary sphincter deficiency. *Stem Cells Transl Med* **4**, 286-294 (2015). https://doi.org:10.5966/sctm.2014-0114

153 Bassols, A. *et al.* The pig as an animal model for human pathologies: A proteomics perspective. *PROTEOMICS – Clinical Applications* **8**, 715-731 (2014). https://doi.org:https://doi.org/10.1002/prca.201300099

154 Hou, N., Du, X. & Wu, S. Advances in pig models of human diseases. *Animal Models and Experimental Medicine* **5**, 141-152 (2022). https://doi.org:https://doi.org/10.1002/ame2.12223

155 Wernersson, R. *et al.* Pigs in sequence space: a 0.66X coverage pig genome survey based on shotgun sequencing. *BMC Genomics* **6**, 70 (2005). https://doi.org:10.1186/1471-2164-6-70

156 Mitterberger, M. *et al.* Functional and Histological Changes after Myoblast Injections in the Porcine Rhabdosphincter. *European Urology* **52**, 1736-1743 (2007). https://doi.org:https://doi.org/10.1016/j.eururo.2007.05.007

157 Zini, L. *et al.* The striated urethral sphincter of the pig shows morphological and functional characteristics essential for the evaluation of treatments for sphincter insufficiency. *J Urol* **176**, 2729-2735 (2006). https://doi.org:10.1016/j.juro.2006.07.135

158 Burdzińska, A. *et al.* The Effect of Endoscopic Administration of Autologous Porcine Muscle-derived Cells Into the Urethral Sphincter. *Urology* **82**, 743.e741-743.e748 (2013). https://doi.org:https://doi.org/10.1016/j.urology.2013.03.030

159 Kelp, A. *et al.* Establishing and monitoring of urethral sphincter deficiency in a large animal model. *World Journal of Urology* **35**, 1977-1986 (2017). https://doi.org:10.1007/s00345-017-2088-3

160 Amend, B. *et al.* Precise injection of human mesenchymal stromal cells in the urethral sphincter complex of Göttingen minipigs without unspecific bulking effects. *Neurourology and Urodynamics* **36**, 1723-1733 (2017). https://doi.org:https://doi.org/10.1002/nau.23182

161 Rosier, P. *et al.* International Continence Society Good Urodynamic Practices and Terms 2016: Urodynamics, uroflowmetry, cystometry, and pressure-flow study. *Neurourol Urodyn* **36**, 1243-1260 (2017). https://doi.org:10.1002/nau.23124

162 Lose, G. *et al.* Standardisation of urethral pressure measurement: Report from the standardisation sub-committee of the International Continence Society. *Neurourology and Urodynamics* **21**, 258-260 (2002). https://doi.org:https://doi.org/10.1002/nau.10051

163 Schumacher, S. & Heidler, H. in *Urodynamik* (eds Daniela Schultz-Lampel, Mark Goepel, & Axel Haferkamp) 115-122 (Springer Berlin Heidelberg, 2012).

164 Klünder, M. *et al.* Assessing the reproducibility of high definition urethral pressure profilometry and its correlation with an air-charged system. *Neurourology and Urodynamics* **36**, 1292-1300 (2017). https://doi.org:https://doi.org/10.1002/nau.23115

165 Klünder, M. *et al.* High definition urethral pressure profilometry: Evaluating a novel microtip catheter. *Neurourology and Urodynamics* **35**, 888-894 (2016). https://doi.org:https://doi.org/10.1002/nau.22835

166 Klünder, M. *et al.* in *2015 37th Annual International Conference of the IEEE Engineering in Medicine and Biology Society (EMBC).* 2779-2783.

167 Klünder, M. *et al.* Signal processing in urodynamics: towards high definition urethral pressure profilometry. *BioMedical Engineering OnLine* **15**, 31 (2016). https://doi.org:10.1186/s12938-016-0145-6

168 Linzenbold, W. *et al.* Rapid and precise delivery of cells in the urethral sphincter complex by a novel needle-free waterjet technology. *BJU International* **127**, 463-472 (2021). https://doi.org:https://doi.org/10.1111/bju.15249

169 Mitterberger, M. *et al.* Comparison of the precision of transurethral endoscopic versus ultrasound-guided application of injectables. *BJU International* **101**, 245-249 (2008). https://doi.org:https://doi.org/10.1111/j.1464-410X.2007.07262.x

170 Hussain, S. M. & Bray, R. Urethral bulking agents for female stress urinary incontinence. *Neurourology and Urodynamics* **38**, 887-892 (2019). https://doi.org:https://doi.org/10.1002/nau.23924

171 Burdzinska, A. *et al.* Limited accuracy of transurethral and periurethral intrasphincteric injections of cellular suspension. *Neurourology and Urodynamics* **37**, 1612-1622 (2018). https://doi.org:https://doi.org/10.1002/nau.23522

172 Linzenbold, W., Fech, A., Hofmann, M., Aicher, W. K. & Enderle, M. D. Novel Techniques to Improve Precise Cell Injection. *Int J Mol Sci* **22** (2021). https://doi.org:10.3390/ijms22126367

173 Jäger, L. *et al.* A novel waterjet technology for transurethral cystoscopic injection of viable cells in the urethral sphincter complex. *Neurourology and Urodynamics* **39**, 594-602 (2020). https://doi.org:https://doi.org/10.1002/nau.24261

VI. Publications

10. Publication 1

Injection of Porcine Adipose Tissue-Derived Stromal Cells by a Novel Waterjet Technology

Marina Danalache[1†], Jasmin Knoll[2†], Walter Linzenbold[3], Markus Enderle[3], Tanja Abruzzese[2], Arnulf Stenzl[2], Wilhelm K. Aicher[2*]

[1] Department of Orthopaedic Surgery, University Hospital Tübingen, Tübingen Germany
[2] Department of Urology, University Hospital Tübingen, Tübingen, Germany
[3] ERBE Elektromedizin GmbH Tübingen, Germany

† The authors MD and JK share first authorship as they contributed equally

* Correspondence author

International Journal of Molecular Sciences

Year 2021, Volume 22, Issue no. 8, Article no. 3958

doi: 10.3390/ijms22083958

MDPI

Received: 8 March 2021 / Revised: 7 April 2021 / Accepted: 8 April 2021 / Published: 12 April 2021

(This article belongs to the Special Issue Role and Application of Stem Cells in Regenerative Medicine 3.0)

Abstract

Previously, we developed a novel, needle-free waterjet (WJ) technology capable of injecting viable cells by visual guided cystoscopy in the urethral sphincter. In the present study, we aimed to investigate the effect of WJ technology on cell viability, surface markers, differentiation and attachment capabilities, and biomechanical features. Porcine adipose tissue-derived stromal cells (pADSCs) were isolated, expanded, and injected by WJ technology. Cell attachment assays were employed to investigate cell–matrix interactions. Cell surface molecules were analyzed by flow cytometry. Cells injected by Williams Needle (WN), normal cannula, or not injected cells served as controls. Biomechanical properties were assessed by atomic force microscopy (AFM). pADSCs injected by the WJ were viable (85.9%), proliferated well, and maintained their in vitro adipogenic and osteogenic differentiation capacities. The attachment of pADSCs was not affected by WJ injection and no major changes were noted for cell surface markers. AFM measurements yielded a significant reduction of cellular stiffness after WJ injections ($p < 0.001$). WJ cell delivery satisfies several key considerations required in a clinical context, including the fast, simple, and reproducible delivery of viable cells. However, the optimization of the WJ device may be necessary to further reduce the effects on the biomechanical properties of cells.

Keywords

atomic force microscopy; elasticity; stromal cells; regeneration; viability; urinary incontinence; waterjet

Introduction

Urinary incontinence (UI) is a highly prevalent condition, affecting 1.8–30.5% of the European population [1]. The most prominent form of UI is stress urinary incontinence (SUI), representing more than a third of patients reporting with UI. SUI in women is associated with mechanical load to the lower pelvic floor during pregnancy or vaginal delivery. In men, it is associated with prostate cancer surgery. In both cases, an insufficient muscular function contributes to incontinence [2]. In terms of treatment options, surgical therapy is opted for when conservative therapies or physiotherapy fail to grant satisfactory improvement. However, one major drawback of such invasive approaches is that they may trigger the occurrence of unwanted side effects, and treated patients, eventually, have to undergo revision surgical procedure after a short period of time [3–5]. Even though the current state-of-the-art regimen can ameliorate the sequela of UI, they do not address the main cause—the malfunction of the sphincter complex. In this framework, regenerative medicine approaches have emerged as an exciting new tool to improve or restore the urethral sphincter function through cell therapy [6,7]. The minimally invasive delivery of cells still bears several challenges with respect to injection precision and coverage of the target, albeit with significant research strides. Recent studies of preclinical cell delivery by needle injection have reported the frequent misplacement or loss of the injected cells [8,9]. Transurethral ultrasound-guided injections increase the precision of cell injection in the urethra [10]. In addition, in preclinical animal studies, a more defined control of the cells' exact localization in combination with a lower risk of complete sphincter penetration by injection needles was achieved by shortening the length of the needle's tip [8]. Nonetheless, it was noticed that shorter needle tips did not, in fact, grant "optimal" cell injections and a considerable percentage of cells were still misplaced [8]. While several circumferential needle injections are often performed to achieve a better cell distribution in the sphincter complex [11], they increase the risk of muscle injury and infections [9,12], and in addition, extend the overall time of treatment considerably.

There is an ongoing demand for new and efficient cell delivery technologies that are tailored to the demanding criteria present in a clinical setup. In this context, the waterjet (WJ) arises as a new tool for the high-throughput delivery of cells [13]. The versatility of WJ technology is unmatched, already being employed in a broad spectrum of medical specialties such as orthopedic surgery, neurosurgery, dermatology, urology, as

well as in dental surgery [14]. In fact, we recently developed a novel, needle-free, flexible WJ technology capable of injecting fluids, as well as particles and viable cells, by a cystoscope under visual control in the urethral sphincter [12]. Cell delivery via the abovementioned WJ technology in isotonic capture fluid actually yielded a significantly higher cell viability when compared to needle injections [12]. Moreover, when we extrapolated the WJ—cell delivery setting to injections in cadaveric urethra tissue—viable cells could be aspirated from the tissue and further expanded in vitro [12].

In the present study, we aimed to expand our understanding of WJ-based cell delivery by addressing the following highly relevant and still pending questions: (1) Does WJ reduce the viability of injected cells? (2) Does shear stress exerted by WJ determine a loss of cell surface molecules? (3) Is the attachment of cells to substrates modulated after WJ injections? (4) Are the biomechanical features of injected cells (as determined by the Young's modulus) compromised by WJ procedures? Cells injected by Williams Needle (WN), hypodermic needles, or not injected cells served as controls.

Results

Viability of Porcine Adipose Tissue-Derived Mesenchymal Stromal Cells after Injection by Waterjet

Unlabeled pADSCs were injected in capture medium by WJ using the E60-10 settings, WN, or a G22 cannula for controls (Figure 1A). Upon injection through the cannula (95.6 ± 0.06%, $n = 4$, $p < 0.002$) or WN (97.2 ± 2%, $n = 10$, $p < 0.002$), the viability of cells was higher when compared to injections by WJ (85.9 ± 0.16%, $n = 12$). The yield of cells recovered after WJ injections was somewhat lower when compared to injections by a G22 cannula or WN needle (Figure S1). After WJ injection, recovered pADSCs were expanded for one week and differences in their morphology (Figure 1B,C) or duplication rate (not shown) were not observed. Moreover, Calcein-labeled pADSCs were injected by WJ in cadaveric tissue samples, extracted, and incubated in expansion medium for up to 6 days. The fluorescence was proof for the viability of the injected cells. Overall, pADSCs proliferated well (Supplementary Figure S2) and maintained their in vitro adipogenic, as well as their osteogenic, differentiation capacities (Supplementary Figure S3).

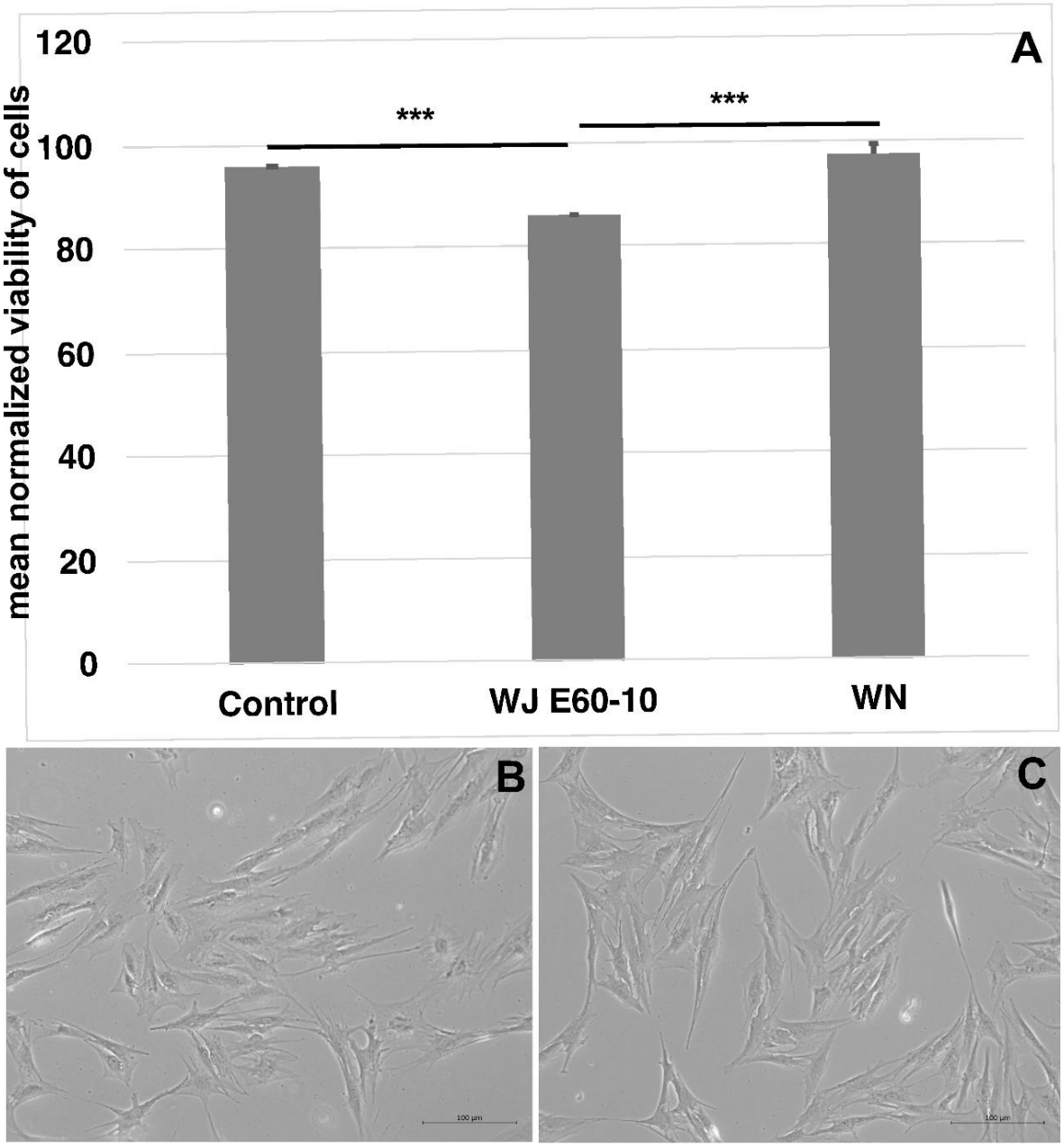

Figure 1: Viability assessment of cells after WN and WJ injections in capture fluid. Cells were injected by WJ in capture fluid (n = 12), collected, and counted by trypan exclusion to determine the viability. WJ injection reduced the viability of pADSCs significantly compared to cells injected through a standard 22G cannula (n = 4) or by WN (n = 10) (A). Microscopic differences in cell morphology or proliferation were not observed between the 22G cannula (B) and the WJ-injected pADSCs (C). *** $p < 0.001$. Abbreviations: WJ—waterjet, WN—Williams needle.

Biomechanical Assessments of Cellular Elasticity upon Injection of pADSCs in Isotonic Fluid and into Urethral Tissue

In the first experimental setting, pADSCs were injected in isotonic capture fluid (2 individual runs). WN injections displayed no significant difference regarding the mean elasticity modulus (EM; 0.992 kPa) when compared to not injected controls (1.176 kPa; Figure 2), while WJ injections caused in one experiment a highly significant reduction of the cellular EM from 0.891 to 0.440 kPa ($p < 0.001$, Figure 3) when compared to their corresponding controls. In a second experimental setup, the EM after WJ injection was reduced from 1.176 to 0.469 kPa (data not shown). This yielded an overall decrease in the cellular EM of 40–50% after WJ injections. Additionally, the cellular EMs after WN and WJ injections exhibited a highly significant difference ($p < 0.001$)—cells subjected to WJ injection showed a markedly lower EM (0.469 kPa) when compared to those subjected to WN injection (0.992 kPa; Figure 4).

Moreover, between two distinct WN injection experiments, a significant difference in the EMs of 1.615 versus 0.992 kPa ($p = 0.028$) was noted (Supplementary Figure S4A). In contrast, WJ injections, respectively, yielded in all experiments a considerably lower cellular EM stiffness (0.440 to 0.469 kPa, n.s.; Supplementary Figure S4B). Significant differences in the cellular EM among all not injected controls were not observed (Supplementary Figure S4C).

Next, pADSCs were injected by WN or WJ in the fresh porcine cadaveric sphincter samples, extracted, and investigated for their cellular EM in comparison to the controls (Figures 6 and 7). Upon WN injections, no significant difference in EMs was observed (1.176 to 1.441 kPa, Figure 5). Contrastingly, a significant reduction in the cellular EM was determined after WJ injections in tissue samples (0.890 to 0.429 kPa; $p < 0.001$) (Figure 6). In such, an overall 51% decrease in the EM for WJ injections was noted.

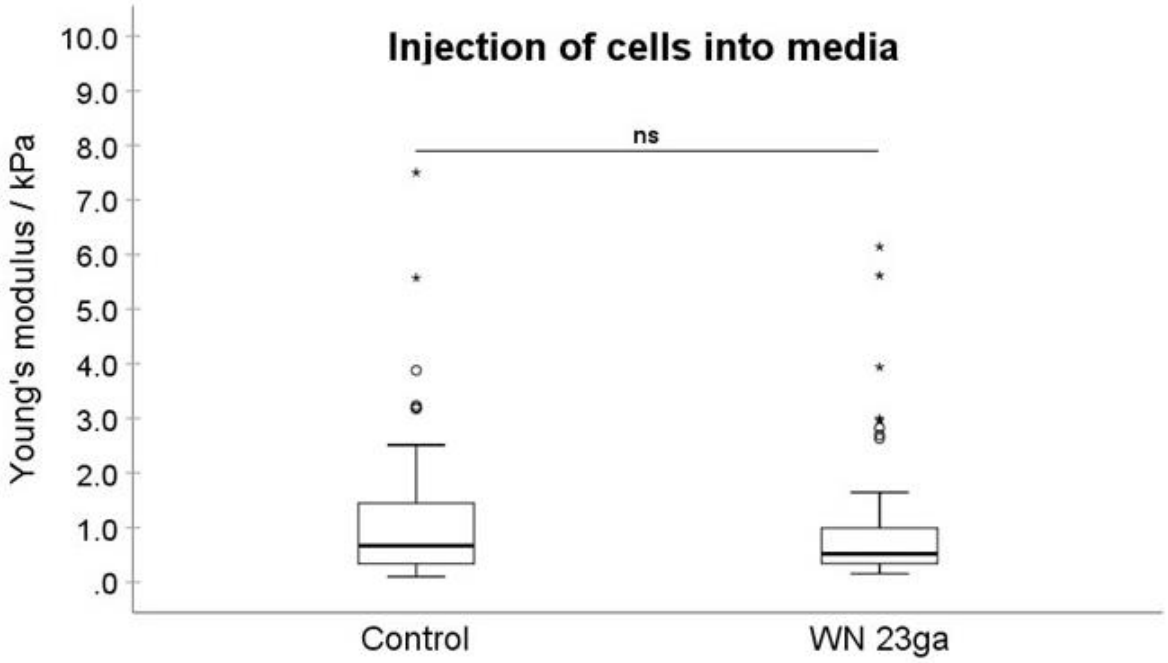

Descriptive statistics	Category	
Injections of cells in media	Control	WN 23ga
Number of cells in evaluation	59	58
Mean	1.176	0.992
Median	0.666	0.517
Minimum	0.100	0.155
Maximum	7.501	6.144
Standard deviation	1.356	1.251
Standard error	0.177	0.164

Figure 2: Analysis of Young's modulus of cell injections by WN in capture fluid. Boxplots (medians, minimum, maximum) of the stiffness (kPa) measured by atomic force microscopy for controls and WN-injected pADSCs in capture fluid are depicted. The control (untreated) cell monolayers revealed no difference in stiffness when compared to the WN group. Descriptive statistics of Young's moduli in the control and WN-injected cells in capture fluid. Medians with minimum and maximum, means, standard deviations, and standard errors of the mean of both groups are depicted. ns $p > 0.05$. Abbreviations: WN—Williams needle.

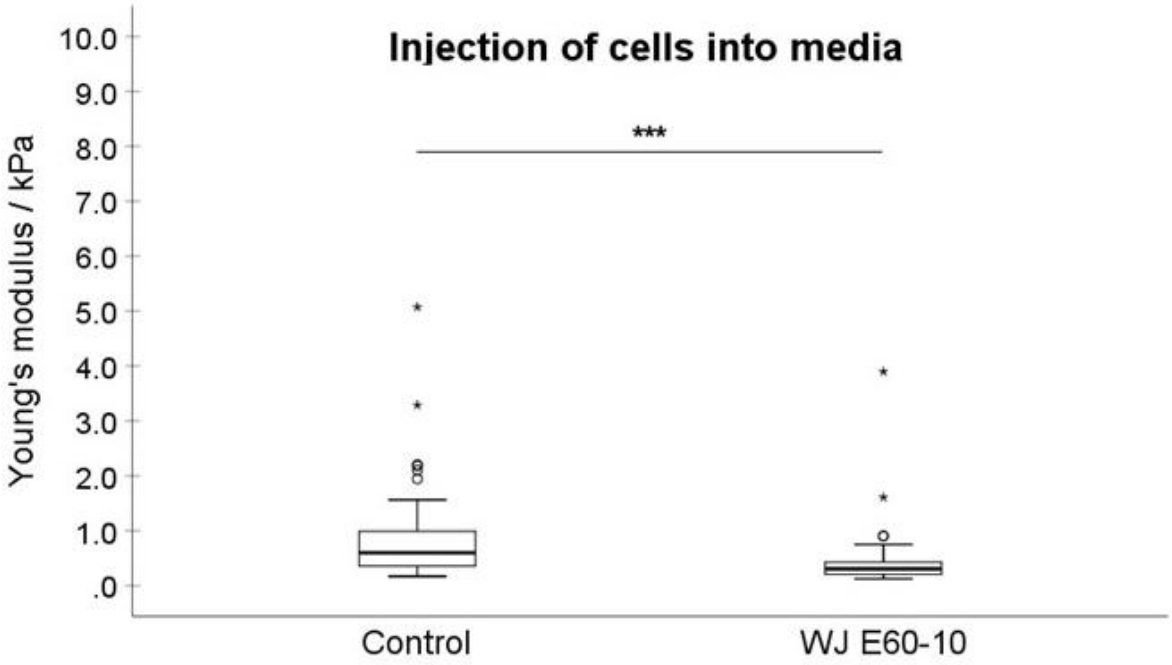

Descriptive statistics	Category	
Injections of cells in media	Control	WJ E60-10
Number of cells in evaluation	50	52
Mean	0.891	0.440
Median	0.598	0.306
Minimum	0.169	0.125
Maximum	5.071	3.898
Standard deviation	0.883	0.552
Standard error	0.125	0.077

Figure 3: Analysis of Young's modulus of cell injections by WJ capture fluid. Boxplots (medians, minimum, maximum) of the stiffness (kPa) measured by atomic force microscopy for controls and WJ-injected pADSCs in capture fluid are depicted. The control (untreated) cell monolayers revealed a higher stiffness when compared to the WJ group. Descriptive statistics of Young's moduli in control and WJ-injected cells in capture fluid. Medians with minimum and maximum, means, standard deviations and standard errors of mean of both groups are depicted. *** $p < 0.001$. Abbreviations: WJ—waterjet.

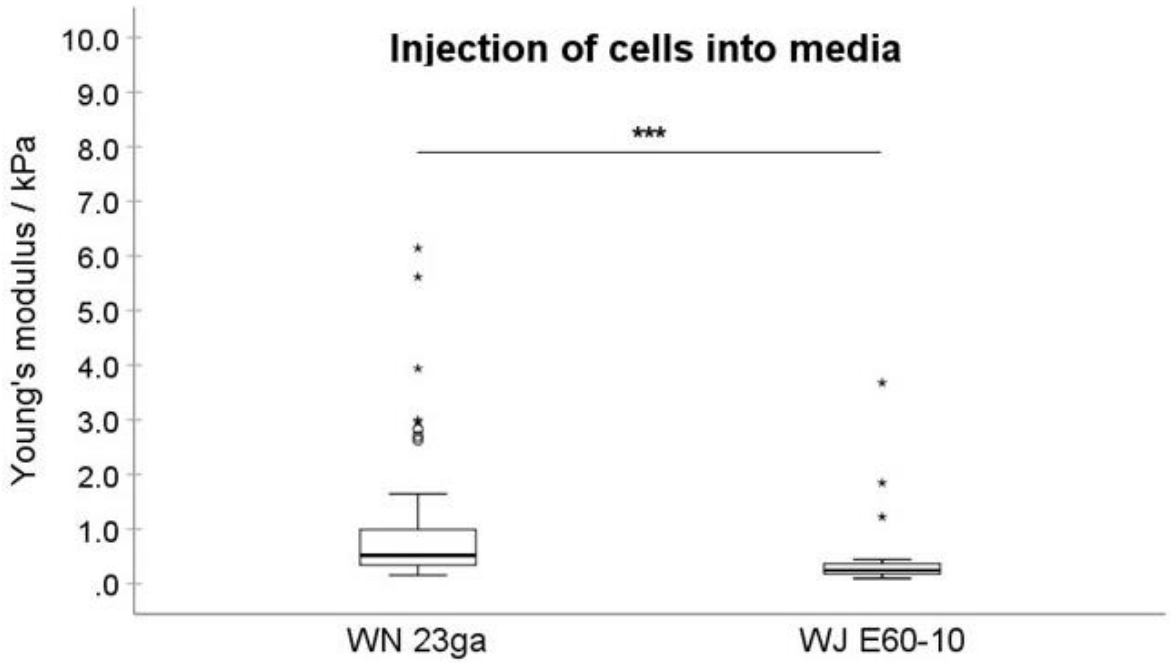

Descriptive statistics	Category	
Injections of cells in media	WN 23ga	WJ E60-10
Number of cells in evaluation	58	27
Mean	0.992	0.469
Median	0.517	0.245
Minimum	0.155	0.096
Maximum	6.144	3.678
Standard deviation	1.251	0.738
Standard error	0.164	0.142

Figure 4: Cellular elasticity after cell injections by WN versus WJ. Boxplots (medians, minimum, maximum) of the stiffness (kPa) measured by atomic force microscopy for WN and WJ-injected pADSCs in capture fluid are depicted. The WN-injected cell monolayers revealed a higher stiffness when compared to the WJ group. Descriptive statistics of Young's moduli in WN and WJ-injected cells in capture fluid. Medians with minimum and maximum, means, standard deviations and standard errors of the mean of both groups are depicted. *** $p < 0.001$. Abbreviations: WJ—waterjet, WN—Williams needle.

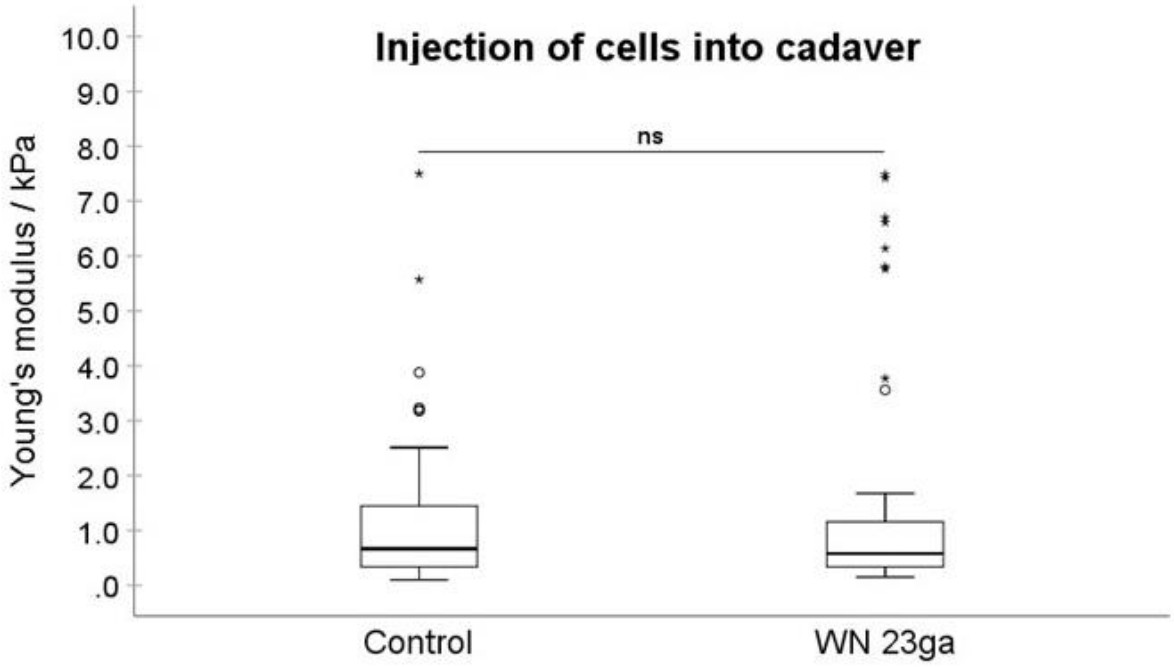

Descriptive statistics	Category	
Injections of cells in cadaver	Control	WN 23ga
Number of cells in evaluation	59	58
Mean	1.176	1.441
Median	0.666	0.578
Minimum	0.100	0.151
Maximum	7.501	7.485
Standard deviation	1.356	2.037
Standard error	0.177	0.268

Figure 5: Analysis of Young's modulus of cell injections by WN in tissue. Boxplots (medians, minimum, maximum) of the stiffness (kPa) measured by atomic force microscopy for controls and WN-injected pADSCs in fresh porcine cadaveric tissue are depicted. The control (untreated) cell monolayers revealed no significant differences in stiffness when compared to the WN group. Descriptive statistics of Young's moduli in the control and WN-injected cells in fresh porcine cadaveric tissue. Medians with minimum and maximum, means, standard deviations and standard errors of the mean of both groups are depicted. ns $p > 0.05$. Abbreviations: WN—Williams needle.

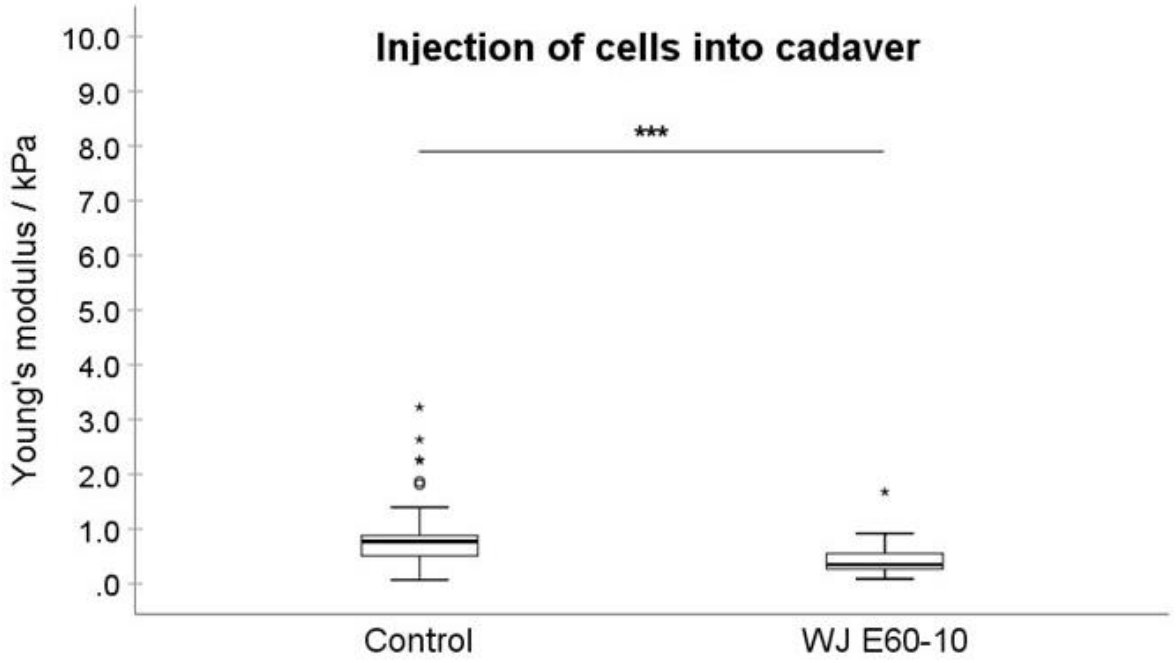

Descriptive statistics	Category	
Injections of cells in cadaver	Control	WJ E60-10
Number of cells in evaluation	51	53
Mean	0.891	0.429
Median	0.771	0.350
Minimum	0.072	0.086
Maximum	3.226	1.679
Standard deviation	0.623	0.274
Standard error	0.087	0.038

Figure 6: Analysis of Young's modulus of cell injections by WJ in tissue. Boxplots (medians, minimum, maximum) of the stiffness (kPa) measured by atomic force microscopy for controls and WJ-injected pADSCs in fresh porcine cadaveric tissue are depicted. The control (untreated) cell monolayers revealed a higher stiffness when compared to the WJ group. Descriptive statistics of Young's moduli in control and WJ-injected cells in fresh porcine cadaveric tissue. Medians with minimum and maximum, means, standard deviations and standard errors of the mean of both groups are depicted. *** $p < 0.001$. Abbreviations: WJ—waterjet.

Cell Attachment Assay

In order to investigate whether the cell attachment was modulated by WN or WJ injections, pADSCs were seeded on spots of serial dilutions of collagen and the attachment was monitored immediately after injections (Figure 7). The strong attachment of control pADSCs was noted on collagen spots diluted 1E02 (Figure 7A) and a moderate one on collagen diluted 1E03 (Figure 7B). However, cells either failed to attach (data not shown) or only slightly attached (Figure 7C) to collagen diluted 1E04. The attachment to BSA served as the control for specificity of the assay and cells did not attach in any of the experiments (Figure 7D,H,L). Immediately after WN and WJ injections of the cells in capture fluid, cell attachment was not affected nor reduced: in both groups, the pADSCs attached strongly to collagen diluted 1E02 (Figure 7E,I) and moderately to collagen diluted 1E03 (Figure 7F,J). To collagen diluted 1E04, pADSCs after WN injection failed to attach (Figure 7G), while after WJ injection, pADSCs showed a weak attachment (Figure 7K). In addition, calceinlabeled cells strongly attached to the 1E02 collagen dilution (Supplementary Figure S5E), moderately to collagen diluted 1E03 (Supplementary Figure S5F), and slightly to collagen diluted 1E04 (Supplementary Figure S5G).

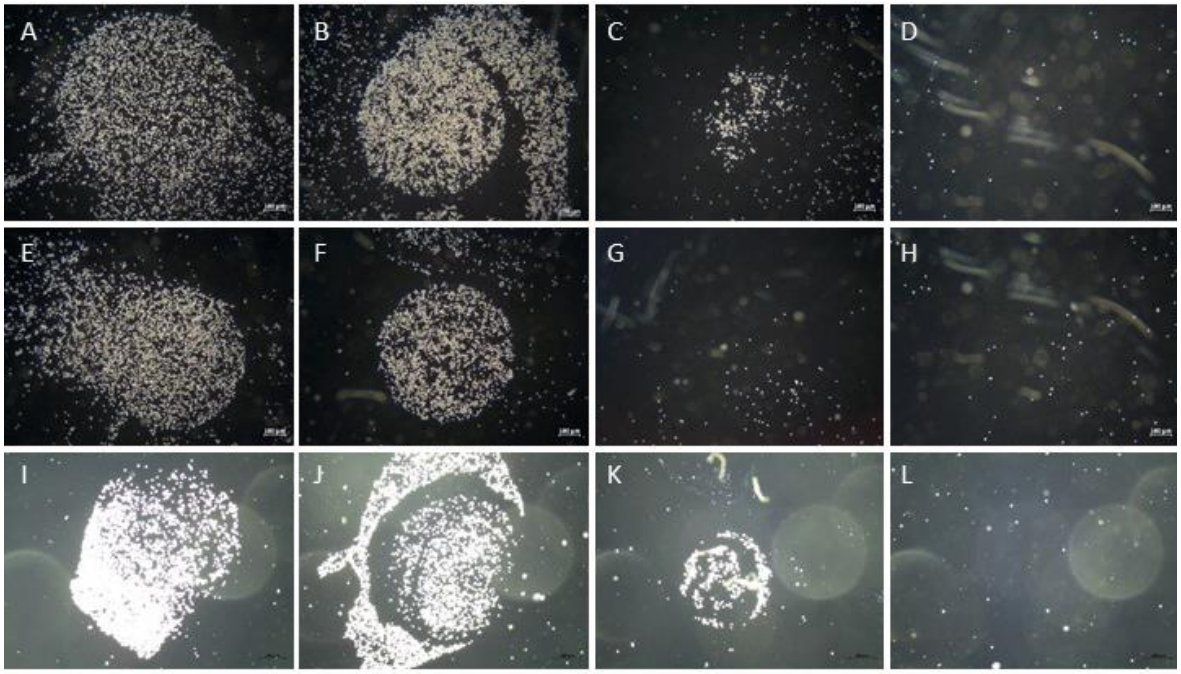

Figure 7: Attachment of cells after WJ injection. pADSCs were harvested and subjected to cell attachment assays (controls (A–D) after WN injection (E–H) and after WJ injection in capture fluid (I–L)). All populations attached to collagen at 1E02 (A,E,I) and 1E03 (B,F,J) dilutions, respectively. Not injected control cells slightly attached to collagen at 1E04 (C), while pADSCs after WN injection failed to attach (G). Cells after WJ injection maintained some attachment capacity (K). The interaction with BSA served as negative controls (D,H,L). Abbreviations: WN—Williams needle, WJ—waterjet.

Detection of Cell Surface Proteins Prior to and after WJ Injections

Flow cytometry was employed to further explore if shear stress triggers changes in cellular parameters such as size, granularity, and cell surface marker density. Differences in the size or granularity of pADSCs were not observed when cells were analyzed before vs. immediately after WJ injection (Figure 8). Even though the numbers of cells expressing cell surface proteins CD44 (97.5% vs. 93.2%) or CD90 (99.3% vs. 97.5%), as well as the mean fluorescence intensities (MFI; MFI CD44: 3174 vs 2554; MFI CD90: 8207 vs. 5923), were slightly reduced by WJ injection, no major differences were observed for the cell surface markers analyzed (Figure 8).

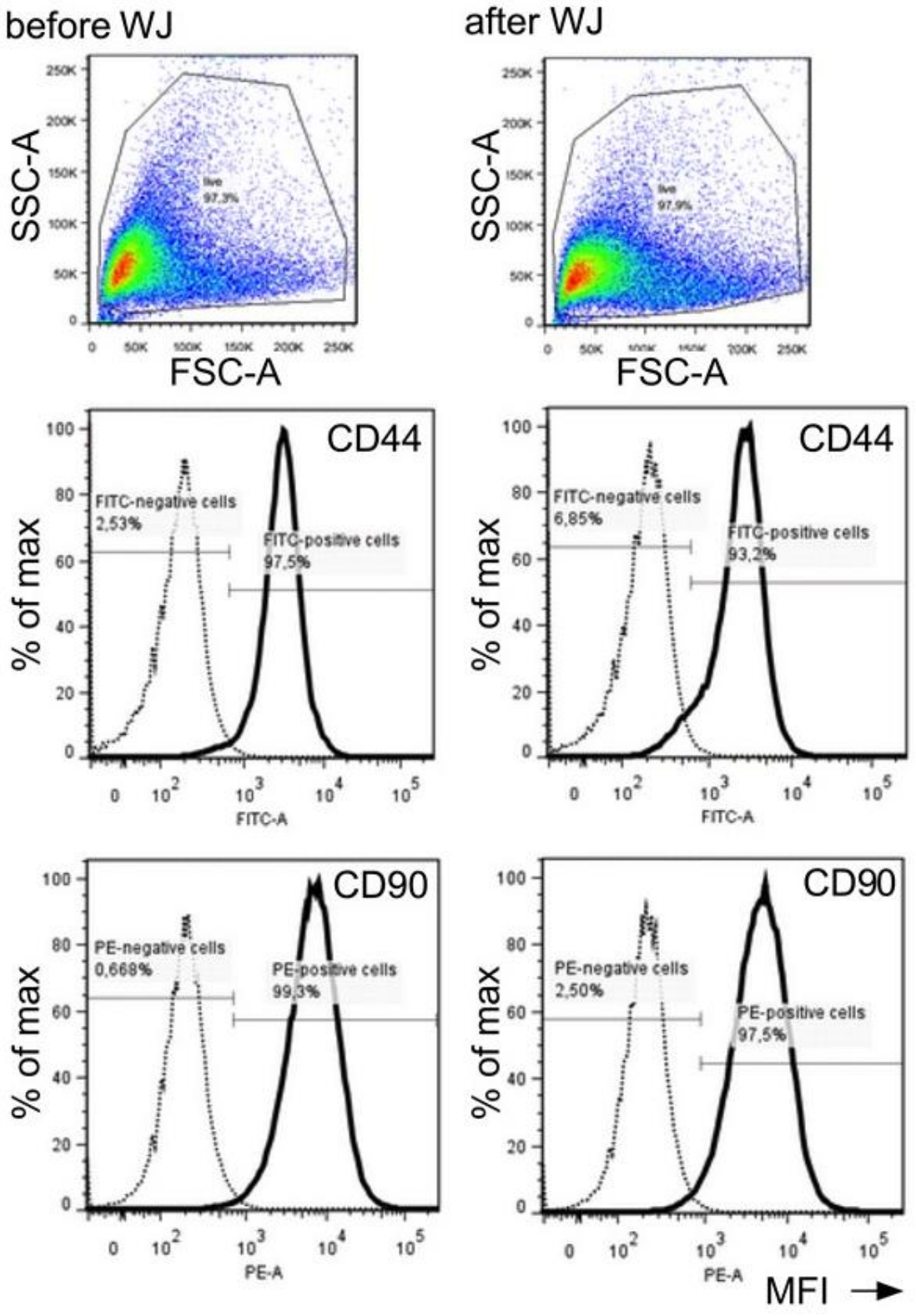

Figure 8: Detection of cell surface markers after WJ injection. Flow cytometry was employed to analyze the effect of WJ injections on pADSCs surface markers. Changes in cell size (forward light scatter; FSC-A), granularity and roughness of the cells (side light scatter, SSC-A), and the expression of mesenchymal markers CD44 and CD90 were determined. The numbers of cells expressing CD44 and CD90 are presented as a percentage (%) of the maximum (Y-axis) and their mean fluorescence intensities (MFI, X-axis). Major differences in cells markers prior to (left panels) versus after WJ injections (right panels) were not observed. Abbreviations: WJ—waterjet.

Discussion

In a clinical setting, the injection of active components including cells is routinely performed by injection needles and syringes. However, cell delivery through a needle-syringe inherits significant disadvantages [15]. Given this background, we have previously developed a novel WJ technology that enables cell delivery through the urothelium in a defined depth of the sphincter muscle [12]. In the present study, we aimed to further enhance our current understanding of the effect the WJ delivery approach has on cellular characteristics, in particular: on cellular viability, attachment, surface markers, and implicitly biomechanical features (i.e., EM). WJ injections of pADSCs in capture fluid determined a lower cell viability when compared to 22G cannula or WN injections of about 10% to 12%. This means that 85.9% of the cells obtained post-injection from WJ were viable, which in a clinical context represents an absolute requirement (>80%) [16].

Previous studies have demonstrated similar results for the delivery of cells using the water jet technology, whereas the results of the needle injection highly varied. For WJ injections of pADSCs, vital cell yields of 84.7% and 74.8% were reported for WJ and WN, respectively [12]. Another study demonstrated no significant difference between WN and WJ (both about 95%) [17]. This demonstrates a high reproducibility of a standardized injection protocol as is realized by WJ compared to needle injections, where the outcome is dependent on the size of the syringe and needle, the pressure of the syringe, flow rate, and the physician who executes the injection itself.

In this study, we noted a lower total yield of cells after WJ injections (74%). This loss of some cells could be explained by the construction of the WJ. The cells are delivered over a long path to the instrument and, therefore, some cells remain in the hose and instrument, not being delivered to the target. This is possibly not critical in clinical situations, as it may be compensated by a somewhat higher dosage of cells in the injection device if required or by re-constructing the device in order to minimize the dead volume within the hose and instrument. We therefore conclude that the WJ technology passes this critical threshold. Of note, WJ injections in living animals showed that by variation in the pressure profile, the penetration depth can be adapted to the tissue targeted and to the clinical need [12,18]. Moreover, preliminary unpublished results indicate that cells could be found in porcine urethrae after WJ injections in more than 95% of animals investigated (not shown). In contrast, upon needle injections in porcine urethrae, cells were found placed correctly only

in less than 50% of animals investigated [8]. This means that a moderate loss of cells by a lower yield after WJ injections is easily compensated by the significantly higher precision of cell placement in the region of interest.

In terms of other cellular characteristics such as cell attachment to substrates, granularity, and size, the expression of cell surface markers and differentiation capacities of WJ, pADSCs were not modulated. In addition, calcein staining does not affect the attachment, as well as the biomechanical features (i.e., elasticity). Correspondingly, no significant changes in cellular characteristics were also reported when the viability, differentiation capacities, expression of cell surface antigens, and in vivo migration of mesenchymal stromal cells injected through narrow needles were investigated [19]. These data are in line with our observations. Although one has to bear in mind that the flow rates of cell injections in blood using conventional needles range from 0.4 to 1.2 mL/min, syringe-needle injections of cells in tissue are performed with considerably lower flow rates [15]. Using the current WJ devices, the fluid injections of the tissue penetration jet at E60 reach flow rates of 45 mL/min, while the cells injected with E10 travel at rates of 15 mL/min. This improved pressure control protocol granted higher cell viability when compared to WJ injections applying a pressure of E60 in a fixed-pressure-level mode.

The exact rate of cells surviving after tissue injections could not be determined in the context of these experiments. In a recent in vivo animal feasibility study, however, we showed that the WJ technology delivers viable cells into the urethral sphincter of pigs that also are morphological intact after an incubation time of 3 days [18]. Functional studies designed to inject cells by WJ and investigating their regenerative potential in appropriate animal models are needed to address these pending questions. However, as cells injected by needle were shown to regenerate the sphincter function in both preclinical and clinical situations [9,20–22], it is conceivable to hypothesize that the precise delivery of cells to the sphincter may grant functional regeneration of the muscle.

The mechanical forces that cells are exposed to as they pass through the injection device represents a crucial factor that modulates their subsequent viability and functionality post-transplantation [23]. When considering the technical background of the WJ cell delivery, we employed a two-phased process: An elevated pressure (effect 60) injects a small aliquot of fluid in the tissue (this jet loosens the targeted tissue). Within milliseconds, the pressure is reduced to moderate levels (effect 10) to inject the cells in a low-pressure jet [12]. When generating even modest pressure and volume profiles at E10, the cells are

accelerated in the apparatus, possibly relaying mechanical shear stress to the cells. Therefore, the next arising question in our study was whether our WJ delivery setting has an effect on the biomechanical features (e.g., elasticity) of the cells in comparison to WN injections. After WN injections, no significant EM differences were observed compared to controls. This suggested that the elastic features of the cells are not affected. However, when comparing two individual needle injection experiments, a significant difference was detected ($p = 0.028$), pinpointing to an increased variability of elastic effects on the cells by WN injections. In contrast, the AFM data after WJ injections were more constant than AFM results after WN injections. This confirmed that the WJ technology yielded more consistent and reproducible conditions. However, a significant decrease in EM after WJ delivery was observed in both the experimental settings compared to the corresponding control: upon injection in isotonic capture fluid ($p < 0.001$) and also in fresh porcine cadaveric sphincter tissue ($p < 0.001$). We conclude that the elastic features of cells are affected by WJ delivery.

It has been suggested that elasticity changes are associated with changes in cellular morphology [24,25]. Wharton's jelly-derived mesenchymal stem cells that present an elevated migration potential are characterized by increased cellular deformability. The study suggested that there is a "selective chemotactic migration" of cells with higher deformabilities and lower Young's modulus values [26]. Similar observations have been stated previously, hence emphasizing that cellular elasticity and migration capabilities are two closely intertwined processes [27]. A lower cell stiffness could facilitate cells migration after WJ injection, thus granting a wider distribution and radius of regenerative action in the tissue targeted. These phenomena might also have facilitated the wide distribution of cells in our recent in vivo animal feasibility study, where a much larger distribution of the cells was observed after 3 days compared to needle injection [18]. When comparing the two experimental setups used in our study—injections in capture fluid (resembling intravenous injections) versus injections in cadaveric sphincter tissue—no significant difference in EM was noted. This indicated that the two-phase injection approach opened the tissue targeted in a sufficient way to facilitate cell injections in micro-cavernae.

To reduce injury and bleeding, small-caliber needles are often used for injections of drugs in solid tissues. However, smaller needles and slower injection rates contribute to an elevated pressure at the ejection point, the needle tip [28]. Tissues actually resemble a solid

or semi-solid target at the spot of cell injection, thus enhancing the pressure on individual cells when entering the tissue. Leaving the needle tip, cells exhibit a sudden deceleration and are pressed against the corresponding tissue. This may cause an increase in cells loss, not investigated in our study in detail. While the loss of cells or lasting changes in gene expression were not observed for mesenchymal stromal cells after needle injections in fluids [29], upon local administration of stromal cells in heart muscle, only 10–30% of the cells were detected [30,31]. Of note, WJ injections in cadaveric samples yielded the recovery of viable cells in 71–86% of samples investigated depending on the pressure profile utilized [12]. The exact enumeration of the cell yield after WJ injections in vivo remains to be determined in future studies. Using the novel WJ technology, ejection from the injector tip is gentle and follows almost the biomechanics of injections in liquids. We corroborate this notion in the present study, as significant differences in the EM of cells after injection in fluid versus tissue injections were not observed, nor significant changes in attachment, proliferation, or differentiation.

The data presented and validated by our study focused primarily on in vitro investigations that pave the way for future in vivo studies. Future research efforts will focus on not only addressing SUI [12,18] but also on other forms of incontinence and pathologies such as heart attack [17]. Overall, the WJ technology satisfies several key considerations required in a clinical context, such as the ease of loading and use, reproducibility of delivery, and precise delivery of viable cells under guided visual control.

Material and Methods

Isolation and Production of Porcine Adipose Tissue-Derived Stromal Cells

Porcine adipose tissue-derived stromal cells (pADSCs) were isolated, characterized, and expanded in DMEM medium enriched by 10% (v/v) fetal bovine serum (FBS, Sigma, Munich, Germany) and antibiotics following published protocols [32]. In brief, the tissue was minced and incubated with 0.1% of collagenase (Gibco) and 1% of bovine serum albumin (BSA, 1% (w/v) in PBS) at 37◦ for 30 min. Incubation was stopped with medium containing 10% of FBS. The adipocyte phase was discarded and the stromal cell fraction was filtered through a 100 µm cell strainer. Cells were washed again with medium and the retrieved cells were seeded and incubated in expansion media containing 10% of FBS and antibiotics [32]. When reaching 70% of confluence, cells were detached (Trypsin-EDTA, Sigma, Munich, Germany), washed twice with PBS, and seeded in 10 mL of medium at an inoculation density of 3E05 ADSCs per 75 cm^2 flask. Cell proliferation and duplication rates (DR) were determined by cell counting over three consecutive passages [33]. To determine the mean size of pADSCs in suspension, cells were detached by Trypsin-EDTA (Sigma, Munich, Germany) and washed with phosphate-buffered saline (PBS, Sigma, Munich, Germany). Cell viability and dimensions were determined with a cell analyzer following the manufacturer's instruction (CASY, Omni Life Science, Bremen, Germany).

Preparation of Urethral Tissue Samples

Urethra and bladder tissue were prepared from fresh cadaveric samples of adult female landrace pigs. The tissue was cleared from any debris, rinsed with cold PBS, and transported to the laboratory in bags on wet ice. The tissue was preserved on wet ice until experiments without additives. Afterward, the urethra was placed on a sponge to mimic the elasticity of the lower pelvic floor. The urethra was opened longitudinally on the dorsal side by scissors and wetted by cold PBS to avoid tissue dehydration. Then, cells were injected in the urethra as described below. The bladder was used only to grant the distal-proximal orientation and positioning of the female urethra for the cell injections. Cells were not injected in bladder tissue. The whole procedure from the preparation of tissue to cell injections was performed within a time frame of 45 min to a maximal 90 min.

Needle Injections of Cells in Fluids and Tissue Samples

For needle injections in capture fluid (DMEM, 10% FBS), pADSCs were harvested, washed with PBS, resuspended in culture media at 2.4E06 cells per mL, aspirated in a syringe (1 mL BD Luer-LokTM Syringe, BD Plastik Inc, Laval, QC, Canada)), and injected through a Williams Cystoscopic Injection Needle (WN; Cook Medical; 23G, 5.0 Fr, 35 cm) by hand. Cells were harvested by centrifugation. In order to determine the yield and viability, the cells were counted by aid of Trypan Blue dye (Sigma, Munich, Germany) exclusion with a hematocytometer. Cells that were not subjected to WN injection served as controls.

WN injections of pADSCs were also performed in fresh porcine cadaveric tissue. The WN was inserted in a flat angle in the tissue and cells were injected by hand. Then, cells were aspirated from the injection dome by the aid of a needle (18G) and syringe (1.2 mL), collected in capture fluid, and washed with cell culture media. Cells harvested from cadaveric samples were further subjected to analyses. Cells that were not subjected to WN injection served as controls.

Waterjet Injections of Cells in Fluids and Tissue Samples

For WJ injections in capture fluid, pADSCs were harvested, washed with PBS, resuspended in injection media at 6E06 per mL, and filled in the dosing unit of the WJ device [12]. Cells were injected using a modified ERBEJET®2 device (Erbe Elektromedizin GmbH; Tuebingen, Germany) and a prototype injection nozzle that allows the injection of fluids in a two-phase manner using high pressures (E = effects) during a tissue penetration phase (E > 60) and low pressures for cell injection (E < 20) [11,18]. The applied pressure settings here were E60-10 in all WJ experiments [12]. After WJ injection in capture fluid, cells were harvested as described above. Cells that were not subjected to WJ injection served as controls. For the viability assessment experiments, injections through a WN and through a standard 22G cannula (B. Braun Sterican®, Melsungen, Germany bore size 0.47 mm, length 1.25 inch) served as additional controls.

For WJ injections of pADSCs in fresh porcine cadaveric tissue samples, the same device and settings were employed as aforementioned. The injection device was mounted perpendicularly on a stand and lowered on the tissue surface by the aid of a micrometer caliper. When approaching the tissue, the injector tip was lowered two more millimeters in

the tissue to avoid the splashing of the cells to the side. WJ injections were performed using the E60-10 settings [12]. After WJ injections in cadaveric tissue, cells were processed as described above. Cells that were not subjected to WJ injection served as controls.

Biomechanical Assessment of Cellular Elasticity by Atomic Force Microscopy (AFM)

The elastic moduli of the cells were assessed as previously described [34]. Briefly, an AFM system (CellHesion 200, Bruker, Billerica, MA, USA) equipped with an inverted microscope (AxioObserver D1, Carl Zeiss AG, Jena, Germany) was employed. This enabled the simultaneous visualization and selection of the cells. In such, the specific positions within the dishes could be user-selected and measured. An AFM cantilever (tip A, k = 0.2 N/m, All-In-One-Al-Tl, Budget Sensors, Sofia, Bulgaria) was used for elasticity determinations. Indentation curves were sampled at 2 kHz, with a force trigger of ≈10 nN and a velocity of 5 µm/s. The elastic properties of the pADSC were evaluated after WJ injection and injections by WN. As described above, two different pADSCs WJ injection experiment settings were performed: For the first experimental setting, pADSCs were injected via WJ or WN in isotonic capture fluid, collected, and subjected to AFM analyses. The second experimental setting consisted of pADSCs injected by WJ or WN in the fresh porcine cadaveric sphincter samples, extracted from the tissue, washed, and subjected to AFM analyses. For both experimental settings, cell cohorts were washed by PBS and counted. A total of 5E05 cells per testing condition were incubated for 3 h in expansion medium to allow cell binding and adhesion to the tissue culture dishes (TPP AG, Trasadingen, Switzerland). Right before commencement of all AFM measurements, cells were first rinsed with PBS and then covered with Leibovitz's L-15 medium without l-glutamine (Merck, Munich, Germany). As controls, cells that were not subjected to any kind of injection procedure were employed. We applied indentations over the chosen region of interest identified by microscopic examination (50 different cells/culture condition; three measurement repetitions/measurement site (Figure 9). The Young's modulus (i.e., elastic modulus (EM)) was calculated from the force–distance curves by using the Hertz-fit model incorporated in the data processing software (Brucker, Billerica, MA, USA).

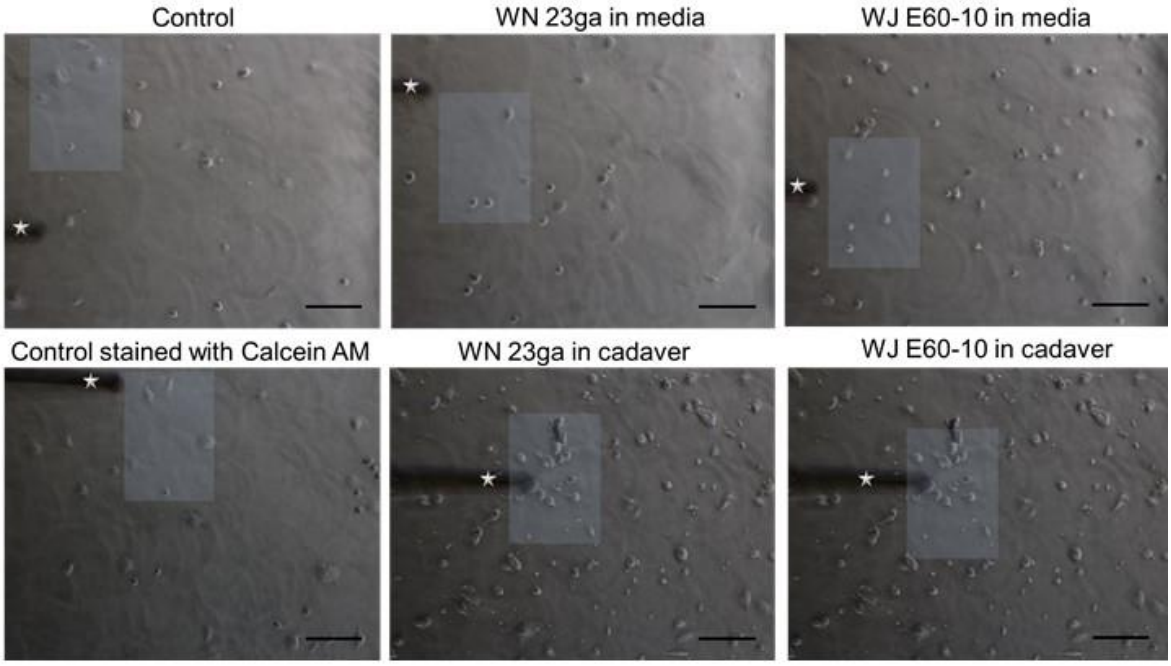

Figure 9: Representative images indicating the regions of interest subjected to elasticity measurements via AFM. Microscopic pictures of AFM-measured porcine adipose tissue-derived stromal cells (pADSCs) control monolayers (left pictures) and pADSCs injected by WN (middle pictures) or WJ (right pictures). Following WN and WJ injection, cells were collected, washed by PBS, and allowed to attach for 3 h in expansion medium before AFM measurements. As controls, cells that were not subjected to an injection procedure were used. The cantilever employed for measurements is also displayed (white star). Representative regions containing cells subjected to AFM measurements are also displayed (white squares). Images were acquired with the inverted AxioObserver D1 light microscope attached to the AFM system at a 10× magnification. Scale bar (black) represents 100 µm. Abbreviations: WJ—waterjet, WN—Williams needle.

Cell Attachment Assay

Cell attachment was analyzed on type I collagen-coated dishes, as previously described [35]. In brief, rat type I collagen (# 354236, 4.52 µg/µL, BD-Biosciences, Franklin Lakes, NJ, USA) was diluted 1E02, 1E03, and 1E04 in PBS, and 1 µL aliquots were distributed and airdried. The dish surface was coated with BSA (1% (w/v) in PBS) and washed. The pADCSs were detached by mild proteolysis (Accutase, Sigma, Munich, Germany), washed and resuspended in medium, and injected by WJ or WN in capture medium. The yield of viable cells was counted, and 1E06 cells were resuspended in 200 µL of cell attachment medium and seeded onto the collagen spots [35]. As controls, pADSCs were detached, washed, resuspended, counted, and directly added to the collagen spots [35]. After incubation (15 min, 37 ◦C, humidified atmosphere), dishes were washed three times by PBS and the spots were recorded by aid of a microscope (AxioVert.A1, 2.5× objective, Carl Zeiss AG, Jena, Germany).

Characterization of pADSCs Prior to and after WJ Injections

The size and granularity of cells were determined by flow cytometry recording the forward scatter area (FSC-A) and side scatter area (SSC-A), respectively. To document their mesenchymal phenotype, the expression of cell surface markers was also analyzed. The expressions of CD44 (mAB # ab19622, 1:10 in PFEA buffer; abcam, Bristol, United Kingdom) and CD90 (PE-labelled mAB # 555596 1:5 in PFEA buffer; BD-Biosciences, Franklin Lakes, NJ, USA) were investigated as previously described [36]. Adipogenic and osteogenic differentiations were induced over 4 weeks by incubation of the pADSCs in the corresponding differentiation media. Controls remained in starvation media. The differentiation was visualized by von Kossa and Oil Red O staining [36].

Statistical Analysis

The normality of the data was assessed by means of the Shapiro–Wilks test and histograms. Based on normality, the AFM values are either presented as a median and range (minimum-maximum) and graphically displayed as boxplots or as a mean ± standard deviation (SD) displayed as bar diagrams. Differences between groups of nonnormally distributed data were analyzed by the nonparametric Mann–Whitney U test. To allow and facilitate a comparison of our AFM data with other studies and due to the fact that our AFM data were not normally distributed, we computed and present the mean, median, SD, and standard error of the mean [37]. For normal-distributed data, a Student’s t-test was used. Statistical analysis was performed with SPSS Statistics 22 (IBM, Endicott, New York, NY, USA).

Study Limitations

Experimental parameters used for AFM testing, such as indentation velocity and depth, indenter shape and size, as well as the accurate representation of tip geometry in model fitting [38], may impact absolute values of the measured mechanical properties [39,40]. They should not, however, affect the results within one study and their relation to each other. It has to be borne in mind that AFM analysis is generally restricted to the analysis of the outer surface of cell membranes. As the AFM is not capable of scanning the inside of a cell membrane, it implicitly means that it is not able to directly investigate intracellular structures. However, our focus of the present study was to investigate the average WJ and WN-related EM changes rather than probing specific cellular/intracellular components. Additionally, due to the limited availability of tissue samples, as well as to animal welfare considerations, the trade-off of using procedures is the mixing of statistically dependent and independent data, which formally is not indicated. Even though the obtained p-values thus need to be interpreted with the necessary caution, the measured tendency should still not be affected.

Conclusions

WJ injections of cells using the two-phase pressure and volume protocol enable applications of viable cells in fluids, as well as in tissues. For minimally invasive injections of cells by endoscope or cystoscope under visual control, the WJ grants a simple, precise, and reproducible method to apply viable cells. While many features of pADSCs such as viability, attachment, or differentiation capacities are not influenced by WJ injections, the overall yield of cells, as well as their biomechanical properties, show differences to cell injection by WN or standard needles.

Author Contributions

M.D.: performed and evaluated MFM measurements, and wrote the manuscript; J.K.: performed the experiments and critical reading of the manuscript; W.L.: constructed the WJ device; M.E.: concept of WJ technology; T.A.: production and quality management of cells; A.S.: critical reading of the manuscript; W.K.A.: design and conception of the study, supervision of experiments, and data evaluation. All authors have read and agreed to the published version of the manuscript.

Funding

The project was funded in part by EU grant # 731377 project MUS.I.C., BMBF grant 13GW0073 project Multimorb-INKO, and the DFG Ai16/27-1 project PoTuS toWKA, and in part by institutional funds.

Institutional Review Board Statement

Not applicable.

Informed Consent Statement

Not applicable.

Data Availability Statement

All data are available to colleagues associated with pubic research enterprises upon reasonable request.

Acknowledgments

We thank the colleagues at the Institute for Experimental Surgery at the University of Tübingen Hospital for providing tissue samples for the preparation of pADSCs. The project was supported in part by grants of WKA and ME (BMBF # 13GW0073A, # 13GW0073C; EU # 731377; DFG # Ai 16/27-1) and in part by institutional funds.

Conflicts of Interest

All authors declare that they have no conflict of interest, except for W. Linzenbold and M. Enderle. They are employed by ERBE GmbH, the manufacturer of the Waterjet device.

Abbreviations

AFM	atomic force microscopy
EM	elastic modulus
pADSCs	porcine adipose tissue-derived stromal cells
WJ	waterjet
WN	Williams needle

References

1. Milsom, I.; Coyne, K.S.; Nicholson, S.; Kvasz, M.; Chen, C.I.; Wein, A.J. Global prevalence and economic burden of urgency urinary incontinence: A systematic review. *Eur. Urol.* **2014**, *65*, 79–95. [CrossRef]
2. Hillary, C.J.; Roman, S.; MacNeil, S.; Aicher, W.K.; Stenzl, A.; Chapple, C.R. Regenerative medicine and injection therapies in stress urinary incontinence. *Nat. Rev. Urol.* **2020**, *17*, 151–161. [CrossRef]
3. Nitti, V.W.; Dmochowski, R.; Herschorn, S.; Sand, P.; Thompson, C.; Nardo, C.; Yan, X.; Haag-Molkenteller, C. OnabotulinumtoxinA for the treatment of patients with overactive bladder and urinary incontinence: Results of a phase 3, randomized, placebo controlled trial. *J. Urol.* **2013**, *189*, 2186–2193. [CrossRef]
4. Ravier, E.; Fassi-Fehri, H.; Crouzet, S.; Gelet, A.; Abid, N.; Martin, X. Complications after artificial urinary sphincter implantation in patients with or without prior radiotherapy. *BJU Int.* **2015**, *115*, 300–307. [CrossRef]
5. Léon, P.; Chartier-Kastler, E.; Rouprêt, M.; Ambrogi, V.; Mozer, P.; Phé, V. Long-term functional outcomes after artificial urinary sphincter implantation in men with stress urinary incontinence. *BJU Int.* **2015**, *115*, 951–957. [CrossRef]
6. Wang, H.J.; Chuang, Y.C.; Chancellor, M.B. Development of cellular therapy for the treatment of stress urinary incontinence. *Int. Urogynecol. J.* **2011**, *22*, 1075–1083. [CrossRef]
7. Vaegler, M.; Lenis, A.T.; Daum, L.; Amend, B.; Stenzl, A.; Toomey, P.; Renninger, M.; Damaser, M.S.; Sievert, K.D. Stem cell therapy for voiding and erectile dysfunction. *Nat. Rev. Urol.* **2012**, *9*, 435–447. [CrossRef]
8. Amend, B.; Kelp, A.; Vaegler, M.; Klünder, M.; Frajs, V.; Klein, G.; Sievert, K.-D.; Sawodny, O.; Stenzl, A.; Aicher, W.K. Precise injection of human mesenchymal stromal cells in the urethral sphincter complex of Göttingen minipigs without unspecific bulking effects. *Neurourol. Urodyn.* **2017**, *36*, 1723–1733. [CrossRef] [PubMed]
9. Burdzinska, A.; Dybowski, B.; Zarychta-Wis´niewska, W.; Kulesza, A.; Butrym, M.; Zagozdzon, R.; Graczyk-Jarzynka, A.; Radziszewski, P.; Gajewski, Z.; Paczek, L. Intraurethral co-transplantation of bone marrow mesenchymal stem cells and

musclederived cells improves the urethral closure. *Stem Cell Res. Ther.* **2018**, *9*, 239. [CrossRef] [PubMed]
10. Strasser, H.; Marksteiner, R.; Margreiter, E.; Pinggera, G.M.; Mitterberger, M.; Frauscher, F.; Hering, S.; Bartsch, G. 328: Transurethral Ultrasound Guided Stem Cell Therapy of Urinary Incontinence. *J. Urol.* **2006**, *175*, 107. [CrossRef]
11. Mitterberger, M.; Pinggera, G.M.; Marksteiner, R.; Margreiter, E.; Fussenegger, M.; Frauscher, F.; Ulmer, H.; Hering, S.; Bartsch, G.; Strasser, H. Adult stem cell therapy of female stress urinary incontinence. *Eur. Urol.* **2008**, *53*, 169–175. [CrossRef] [PubMed]
12. Jäger, L.; Linzenbold, W.; Fech, A.; Enderle, M.; Abruzzese, T.; Stenzl, A.; Aicher, W.K. A novel waterjet technology for transurethral cystoscopic injection of viable cells in the urethral sphincter complex. *Neurourol. Urodyn.* **2020**, *39*, 594–602. [CrossRef] [PubMed]
13. Adamo, A.; Roushdy, O.; Dokov, R.; Sharei, A.; Jensen, K.F. Microfluidic jet injection for delivering macromolecules into cells. *J. Micromech. Microeng.* **2013**, *23*, 035026. [CrossRef] [PubMed]
14. Hreha, P.; Hloch, S.; Magurov, D.; ValÓek, J.; Kozak, D.; Harni rov, M.; Rakin, M. Water Jet Technology Used in Medicine. *Teh. Vjesn. Tech. Gaz.* **2010**, *17*, 237–240.
15. Wahlberg, B.; Ghuman, H.; Liu, J.R.; Modo, M. Ex vivo biomechanical characterization of syringe-needle ejections for intracerebral cell delivery. *Sci. Rep.* **2018**, *8*, 9194. [CrossRef]
16. Gálvez-Martín, P.; Hmadcha, A.; Soria, B.; Calpena-Campmany, A.C.; Clares-Naveros, B. Study of the stability of packaging and storage conditions of human mesenchymal stem cell for intra-arterial clinical application in patient with critical limb ischemia. *Eur. J. Pharm. Biopharm. Off. J. Arb. Fur Pharm. Verfahr. e.V* **2014**, *86*, 459–468. [CrossRef] [PubMed]
17. Weber, M.; Fech, A.; Jäger, L.; Steinle, H.; Bühler, L.; Perl, R.M.; Martirosian, P.; Mehling, R.; Sonanini, D.; Aicher, W.K.; et al. Hydrojet-based delivery of footprint-free iPSC-derived cardiomyocytes into porcine myocardium. *Sci. Rep.* **2020**, *10*, 16787. [CrossRef]
18. Linzenbold, W.; Jäger, L.; Stoll, H.; Abruzzese, T.; Harland, N.; Bézière, N.; Fech, A.; Enderle, M.; Amend, B.; Stenzl, A.; et al. Rapid and precise delivery of cells in the urethral sphincter complex by a novel needle-free waterjet technology. *BJU Int.* **2020**. [CrossRef]
19. Mamidi, M.K.; Singh, G.; Husin, J.M.; Nathan, K.G.; Sasidharan, G.; Zakaria, Z.; Bhonde, R.; Majumdar, A.S.; Das, A.K. Impact of passing mesenchymal stem cells through smaller bore size needles for subsequent use in patients for clinical or cosmetic indications. *J. Transl. Med.* **2012**, *10*, 229. [CrossRef]
20. Eberli, D.; Aboushwareb, T.; Soker, S.; Yoo, J.J.; Atala, A. Muscle Precursor Cells for the Restoration of Irreversibly Damaged Sphincter Function. *Cell Transplant.* **2012**, *21*, 2089–2098. [CrossRef] [PubMed]
21. Gotoh, M.; Yamamoto, T.; Kato, M.; Majima, T.; Toriyama, K.; Kamei, Y.; Matsukawa, Y.; Hirakawa, A.; Funahashi, Y. Regenerative treatment of male stress urinary incontinence by periurethral injection of autologous adipose-derived

regenerative cells: 1-year outcomes in 11 patients. *Int. J. Urol.* **2014**, *21*, 294–300. [CrossRef] [PubMed]
22. Peters, K.M.; Dmochowski, R.R.; Carr, L.K.; Robert, M.; Kaufman, M.R.; Sirls, L.T.; Herschorn, S.; Birch, C.; Kultgen, P.L.; Chancellor, M.B. Autologous muscle derived cells for treatment of stress urinary incontinence in women. *J. Urol.* **2014**, *192*, 469–476. [CrossRef]
23. Amer, M.H.; Rose, F.R.A.J.; Shakesheff, K.M.; Modo, M.; White, L.J. Translational considerations in injectable cell-based therapeutics for neurological applications: Concepts, progress and challenges. *NPJ Regen. Med.* **2017**, *2*, 23. [CrossRef] [PubMed]
24. Grady, M.E.; Composto, R.J.; Eckmann, D.M. Cell elasticity with altered cytoskeletal architectures across multiple cell types. *J. Mech. Behav. Biomed. Mater.* **2016**, *61*, 197–207. [CrossRef]
25. Safrana, S.A.; Govb, N.; Nicolasc, A.; Schwarzd, U.S.; Tlustya, T. Physics of cell elasticity, shape and adhesion. *Physica A* **2005**, *352*, 171–201. [CrossRef]
26. Szydlak, R.; Majka, M.; Lekka, M.; Kot, M.; Laidler, P. AFM-based Analysis of Wharton's Jelly Mesenchymal Stem Cells. *Int. J. Mol. Sci.* **2019**, *20*, 4351. [CrossRef] [PubMed]
27. Xu, W.; Mezencev, R.; Kim, B.; Wang, L.; McDonald, J.; Sulchek, T. Cell stiffness is a biomarker of the metastatic potential of ovarian cancer cells. *PLoS ONE* **2012**, *7*, e46609. [CrossRef] [PubMed]
28. Amer, M.H.; White, L.J.; Shakesheff, K.M. The effect of injection using narrow-bore needles on mammalian cells: Administration and formulation considerations for cell therapies. *J. Pharm. Pharmacol.* **2015**, *67*, 640–650. [CrossRef] [PubMed]
29. Heng, B.C.; Hsu, S.H.; Cowan, C.M.; Liu, A.; Tai, J.; Chan, Y.; Sherman, W.; Basu, S. Transcatheter Injection-Induced Changes in Human Bone Marrow-Derived Mesenchymal Stem Cells. *Cell Transplant.* **2009**, *18*, 1111–1121. [CrossRef]
30. Liu, S.; Zhou, J.; Zhang, X.; Liu, Y.; Chen, J.; Hu, B.; Song, J.; Zhang, Y. Strategies to Optimize Adult Stem Cell Therapy for Tissue Regeneration. *Int. J. Mol. Sci.* **2016**, *17*, 982. [CrossRef]
31. Karp, J.M.; Leng Teo, G.S. Mesenchymal stem cell homing: The devil is in the details. *Cell Stem. Cell* **2009**, *4*, 206–216. [CrossRef]
32. Zuk, P.A.; Zhu, M.; Mizuno, H.; Huang, J.; Futrell, J.W.; Katz, A.J.; Benhaim, P.; Lorenz, H.P.; Hedrick, M.H. Multilineage cells from human adipose tissue: Implications for cell-based therapies. *Tissue Eng.* **2001**, *7*, 211–228. [CrossRef] [PubMed]
33. Cristofalo, V.J.; Allen, R.G.; Pignolo, R.J.; Martin, B.G.; Beck, J.C. Relationship between donor age and the replicative lifespan of human cells in culture: A reevaluation. *Proc. Natl. Acad. Sci. USA* **1998**, *95*, 10614–10619. [CrossRef]
34. Danalache, M.; Kliesch, S.-M.; Munz, M.; Naros, A.; Reinert, S.; Alexander, D. Quality Analysis of Minerals Formed by Jaw Periosteal Cells under Different Culture Conditions. *Int. J. Mol. Sci.* **2019**, *20*, 4193. [CrossRef] [PubMed]
35. Klein, G.; Langegger, M.; Timpl, R.; Ekblom, P. Role of laminin A chain in the development of epithelial cell polarity. *Cell* **1988**, *55*, 331–341. [CrossRef]

36. Pilz, G.A.; Braun, J.; Ulrich, C.; Felka, T.; Warstat, K.; Ruh, M.; Schewe, B.; Abele, H.; Larbi, A.; Aicher, W.K. Human mesenchymal stromal cells express CD14 cross-reactive epitopes. *Cytom. Part A J. Int. Soc. Anal. Cytol.* **2011**, *79*, 635–645. [CrossRef]
37. Danalache, M.; Kleinert, R.; Schneider, J.; Erler, A.L.; Schwitalle, M.; Riester, R.; Traub, F.; Hofmann, U.K. Changes in stiffness and biochemical composition of the pericellular matrix as a function of spatial chondrocyte organisation in osteoarthritic cartilage. *Osteoarthr. Cartil.* **2019**, *27*, 823–832. [CrossRef] [PubMed]
38. Costa, K.D.; Yin, F.C. Analysis of indentation: Implications for measuring mechanical properties with atomic force microscopy. *J. Biomech. Eng.* **1999**, *121*, 462–471. [CrossRef]
39. Stolz, M.; Raiteri, R.; Daniels, A.U.; VanLandingham, M.R.; Baschong, W.; Aebi, U. Dynamic elastic modulus of porcine articular cartilage determined at two different levels of tissue organization by indentation-type atomic force microscopy. *Biophys. J.* **2004**, *86*, 3269–3283. [CrossRef]
40. Park, S.; Costa, K.D.; Ateshian, G.A.; Hong, K.S. Mechanical properties of bovine articular cartilage under microscale indentation loading from atomic force microscopy. *Proc. Inst. Mech. Eng. Part H J. Eng. Med.* **2009**, *223*, 339–347. [CrossRef] [PubMed]

Supplementary Materials

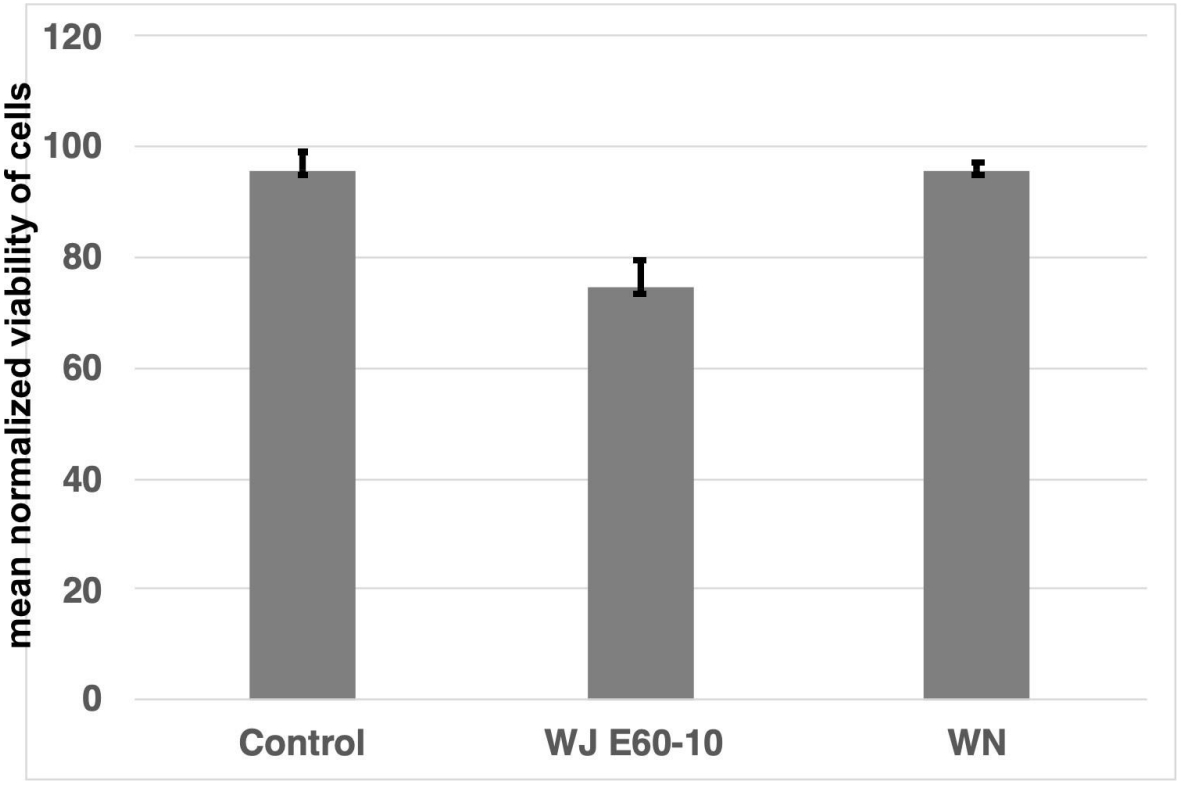

Figure S1: Yield assessment after WN and WJ injections in capture fluid. Injections of pADSCs by cannula (control; 95.8±3.2%; $p<0.001$) or WN (95.8±1.3%, $p<0.001$) yielded higher total yields of cells when compared to WJ injections (74.4 ± 4.94%). Abbreviations: WJ – waterjet, WN – Williams needle.

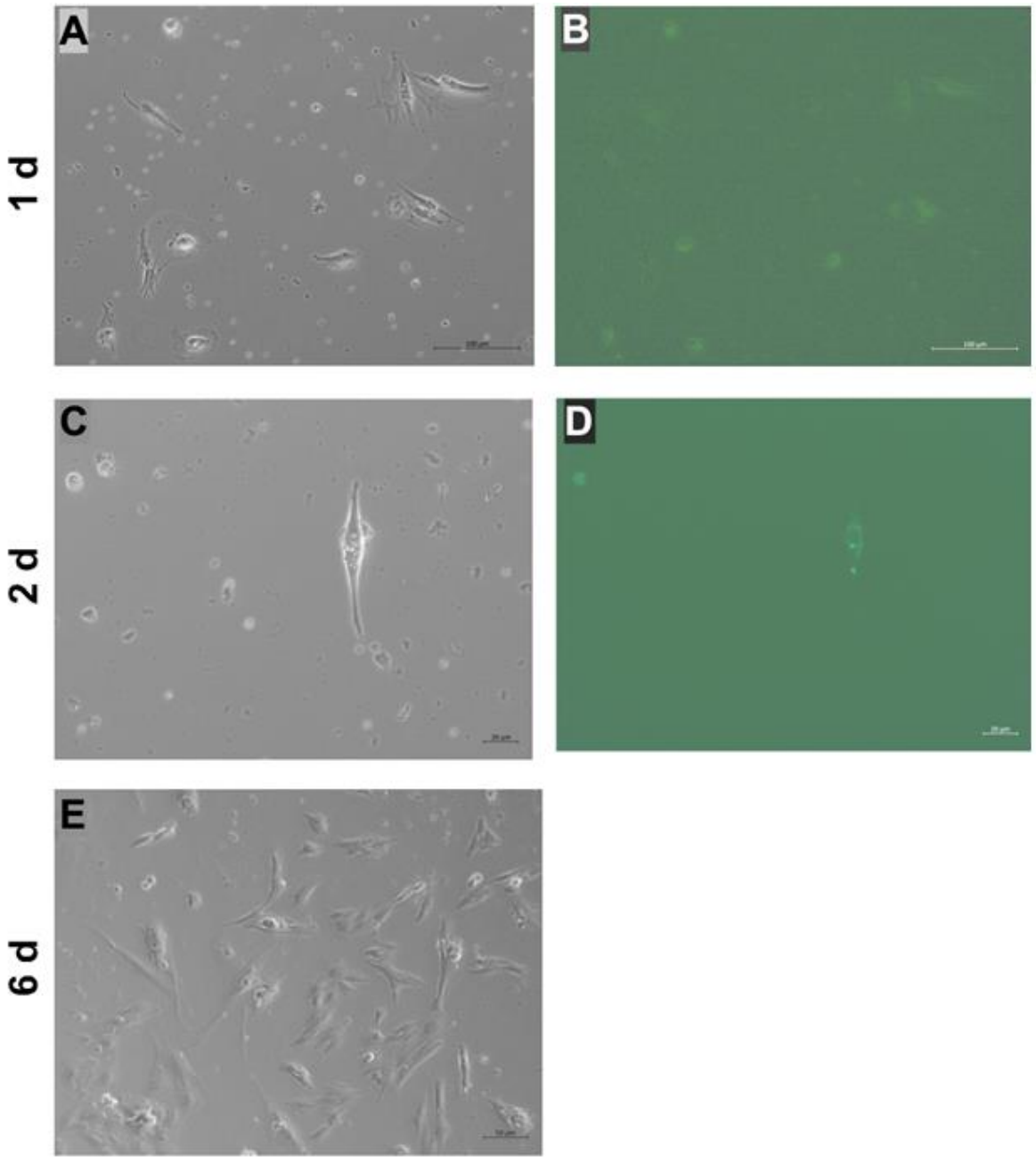

Figure S2: Seeding and proliferation of fluorescence - labelled cells. Cells were labelled with calcein-AM to identify viable cells by green fluorescence. Calcein-labelled cells were WJ injected in tissue samples, collected, washed and seeded in cell culture vessels. By dark field microscopy (A,C,E) cells binding to the vessel were recorded. Fluorescence microscopy (B, D) visualized viable cells. As the calcein coloring dilutes with each cell division, fluorescent cells could not be recorded 6 days after inoculation of the cultures.

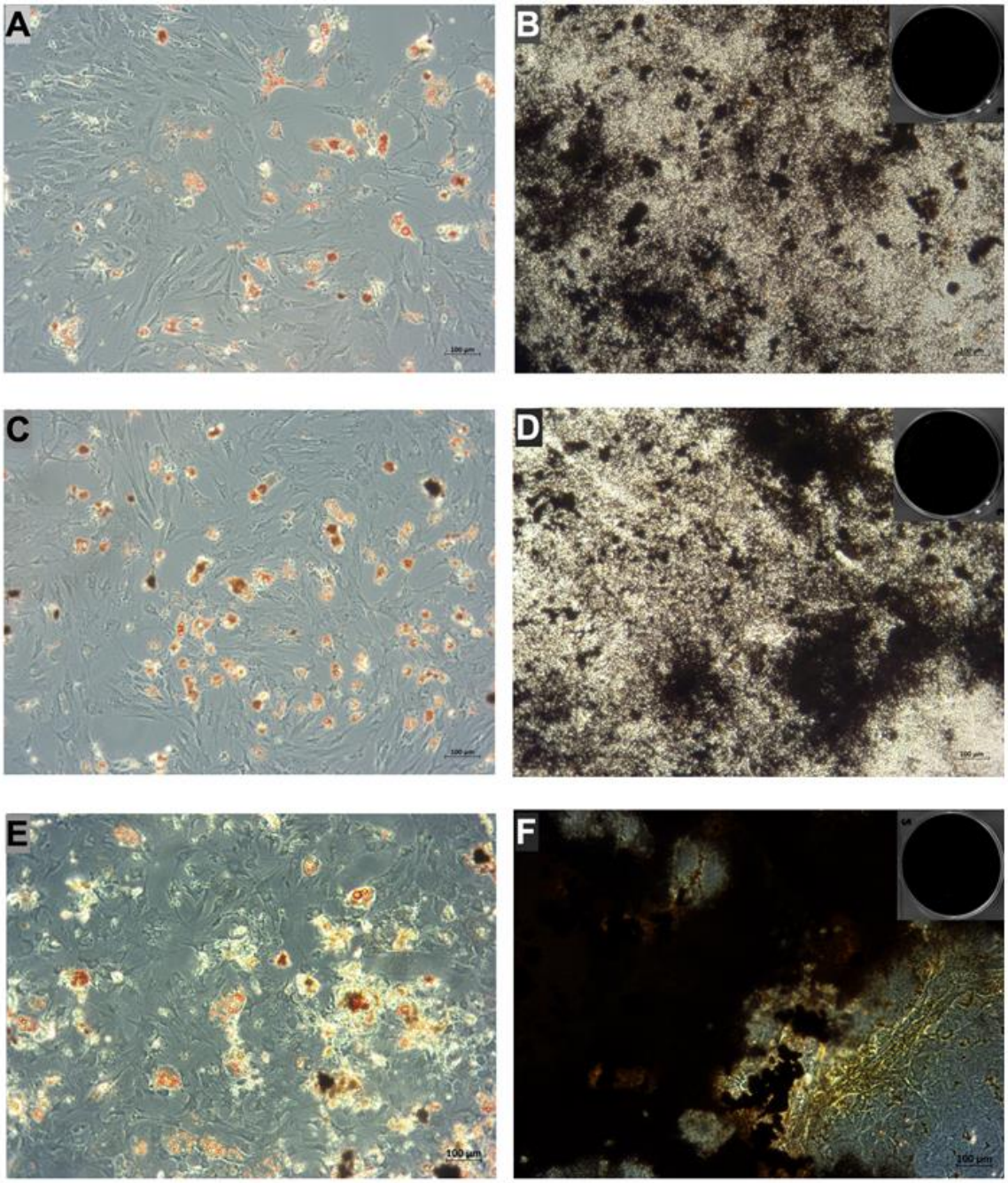

Figure S3: Differentiation of pADSCs after injection by WJ. Adipogenic (A,C,E) and osteogenic (B,D,F) differentiations of pADSCs were induced in vitro by incubation of the cells in the corresponding differentiation media for 4 weeks in 6-well plates. Cells not injected by WJ served as controls (A,B). Cells injected by WJ in capture media (C,D) or in fresh cadaveric porcine sphincter tissue samples (E,F) were collected after WJ injection, washed, counted and incubated as the controls (A,B). After 4 weeks of differentiation, adipocytes were visualized by Oil Red O staining (A,C,E), while mineralization of the matrix by osteoblasts was detected by von Kossa staining (B,D,F) by microscopy. A scan of the total 6-wells is inserted in the upper right micrographs to facilitate the comparison of osteogenesis in the different populations.

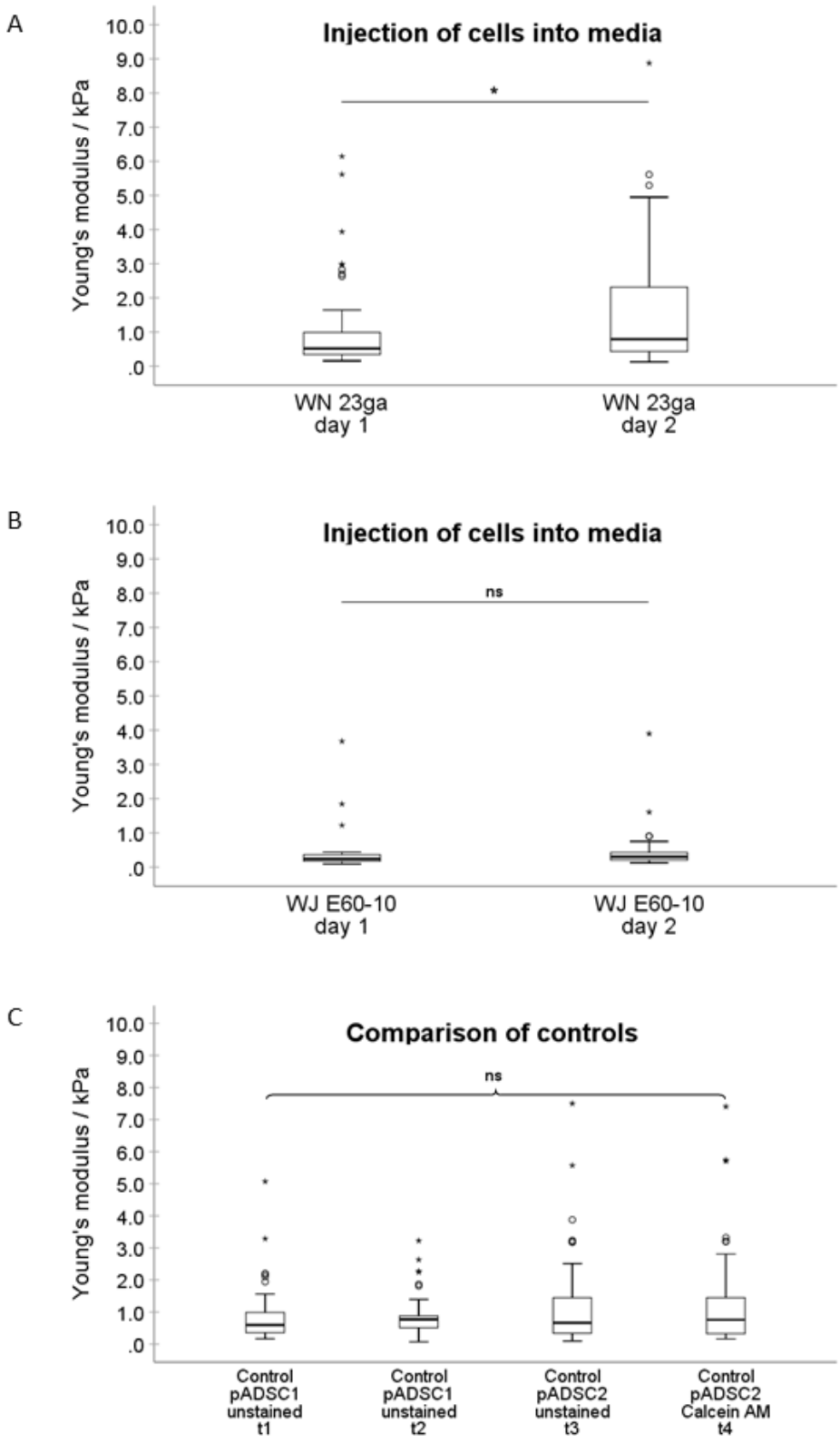

Figure S4: Comparing the results of the Young's modulus in individual experiments. Boxplots (medians, minimum, maximum) of the stiffness (kPa) measured by atomic force microscopy for WN injected pADSCs in capture fluid (A), WJ injected pADSCs in capture fluid (B) and controls at different time points (t, C) are depicted. WN injected pADSCs of two distinct injections revealed a significant difference in stiffness while two distinct WJ injections displayed low but not significant different EM. The compared controls revealed no differences in stiffness even when stained with calcein AM. * $p < 0.05$; ns $p > 0.05$. Abbreviations: WJ – waterjet, WN – Williams needle.

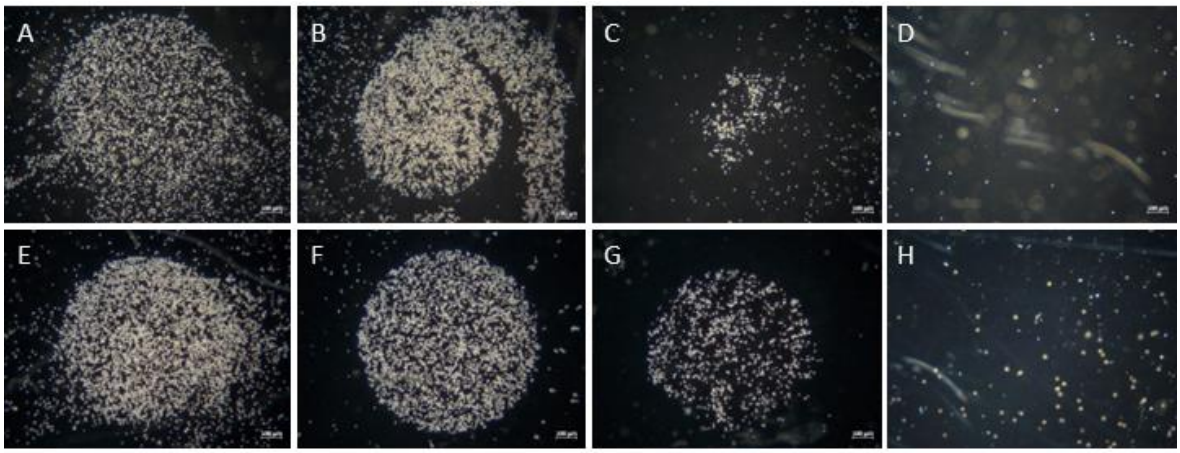

Figure S5: Investigation of the attachment of fluorescence-labelled cells after WJ injection. pADSCs were harvested and subjected to cell attachment assays (unstained controls (A-D) and Calcein AM stained controls (E-H)). Both populations attached to collagen at 1E02 (A,E) and 1E03 (B,F) dilutions, respectively. Unstained control cells weakly attached to collagen at 1E04 (C), while stained control cells showed slightly more attachment. Interaction with BSA served as negative controls (D,H).

11. Publication 2

Replacing Needle Injection by a Novel Waterjet Technology Grants Improved Muscle Cell Delivery in Target Tissues

Ruizhi Geng[1], Jasmin Knoll[1], Niklas Harland[2], Bastian Amend[2], Markus D. Enderle[3], Walter Linzenbold[3], Tanja Abruzzese[1], Claudia Kalbe[4], Elisabeth Kemter[5,6], Eckhard Wolf[5,6], Martin Schenk[7], Arnulf Stenzl[2], and Wilhelm K. Aicher[1*]

[1] Department of Urology, Center for Medical Research, Eberhard Karl University of Tübingen, Tübingen, Germany
[2] Department of Urology, University of Tübingen Hospital, Eberhard Karl University of Tübingen, Tübingen, Germany
[3] Erbe Elektromedizin GmbH, Tübingen, Germany
[4] Institute of Muscle Biology and Growth, Research Institute for Farm Animal Biology, Dummerstorf, Germany
[5] Department of Molecular Animal Breeding and Biotechnology, LMU Munich, Oberschleißheim, Germany
[6] Center for Innovative Medical Models, LMU Munich, Oberschleißheim, Germany
[7] Department of Surgery, University of Tübingen Hospital, Eberhard Karl University of Tübingen, Tübingen, Germany

* Correspondence author

Cell Transplantation

Year 2022, Volume 31, Pages 1–17

doi: 10.1177/09636897221080943

SAGE

Received: 4 August 2021 / Revised: 8 November 2021 / Accepted: 31 January 2022

Abstract

Current regimen to treat patients suffering from stress urinary incontinence often seems not to yield satisfactory improvement or may come with severe side effects. To overcome these hurdles, preclinical studies and clinical feasibility studies explored the potential of cell therapies successfully and raised high hopes for better outcome. However, other studies were rather disappointing. We therefore developed a novel cell injection technology to deliver viable cells in the urethral sphincter complex by waterjet instead of using injection needles. We hypothesized that the risk of tissue injury and loss of cells could be reduced by a needle-free injection technology. Muscle-derived cells were obtained from young male piglets and characterized. Upon expansion and fluorescent labeling, cells were injected into cadaveric tissue samples by either waterjet or injection needle. In other experiments, labeled cells were injected by waterjet in the urethra of living pigs and incubated for up to 7 days of follow-up. The analyses documented that the cells injected by waterjet in vitro were viable and proliferated well. Upon injection in live animals, cells appeared undamaged, showed defined cellular somata with distinct nuclei, and contained intact chromosomal DNA. Most importantly, by in vivo waterjet injections, a significantly wider cell distribution was observed when compared with needle injections ($P < .05$, $n \geq 12$ samples). The success rates of waterjet cell application in living animals were significantly higher (≥95%, $n = 24$) when compared with needle injections, and the injection depth of cells in the urethra could be adapted to the need by adjusting waterjet pressures. We conclude that the novel waterjet technology injects viable muscle cells in tissues at distinct and predetermined depth depending on the injection pressure employed. After waterjet injection, loss of cells by full penetration or injury of the tissue targeted was reduced significantly in comparison with our previous studies employing needle injections.

Keywords

myoblast injection, waterjet technology, cell therapy, muscle regeneration, urinary incontinence, porcine model

Introduction

Urinary incontinence (UI) is a rather frequent condition. The prevalence in adult populations was reported to range from 15% to 35%[1–4]. Stress urinary incontinence (SUI), the most common form of UI, is characterized by involuntary loss of urine under mechanical stress to the lower pelvic floor, for example, by lifting, coughing, or sneezing. In men, prostate surgery is the main risk factor for SUI. In women, SUI is associated with pregnancy and vaginal delivery. SUI is caused by a functional deficiency of the urethral sphincter complex. This may stem from loss of muscle tissue, apoptosis of muscle cells, or loss of muscular enervation[5]. When diagnosed in time, physical exercise of lower pelvic floor muscles may improve sphincter function. Exercise in combination with bio-feedback and/or electrostimulation is a suggested regimen as well[6]. Activation of muscle precursor cells residing in the sphincter tissue may contribute to functional regeneration upon exercise or electrophysiological stimulation[7]. But SUI is a condition caused by severe reduction in sphincter performance due to loss of muscle cells or muscular enervation. Therefore, treatment of SUI requires other strategies[8]. For more severe cases and after failed conservative treatment, current guidelines advice for surgical approaches: Implantation of artificial sphincters and fixing the position of the urethra by artificial supports, for example, by tapes, are common regimens SUI treatment. But the median durability and biocompatibility of implants still fall short of expectations. This motivated preclinical research and clinical feasibility studies investigating the prospects of SUI cell therapy[9–12].

The sphincter complex includes two types of muscle tissue: the lissosphincter, composed of smooth muscles, and the rhabdosphincter, composed of striated muscles. Accordingly, cell therapy of SUI in (pre)clinical studies employed two distinct strategies: strengthening the striated muscle by injection of muscle-derived cells (MDCs)[13–15] or improving smooth muscle function as well as the vascularization and enervation by injection of mesenchymal stromal cells (MSCs), adipose tissue–derived stromal cells (ADSCs), or related cells[11,16,17]. For cell injections, minimally invasive and transurethral approaches are preferred, and cells are injected by needles under visual control using a cystoscope. But recent animal studies provided evidence that needle injections of cells in the sphincter complex by transurethral route using a cystoscope often misplaced the cells[18,19]. Deposition of cells at suboptimal sites or even loss of cells by full penetration of the needle through the delicate urethral

sphincter may in part explain the contradictory situation in reports on SUI cell therapy[10]. To improve precision of cell injection in the urethral sphincter, we developed a novel waterjet (WJ) technology and used primarily ADSCs[20–22]. By this novel technology, cells ride gently in a stream of an isotonic buffer less than 200 μm wide and, if needed, enriched by bioactive molecules such as growth factors or by components facilitating attachment of cells to the injection side[20,21]. The energy of this narrow jet is sufficient to open the smallest cavities, probably less than 500 μm wide, without direct contact of the jet's nozzle to the tissue surface. By preselection of the injection pressure, the energy of the jet can be adapted to the tissue targeted. Thus, full penetration of the urethra by the jet can be avoided[21]. Moreover, in contrast to sturdy injection needles, a WJ does not punch "wide holes" in tissues targeted, thus reducing loss of any active components by reflux and tissue damage, inflammation, or entry of urine in submucosal layers[18,19]. To discover whether regeneration of muscular tissues was potentially facilitated by WJ injection of MDCs, we had to investigate whether myoblasts derived from satellite cells of skeletal muscle tissue can be delivered and recovered with sufficient viability upon injection in tissue samples and survive WJ injection in live animals. In this study, we present evidence that injection of MDCs by WJ in the porcine urethra delivers viable cells fast, simple, and with high precision, minimal tissue damage, and convincing yield.

Material and Methods

Isolation, Cultivation, and Labeling of Porcine MDCs

MDCs were isolated from male wild-type (WT; German Landrace) or transgenic (TG) piglets expressing a near-infrared fluorescent protein (iRFP720 transgene under the control of the ubiquitous active chicken beta actin promoter)[23] about 4 to 5 days after birth and expanded as described[24–26]. In brief, WT piglets were sacrificed using carotid artery bleeding after captive-bolt pistol. TG piglets were sedated (atropine 0.05 mg/kg, intramuscularly and azaperone 4 mg/kg, intramuscularly). After initial sedation, deep anesthesia was established by phenobarbital (150 mg/kg, intramuscularly), confirmed by checking reflexes, and the piglets were sacrificed by carotid artery bleeding. Then the dermis was cleaned and sterilized. The dermis was opened by the aid of scalpel and scissors to prepare musculus longissimus or musculus semitendinosus. Pieces of the muscles were excised aseptically (approximately 15 g wet weight), washed, and transported in enriched phosphate-buffered saline (PBS) on wet ice. Then, the tissue was minced by blade and enzymatically degraded (20 min, 37°C, agitation in digestion buffer: 0.025% trypsin, 0.2% mixed collagenases I + II, 0.01% DNase I in PBS). The supernatant was filtered (100 μm nylon strainer), sedimented (800 × g, 4°C, 10 min), and the pellet was resuspended in Dulbecco's Modified Eagle Medium (DMEM), mixed with digestion buffer again for two additional rounds of tissue degradation. Muscle extracts were pooled. The MDCs were enriched by Percoll step-gradient centrifugation as described (15,000 × g, 4°C, 9 min)[26]. The interface containing mononuclear cells was aspirated, diluted in DMEM, and washed twice by centrifugation. Purified MDCs were expanded in type I collagen–coated flasks in growth medium containing DMEM complemented with 10% fetal bovine serum (FBS), glutamine, and antibiotics as described[24–26]. At cell densities of approximately 70% of confluence, cells were harvested, counted, split in a 1:3 ratio, and expanded further up to their third or fourth passage of in vitro culture to generate cells for characterization and injection experiments.

To visualize injected MDCs and discriminate them from the target tissue, cells were labeled by fluorescent dyes prior to injections in cadaveric urethra samples or in live pigs. In some experiments, MDCs expressing the iRPF720 reporter were employed. Generation of TG pigs was licensed by the Bavarian State Authorities (file # ROB-55.2-2532. Vet_0217-136). For in vitro experiments, MDCs were labeled by calcein-AM and ethidium

homodimer following the manual (Life/dead viability/cytotoxicity kit; Thermo Fisher Scientific, Schwerte, Germany) and injected into fresh porcine cadaveric urethra samples by Williams needle (WN; Cook Medical, Bloomington, IN, USA)[18] or by WJ (Erbe Elektromedizin GmbH, Tübingen, Germany)[20]. For in vivo experiments, MDCs were labeled immediately prior to injections by PKH26 following the manual (PKH26 label kit; Thermo Fisher Scientific)[27], washed with PBS, counted, and prepared for WJ injections. In some experiments, 70% of MDCs were labeled by PKH26 and 30% by a baculovirus system expressing a recombinant enhanced green fluorescent protein (eGFP) as fusion protein to histone 2B as requested by the supplier (CellLight BacMam 2.0; Thermo Fisher Scientific). Efficacies of cell labeling were visualized by microscopy in phase contrast transmitted light versus fluorescence mode (Axiovert A1; Zeiss, Oberkochen, Germany).

Characterization of Porcine MDCs

For analysis of transcript expression, cells were detached by aid of trypsin-EDTA, washed twice with PBS, and sedimented in 1.5 ml centrifugation tubes. Total RNA was extracted using RNeasy mini kits following the manual (Qiagen, Hilden, Germany) and DNA was removed by DNase. Yield and purity of RNA were measured by UV-spectrophotometry (Nanodrop; Implen, München, Germany). Complementary DNA (cDNA) was reverse-transcribed following the manuals (oligo-dT priming, MMLV enzyme, 42°C, 60 min, cDNA kit; Takara Bio Inc., Kusatsu, Shiga, Japan). Transcripts encoding myostatin (*MSTN*), the transcription factors myogenic factor-5 and myogenic factor-6 (*MYF5*, *MYF6*), myogenic differentiation 1 (*MYOD1*), myosin light chain 1 (*MYL1*), as well actin (*ACTA2*) and desmin (*DES*) were detected by quantitative polymerase chain reaction (qPCR) of cDNAs using swine-specific primer pairs (Table 1) and the following amplification protocol: 2 min 94°C for separation of RNA from cDNA and 35 cycles of amplification (30 s 58°C for primer annealing, 60 s 72°C for primer extension, 30 s 94°C for melting of double stands), followed by product completion for 5 min at 72°C (LightCycler 480; SybrGreen PCR amplification kit; Roche, Basel, Switzerland). PCR product amounts of the individual myogenic target genes were normalized to β2-microglobulin (*B2M*) as a housekeeping gene and in addition to an established DNA standard in each run[31,32]. Amplifications without DNA served as negative controls. Melting point analyses and agarose gel electrophoresis of the PCR products confirmed quality and sizes of the amplifications[33].

Table 1: Primers Employed for PCR

Gene	Upper primer	Lower primer	Size	Acc. number	Ref.
ACTA2	CGGGCAGGTCATCACCATC	CGTGTTGGCGTAGAGGTCCTT	160	NM_001164650.1	Maak and Wicke[28]
DES	ACACCTCAAGGATGAGATGGC	CAGGGCTTGTTTCTCGGAAG	176	NM_001001535.1	
MYF5	GCTGCTGAGGGAACAGGTGGA	CTGCTGTTCTTTCGGGACCAGAC	135	NM_001278775.1	Maak and Wicke[28]
MYF6	CGCCATCAACTACATCGAGAGGT	ATCACGAGCCCCCTGGAAT	189	NM_001244672.1	Maak and Wicke[28]
MYL1	CTCTCAAGATCAAGCACTGCG	GCAGACACTTGGTTTGTGTGG	198	NM_214374.2	Maak and Wicke[28]
MYOD1	CACTACAGCGGTGACTCAGACGCA	GACCGGGGTCGCTGGGCGCCTCGCT	145	NM_001002824.1	Maak and Wicke[28]
MSTN	CCCGTCAAGACTCCTACAACA	CACATCAATGCTCTGCCAA	141	NM_214435.2	Maak and Wicke[28]
B2M	ACGGAAAGCCAAATTACCTGAACTG	TCTGTGATGCCGGTTAGTGGTCT	261	NM_213978.1	Kalbe et al[29]
SRY	GACAATCATAGCTCAAACGATG	TCTCTAGAGCCACTTTTCTCC	133	NC_010462.3	Jaillard et al[30]

PCR primer pairs for specific amplification of porcine cDNA and chromosomal DNA. The column “Gene” refers to chromosomal DNA or complementary DNA; columns “upper primer” and “lower primer” refer to all primers in 5′ > 3′ orientation; column “Size” refers to PCR product lengths according to the published sequences in base pairs (bp) and confirmed by electrophoresis in agarose gels; column “Accession Number” denotes the gene bank accession numbers (www.ncbi.nlm.nih.gov); and column “Ref.” refers to a citation where applicable.

The expression of muscle-associated proteins desmin, and fast and slow myosin was investigated on cells by immunofluorescence[34]. To this end, MDCs were seeded in coated chamber slides, incubated overnight in complete medium, washed twice with cold PBS, and fixed by methanol (10 min, −24°C). Methanol was aspirated and cells were rinsed twice with PBS at ambient temperature (AT). Unspecific binding sites were saturated by blocking buffer [5% dry milk powder in 0.1% Tween-20 in PBS (T-PBS), 37°C, 30 min]. The samples were washed twice with T-PBS. Primary antibodies reactive with porcine antigens (Table 2) were dissolved in blocking buffer and incubated in a humidified chamber in the dark at 37°C for 2 h. The primary antibodies were aspirated, and the samples were washed three times with T-PBS at AT. Then fluorescent-labeled detection antibodies were added and incubated (37°C, 1 h, dark; Table 2). The samples were washed

three times with T-PBS at AT, and nuclei were stained by 4′,6-diamidino-2-phenylindole (DAPI). The cells were visualized by fluorescence microscopy (LSM 510 meta; Zeiss). Samples omitting the primary antibodies served as controls.

Table 2: Antibodies Employed

Antigen	Antibody	Source	Label	Dilution	Company
Desmin	IgG, pAB	Rabbit	ø	1:200	Abcam 15200
Fast myosin	Serum	Rabbit	ø	1:200	Abcam 91506
Slow myosin	IgG, mAB	Mouse	ø	1:100	Abcam 11083
Rabbit IgG	IgG, pAB F(ab′)2	Donkey	FITC	1:100	Jackson 711-096-152
Mouse IgG	IgG, pAB F(ab′)2	Donkey	Alexa Fluor 488	1:2,000	Abcam 181289

Antibodies for immunocytochemistry and immunohistochemistry. Antibodies utilized as primary antibodies (lines 1–3) and for detection of primary antibodies (lines 4, 5) of cells in chamber slides or on cryosection. FITC: fluorescein isothiocyanate; pAB: polyclonal antibody; mAB: monoclonal antibody.

Injections of Cells in Porcine Cadaveric Urethra Samples

Fresh cadaveric female porcine urethra samples were obtained from the local abattoir. Debris was removed and a catheter was inserted in the urethra. To mimic the elasticity of lower pelvic floor tissues during cell injections, the urethra was placed on a soft sponge with the ventral side up. By scissors, the urethra was opened longitudinally to gain access to the inner side of the tube as described[20]. For needle injections, a 2-ml syringe was filled with labeled MDCs (2.4E06 ml^{-1} in complete medium) and aliquots of 250 µl were injected by WN (23 gauge; 8 mm tip; Cook Medical; Fig. 1A). For WJ injections, labeled MDCs (6.0E06 ml^{-1} in complete medium) were loaded in the dosing unit of the WJ device and aliquots of 100 µl were injected in orthogonal position using an upgraded pump and controller system (UPaCS) based on an ErbeJet2 device in an improved pressure control mode (IPCM). With this system, cell administration into the desired layer is performed by a two-phase injection. In the first phase, a high-pressure jet of a transport medium is applied at a pressure ≥60 bar to loosen the extracellular matrix of the tissue on its way to the point of treatment and to open small interconnecting micro-lacunae for the cells next to or within the muscle. In a second step, the pressure of the jet is reduced fast to a low level (eg, 10 bars) and cells are gently added to the jet exiting the nozzle[35]. In these experiments, we used pressure settings of 60 bars (Effect 60 = E60) and 80 bars (Effect 80 = E80) for tissue penetration and a pressure of 10 bar (E10) for cell injection[20]. In one set of experiments, cells injected by WN or WJ in cadaveric tissue samples were recovered by

careful aspiration using a G18 needle and syringe. The injection area was flushed once with complete medium to harvest the remaining cells. Cells extracted were pooled, washed once with complete medium, seeded in coated six-well plates, and cultured in complete medium to determine the yield of fluorescent viable MDCs and to study their proliferation after in vitro injections as described recently[20]. In a second set of experiments, injection sides were sealed immediately after cell injections by superglue. The tissue pieces injected were excised to prepare cryosections for histology (see below).

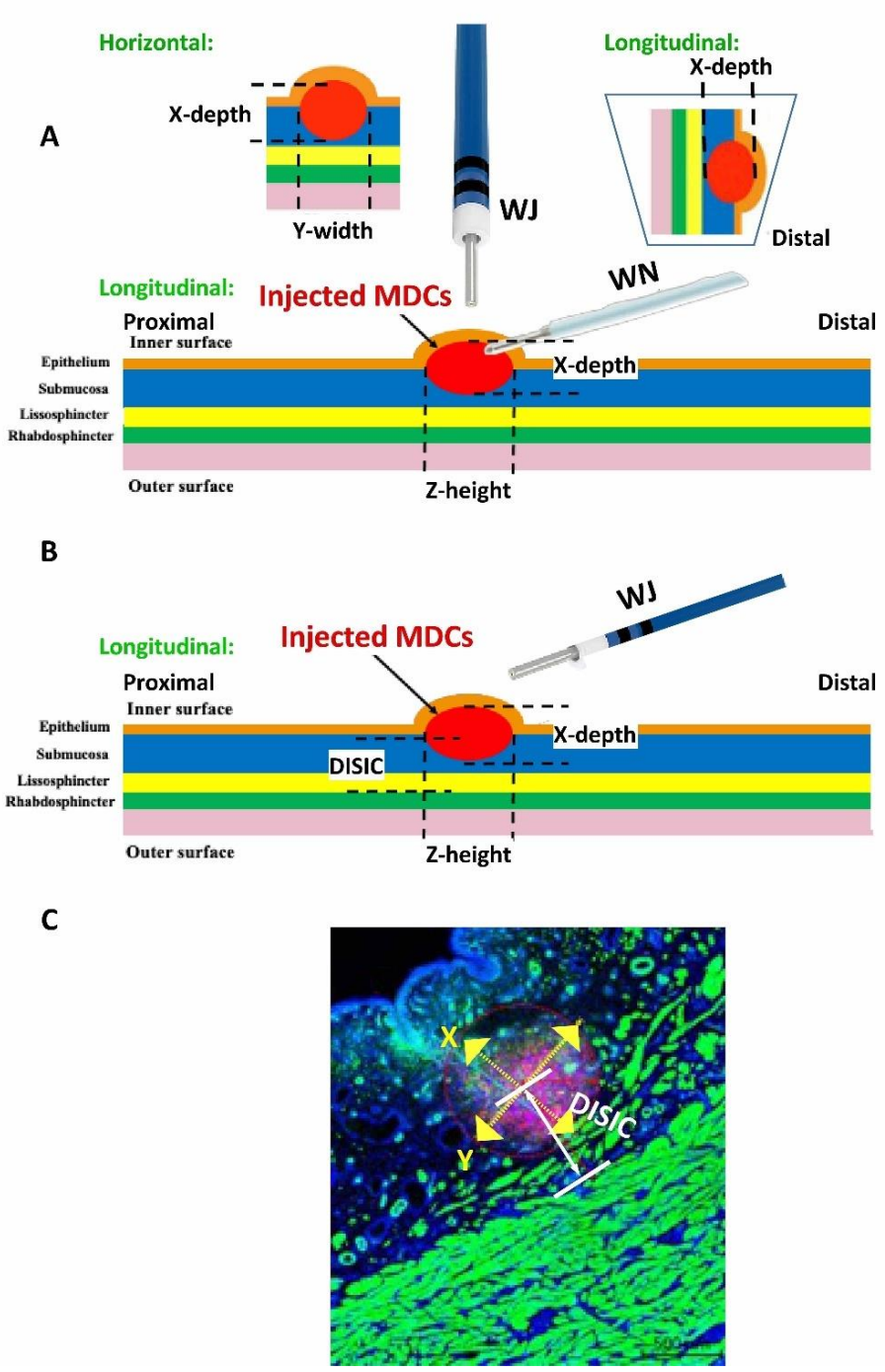

Figure 1: Schematic overview of cell injections. For cell injections in cadaveric urethra samples, the urethra was opened and placed on a sponge with the epithelium (ie, urothelial cell layer) facing up. (A) Injections in the submucosal layer by WN were performed at an angle of approximately 30° to 45°. For cell injections, the tip of the WN was inserted in the tissue for a few millimeters. Injections by WJ were performed vertically. The tip of the WJ lance was lowered by a gauge to the surface of the urothelial layer and moved 2 mm down without tissue penetration to avoid loss of cells by splash to the side caused by the Bernoulli effect. The X- and Y-dimensions for histologic evaluation are explained in the inserts on top. (B) For transurethral cell injections in living animals by aid of cystoscope under visual control, WJ injections were performed. After slightly tilting the device in the urethra, the flexible tip of the injection lance enabled angulated WJ injections in the urethra without penetration of the urothelium. (C) Schematic overview for determination of the distribution of cells in the tissue targeted and determination of DISIC. WN: Williams needle; WJ: waterjet; DISIC: distance between sphincter muscle and injected cells.

WJ Injection of MDCs in the Urethra of Female Pigs

The efficacy of WJ injections of MDCs was studied in vivo in a large animal model[18]. Healthy female landrace hybrid pigs (n = 24, average weight 45 kg) were purchased and adapted to the new habitat at six animals per pen in the University's Animal Facilities under ethical husbandry and veterinarian observation for 7 days prior to surgery. On the day of surgery (day 1), animals were sedated by atropine (0.05 mg/kg, intramuscularly) and azaperone (4 mg/kg, intramuscularly) and then anesthetized (propofol, 4 mg/ kg//h intravenously; fentanyl, 30–100 µg/kg/h intravenously; isoflurane, 0.8–1.6 vol%). The urethra and bladder of each animal were examined prior to the injections by cystoscopy, and healthy urine status was confirmed by urine test strips (Combur10 Test M; Roche). A sensor catheter for determination of the urethral wall pressure was introduced by aid of a cystoscope under visual control (T-Doc 7 Fr dual sensor catheter; Laborie, Enschede, The Netherlands). The urethral wall pressure and the localization of the sphincter complex were determined by urodynamic measurement (Aquarius TT UDS120; Laborie) as described[36]. Fluorescent MDCs were injected in the area of urethral wall pressure maxima (Supplemental Fig. S1) by WJ employing the UPaCS and IPCM at E60-10 and E80-10 settings (Supplemental Fig. S2). After surgical intervention, animals were either sacrificed to prepare urethral tissue samples for immediate analyses (subcutaneously, day 1) or kept in husbandry under veterinarian supervision for a follow-up of 3 or 7 days, respectively, and analyzed thereafter. The animal study was approved by the local Animal Welfare Authorities (file: CU-01/16; NTP: 33978-3-1).

Detection of Injected Cells

For preparation of urethra samples from injected animals, pigs were sedated (atropine 0.05 mg/kg intramuscularly + azaperone 4 mg/kg intramuscularly) and then anesthetized (phenobarbital intravenously, 100 mg/kg), and reflexes were checked. Pigs were sacrificed in deep anesthesia by injection of T61 (0.3 ml/kg). Death was confirmed by checking reflexes and bladder and urethra were prepared. After retrieval, the tissue samples were transported in bags on wet ice immediately to an *In Vivo* Imaging System (IVIS Spectrum; PerkinElmer, Waltham, MA, USA). Fluorescent cells were localized in the urethra by IVIS (Supplemental Fig. S3) and the region of interest was excised. These pieces were embedded in molds in freezing compound (TissueTec O.C.T.; Sakura, Umkirch, Germany) and frozen in liquid nitrogen.

Cryosections were generated (20 μm; CM1860UV; Leica, Wetzlar, Germany), stained by DAPI, and mounted as described[21]. PKH26-labeled cells and cells expressing green fluorescent protein (GFP) were detected by fluorescence microscopy (Observer C1, LSM510 meta; Zeiss). Muscular cells and muscle tissues were visualized by incubation of cryosections with a phalloidin-iFluor488 conjugate (1:1,000; AAT Bioquest; Biomol, Hamburg, Germany). Urethral tissue samples were explored by H&E and AZAN staining as well[36]. Investigating injected MDCs in consecutive cryosections by microscopy determined the distribution of cells in the urethra depending on tissue height (Z-axis; Fig. 1). By automated lateral scanning, the width (Y-axis) and depth (X-axis) of cell distribution were determined in the area of widest distribution of fluorescent MDCs (Observer Z1 with apotome, LSM510 meta, fully automated motorized table; Zeiss). In addition, the distance between sphincter muscle and injected cells (DISIC) was determined. To measure the DISIC, the center of the injected cells was computed on stitched microscopy pictures and the mean distance of the cell center to the rhabdosphincter muscle was computed (Fig. 1C; Zen software; Zeiss). To determine whether cells were intact after WJ injections, DNA was isolated from four to six consecutive cryosections containing PKH26-positive cells. To this end, tissue was scratched off, collected in centrifugation tubes, and DNA extracted following the instructions of the kit (DNeasy blood and tissue DNA extraction kit; Qiagen). The yield and purity of chromosomal DNA were determined by UV spectroscopy (Nanodrop, Implen), and intact chromosomal DNA was confirmed by the detection of the gene encoding sex-determining region (SRY) using pig-specific primers (Table 1) and PCR as described above but using 60°C for primer annealing. The product quality was confirmed by melting point analysis and agarose gel electrophoresis.

Statistics

Experimental data were recorded by proprietary software programs of the individual devices or generated by spreadsheet app (Excel; Microsoft, Albuquerque, NM, USA). For statistical analyses, two-sided unbiased *t* tests were employed (PRISM; GraphPad Software, San Diego, CA, USA). P values below .05 (*) or smaller were regarded significant and marked in the artwork accordingly.

Results

Characterization of Porcine MDCs

Muscle cells were isolated from muscle tissue of young male WT or TG landrace piglets and expanded as described[26]. The MDCs proliferated well *in vitro* up to the sixth passage (Fig. 2A). Prominent expression of the myogenic marker genes *MYOD1*, *DES*, *ACTA2*, and *MYL1* was confirmed by reverse transcription qPCR (RT-qPCR) in all MDC preparations in the third or fourth passage of *in vitro* culture (Fig. 2B). The expression of *MYF5* was lower in MDCs from TG piglets when compared with MDCs from WT piglets, while *MYF6* and *MSTN* were low in both populations (Fig. 2B). In addition, the expression of desmin, and fast- and slow-twitch myosin in MDCs was investigated by immune fluorescence microscopy (Fig. 2C). Desmin expression was observed in MDCs from WT and TG piglets. The expression of fast-twitch myosin was low in WT MDCs and somewhat higher in MDCs from TG animals. The expression of slow-twitch myosin was observed only in a few MDCs of TG animals (Fig. 2C).

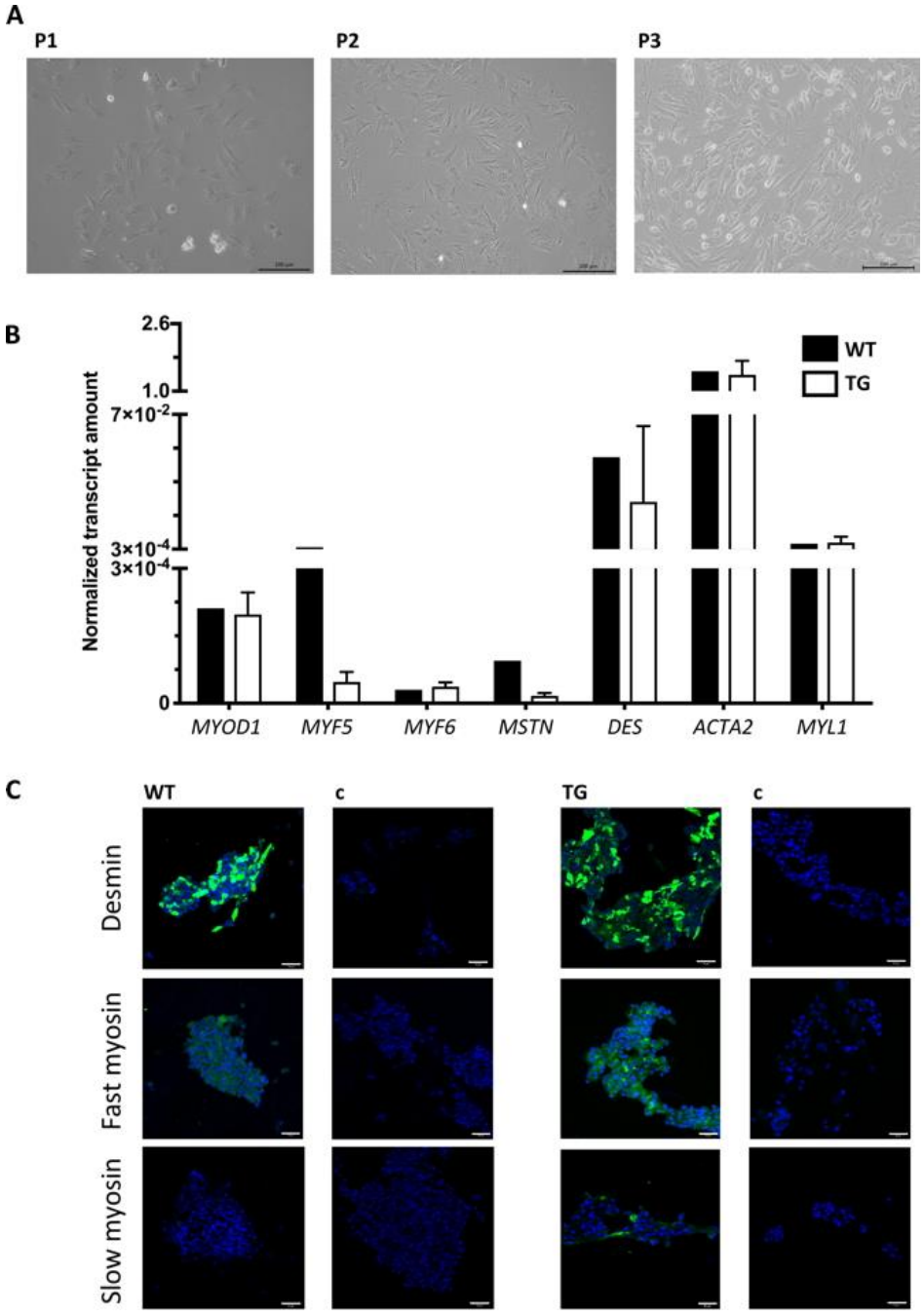

Figure 2: Characterization of porcine MDCs. (A) MDCs were isolated and expanded in vitro. The proliferating MDCs appeared as adherent populations as exemplified for the first three passages P1 to P3. Size bars = 100 µm. (B) The expression of myogenic marker transcripts was explored by RT-qPCR to compare the populations isolated from young WT and TG piglets. The graphic presents the normalized mean transcripts amounts and standard deviations (Y-axis) of seven genes as indicated (X-axis; WT: n = 1, TG: n = 4). (C) The expression of myogenic marker proteins desmin, and fast-twitch and slow-twitch myosin in WT and TG MDCs with specific primary antibodies, followed by counterstaining with FITC-labeled or Alexa 488–labeled detection antibodies (green). Nuclei were counterstained by DAPI (blue). Both populations expressed desmin. Fast myosin was expressed by WT MDCs at low and by TG MDCs at moderate levels. Slow myosin was detected only on a few cells from TG piglets. Size bars = 50 µm. Cells reacted with detection antibodies only served as controls (c). MDCs: muscle-derived cells; WT: wildtype; TG: transgenic; FITC: fluorescein isothiocyanate; DAPI: 4′,6-diamidino-2-phenylindole; RT-qPCR: reverse transcription quantitative polymerase chain reaction.

Injection of MDCs by WJ and WM in Tissue Samples

To explore whether porcine MDCs can be injected by WJ with high viability employing the unmodified prototype lance, cells from male piglets were expanded, harvested, counted, and injected in capture fluid in 16 independent tests. WJ injection using this lance yielded an average normalized MDC viability of 77% ± 10%. In the next experiments, MDCs from young WT piglets were expanded and labeled by calcein-AM to flag viable cells by green fluorescence and injected by WJ or WN in fresh cadaveric urethra samples (n = 12 tests). In addition, injections were performed with TG MDCs (n = 13 tests). In one set (ie, 8× WJ injection and 4× WN injection), cells were collected immediately after injection, washed, and expanded in vitro for up to 5 days of culture. Prominent differences in the yields of fluorescent viable cells were not observed between samples injected by WJ versus WN. Cells directly seeded in culture vessels served as control (Fig. 3A). This corroborated that WJ injections of MDCs delivered viable cells in tissue samples at efficacies comparable to injections by WN, and at the same time confirmed recent studies employing WJ injections of porcine stromal cells[25]. In a second set of experiments, cryosections were generated from cadaveric tissue samples immediately after cell injection of TG or calcein-AM-labeled MDCs by WJ (n = 8) or WN (n = 5). Immune fluorescence microscopy determined the localization of MDCs in cadaveric tissue samples. Fluorescent cells were detected after injections by WN and WJ in all samples investigated (n = 13; Fig. 3B, C). Injections by WN generated fluid-filled domes in the submucosal layer of cadaveric urethrae, and cells tended to cluster at the injection front (Fig. 3B). Injections by WJ stretched the submucosal layer of cadaveric urethrae as well, but the cells tended to yield less compact clusters (Fig. 3C). Comparable patterns were observed upon WJ injection of nano- and microparticles in cadaveric samples (data not shown).

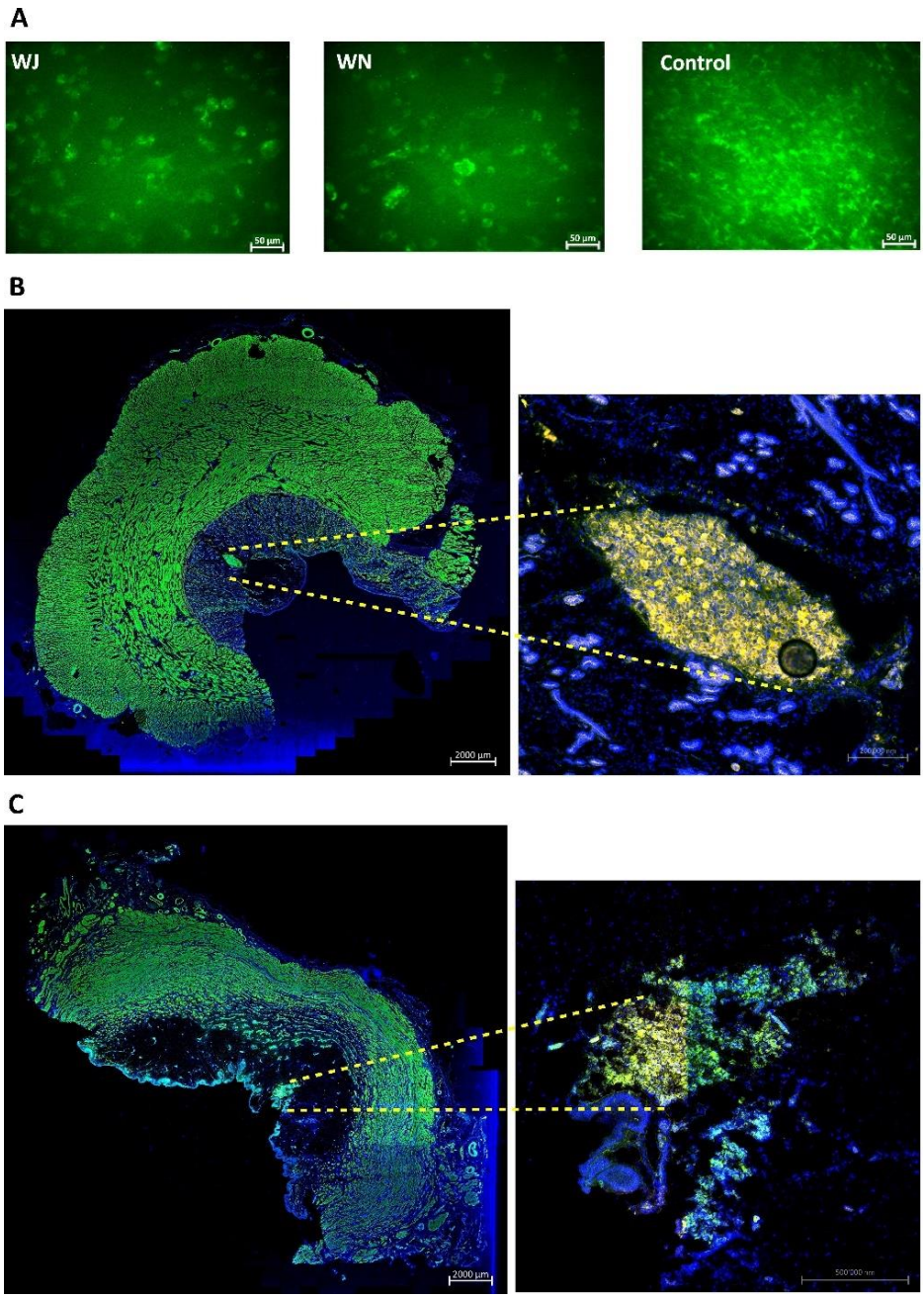

Figure 3: Cell injections in cadaveric tissue samples. (A) Examples of calcein-AM-labeled MDCs injected by WJ or WN in fresh porcine cadaveric urethra samples, aspirated, washed, and seeded in six-well plates for further expansion in culture. Significant differences between yield of viable cells and their proliferation rates were not observed. Noninjected calcein-AM-labeled MDCs served as controls. The pictures are representative artwork from a 5-day follow-up. Size bars indicate 50 µm. (B) TG MDCs were injected by WN in fresh porcine cadaveric urethra samples. Cryosections were generated and stained by fluorescent phalloidin to visualize the injected cells and muscular tissue. The sphincter muscle and injected MDCs appear green in the stitched overview (10× objective, left, size bar 2 mm). Injected TG MDCs appear yellow in the magnified micrograph (20× objective, right, size bar 0.2 mm). (C) TG MDCs were injected by WJ in fresh porcine cadaveric urethra samples. Cryosections were generated and stained by fluorescent phalloidin to visualize the injected cells and muscular tissue. The sphincter muscle and injected MDCs appear green in the stitched overview (10× objective, left, size bar 2 mm). Injected TG MDCs appear yellow in the magnified micrograph (20× objective, right, size bar 0.5 mm). Cell nuclei were counterstained by DAPI (blue). MDCs: musclederived cells; WJ: waterjet; WN: Williams needle; TG: transgenic; DAPI: 4′,6-diamidino-2-phenylindole.

Transurethral Injection of MDCs by WJ in Live Animals

Based on the *in vitro* injections of MDCs (Fig. 3), a preclinical animal study was performed with WJ cell injections. MDCs were produced as described above, characterized, and labeled by PKH26 staining. Prior to each WJ injection, the sphincter complex was localized by measurement of the urethral wall pressure (Supplemental Fig. S1). In the first series of experiments, MDCs were injected by the improved WJ protocol (UPaCS / IPCM) at pressure settings E60-10^{20} (Supplemental Fig. S2) using a further improved prototype lance allowing sidewise injections by bending the lance nozzle. Urethral tissue samples were prepared after 1 h of *in vivo* incubation (ie, day 1) or after 3 and 7 days of follow-up. The injected cells were localized in the urethrae by IVIS (Supplemental Fig. S3), followed by (immuno)fluorescence microscopy of cryosections (Fig. 4A–C). Injected MDCs were observed in 94% of treated animals in the submucosa of the urethra (17/18 animals; Fig. 4A–C). Higher magnification presented fluorescent cell somata with intact nuclei 3 and 7 days after injection (Fig. 4D, E). In a second set of experiments, MDCs were injected by WJ using the improved UPaCS / IPCM at elevated pressure settings (E80-10) and analyzed as described above after 3 days of follow-up (Fig. 5). In 11 of 12 injection sites (ie, 91%), corresponding to treatment of six animals by E80-10 WJ injections, fluorescent MDCs were detected. In stitched micrographs, fluorescent cells were localized mainly in the submucosa of the porcine urethra (Fig. 5A). However, cells appeared somewhat closer to the lissosphincter and rhabdosphincter muscle layers when compared with E60-10 injections. Again, micrographs taken at higher magnification demonstrated fluorescent cell somata with intact cell nuclei (Fig. 5B).

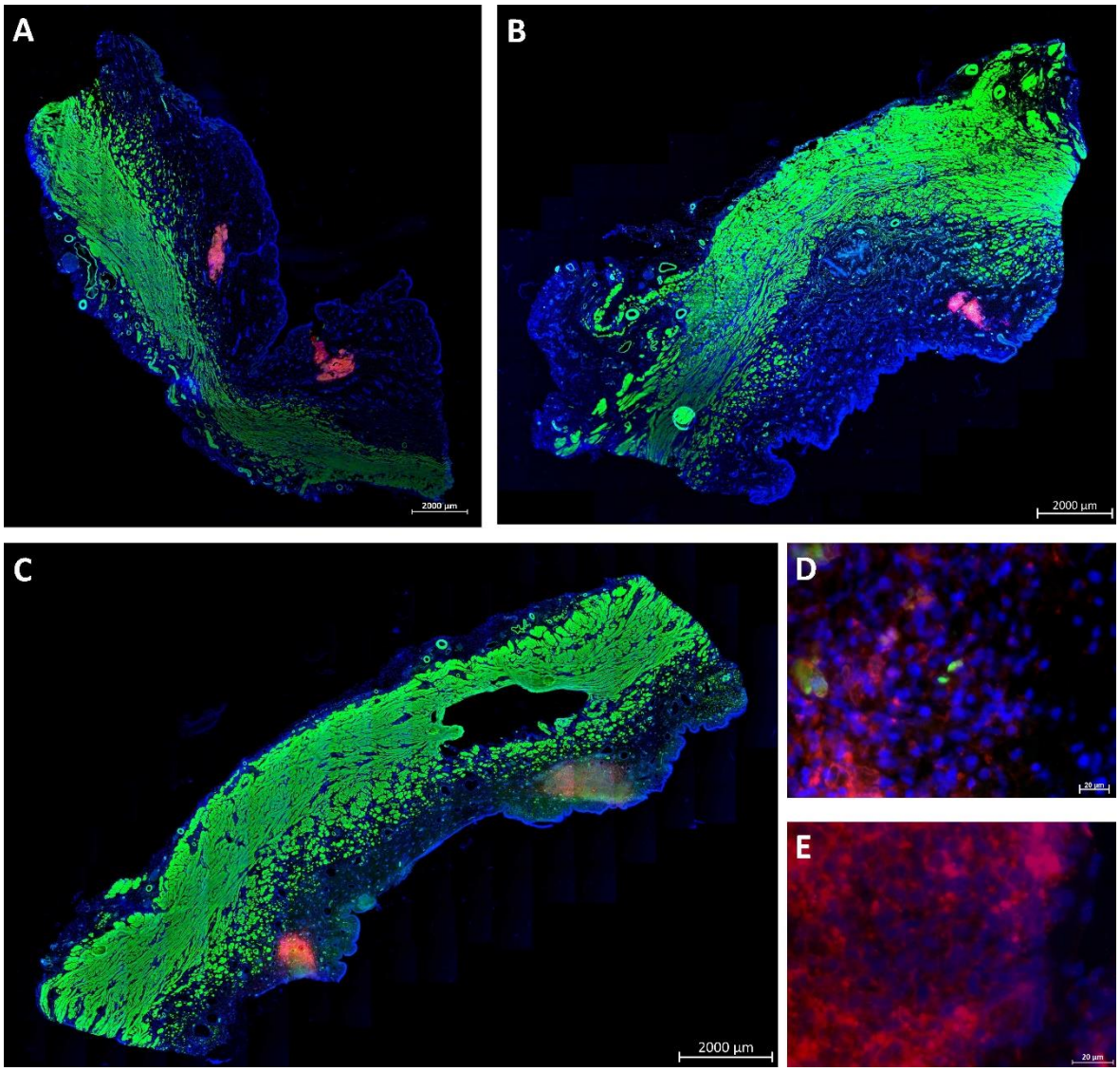

Figure 4: WJ injections in living animals at moderate pressure levels. Stitched micrographs (10× objective) of complete cryosection samples document PKH26-labeled fluorescent red cells in pigs treated by WJ and E60-10 protocol (A) prepared on day 1, (B) on day 3, and (C) on day 7 after injections. Cells are localized in the submucosa. Muscle tissue is stained by phalloidin and appears green, and cell nuclei are counterstained by DAPI and appear blue. Size bars = 2 mm. (D) By larger magnification (40× objective), PKH26 fluorescent cell somata surrounded by defined nuclei and detection of the expression of recombinant GFP suggest that cells injected are intact and alive after 3 days of follow-up. (E) PKH26-labeled cells were also detected after 7 days of follow-up. Size bars = 20 µm. WJ: waterjet; DAPI: 4′,6-diamidino-2-phenylindole; GFP: green fluorescent protein.

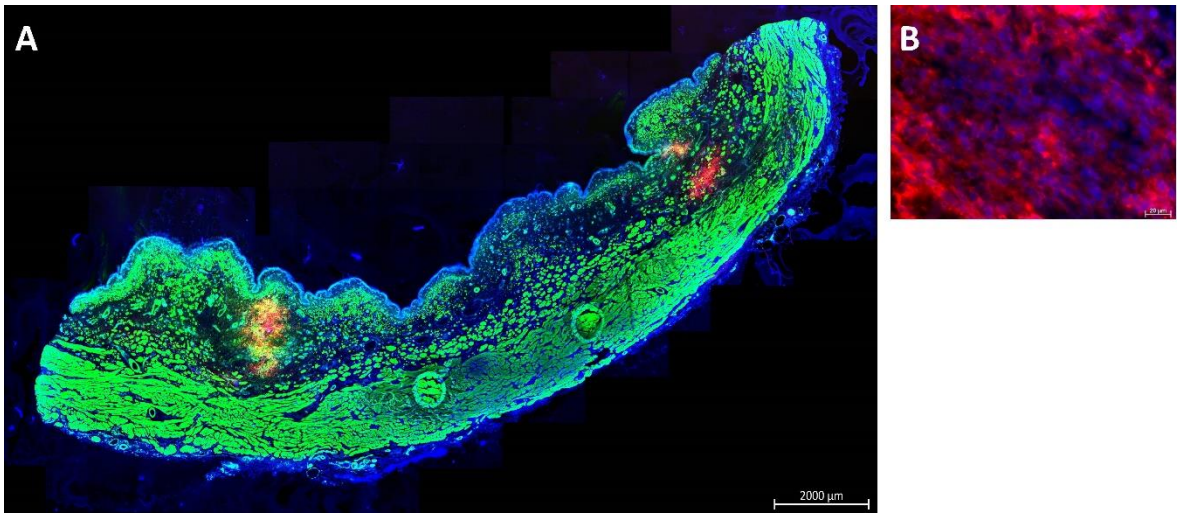

Figure 5: WJ injections in living animals with elevated pressure levels. Stitched micrographs (10× objective, size bar = 2 mm) of complete cryosection samples document PKH26-labeled fluorescent red cells in pigs treated by WJ and E80-10 protocol (A) on day 3 after injection. Cells are localized in the submucosa closer to the muscle. Muscle tissue is stained by phalloidin and appears green, and cell nuclei are counterstained by DAPI and appear blue. (B) By larger magnification (40× objective, size bar = 20 µm), PKH26-labeled fluorescent cell somata surrounded by defined nuclei indicate that the injected cells are intact. WJ: waterjet; DAPI: 4′,6-diamidino-2-phenylindole.

The three-dimensional distribution of cells and the injection depths after injections by WJ versus WN in cadaveric urethra samples, as well as the distribution and injection depths of cells after WJ injection in the urethra of living cells were measured in consecutive cryosections by fluorescence microscopy (Figs. 1 and 6). Rather, narrow cell distribution and no major differences were computed in the X- and Y-dimensions of MDC injections in cadaveric samples in comparison with living animal injections using the E60-10 protocol (Fig. 6A). The computed statistically significant differences between E60-10 injections in X-dimensions in living animals versus cadaveric samples as well as the significance between E80-10 and E60-10 WJ injections in living animals in Y-dimensions were considered biologically irrelevant (Fig. 6A). In contrast, significant differences were noted in the Z-dimension between injections in living animals employing the E80-10 versus E60-10 injection protocol ($n \leq 12$, $P < .005$; Fig. 6A). Comparably, the distribution of cells along the Z-dimension after WN injections in cadaveric samples was significantly higher when compared with WJ injections using the E60-10 protocol ($n \geq 5$, $P < .01$; Fig. 6A).

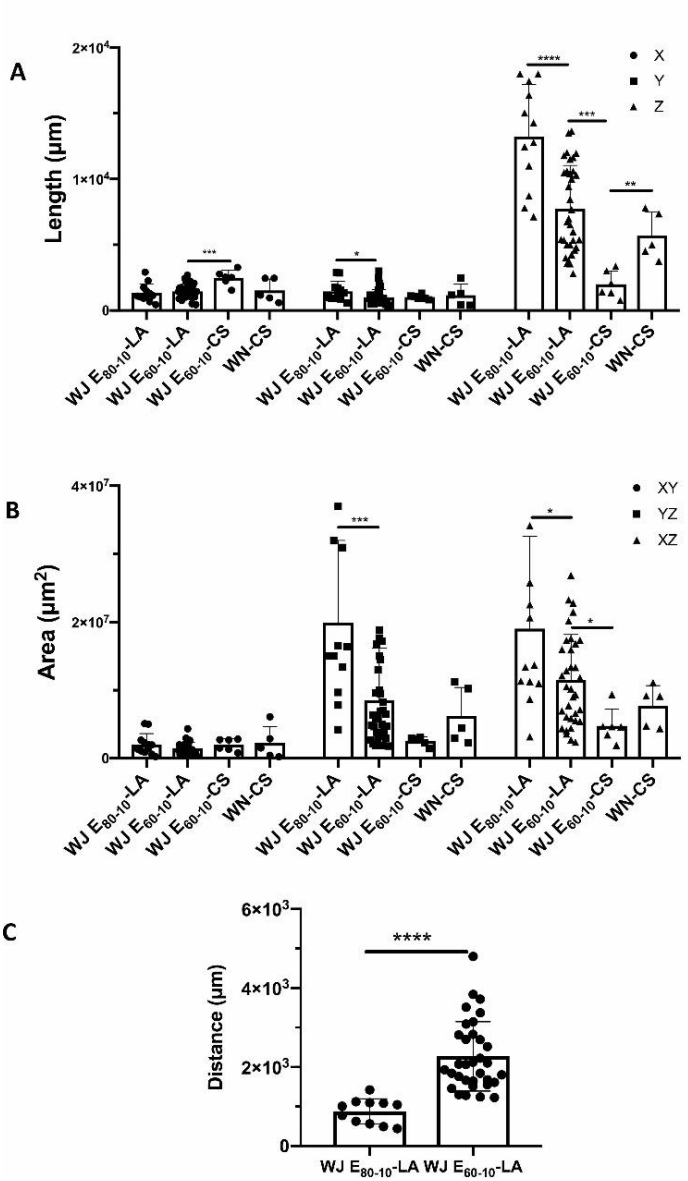

Figure 6: Three-dimensional cell distribution in tissues targeted. (A) Consecutive stacks of cryosections were investigated to determine the distribution of cells in three dimensions after injection by WJ using the E60-10 or E80-10 protocol in LA and after injection in CS by WJ using the E60-10 protocol or by WN as indicated. In the X- and Y-axes, only minor differences were measured. Distribution of MDCs in the height (ie, Z-axis) was significantly higher after WJ E80-10 injections in living animals when compared with WJ E60-10 injections. WJ E60-10 injections in living animals yielded a significantly higher cell distribution when compared with WJ E60-10 injections of MDCs in cadaveric tissue samples. Due to the angular WN injection in cadaveric samples, MDC distribution along the X-axis was significantly higher after WN injection in cadaver tissue samples when compared with perpendicular WJ E60-10 injections. (B) Distribution of cells was also investigated in XY-, YZ-, and XZ-planes as indicated. WJ E80-10 injections in living animals showed a significantly wider distribution in the YZ-plane when compared with WJ 60-10 injections. Comparably, in the XZ-plane, WJ E80-10 injections showed a significantly wider distribution when compared with WJ 60-10 injections. WJ E60-10 LA injections yielded significantly larger distribution in the XZ-plane when compared with injections in cadaveric urethra samples. (C) The distance between the sphincter muscle and the injected cells was significantly higher after WJ E60-10 injections in living animals when compared with WJ E80-10 injections. WJ: waterjet; LA: living animals; CS: cadaveric tissue samples; WN: Williams needle; MDCs: muscle derived cells. Significance levels were *$p \leq 0.05$, **$p \leq 0.01$, ***$p \leq 0.001$, ****$p \leq 0.0001$.

When the cell distribution was calculated from consecutive samples in a two-dimensional manner, the X-Ydistribution ("depth–width") did not differ between E60-10 WJ and WN injections in living animals versus cadaveric samples (Fig. 6B). But in Y-Z-dimensions ("width-height"), the E80-10 in the injection area was significantly larger when compared with E60-10 injections ($n \geq 12$, $P < .005$; Fig. 6B), while E60-10 WJ injections in cadaveric samples in comparison with WN injections did not yield different cell distributions in the Y-Z-dimensions (Fig. 6B). Comparing the cell distribution in the X-Z-plane ("depth– height"), significant differences were obtained upon WJ injections using the E60-10 versus E80-10 mode in living animals ($n \geq 12$, $P < .05$; Fig. 6B). WJ injections in the elevated pressure mode E80-10 generated a wider cell distribution in X-Z-dimensions.

In addition, the DISIC was measured after WJ injections in living animals. Using the E80-10 WJ protocol, cells were injected significantly deeper in the urethra and closer to the rhabdosphincter muscle when compared with E60-10 WJ injections ($n \geq 11$, $P < .005$; Fig. 6C). However, a full penetration of the jet was observed in 1 of 6 animals using the E80-10 WJ protocol (83% success rate; Fig. 7A) but not in any of the 18 animals using the E60-10 protocol. In 1 of 18 animals treated by E60-10 WJ injection, MDCs were found deep in the urethra within the lissosphincter and rhabdosphicter muscles (Fig. 7B). Upon WJ injections, cells were detected by IVIS and in cryosections in samples from 23 of 24 pigs treated. The WJ injections reported here yielded an overall success rate of 95.8%. WJ injections caused a minor bleeding in 8 of 24 animals. This was observed during surgery by transurethral cystoscopy. Small injuries of the inner surface of the porcine urethra were noted in cryosection samples prepared immediately after WJ injections. No visible injuries but small hematoma was observed 3 days after WJ injection, while after 7 days of follow-up hematoma was resolved and only minor tissue coloring was noted (not shown). Infiltration of mononuclear cells was not observed in tissue samples 3 and 7 days after WJ injection (Fig. 8), and the urine status was without pathology in all animals (not shown).

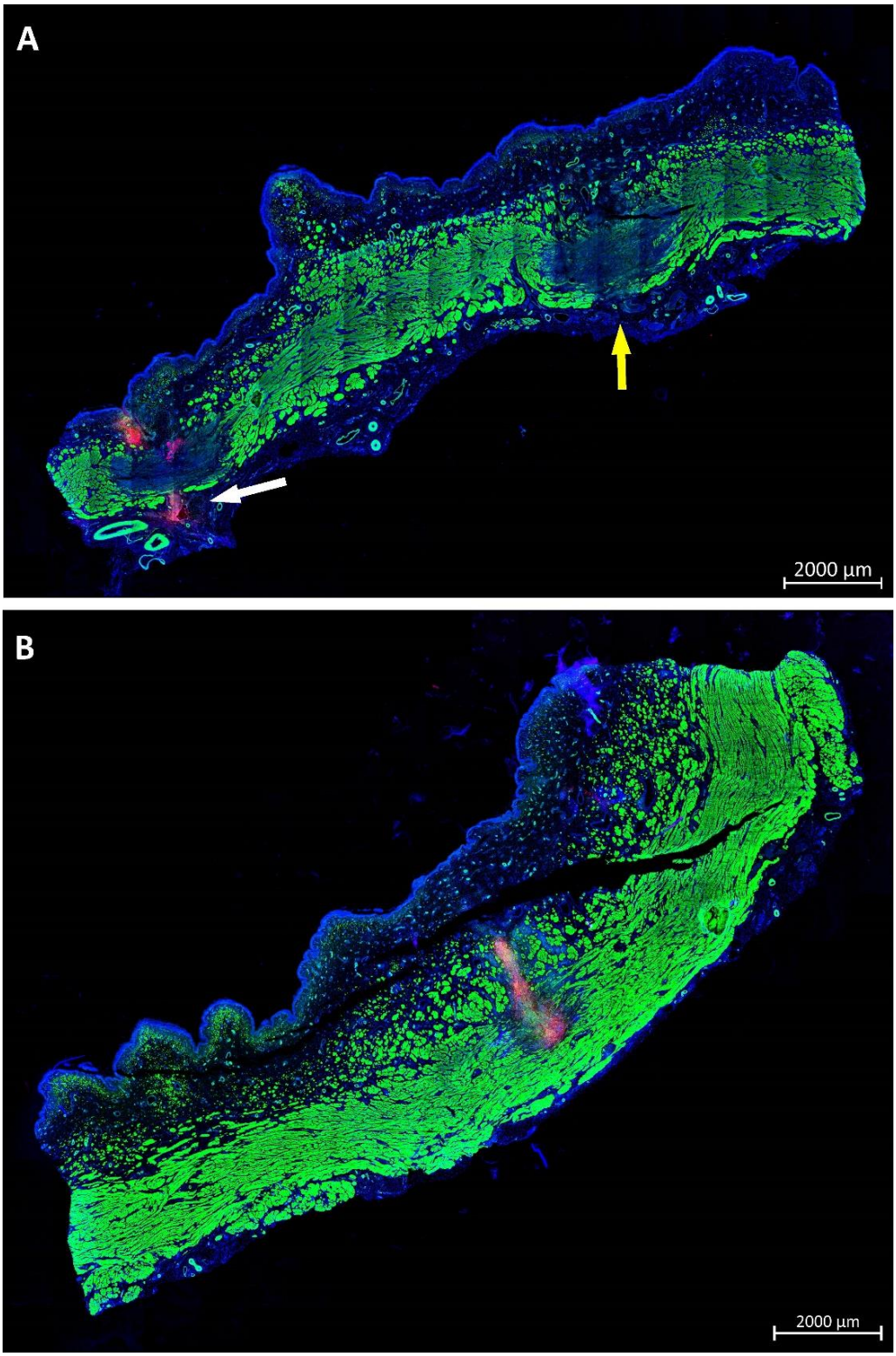

Figure 7: Injection depth reached by WJ in living animals. (A) Cryosamples were generated after WJ injections in living animals and stained by phalloidin and DAPI to label muscle in green and cell nuclei in blue. WJ E80-10 injection of MDCs caused full penetrations on both lateral injection spots in one of six pigs. In one penetration spot, PKH26-labeled MDCs were not detected (yellow arrow), while on the other site PKH26-labeled MDCs were observed outside the urethra (white arrow). (B) WJ E60-10 injections yielded a deep penetration in 1 of 18 pigs, and PKH26-labeled MDCs were detected in the muscular layers of the sphincter complex. Size bars = 2 mm. WJ: waterjet; MDCs: muscle-derived cells; DAPI: 4′,6-diamidino-2-phenylindole.

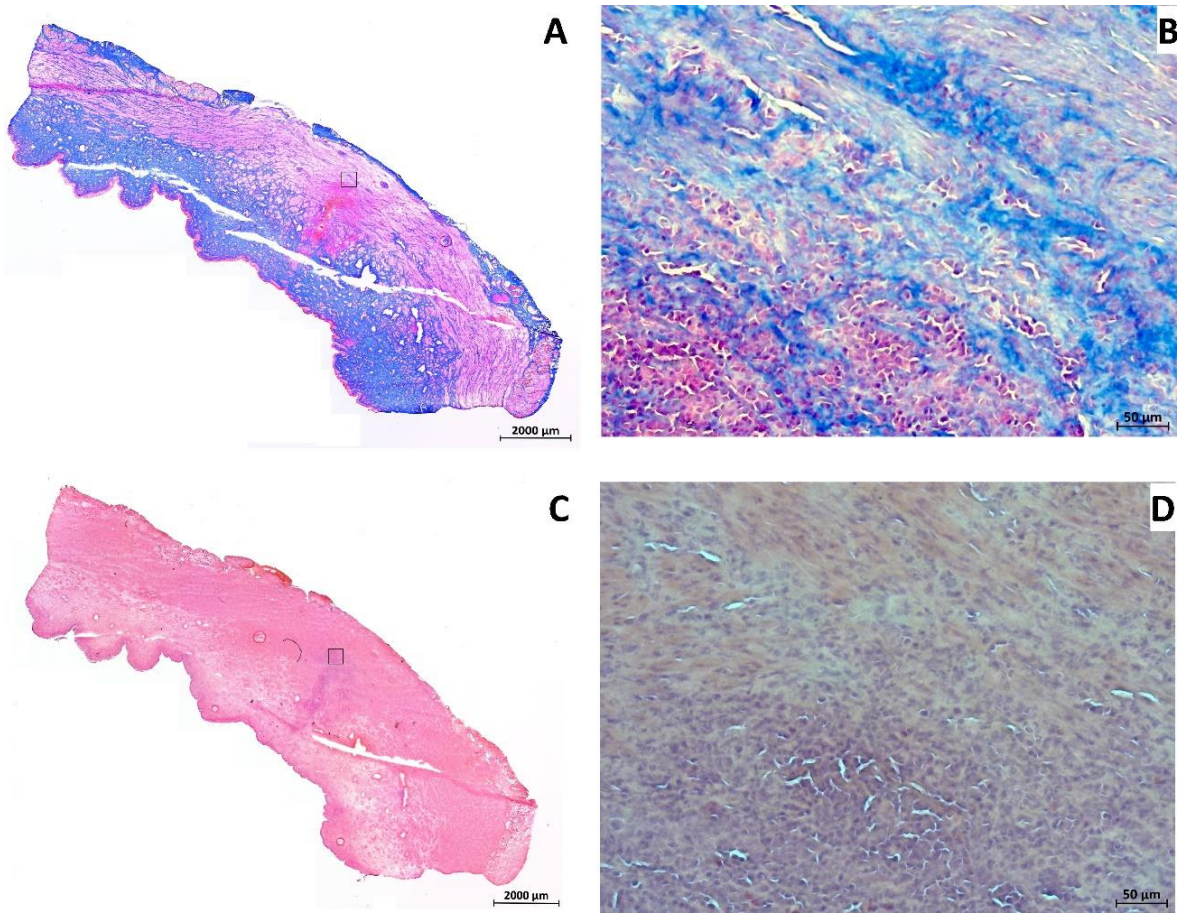

Figure 8: Histological analysis of the urethral tissue after WJ injection. (A) Cryosections from layers containing WJ-injected cells from animals after 7 days of follow-up were stained by AZAN to detect the injected MDCs (red color) within the submucosal connective tissue (blue color; stitched overview; 2.5× objective, size bar = 2 mm). The area of the magnified picture on the left is marked by rectangle. (B) Magnified aspect of the area of MDC injection as indicated (20× objective, size bar = 50 µm). (C) Cryosections from layers containing WJ-injected cells from animals after 7 days of follow-up were stained by H&E to visualize the tissue structure and to detect infiltration of inflammatory cells (stitched overview; 2.5× objective, size bar = 2 mm). The area of the magnified picture on the left is marked by rectangle. (D) Magnified aspect of the area of MDC injection as indicated does not show infiltration of mononuclear cells (20× objective, size bar = 50 µm). WJ: waterjet; MDCs: muscle-derived cells; H&E: hematoxylin and eosin.

Detection of Intact Male DNA in Cryosections of Tissue Samples After WJ Injection

Injection of MDCs in cadaveric samples and retrieval for further culture indicated that WJ injections delivered viable cells at yields comparable to needle injections (Fig. 3). By fluorescence microscopy, intact nuclei of fluorescent cells indicated that the MDCs injected by WJ in living animals appeared intact (Figs. 4 and 5). Infiltration of mononuclear cells as response to necrosis of injected cells was not observed (Fig. 8). This implied that cells injected by WJ were not dead. To verify intact chromosomes in MDCs

after WJ injections in living animals, DNA was isolated from consecutive cryosections containing fluorescent cells to search for the male *SRY* allele by PCR. In samples from all animals investigated, the 133-bp PCR product was detected (Fig. 9). This is evidence that after E60-10 WJ injections and followup of up to 7 days (in 17/18 animals injected) as well as after E80-10 WJ injections with a follow-up of 3 days (in 6/6 animals injected), sufficient numbers of male cells with intact Y-chromosomes remained in the tissue targeted (Fig. 9). From this, we infer that WJ injections delivered cells fast, precisely, and gently in the urethra in this preclinical SUI therapy model in 95.8% of animals included, without provoking a notable inflammatory response.

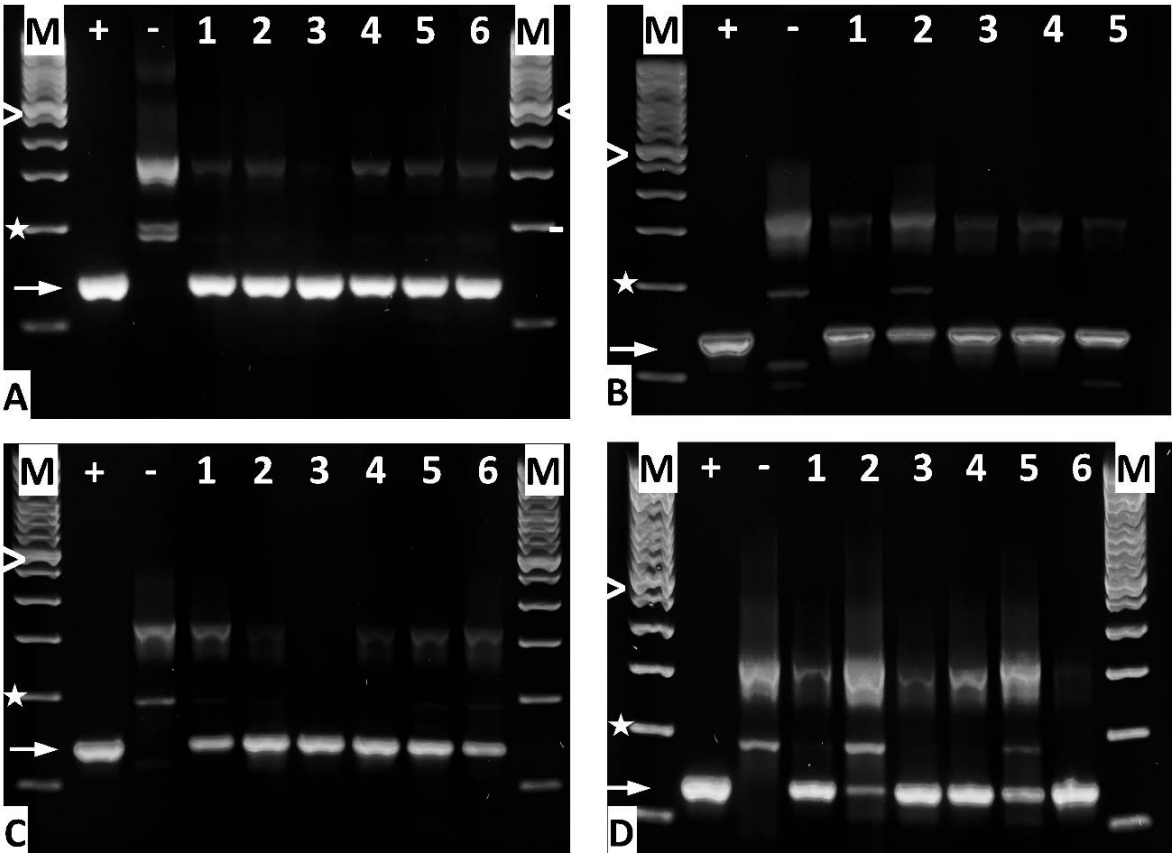

Figure 9: Amplification of the male-specific SRY gene by PCR from cryosections. DNA was prepared to detect the intact SRY gene by PCR after WJ of MDCs using the (A) E60-10 method at day 1 of f/u, (B) E60-10 method on day 3 of f/u, (C) E60-10 method on day 7 of f/u, and (D) E80-10 method on day 3 of f/u. "M" denotes the 100-bp DNA ladder size marker; ">" = 600 bp, "*" = 200 bp, "+" = positive control (DNA from porcine male adipocytes), "–" = negative control (DNA from female porcine adipocytes), and "→" = the 133-bp SRY PCR product. DNA samples from animals are numbered. Note that for E60-10 at 3 days of f/u, cells were found only in five of six animals treated. SRY: sex-determining region; WJ: waterjet; f/u: follow-up.

Discussion

Cell therapy of SUI is not yet a standard procedure despite many successfully completed preclinical animal studies reporting promising results[9,37]. Initially, only a few clinically feasible studies reported success4, the quality and type of cells injected varied considerably[37], large cohort studies with the corresponding control groups were mostly missing[38], follow-up in many studies remained rather short, and outcome was variable and not evaluated consistently. Drop-out during clinical feasibility trials seemed not to be worth reporting. But a recent meta-analysis comparing outcome of midurethral sling surgery versus injection of minced muscular tissue versus *in vitro* expanded myoblasts suggested better efficacy of myoblast injections with a lower risk of adverse effects and less invasiveness, albeit at higher costs[39]. Improving effectiveness of SUI cell therapy was explored by complementing cell injections, for instance, by application of cytokines, chemokines, or extracellular vesicles[4,10,40]. But there is ample evidence that such factors act only for a limited time. They are rapidly adsorbed to different molecules including receptors in the region of interest; they are diluted by serum or lymph, distributed by natural movement of the tissue targeted, or degraded in time. We therefore hypothesized that effectiveness of cell therapies could also be improved further by a simplified, rapid, and even less invasive transurethral cell injection technique.

SUI cell therapies may support self-healing of the urethral sphincter muscle by activating local satellite cells[7], by improving vascularization and reducing inflammation[41,42], or by complementing the deficient sphincter muscle by myogenic cells[5,13–15,43,44]. But these processes may take some time. Cells injected for tissue regeneration or immune modulation can stay in situ and survive for several days[45]. This grants prolonged regenerative activity. However, after injection of cells by needle in the heart muscle, significant loss of cells in time and appearance of injected cells in remote tissues were reported[46]. We conclude that variable outcome of cell therapies and possibly even failure may in part be associated with loss of cells from the tissue targeted by reflux through the injection canal and migration of such cell by lymph or blood through the body. To reduce loss of cells, injection of regeneration competent cells in the presence of biomaterials providing domains for cell attachment was performed[47–49]. Biomaterials were designed to facilitate in situ tissue engineering as well[50]. But all these attempts included needle injections. Moreover, approval of combination therapies of cells plus bioactive components

through authorities such as European Medicines Agency or Food and Drug Administration is very complex. Therefore, improving cell injection technologies in the first place without need for any other components may improve outcome of cell therapies with less efforts.

The MDCs employed in this study expressed *MYOD1*, *MYF5*, and *DES*. This suggested that the cells were enriched for proliferation-competent myogenic progenitor cells (myoblasts)[51]. The expression of *MYL1* and fast-twitch myosin implied that these cells may match the phenotype of fasttwitch muscles cells of the urethral closure complex[52]. But detailed analyses of individual subsets of the MDC phenotype of cells employed here are beyond the focus of this study. However, our study provides evidence that viable MDCs were injected in capture fluid and in cadaveric tissue samples. This confirmed our recent studies[25]. As seen before, WJ injections in cadaveric tissue tended to produce injection bubbles in the urethrae presenting as domes about 2–3 mm wide and 3–4 mm high. In cadaver samples, cells injected were not found distributed in the whole injection area but clustered in the center of the bubble. This could not be prevented by complementing the transportation fluid or injection media by gelatin, serum, or other carrier materials covering integrins and other matrix receptors to avoid cell-to-cell binding (data not shown). We consider this an artifact caused by the tissue stiffness reflecting the cells injected by WJ impulse from the tissue to the center of the bubble. Comparable patterns were observed upon injection of nano- and microparticles in cadaveric samples[20,53,54]. The significantly larger distribution of cells in the z-dimension after angulated WN injection in cadaveric tissue compared with orthogonal WJ application reflects probably efflux of MDCs through the canal punched by the angulated needle in the tissue in combination with the fluid pressure of the injection dome. The significant differences in Z-distribution between WJ injections in living animals and WJ injections in cadaveric tissue may in part be explained by differences in tissue elasticity.

We noted small bleeding during WJ injection in living animals and small hematoma right after it. But hematoma was resolved within a week’s time completely. Infiltration of mononuclear cells was not observed 1 week after injection, although pigs did not get any immune suppressive treatment such as corticosteroids, tacrolimus, or ciclosporin[55]. This confirmed that WJ did not cause major injury, and the small injection canal excised by the narrow WJ was probably spontaneously closing. Urine or infectious microorganisms were therefore not intruding the urethra to a relevant extent, thus facilitating rapid self-healing of the injection site. This selfsealing of epithelia and submucosal tissues after WJ injections is

a well-described observation in gastrointestinal WJ applications and clearly marks a key advantage of this novel method[56–58].

In our recent study, transurethral injections in the porcine urethra by WN reported frequent misplacement or loss of cells (*n* = 96 female pigs). Cells were detected in the urethral mucosa or muscle only in about 50% of animals investigated[18]. Others reported limited accuracy of cystoscope-mediated needle injections as well[19]. In contrast, upon transurethral WJ injection, fluorescent MDCs were found in urethrae in 95% of animals included (23/24) by IVIS in tissue samples and by fluorescence microscopy in the corresponding cryosections. Moreover, full penetration of the urethra, often observed after injection of cells by WN[18], was noticed only in one pig after an E80-10 WJ injection, but not at all after E60-10 WJ injection. On the other hand, the E80-10 injection delivered cells significantly closer to the urethral muscle layer when compared with E60-10 injection, corroborating our recent study with stromal cells[21]. However, in (pre)clinical situations, the deeper penetration of the E80-10 jet and precise delivery of cells close to the sphincter muscle must be balanced with the elevated risk of cell loss by full penetration and raised up tissue injury. In this study, we also did not investigate the localization and distribution of cells after two versus four WJ injections. Due to the comparably low impact of the E60-10 WJ, repeated E60-10 injections could improve the distribution and place more cells closer to the urethral muscle when compared with two E80-10 applications without increasing the risk of unwanted side effects. Moreover, a precise, deeper, and wider delivery of cells may be achieved by adjusting the duration of the twophase injection. Here, we held the duration constant to avoid any parameter changes during the study. But this remains to be investigated in the next level of studies. Investigation of cell survival upon needle injection reported that slow flow rates decreased the percentage of viable cells delivered and increased the percentage of cells undergoing apoptosis within 2 days[59]. This result is in favor of short contact times of cells to any narrow injection devices. The two-phased WJ technology grants such a short transportation time.

Detection of the *SRY* gene by PCR in samples from animals 3 and 7 days after WJ injection documented that the injected male cells contained sufficiently intact DNA for amplification of this allele. As this experiment was performed as end-point PCR, a quantification of the products to determine the number of intact cells is technically impossible. But it supports the notion that intact appearing cells with defined nuclei were observed immediately after WJ injection, as well as after 3 and 7 days of follow-up.

Evidence for necrosis of injected cells or tissue nearby was not detected by H&E staining of cryosections. However, in the preclinical context of this study, investigation of cell viabilities is only the first level of evaluation. To examine the efficacy of the WJ technology for the clinical use intended, future experiments must include additional studies to determine optimal cell doses, single versus multiple injections in one session, repeating cell injections during follow-up, and possibly other therapies in a suitable animal model documenting functional sphincter regeneration. To this end, a porcine model of UI was developed recently[36]. But these aspects were not yet addressed in our current studies.

Conclusion

Based on this preclinical model of cell therapy of UI, we conclude that MCDs can be injected by cystoscope under visual control precisely and close to the urethral sphincter muscle by the novel WJ technology. Using the moderate E60-10 pressure mode, cells are delivered with significantly higher success rates when compared with cell injections by WN and appear intact during a follow-up of up to 7 days. However, the regenerative potential of MDCs to regenerate a deficient sphincter muscle must be investigated in an animal model with UI in future studies.

Author Contributions

RG, JK, NH, TA, and WKA were involved in cell production, quality management, animal study, and evaluation of data. WL and MDE were involved in the development of waterjet. JK, TA, and WKA were involved in cell transduction. CK helped in obtaining the WT cells. EK and EW helped in obtaining the CAGiRFP720 tg pigs. MS helped with animal husbandry. BA, MDE, AS, and WKA were involved in study design and funds. All authors contributed to the preparation of the manuscript and critically revising it.

Acknowledgments

The authors thank Dr Barbara Keßler for essential logistics and tissue samples; Christine Fahrner, Andreas Fech, A. Luise Jäger, Anne Berndt, Marie Jugert-Lund, and Vera Rothfuß for experimental support; and Dr. Nicolas Beziere for IVIS analyses.

Ethical Approval

This article does not contain any studies with human subjects. Ethical approval is therefore not applicable.

Statement on Human and Animal Rights, Approval of Animal Study

This article does not contain any studies with human subjects. The animal study was approved by the State of Baden-Württemberg Animal Welfare Authorities under file number CU-01/16 and was registered in the Federal NTP Registry under file number 33978-31. All experiments involving animals were conducted in accordance with the guidelines and recommendations of the Federation of European Laboratory Animal Science Associations (FELASA) according to the “ARRIVE” rules and National Law[60].

Statement of Informed Consent

There are no human subjects in this article. Informed consent is not applicable.

Declaration of Conflicting Interest

The author(s) declared the following potential conflicts of interest with respect to the research, authorship, and/or publication of this article: WL and MDE are employed by ERBE Elektromedizin GmbH. ERBE Elektromedizin GmbH and WKA have received joined public funding from the Federal Government under file # 13GW007. All other authors declare that the research presented in this study was conducted in the absence of any commercial or financial relationships that could be construed as a potential conflict of interest.

Funding

The author(s) disclosed receipt of the following financial support for the research, authorship, and/or publication of this article: This project was supported in part by grants from the EU to WKA (MUS.I.C., #731377); the BMBF to MDE and WKA (Multimorb-INKO, # 13GW007); the DFG to BA, AS, and WKA (PoTuS, #429049495); from the EU's Horizon 2020 program to EK and EW (iNanoBIT, # 760986); from the BMBF to the German Centre for Diabetes Research to EW (DZD e.V., # 82DZD00802); from Zukunftsfonds, FBN Dummerstorf to CK; and in part by institutional funds.

References

1. Broome BAS. The impact of urinary incontinence on self-efficacy and quality of life. Health Qual Life Outcomes. 2003; 1(1):35.
2. Irwin DE, Kopp ZS, Agatep B, Milsom I, Abrams P. Worldwide prevalence estimates of lower urinary tract symptoms, overactive bladder, urinary incontinence and bladder outlet obstruction. BJU Int. 2011;108(7):1132–38.
3. Norton P, Brubaker L. Urinary incontinence in women. Lancet. 2006;367(9504):57–67.
4. Hillary CJ, Roman S, MacNeil S, Aicher WK, Stenzl A, Chapple CR. Regenerative medicine and injection therapies in stress urinary incontinence. Nat Rev Urol. 2020;17(3):151–61.
5. Schmid FA, Williams JK, Kessler TM, Stenzl A, Aicher WK, Andersson KE, Eberli D. Treatment of stress urinary incontinence with muscle stem cells and stem cell components: chances, challenges and future prospects. Int J Mol Sci. 2021;22(8):3981.
6. Lukacz ES, Santiago-Lastra Y, Albo ME, Brubaker L. Urinary incontinence in women: a review. JAMA. 2017;318(16):1592– 604.

7. Yiou R, Lefaucheur JP, Atala A. The regeneration process of the striated urethral sphincter involves activation of intrinsic satellite cells. Anat Embryol (Berl). 2003;206(6):429–35.
8. Klauser A, Frauscher F, Strasser H, Helweg G, Kölle D, Strohmeyer D, Stenzl A, zur Nedden D. Age-related rhabdosphincter function in female urinary stress incontinence. J Ultrasound Med. 2004;23(5):631–37.
9. Herrera-Imbroda B, Lara MF, Izeta A, Sievert KD, Hart ML. Stress urinary incontinence animal models as a tool to study cell-based regenerative therapies targeting the urethral sphincter. Adv Drug Deliv Rev. 2015;82–83:106–16.
10. Bennington J, Williams JK, Andersson K-E. New concepts in regenerative medicine approaches to the treatment of female stress urinary incontinence. Curr Opin Urol. 2019;29(4):380–84.
11. Yiou R, Mahrouf-Yorgov M, Trebeau C, Zanaty M, Lecointe C, Souktani R, Zadigue P, Figeac F, Rodriguez AM. Delivery of human mesenchymal adipose-derived stem cells restores multiple urological dysfunctions in a rat model mimicking radical prostatectomy damages through tissue-specific paracrine mechanisms. Stem Cells. 2016;34(2):392–404.
12. Williams JK, Dean A, Badlani G, Andersson K-E. Regenerative medicine therapies for stress urinary incontinence. J Urol. 2016;196(6):1619–26.
13. Eberli D, Aboushwareb T, Soker S, Yoo JJ, Atala A. Muscle precursor cells for the restoration of irreversibly damaged sphincter function. Cell Transplant. 2012;21(9):2089–98.
14. Mitterberger M, Pinggera GM, Marksteiner R, Margreiter E, Plattner R, Klima G, Bartsch G, Strasser H. Functional and histological changes after myoblast injections in the porcine rhabdosphincter. Euro Urol. 2007;52(6):1736–43.
15. Peters KM, Dmochowski RR, Carr LK, Robert M, Kaufman MR, Sirls LT, Herschorn S, Birch C, Kultgen PL, Chancellor MB. Autologous muscle derived cells for treatment of stress urinary incontinence in women. J Urol. 2014;192(2): 469–76.
16. Gotoh M, Yamamoto T, Shimizu S, Matsukawa Y, Kato M, Majima T, Takai S, Funahashi Y, Toriyama K. Treatment of male stress urinary incontinence using autologous adiposederived regenerative cells: long-term efficacy and safety. Int J Urol. 2019;26(3):400–405.
17. Kuismanen K, Sartoneva R, Haimi S, Mannerström B, Tomás E, Miettinen S, Nieminen K. Autologous adipose stem cells in treatment of female stress urinary incontinence: results of a pilot study. Stem Cells Transl Med. 2014;3(8):936–41.
18. Amend B, Kelp A, Vaegler M, Klunder M, Frajs V, Klein G, Sievert KD, Sawodny O, Stenzl A, Aicher WK. Precise injection of human mesenchymal stromal cells in the urethral sphincter complex of Gottingen minipigs without unspecific bulking effects. Neurourol Urodyn. 2017;36(7):1723–33.
19. Burdzinska A, Dybowski B, Zarychta-Wisniewska W, Kulesza A, Hawryluk J, Graczyk-Jarzynka A, Kaupa P, Gajewski Z, Paczek L. Limited accuracy of transurethral and periurethral intrasphincteric injections of cellular suspension. Neurourol Urodyn. 2018;37(5):1612–22.

20. Jager L, Linzenbold W, Fech A, Enderle M, Abruzzese T, Stenzl A, Aicher WK. A novel waterjet technology for transurethral cystoscopic injection of viable cells in the urethral sphincter complex. Neurourol Urodyn. 2020;39(2):594–602.
21. Linzenbold W, Jager L, Stoll H, Abruzzese T, Harland N, Beziere N, Fech A, Enderle M, Amend B, Stenzl A, Aicher WK. Rapid and precise delivery of cells in the urethral sphincter complex by a novel needle-free waterjet technology. BJU Int. 2021;127(4):463–72.
22. Danalache M, Knoll J, Linzenbold W, Enderle M, Abruzzese T, Stenzl A, Aicher WK. Injection of porcine adipose tissuederived stromal cells by a novel waterjet technology. Int J Mol Sci. 2021;22(8):3958.
23. Dinnyes A, Schnur A, Muenthaisong S, Bartenstein P, Burcez CT, Burton N, Cyran C, Gianello P, Kemter E, Nemeth G, Nicotra F, et al. Integration of nano- and biotechnology for beta-cell and islet transplantation in type-1 diabetes treatment. Cell Prolif. 2020;53(5):e12785.
24. Mau M, Kalbe C, Viergutz T, Nurnberg G, Rehfeldt C. Effects of dietary isoflavones on proliferation and DNA integrity of myoblasts derived from newborn piglets. Pediatr Res. 2008;63(1):39–45.
25. Kalbe C, Mau M, Wollenhaupt K, Rehfeldt C. Evidence for estrogen receptor alpha and beta expression in skeletal muscle of pigs. Histochem Cell Biol. 2007;127(1):95–107.
26. Metzger K, Tuchscherer A, Palin MF, Ponsuksili S, Kalbe C. Establishment and validation of cell pools using primary muscle cells derived from satellite cells of pig skeletal muscle. In Vitro Cell Dev Biol Anim. 2020;56(3):193–99.
27. Kelp A, Abruzzese T, Wöhrle S, Frajs V, Aicher WK. Labeling mesenchymal stromal cells with PKH26 or vybrantdil significantly diminishes their migration, but does not affect their viability, attachment, proliferation and differentiation capacities. J Tissue Sci Engin. 2017;8:199.
28. Maak S, Wicke M. Analysis of gene expression in specific muscles of swine and turkey. Arch. Tierz. 2005;48:135–40.
29. Kalbe C, Mau M, Rehfeldt C. Developmental changes and the impact of isoflavones on mRNA expression of IGF-I receptor, EGF receptor and related growth factors in porcine skeletal muscle cell cultures. Growth Horm IGF Res. 2008;18(5):424–33.
30. Jaillard S, Holder-Espinasse M, Hubert T, Copin MC, DuterqueCoquillaud M, Wurtz A, Marquette CH. Tracheal replacement by allogenic aorta in the pig. Chest. 2006;130(5):1397–404.
31. Rasmussen R, Morrison T, Herrmann M, Wittwer C. Quantitative PCR by continuous fluorescence monitoring of a double strand DNA specific binding dye. Biochemica. 1998;2:8–11.
32. Pfaffl MW. A new mathematical model for relative quantification in real-time RT-PCR. Nucleic Acids Res. 2001;29(9):e45.
33. Ausubel FM, Brent R, Kingston RE, Moore DD, Seidman JG, Smith JA, Struhl K. Current protocols in molecular biology. In: Ausubel FM, editor. Current protocols. New York (NY): John Wiley; 1994.
34. Coligan JE, Kruisbeek A, Margulies DH, Shevach EM, Strober W. Current protocols in immunology. Colligan JE, editor. New York (NY): John Wiley; 1994.

35. Linzenbold W, Fech A, Hofmann M, Aicher WK, Enderle MD. Novel techniques to improve precise cell injection. Int J Mol Sci. 2021;22(12):6367.
36. Kelp A, Albrecht A, Amend B, Klunder M, Rapp P, Sawodny O, Stenzl A, Aicher W. Establishing and monitoring of urethral sphincter deficiency in a large animal model. World J Urol. 2017;35(12):1977–86.
37. Aragon IM, Imbroda BH, Lara MF. Cell therapy clinical trials for stress urinary incontinence: current status and perspectives. Int J Med Sci. 2018;15(3):195–204.
38. Barakat B, Franke K, Schakaki S, Hijazi S, Hasselhof V, Vogeli TA. Stem cell applications in regenerative medicine for stress urinary incontinence: a review of effectiveness based on clinical trials. Arab J Urol. 2020;18(3):194–205.
39. Vilsboll AW, Mouritsen JM, Jensen LP, Bodker N, Holst AW, Pennisi CP, Ehlers. Cell-based therapy for the treatment of female stress urinary incontinence: an early cost-effectiveness analysis. Regen Med. 2018;13(3):321–30.
40. Sun X, Zhu H, Li W, Zhao L, Li W, Li X, Xie Z. Small extracellular vesicles secreted by vaginal fibroblasts exert inhibitory effect in female stress urinary incontinence through regulating the function of fibroblasts. PLoS ONE. 2021;16(4):e0249977.
41. Noronha NC, Mizukami A, Caliinari-Oliveira C, Cominal JG, Rocha JLM, Covas DT, Swiech K, Malmegrim KCR. Priming approaches to improve the efficacy of mesenchymal stromal cell-based therapies. Stem Cell Res Ther. 2019;10(1):131.
42. Gorodetsky R, Aicher WK. Allogenic use of human placentaderived stromal cells as highly active and competent cells for regenerative therapies. Int J Mol Sci. 2021;22(10):5302.
43. Yiou R, Dreyfus P, Chopin DK, Abbou CC, Lefaucheur JP. Muscle precursor cell autografting in a murine model of urethral sphincter injury. BJU Int. 2002;89(3):298–302.
44. Gräs S, Klarskov N, Lose G. Intraurethral injection of autologous minced skeletal muscle: a simple surgical treatment for stress urinary incontinence. J Urol. 2014;192(3):850–55.
45. Yokoyama T, Yoshimura N, Dhir R, Qu Z, Fraser MO, Kumon H, de Groat WC, Huard J, Chancellor MB. Persistence and survival of autologous muscle derived cells versus bovine collagen as potential treatment of stress urinary incontinence. J Urol. 2001;165(1):271–76.
46. Yasuda T, Weisel RD, Kiani C, Mickle DA, Maganti M, Li RK. Quantitative analysis of survival of transplanted smooth muscle cells with real-time polymerase chain reaction. J Thorac Cardiovasc Surg. 2005;129(4):904–11.
47. Marquardt LM, Heilshorn SC. Design of injectable materials to improve stem cell transplantation. Curr Stem Cell Rep. 2016; 2(3):207–20.
48. Habib M, Shapira-Schweitzer K, Caspi O, Gepstein A, Arbel G, Aronson D, Seliktar D, Gepstein L. A combined cell therapy and in-situ tissue-engineering approach for myocardial repair. Biomaterials. 2011;32(30):7514–23.
49. Hashemzadeh MR, Taghavizadeh Yazdi ME, Amiri MS, Mousavi SH. Stem cell therapy in the heart: biomaterials as a key route. Tissue Cell. 2021;71:101504.
50. Luan C, Liu P, Chen R, Chen B. Hydrogel based 3D carriers in the application of stem cell therapy by direct injection. Nanotechnol Rev. 2017;6(5):435–48.

51. Jankowski RJ, Deasy BM, Huard J. Muscle-derived stem cells. Gene Ther. 2002;9(10):642–47.
52. Koraitim MM. The male urethral sphincter complex revisited: an anatomical concept and its physiological correlate. J Urol. 2008;179(5):1683–89.
53. Schreiber J. *Investigation of the penetration depth of microparticles by water jet application in porcine urethra* [German]. Tübingen (Germany): Eberhard-Karls-Universität; 2020.
54. Beck F. *Penetration depth and distribution of nanoparticles after injection into the porcine urethra using a new water jet technology* [German]. Tübingen (Germany): Eberhard-KarlsUniversität; 2020.
55. Enosawa S, Kobayashi E. Controllable immunosuppression in pigs as a basis for preclinical studies on human cell therapy. In: Miyagawa S, editor. Xenotransplantaton—comprehensive study, vol. 1. Osaka (Japan): Osaka University; 2020.
56. Castro R, Libanio D, Pita I, Dinis-Ribeiro M. Solutions for submucosal injection: what to choose and how to do it. World J Gastroenterol. 2019;25(7):777–88.
57. Jacques J, Kerever S, Carrier P, Couquet CY, Debette-Gratien M, Tabouret T, Lepetit H, Geyl S, Loustaud-Ratti V, Sautereau D, Legros R. HybridKnife high-pressure glycerol jet injection for endoscopic submucosal dissection increases procedural ease and speed: a randomised study in pigs and a human case series. Surg Endosc. 2016;30(7):3152–59.
58. Repici A, Maselli R, Carrara S, Anderloni A, Enderle M, Hassan C. Standard needle versus needleless injection modality: animal study on different fluids for submucosal elevation. Gastrointest Endosc. 2017;86(3):553–58.
59. Amer MH, White LJ, Shakesheff KM. The effect of injection using narrow-bore needles on mammalian cells: administration and formulation considerations for cell therapies. J Pharm Pharmacol. 2015;67(5):640–50.
60. FELASA. https://felasa.eu/working-groups/guidelines [accessed 2022 Feb 14].

Supplementary Materials

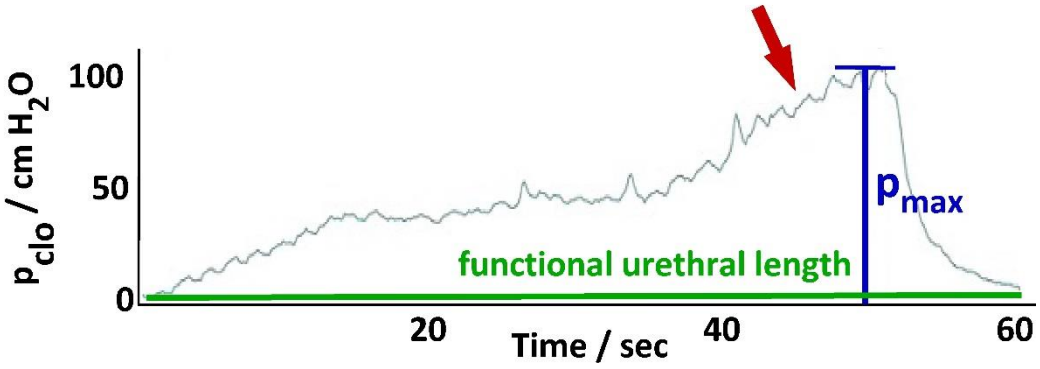

Supplemental Figure S1: Determination of Urothelial Muscle Strength by Urodynamics. The urethral muscle strength and closure function was determined by a sensor and urodynamics. The scale on this sensor facilitated the injection of MDCs by WJ in the area of maximal muscle strength. The maximal urethral closure pressure (pmax) describes the location of main sphincter muscle in the urethra. The functional urethral length describes the part in which the closure pressure is higher than the intravesical pressure. The area under the curve (AUC) describes the integral of urethral wall pressures over the functional length. The arrow points at the WJ injection site.

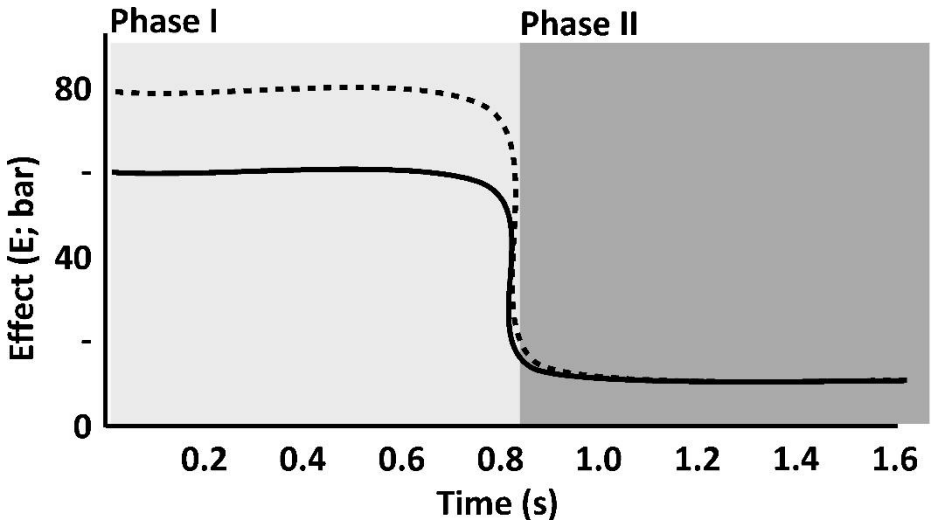

Supplemental Figure S2: Pressure Profiles of the Waterjet System. An upgraded pump and controller system (UPaCS) was operated in an improved pressure control mode (IPCM) to facilitate a short water impulse at elevated pressures ranging from E40 to E80, which is an equivalent of approx. 40 to 80 bars, respectively (= phase I). By this water impulse the tissue targeted is stretched and microchannels are opened in phase I. Within milliseconds pressure levels are reduced to E5 – E10 (= phase II). This low pressure is optimal for injection of viable cells in the open microchannels with high efficacy in phase II. In this study, pressure profiles of E80-10 (dashed line) and E60-10 (solid line) were employed.

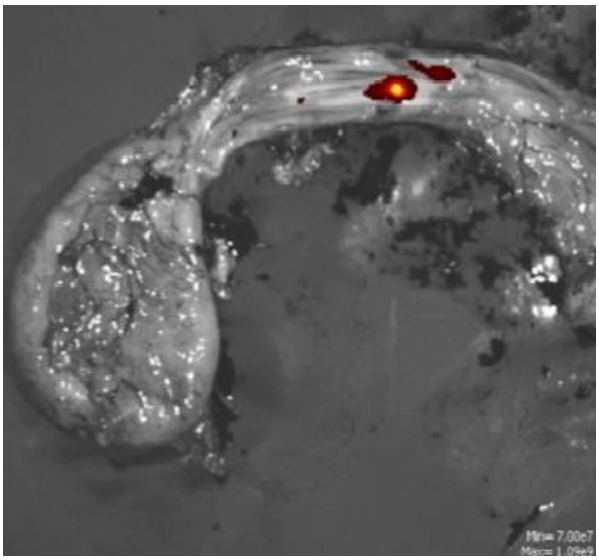

Supplemental Figure S3: Localization of Injected MDCs in the Urethra by IVIS Imaging. Fluorescent MDCs were localized in the urethrae after in vivo injections by an In Vivo Imaging System (IVIS) and visualized by a false-color heat map, while the remaining organ is shown in grey. This facilitated fast preparations of frozen tissue samples from the region of interest and further processing of the samples.

12. Publication 3

Improved protocol for production of proliferation- and differentiation-competent porcine striated muscle-derived myoblasts

Jasmin Knoll[1], Bastian Amend[2], Tanja Abruzzese[1], Arnulf Stenzl[2], Wilhelm K. Aicher[1*]

[1] Centre of Medical Research, Department of Urology at UKT, Eberhard-Karls-University, 72072 Tuebingen, Germany
[2] Department of Urology, University of Tuebingen Hospital, 72076 Tuebingen, Germany

* Correspondence author

Tissue Engineering and Regenerative Medicine

Year 2023

Springer

Submitted: 20 December 2022

Abstract

BACKGROUND: Urinary incontinence is associated with functional deficiency of the urethral sphincter muscle. A causative cell therapy is currently not state-of-the-art. We recently developed a swine animal model of urinary incontinence to investigate the potential of different cells to improve debilitated sphincter functions. In this study, we now developed improved protocols to produce myoblasts suitable for pre-clinical muscle therapy studies.

METHODS: Cells were isolated from striated muscle tissue of 3 boars, expanded employing five different protocols for isolation and expansion of cells, and characterized on transcript and protein expression levels to determine procedures which yielded muscle regeneration-competent cells and multi-nucleated myofibers.

RESULTS: Swine skeletal myoblasts proliferated well under optimized conditions without premature signs of cellular senescence, expressed significant levels of myogenic markers including Pax7, MyoD1, Myf5, MyoG, Des, Myf6, CD56, and others, while cells expanded following other procedures expressed several of the myogenic genes significantly less ($p \leq 0.05$ each). Upon induction of terminal differentiation, myoblasts ceased proliferation and generated multi-nucleated myofibers.

CONCLUSIONS: Expansion of porcine myoblasts in medium enriched by 15% bovine serum and complemented with basic fibroblast growth factor facilitates the production of proliferation- and differentiation-competent swine myoblasts.

Keywords

Porcine myoblast, myogenic differentiation, myofiber, cell-based muscle regeneration, large animal model of cell therapy

Introduction

Stress urinary incontinence (SUI) is a debilitating condition affecting more 15% of the elderly in our communities [1]. It reduces quality of life for the people affected, is associated with psychological distress, and may cause social isolation [2]. In addition, SUI is a challenge to medical personnel and health care systems [3]. In women, SUI is associated with pregnancy, vaginal delivery, and menopause [4]. In men, SUI is a sequela of prostate surgery [5]. For both sexes, injury or persisting inflammation of urogenital structures in the lower pelvic region, neuronal failure, age, and dementia also contribute to SUI. SUI therapy therefore aims at strengthening this muscle complex or supporting its function by other means.

Along these lines, physical exercise of the lower pelvic floor, complemented by electrophysiological stimulation therapy was shown to improve the strength of the lower pelvic floor muscles and thus ameliorate or even cure SUI [6]. If such therapies fail to satisfy the patients expectations or medical need, cell therapies were considered to regenerate urethral sphincter contraction [7-9]. However, despite intensive research, especially in the last two decades, a standard cell therapy for SUI of human patients was not established and the optimal active component for such cell therapy – myoblasts or stromal cells - has not been determined yet [10, 11]. Several preclinical and clinical studies employed myoblasts to replace lost or not functional cells of the striated rhabdosphincter muscle [9]. Others injected adipose tissue-derived mesenchymal stromal cells to facilitate vascularization and tissue regeneration [12].

To explore the regenerative potential of porcine myoblasts for future studies in a large animal SUI model, we investigated the cell proliferation, marker gene expression and differentiation potential of swine striated muscle-derived myoblasts based on two distinct protocols [13, 14] and variants of them employing a total of five study cohorts (Fig. 1). We report that expansion of swine myoblasts in medium containing fetal bovine serum (FBS) and basic fibroblast growth factor (bFGF) facilitates extended cell expansion without signs of premature cellular senescence. Such cells expressed significantly higher levels of myogenic marker genes, generated multinuclear myofibers more efficiently, and thus are recommended for preclinical cell therapy studies focusing on the regeneration of striated muscle tissue.

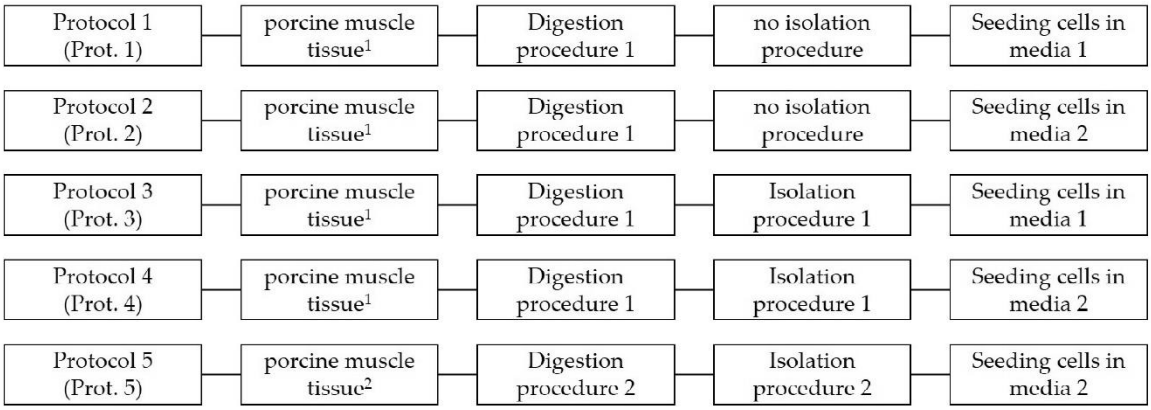

Figure 1: Schematic illustration of the five protocols employed. The different combinations of tissue digestion, cell isolation procedures, and myoblast expansions in the two different media are summarized. An "1" refers to Metzger et al. [13], a "2" points to Ding et al. [14]. Footnote [1] indicates that the tissue was transported to the lab in PBS-D (144mM NaCl, 25mM glucose, 5.4mM KCl, 14mM sucrose, 5mM Na2HPO4, 1% ml P/S; titrated with NaOH to pH 7.4) complemented with 10% P/S and 10% amphotericin B [13]. Footnote [2] indicates that muscle was transported to the lab in DMEM-HG [14].

Material and Methods

Isolation of swine muscle-derived cells and cell culture procedures

For isolation of cells, the *Musculus (M.) semitendinosus* of three fresh cadavers of five to seven days old German Landrace boars was prepared. Tissue samples were excised aseptically and transported at 0°C in the respective media in a sterile container to the laboratory (Fig. 1). Myoblasts were isolated, enriched, and expanded following 5 distinct procedures based on two different publications [13, 14](Fig. 1). The phenotypic appearance of the cells was recorded by microscopy. To determine duplication rate (DR), cells were washed with cold PBS, detached by aid of trypsin-EDTA, resuspended in media, counted by trypan blue exclusion in a hematocytometer, seeded at an inoculation density of 2E05 cells per flask, and expanded to approximately 70% of confluence for consecutive passages in either M-medium [13] or in D-medium [14]. Terminal differentiation was induced by incubation of the cells in differentiation media complemented by 2% horse serum as described [14]. Progress of differentiation and generation of syncytia or extended fiber-like cells was recorded by microscopy. The study was approved by the State Authorities under file number CU01-20G.

Evaluation of gene expression on transcript levels

For RNA extraction, cell expansion media was aspirated, adherent myoblasts were washed twice with PBS, and cells were detached by trypsin-EDTA. Trypsin activity was stopped by the addition of corresponding media supplemented with FCS. The cells were sedimented by centrifugation (700 g, 10 min, 4°C), washed twice with cold PBS, and lysed to extract total RNA with the RNeasy kit (Qiagen). For cDNA synthesis, the yield and purity of RNA were measured by UV spectroscopy (Nanodrop; Implen) and 1 µg of RNA was reverse-transcribed using oligo-(dT) primers and MMLV reverse transcriptase (RT) (PrimeScript cDNA synthesis kit; TaKaRa). Quantitative real-time polymerase chain reaction (qPCR) was performed from cDNA using target gene-specific oligonucleotides (Table 1) [15]. After a hot start (5 min, 95°C), cDNA was amplified by PCR in 39 cycles (10 sec. 95°C melting, 20 sec. 60°C or 62°C (for primers of Des and MyoD1) annealing, 30 sec. 72°C extension), and followed by a melting curve analysis for quality management (LightCycler 480 II; Roche). The size of PCR products was confirmed by DNA agarose

gel electrophoresis. Expression of swine glycerinaldehydephosphate dehydrogenase (sGAPDH) and β2-microglobuline (sb2MG) served as housekeeping controls and to enumerate the transcript levels of the target genes using efficiency-corrected advanced relative quantification program of the LightCycler480 II as suggested by the instruction for use of the manufacturer[16].

Table 1: Oligonucleotides employed for quantitative reverse-transcription polymerase chain reaction

Gene	Forward Sequence	Reverse Sequence	Accession No.	Reference	Size
GAPDH	CCATCACCATCTTCCAGGAG	ACAGTCTTCTGGGTGGCAGT	NM_001206359.1	Kobayashi-Kinoshita, 2016	346
B2MG	ACGGAAAGCCAAATTACCTGAACTG	TCTGTGATGCCGGTTAGTGGTCT	NM_213978.1[#]	[47]	261
MyoG	CGCCATCCAGTACATCGAG	TGTGGGAACTGCATTCACTG	NM_001012406.1	[48]	125
Pax7	AGATCGCAGCAGGGGTAAAG	GACCCCACCAAGCTGATTGA	XM_021095458.1	Primerblast	209
Myl1	CTCTCAAGATCAAGCACTGCG	GCAGACACTTGGTTTGTGTGG	NM_214374.2	[49]	198
Myf5	GCTGCTGAGGGAACAGGTGGA	CTGCTGTTCTTTCGGGACCAGAC	NM_001278775.1	[50]	135
MSTN	CCCGTCAAGACTCCTACAACA	CACATCAATGCTCTGCCAA	NM_005259.3	[50]	141
ACT	CGGGCAGGTCATCACCATC	CGTGTTGGCGTAGAGGTCCTT	XM_005670976.2[##]	[50]	160
MYH1	CCAGGGAGAGATGGAGGACA	TCAAGTTCACGTACCCTGGC	NM_001104951.2	Primerblast	258
Des	ACACCTCAAGGATGAGATGGC	CAGGGCTTGTTTCTCGGAAG	NM _001001535.1	[49]	176
Myf6	AGTGGCCAAGTGTTTCGGATC	CGCGAGTTATTTCTCCCCCA	NM_001244672.1	Primerblast	179
ACTA1	ACCCGACGCCATGTGTGA	GTCGCCCACGTAGGAATCTT	NM_001167795.1	Primerblast	184
MyoD1	CACTACAGCGGTGACTCAGACGCA	GACCGGGGTCGCTGGGCGCCTCGCT	NM_001002824.1	[50]	145

Oligonucleotides employed for quantitative reverse-transcription polymerase chain reaction of swine (s) cDNAs in 5'-3' orientation, including gene bank access, reference, and expected DNA product size in base pairs. Primers also amplify alternative transcripts for sB2M: [#] XM_021096362.1; or for sACT: [##] XM_021071931.1 and XM_021071930.1, respectively.

Protein detection by immunofluorescence

Myoblasts were grown on chamber slides to the confluence intended. Medium was aspirated, cells were washed twice with cold PBS, fixed by 4% paraformaldehyde (Morphisto), and permeabilized with 0.1% Triton X-100 (Merck) at ambient temperature. To reduce unspecific binding of antibodies, samples were preincubated with a blocking solution (5% dry milk powder in 0.1% Tween-20 in PBS (T-PBS)). The blocking solution was aspirated, the primary anti-desmin antibody (1:200 in 0.1%BSA in PBS; Abcam) was resuspended, and incubated in black humidified chambers at 37°C for 90 min. Unbound primary antibodies were aspirated, the samples were washed three times with T-PBS detection antibody (FITC-F(ab')$_2$ -dk-anti-rbt IgG (H+L), 1:200; Jackson ImmunoResearch Laboratories) was added to the samples for incubation in black humidified chambers at 37°C for 45 min. Samples omitting primary antibodies served as controls. Samples were

counterstained by 4′,6-diamidino-2-phenylindole (DAPI; Sigma) to visualize cell nuclei. Staining was visualized and recorded by fluorescence microscopy (Axiovert 200 M, Axiovision software; Zeiss). Desmin-positive cells were counted with aid of ImageJ software (NIH).

Flow cytometry

Flow cytometry (FC) was employed to explore the expression of myogenic marker CD56 antigen on the cells, [17, 18]. Cells were detached by mild proteolysis (Accutase; Sigma Aldrich), and aliquots of 5E05 cells were resuspended in PFEA sample buffer and sedimented in microtubes [17]. To avoid unspecific antibody binding, cells were incubated with preimmune serum (Gamunex, 1:20 in PBS; 20 min, 0°C; Grifols; [17]), washed, and incubated with directly labeled antibody (PE anti-human CD56 (NCAM) antibody, Biolegend, diluted 1:10 in PFEA) at 0°C for 20 min. Samples were diluted with PFEA, cells with bound antibodies were sedimented, and supernatant with unbound antibodies was discarded. The cells were resuspended in 300 µl PFEA. Size and granularity of the cells were recorded by FC employing forward (FSC-A) and side scatter (SSC-A; LSRII; BD Bioscience) to gate for living cells. Then, antibody staining intensities were measured by FC [17, 18]. Cells with no antibody staining and FC compensation particles (BD Bioscience) were employed for gating. Data were evaluated by FACS-Diva (BD Bioscience) and FlowJo (TreeStar Inc.) software. The FCS- and SSC-scatters are presented as 2D dot blots, median fluorescence intensity (MFI) of cells staining as histograms (thin black line), background fluorescence of unstained cells as shaded histograms (grey).

Statistics

Data generated were processed by Excel (Microsoft). Statistical analyses were performed with GraphPad Prism version 5.04 for Windows (GraphPad Software) and IBM SPSS Statistics for Windows, version 29.0 (Armonk: IBM Corpversion 26). Depending on the normality distribution, either normal data were used, or the data were transformed via log10 to result in an approximately normal distribution. Afterwards, either One-Way-ANOVAs were performed. The One-Way-ANOVAs were completed by post hoc tests of Tukey. If the transformation to normal distribution failed non-parametric tests were performed (Mann-Whitney-U- or Kruskal-Wallis-Test). P-values between 0.05 and

0.01 were considered as significant (*), between 0.01 and 0.001 as very significant (**), and p-values smaller than 0.001 as highly significant (***).

Results

Proliferation and morphology of swine myoblasts

Myoblasts were prepared from 3 individual boars. The cells were expanded employing five different procedures Prot. 1 to Prot. 5, in either M-media containing horse serum [13] or in D-medium complemented with bFGF [14]. The mean cell DR of cells in M-media containing horse serum was significantly higher (mean DR M-media: 1.99) when compared to expansion in D-media (mean DR: D-media: 1.37; $p = 0.038$, Mann-Whitney-U-Test; *). Cells produced according to Prot.3 presented with the lowest mitotic activity (DR: 2.21), while cells produced by Prot.4 showed the highest (DR: 1.18). Furthermore, cells appeared with different morphologies (Fig. 2). Cells produced by Prot.1 and Prot.3 appeared with wider somata and increased granularity (Fig 2A, 2C). Several cells in these protocols appeared flat, enlarged, and stretched (Fig. 2E). This resembles features of replicative senescence [19]. Cells produced by Prot.2, Prot.4, and Prot.5 appeared slim and without prominent granularity (Fig. 2B, 2D, 2F). We conclude that M-medium containing horse serum leads to cellular senescence and thus prolonged duplication rates of porcine muscle-derived cells, whereas D-medium promotes faster growth and healthier appearance.

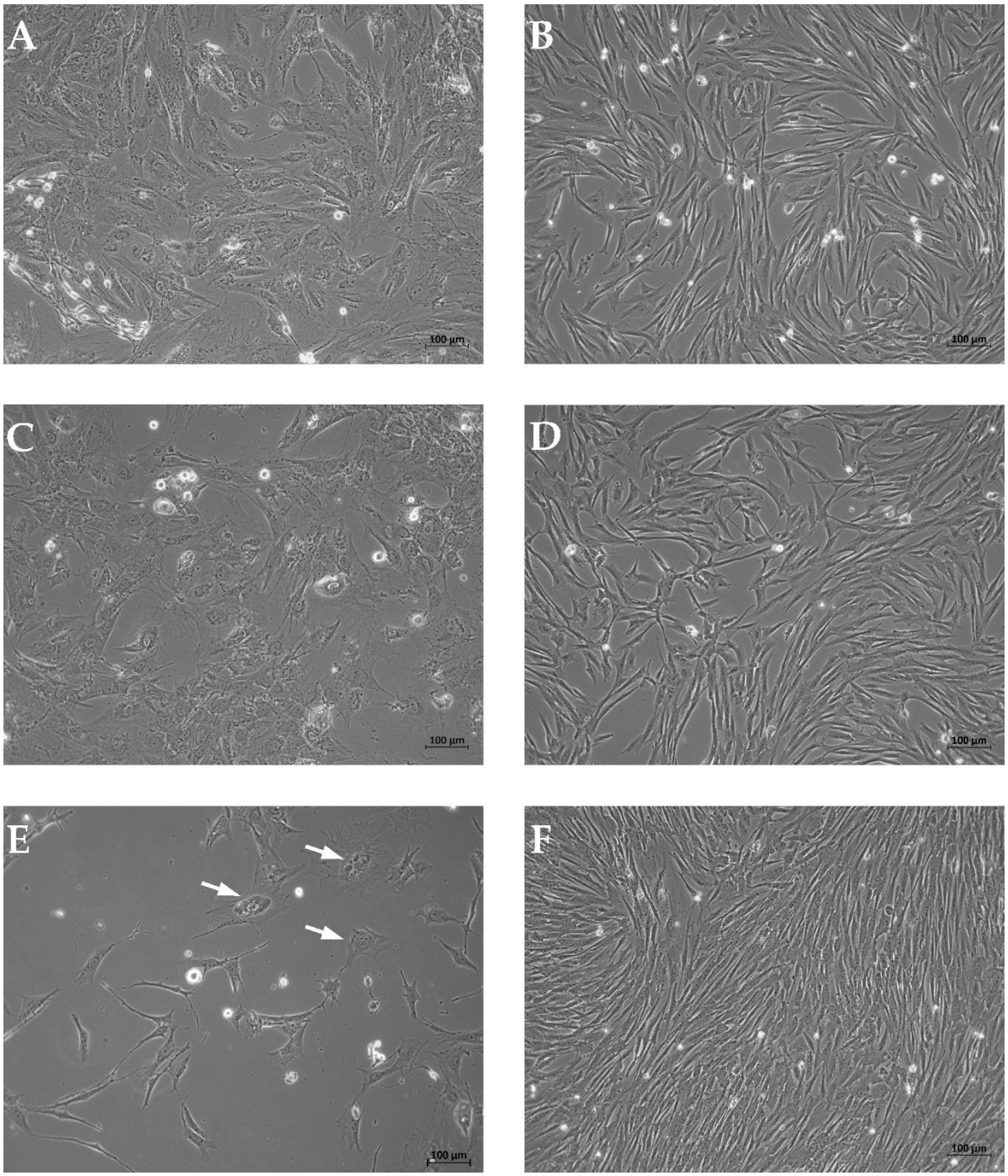

Figure 2: Morphology of myoblasts expanded following different protocols. Myoblasts produced following Prot.1 (A) and Prot.3 (C) appeared wider and contained more granula when compared to cells expanded following Prot.2 (B), Prot.4 (D), or Prot.5 (F), respectively. Myoblasts expanded in K-media (left panel) contained more cells with a perinuclear hallow or stretched cells (E, arrows). Size bars indicate 100 µm. The pictures are representative artwork for cultures generated from the three individual boars and expanded by different protocols included in this study.

Expression of transcripts encoding myogenic markers

Several marker genes have been identified to play a central role in myogenesis. These factors include the gene Pax7 (paired box 7), which is specific for proliferating myoblasts, and myogenic regulatory factors [MRFs: MyoD1 (myoblast determination protein 1), Myf5 (myogenic factor 5), MyoG (myogenin), Myf6 (myogenic factor 6, alias MRF4)] [20, 21]. Therefore, the expression levels of these marker genes, complemented with the intermediate filament desmin (Des) found in muscle, were investigated by qPCR (Fig. 3). In addition, muscle cell markers ACTA1 (skeletal muscle actin alpha 1), Myl1 (myosin light chain-1), MSTN (myostatin), MYH1 (myosin heavy chain 1), ACT (actin) were detected by qPCR as well (data not shown). Myoblasts generated by Prot.4 expressed all myogenic markers at the highest levels, followed by cells produced by Prot.2 and Prot.5. Again, myoblasts generated by Prot.1 and Prot.3 significantly lagged behind (Fig. 3, Tab. 2). We therefore conclude that the expansion of porcine myoblasts in D-medium favored a skeletal muscle phenotype of pig muscle-derived cells.

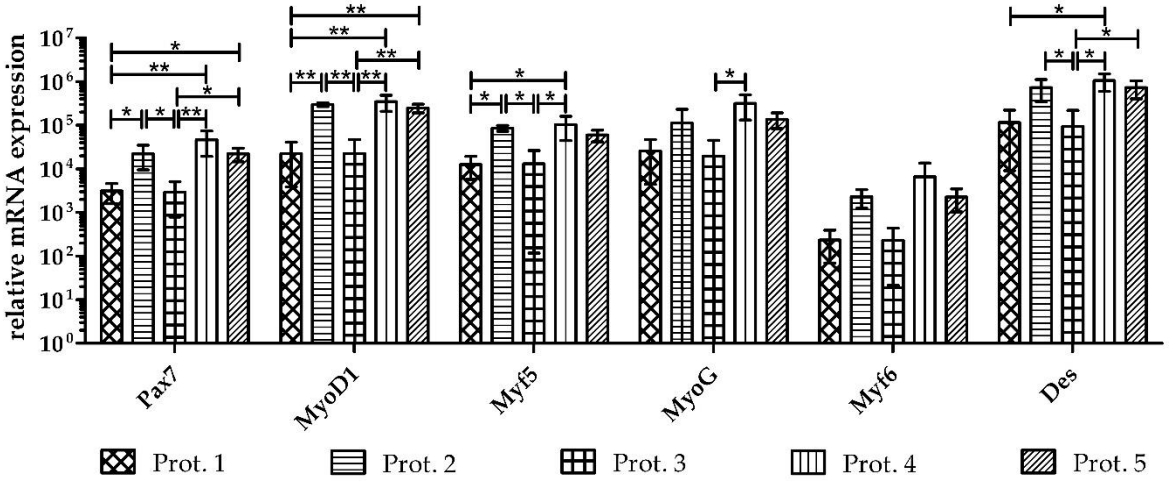

Figure 3: Transcript expression of myogenic marker genes in myoblasts. Expression of myogenic markers was enumerated by RT-qPCR of cDNA isolated from cells of all three donors upon expansion to the third passage following protocols as indicated in three individual sets of experiments. Cells expanded in D-media expressed all myogenic markers at higher levels when compared to cells expanded in K-media. The data present the mean values ± standard deviations of target gene expression normalized to housekeeping controls. Significant differences are indicated: One-Way-ANOVAs with Tukey-Post-Hoc-Tests performed on log-transformed values: *, **. All One-Way-ANOVAs calculated displayed significant results (Tab. 2) even if Post-Hoc-Tests could not identify the groupwise differences for all genes (e.g. Myf6).

Table 2: Results of One-Way-ANOVA performed on log-transformed values indicating significant results for all genes

Gene	p-value
Pax7	0.001
MyoD1	<0.001
Myf5	0.005
MyoG	0.017
Myf6	0.019
Des	0.005

Detection of CD56 by flow cytometry

The cell adhesion molecule CD56 is a multifunctional protein which is expressed in satellite cells and myoblasts [22-24]. We therefore investigated the expression of CD56 on swine myoblasts by FC in three independent sets of analyses (Fig. 4). Differences in cell size and granularity observed by microscopy were confirmed by FC, as myoblasts expanded in M-media had a wider scatter and particle distribution when compared to myoblasts expanded in D-media (Fig. 4A). Expression of CD56 in cells expanded in M-media following Prot.1 and Prot.3 was very low (Fig. 4B-1, -3). A clear separation of the staining peak background was barely recorded in these cells. The percentage of CD56 positive myoblasts was raised highly significantly in cells expanded in D-media when compared to cells in M-media (Fig. 4B-2,-4,-5, 4C). Additionally, the means of MFI of myoblasts cultivated in K-media (Prot.1: 410, Prot.3: 475) were lower than the means of MFI of myoblasts cultivated in D-media (Prot.2: 8379, Prot.4: 13700, Prot.5: 6730). The highest expression levels among all five protocols were recorded in Prot.4 cells (Fig. 4D). This corroborated that elevated expression of CD56 on porcine myoblasts was facilitated by cell expansion in the D-media lacking horse serum.

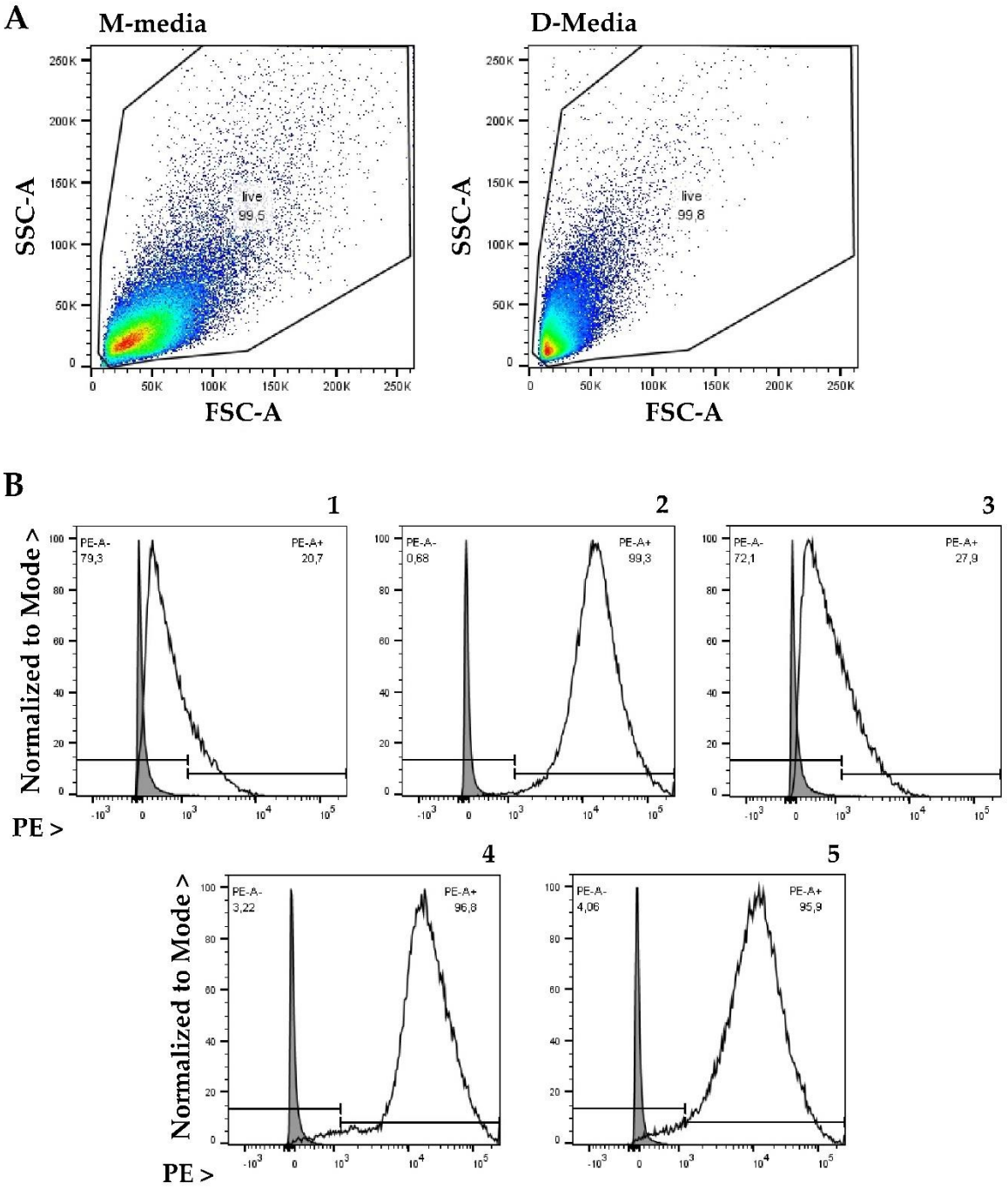
A
M-media
D-Media
SSC-A
FSC-A
live
99,5
live
99,8
B
1
2
3
4
5
Normalized to Mode >
PE >
PE-A-
79,3
PE-A+
20,7
PE-A-
0,68
PE-A+
99,3
PE-A-
72,1
PE-A+
27,9
PE-A-
3,22
PE-A+
96,8
PE-A-
4,06
PE-A+
95,9

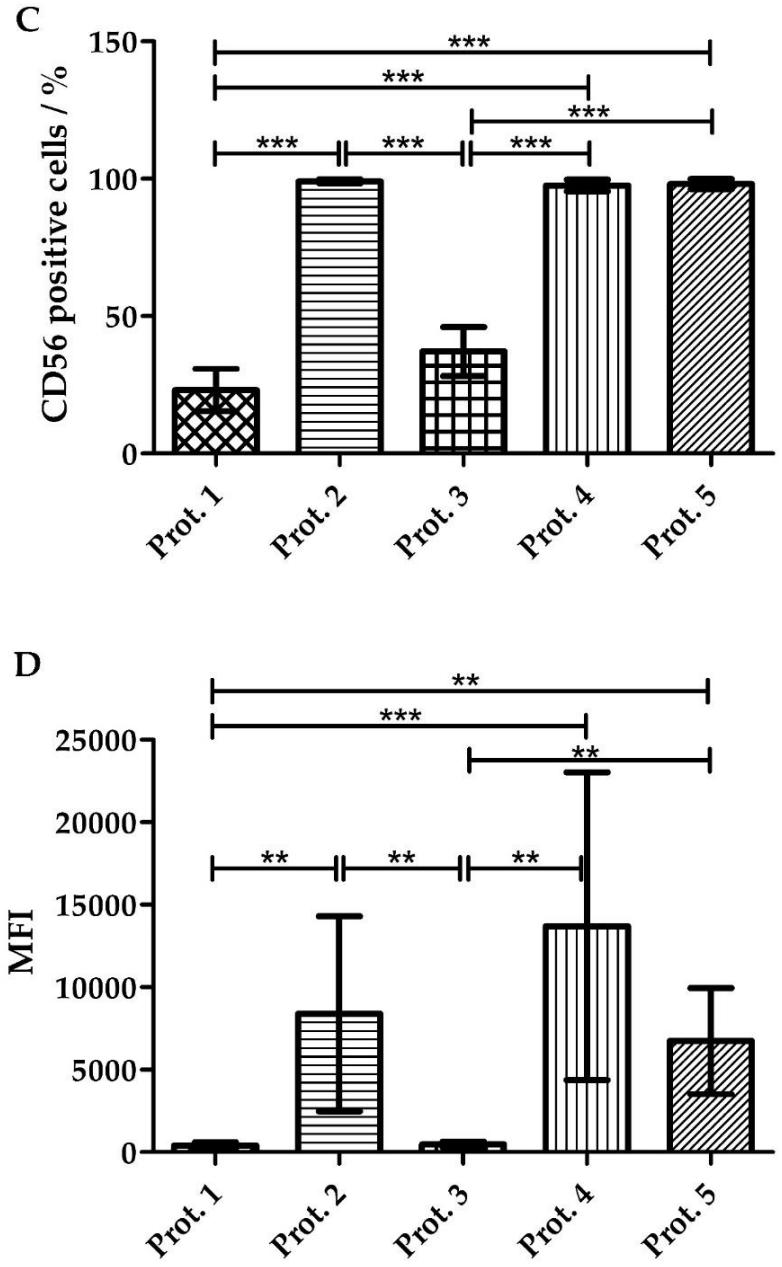

Figure 4: Characterization of myoblasts by flowcytometry (FC). Size (forward scatter; FSC-A) and complexity (side scatter; SSC-A) of myoblasts were determined by FC (A). Myoblasts expanded in M-media showed a broader distribution in FSC and SSC, when compared to cells in D-media. Expression of CD56 was enumerated by FC as well (B). Representative cells derived from the three boars and expanded by procedures following Prot.1 to Prot.5 are displayed as indicated in panels B1 to B5. Expression of CD56 is higher in cells expanded in D-media (B2, B4, B5), when compared to cells from K-media (B1, B3), respectively. Gating of CD56-negativ cells (see B) facilitated the enumeration of CD56-positive cells (C). Significant differences were found between cells produced in the different protocols as indicated: One-Way-ANOVA ($p<0.001$) with Tukey-Post-Hoc-Tests (***). The median fluorescence intensities (MFI) (see B) of the different cells are depicted as well (D). Cells produced in K-media expressed less CD56 per cell which translated in a low MFI when compared to cells in D-media (D). Similar significant differences were found between cells produced in the different protocols as indicated: One-Way-ANOVA ($p<0.001$) with Tukey-Post-Hoc-Tests performed on log-transformed values (**, ***). The data present the mean values ± standard deviations from 3 independent experiments with cells from the 3 donors expanded in the different media.

Expression of desmin in swine myoblasts

Desmin is a muscle-specific intermediate filament contributing to proper structure and function of contractile cells [25, 26]. We therefore compared the expression of desmin in myoblasts from all three individual donors after expansion by the five different protocols employing immunofluorescence (IF). Desmin was detected by IF in all batches generated (Fig. 5A). As the expression levels of an individual protein cannot be delineated from IF signal intensities directly, nuclei were counterstained by DAPI, allowing enumeration of cell counts of desmin-positive versus desmin-negative myoblasts (Fig. 5B). Populations produced by Prot.2 (48.9%; *), Prot.4 (49.1%, *), and Prot.5 (38.7%; not significant) presented with significantly more desmin-positive cells, when compared to Prot.1 (8.2%) and Prot.3 (7.4%) cultures (Fig. 5B). This confirmed that culture of porcine muscle-derived cells in D-media yielded populations enriched for myoblasts when compared to the same cells expanded in M-media.

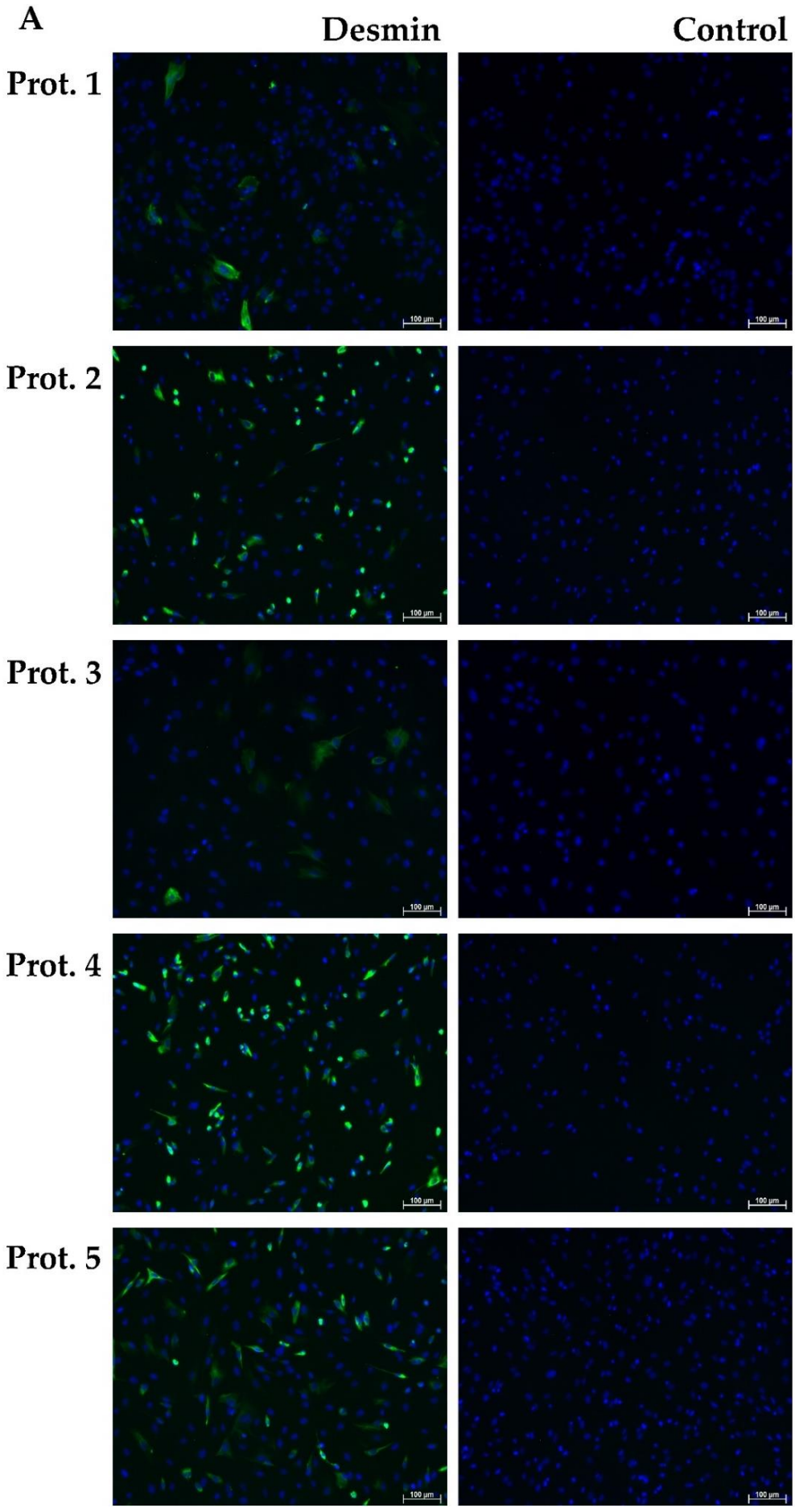
A
Desmin
Control
Prot. 1
Prot. 2
Prot. 3
Prot. 4
Prot. 5
100 µm

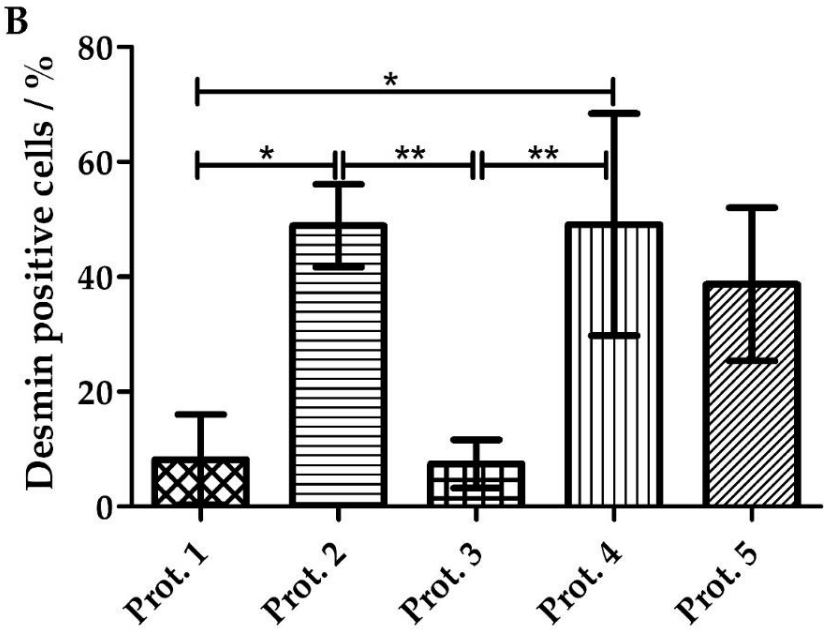

Figure 5: Detection of intracellular desmin by immunofluorescence. Myoblasts were prepared following the five different protocols as indicated, fixed, and stained with anti-desmin reagents as indicated (A, left panel). Incubation of cells with secondary antibody only served as control (A, right panel). Nuclei were visualized by DAPI. The micrographs are representative for cells from all batches included in this study. More cells expressed desmin upon expansion in D-media when compared to cells in M-media (A). Size bars indicate 100 µm. The percentage of desmin expressing cells as function of the protocol employed was enumerated in micrographs using ImageJ (B). Desmin was detected in significantly less myoblasts generated by Prot.1 or Prot.3 when compared to cells produced by Prot.2, Prot.4, or Prot.5. The data present the mean values of 3 independent experiments ± standard deviations. Significant differences are indicated: One-Way-ANOVA (p=0.002) with Tukey-Post-Hoc-Tests (*, **).

Myogenic differentiation to generate myofibers

Terminal differentiation and formation of myofibers was stimulated in myoblasts, expanded from cells of all three donor animals by Prot.1 to Prot.5, and differentiated following established protocols [14]. As controls, cells were maintained in either M-media (Fig. 6, left column) or D-media (Fig. 6, middle column). After incubation in differentiation media (Fig. 6, right column), extension of cells was noted by microscopy in cells produced by Prot.2, Prot.4, and Prot.5 after 2-3 days (not shown). After 4 days of differentiation, cells were fixed to visualize desmin expression and multinucleated myofibers by IF (Fig. 6). Myoblasts expanded following Prot.2, Prot.4, and Prot.5, yielded long myofibers and expressed desmin (Fig. 6), while the other cultures yielded short and less (Prof.1) or no (Prot.3) elongated myofibers (Fig. 6). Most of the myoblasts expanded initially in M-media (Prot.1, Prot.3) did not survive the media change to D-media. Only very few intact cells and nuclei were recorded after DAPI staining. But they survived the media change to differentiation media, however, without efficient myotube formation

(Fig. 6). Interestingly, cells expanded initially in D-media, survived the media change to M-media, and even started a kind of differentiation as well (Fig. 6). This difference in syncycia and myotube formation was corroborated by investigating the transcripts of the differentiated populations (Fig. 7, Tab. 3). Expression of Pax7 were low in myoblasts and remained low in myofibers of cells generated by Prot.1 and Prot.3. This indicated a lower amount of progenitor cells prior to differentiation. In addition, upon differentiation to myofibers, a reduction of Pax7 was expected but not recorded (Fig. 7). Expression patterns of MyoD1, Myf5, and Des were comparably low. Transcripts encoding Myf6 were reduced in Prot.1 cells or remained low in Prot.3 cells after differentiation (Fig. 7). In contrast, the expression of Pax7 was elevated in Prot.2, Prot.4, and Prot.5 myoblasts and was reduced upon differentiation (Fig. 7). Myf6, a factor associated with terminal differentiation, was elevated in myofibers differentiated from Prot.2, Prot.4, and Prot.5 cells, respectively (Fig. 7). The changes in transcript levels recorded for Pax7 and Myf6 confirmed the success of terminal differentiation of porcine myoblasts. [27, 28]. Expression of Des was and stayed high in Prot.2, Prot.4, and Prot.5 cells (Fig. 7). We conclude that expansion of porcine muscle-derived cells in D-media facilitated the expansion of differentiation-competent myoblasts without promoting premature replicative senescence.

Table 3: Results of Kruskal-Wallis-Tests indicating significant results for all genes except for Pax7

Gene	**p-value**
Pax7	0.184
MyoD1	0.006
Myf5	0.028
MyoG	0.017
Myf6	0.045
Des	0.008

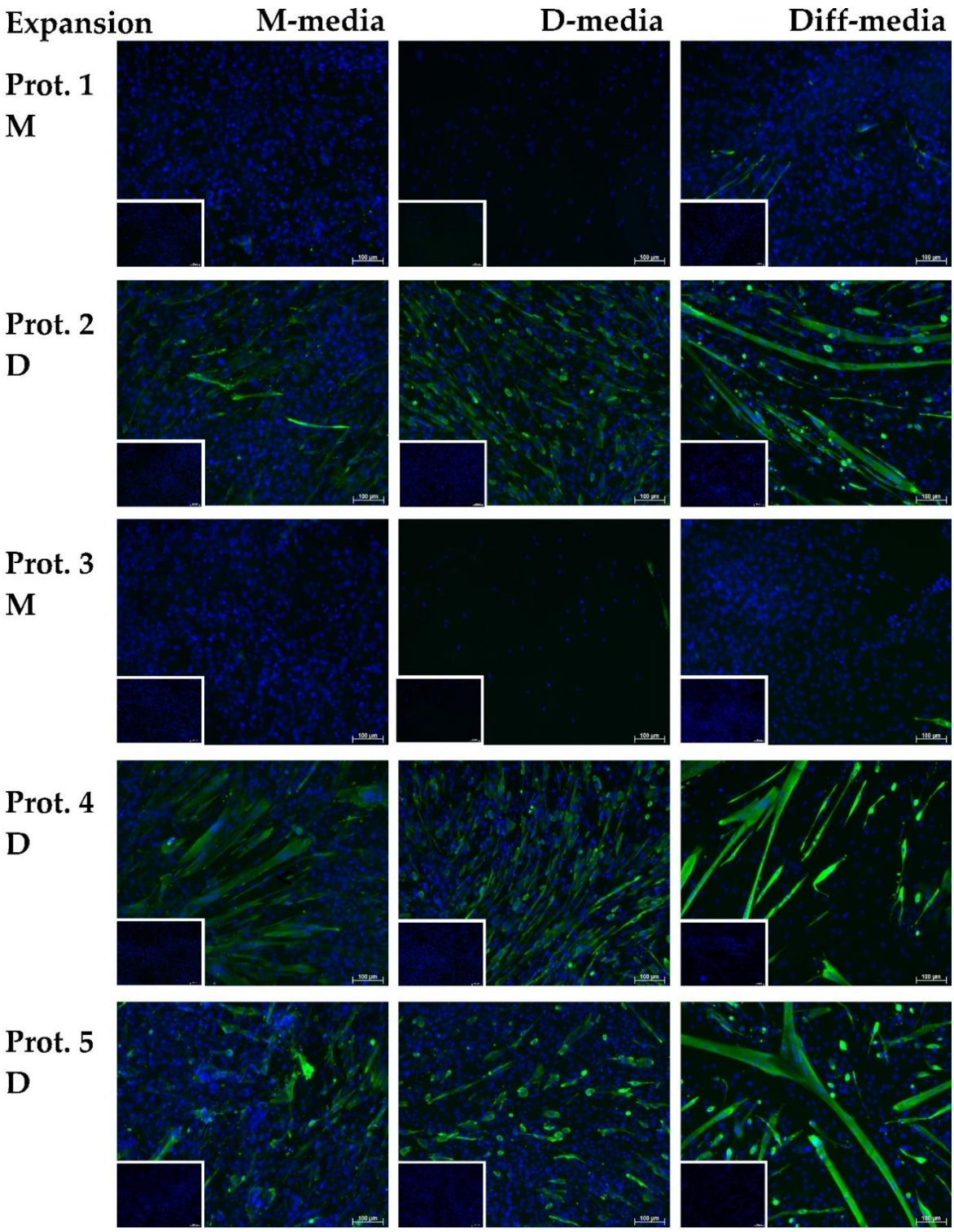

Figure 6: Terminal differentiation of myoblasts. Myoblasts were expanded by Prot.1 to Prot.5 in M- or D-medium and maintained in M- and D-medium for controls as indicated. Differentiation of cells was induced. Generation of elongated muscle fibers was recorded by immunofluorescence of desmin expression. Nuclei were counterstained by DAPI. Myoblasts expanded in D-media generated multinucleated elongated myofibers, while cells expanded by Prot.1 and Prot.3 died upon change to D-medium and did not generate myofibers efficiently. Inserts show control staining omitting the primary antibody. Size markers indicate 100 µm. The figure shows representative micrographs from a series of three independent experiment using cells from three individual boars each.

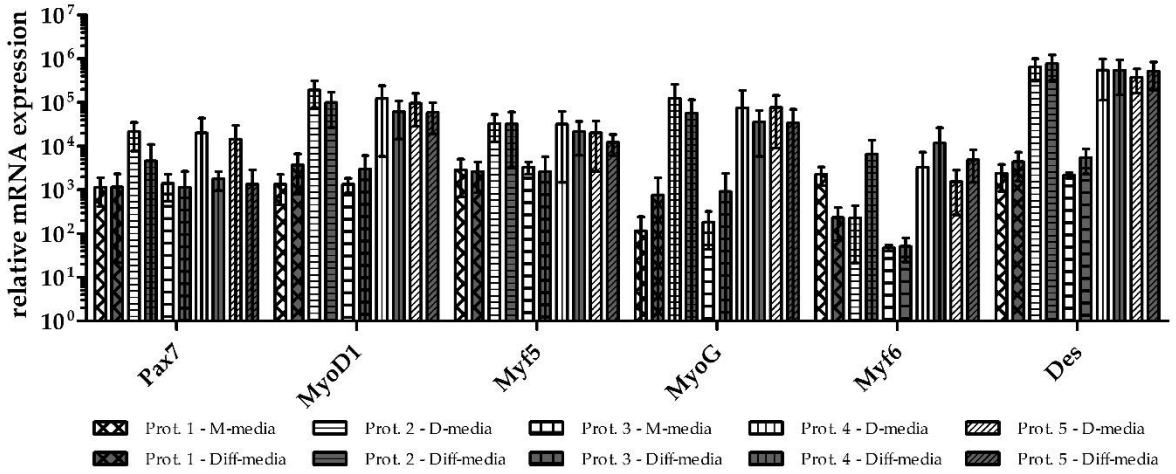

Figure 7: Expression of marker genes in myofibers. Transcripts encoding myogenic marker genes were enumerated by RT-qPCR in Prot.1 to Prot.5 cells after terminal differentiation and in corresponding controls. Data are mean values ± standard differentiation from three independent experiments using cell from three donors produced by the five different protocols. Most overall test values appeared to be significant (Kruskal-Wallis-Test) (Tab. 3) except for Pax7. However, all performed Post-Tests were not significant.

Discussion

Success of preclinical animal studies paved way for clinical feasibility studies aiming at cell therapy of stress urinary incontinence (SUI) by autologous cells [7, 29, 30]. Despite initial enthusiasm some years ago, cell therapy of SUI is not yet a clinical standard [10, 11]. Various reasons for this seemingly contradictory situation must be considered, including the lineage and quality of the cells applied in preclinical animal studies. The tissue targeted by SUI cell therapy – the urethral sphincter muscle - consists in part of smooth muscle tissue, which resembles anatomically the lissosphincter [31]. In addition, striated muscle cells of the outer rhabdosphincter reinforce the contractile complex [31]. Therefore, either stromal cells derived, for instance from adipose tissue [12] or skeletal myoblasts [9, 32, 33] were employed in both, preclinical or in clinical studies [7, 8]. Production of regeneration competent human mesenchymal stromal cells from bone marrow, adipose tissue, and other sources as well as the production of skeletal myoblasts, e.g., from *M. soleus* under good medical procedure conditions is state-of-the-art [8, 9, 32, 33]. In contrast, production protocols or phenotypes of cells applied in animal SUI studies were not always disclosed in great detail, thus impeding the interpretation of therapy versus outcome [34]. In some studies, the myoblasts employed were investigated prior to their application to some extent [35-37]. But sufficient information regarding the quality measures of porcine muscle cells, which had been used in SUI models for regenerative therapy, has not been found.

In preclinical and clinical studies, quality measures for muscle cells applied should address several analyses, including phenotype, stage of differentiation, stress resilience, and replicative senescence. Expression of Pax-7, MyoD-1, and Myf-5 are expressed in activated satellite cells and proliferating skeletal myoblasts, and therefore seem specific for the desired phenotype [20, 21, 28, 38]. Myogenin is especially expressed during the myogenesis [28], whereas desmin, muscle-specific intermediate filament, is found in different stages of myoblasts differentiation corresponding to the prominent expression in our cultures [25]. The expression profile of cells expanded with Prot.4 showed the highest accordance with the expected markers of myoblasts.

The source of cells used for cell-based therapy or tissue engineering may also influence the outcome. In clinical situations, *M. soleus* is one of the preferred sources for myoblast production [9]. Even-toed ungulates such as pigs do not have *M. soleus*. In our preparatory

studies, we therefore explored the phenotypes of myoblasts isolated from other skeletal muscles of adult animals. With the exception of desmin, expression of the markers investigated in cells from adult pigs was not quite convincing (not shown). To get the first clues of an improved myoblast culture, we therefore included in this study only cells isolated from *M. semitendinosus* of very young boars, as they contained sufficient amounts of myogenic progenitors, including satellite cells [39]. But many patients suffering from SUI are not quite young anymore. Thus, rejuvenation of cells prior to their application may become a challenge for future research. Moreover, muscle tissue may contain fast- and slow-twitch fibers. In the omega-shaped rhabdosphincter muscle type I slow-twitch fibers prevail and enable baseline tonic activity and to a large part voluntary sphincter control. Depending on the clinical situation, this difference in muscle type may influence the outcome of a cell therapy as well.

The quality of cells produced *in vitro* depends on cell culture conditions. Supplementation of expansion media by 10% bovine plus 10% horse serum yielded a prolonged proliferation rate in our study and seemed at the same time to facilitate replicative senescence [13, 19]. Recently, horse serum was used as a stimulus to induce the differentiation of preconditioned mesenchymal stromal cells to become elongated myogenin-positive cells [40], while serum deprivation of C2C12 myoblasts reduced the percentage of myogenin- and MyoD-positive cells, indicating a reduction of cells undergoing terminal differentiation and cell fusion [41]. In our study, complementation of differentiation media by horse serum facilitated the generation of multinucleated myofibers in cells expanded in D-media. This was not only obvious by comparing the number of elongated myofibers expressing desmin, but also by investigation of the changes in marker gene expression after differentiation. The phenotype of proliferation-competent myoblasts and of myofiber formation is also regulated *in vitro* by aFGF (FGF-1) and bFGF (FGF-2) [42]. While autocrine and exogenous FGF supported the expansion of myoblasts and blocked terminal differentiation, deprivation of bFGF from myoblast media facilitated generation of myofibers [14]. In combination with the other parameters investigated in this study, generation of myofibers induced by bFGF deprivation may be a sufficient proof for regeneration competent myoblasts for SUI treatment.

However, in our control experiments, cells expanded *ex vivo* in M-media did not survive a media change to D- media. This indicated that the factors contained in M-media allowed for myoblast expansion but failed to mount resilience to cell death. The cell death observed

after a change from M- to D-media was associated with a kind of factor deprivation. Resilience to cell death induced by factor starvation after injection may be a key for the success of clinical application of cells. But detailed analyses of the factors participating in enhancing cell viability in D-media are beyond the focus of this study. Of note, cell death upon media change correlated with low expression of CD56 in myoblasts expanded in M-media and CD56 expression is needed for efficient muscle differentiation [23].

Injection of cells in a tissue is known to cause stress [43] and cell death was reported upon injection of cells in the urethral sphincter [44]. An elevated expression of CD56 on myoblasts seems important in this regard. CD56 is not only expressed on myoblasts and may therefore serve as a cell surface marker for such cells. It also was associated with resistance to cellular stress [45]. But it remains to be investigated *in vivo* in an animal model of SUI therapy to explore if the myoblasts generated by the procedures investigated here are able to recover muscle deficiency significantly.

However, upon isolation of cells from three individual boars from three independent litters and different parents, we noted that myoblasts from the third donor expressed the marker genes investigated at lower levels when compared to the two earlier preparations (not shown). As the cells were produced under identical procedures and protocols, to the best of our knowledge, we conclude that interindividual differences in tissue characteristics may exist in domestic pigs. Such interindividual differences were noted, for instance, by epigenetic analyses of cohorts [46]. In clinical situations, complementing quality measures by epigenetic analyses could help to generate even better cells for muscle regeneration and thus avoid cell therapy with less potent myoblasts. But such strategies are beyond the focus of this study. Moreover, improved selection or enrichment of regeneration competent cells, for instance by antibody-dependent techniques such as panning, MACS, or FACS, may yield better clinical outcome for SUI patients as well. But the definition of suitable markers for human myoblasts selection must await further studies.

Acknowledgements

The authors express their great gratitude to Mrs. Lina M. Serna-Higuita, M.S. for support in statistical analyses, Mr. Chaim Goziga for expert help in preparation of the artwork. This study was supported in part by a joint grant to BA, AS, and WKA (DFG project PoTuS #429049495), by a grant to WKA (DFG project MyoRepair # 468616715), and in part by institutional research funds.

Conflict of interest

There is no conflict of interest for any of the authors in the context of this study.

Ethical statement

Use of animal cells was approved by the State of Baden-Württemberg Authorities under file number 35/9185.81-2 / CU01-20G.

References

1. Broome, B. A., The impact of urinary incontinence on self-efficacy and quality of life. *Health and quality of life outcomes* **2003,** 1, 35.
2. Fultz, N. H.; Herzog, A. R., Self-reported social and emotional impact of urinary incontinence. *J Am Geriatr Soc* **2001,** 49, (7), 892-9.
3. Subak, L. L.; Brubaker, L.; Chai, T. C.; Creasman, J. M.; Diokno, A. C.; Goode, P. S.; Kraus, S. R.; Kusek, J. W.; Leng, W. W.; Lukacz, E. S.; Norton, P.; Tennstedt, S.; Urinary Incontinence Treatment, N., High costs of urinary incontinence among women electing surgery to treat stress incontinence. *Obstetrics and gynecology* **2008,** 111, (4), 899-907.
4. Delancey, J. O., Why do women have stress urinary incontinence? *Neurourol Urodyn* **2010,** 29 Suppl 1, (Suppl 1), S13-7.
5. Markland, A. D.; Goode, P. S.; Redden, D. T.; Borrud, L. G.; Burgio, K. L., Prevalence of urinary incontinence in men: results from the national health and nutrition examination survey. *J Urol* **2010,** 184, (3), 1022-7.
6. Ptak, M.; Brodowska, A.; Ciećwież, S.; Rotter, I., Quality of Life in Women with Stage 1 Stress Urinary Incontinence after Application of Conservative Treatment—A Randomized Trial. International Journal of Environmental Research and Public Health 2017, 14, (6), 577.
7. Aicher, W. K.; Hart, M. L.; Stallkamp, J.; Klunder, M.; Ederer, M.; Sawodny, O.; Vaegler, M.; Amend, B.; Sievert, K. D.; Stenzl, A., Towards a Treatment of Stress Urinary Incontinence: Application of Mesenchymal Stromal Cells for Regeneration of the Sphincter Muscle. *J Clin Med* **2014,** 3, (1), 197-215.

8. Aragón, I. M.; Imbroda, B. H.; Lara, M. F., Cell Therapy Clinical Trials for Stress Urinary Incontinence: Current Status and Perspectives. *Int J Med Sci* **2018,** 15, (3), 195-204.
9. Schmid, F. A.; Williams, J. K.; Kessler, T. M.; Stenzl, A.; Aicher, W. K.; Andersson, K. E.; Eberli, D., Treatment of Stress Urinary Incontinence with Muscle Stem Cells and Stem Cell Components: Chances, Challenges and Future Prospects. *Int J Mol Sci* **2021,** 22, (8).
10. Pokrywczynska, M.; Adamowicz, J.; Czapiewska, M.; Balcerczyk, D.; Jundzill, A.; Nowacki, M.; Petros, P.; Drewa, T., Targeted therapy for stress urinary incontinence: a systematic review based on clinical trials. *Expert Opinion on Biological Therapy* **2016,** 16, (2), 233-242.
11. Vilsbøll, A. W.; Mouritsen, J. M.; Jensen, L. P.; Bødker, N.; Holst, A. W.; Pennisi, C. P.; Ehlers, L., Cell-based therapy for the treatment of female stress urinary incontinence: an early cost–effectiveness analysis. *Regenerative Medicine* **2018,** 13, (3), 321-330.
12. Gotoh, M.; Yamamoto, T.; Shimizu, S.; Matsukawa, Y.; Kato, M.; Majima, T.; Takai, S.; Funahashi, Y.; Toriyama, K., Treatment of male stress urinary incontinence using autologous adipose-derived regenerative cells: Long-term efficacy and safety. *International Journal of Urology* **2019,** 26, (3), 400-405.
13. Metzger, K.; Tuchscherer, A.; Palin, M. F.; Ponsuksili, S.; Kalbe, C., Establishment and validation of cell pools using primary muscle cells derived from satellite cells of pig skeletal muscle. *In Vitro Cell Dev Biol Anim* **2020,** 56, (3), 193-199.
14. Ding, S.; Wang, F.; Liu, Y.; Li, S.; Zhou, G.; Hu, P., Characterization and isolation of highly purified porcine satellite cells. *Cell Death Discovery* **2017,** 3, (1), 17003.
15. Brun, J.; Lutz, K. A.; Neumayer, K. M.; Klein, G.; Seeger, T.; Uynuk-Ool, T.; Worgotter, K.; Schmid, S.; Kraushaar, U.; Guenther, E.; Rolauffs, B.; Aicher, W. K.; Hart, M. L., Smooth Muscle-Like Cells Generated from Human Mesenchymal Stromal Cells Display Marker Gene Expression and Electrophysiological Competence Comparable to Bladder Smooth Muscle Cells. *PLoS One* **2015,** 10, (12), e0145153.
16. Rasmussen, R.; Morrison, T.; Herrmann, M.; Wittwer, C., Quantitative PCR by continuous fluorescence monitoring of a double strand dna specific binding dye. *Biochemica* **1998,** 2, 8 - 11.
17. Pilz, G. A.; Braun, J.; Ulrich, C.; Felka, T.; Warstat, K.; Ruh, M.; Schewe, B.; Abele, H.; Larbi, A.; Aicher, W. K., Human mesenchymal stromal cells express CD14 cross-reactive epitopes. *Cytometry A* **2011,** 79, (8), 635-45.
18. Robinson, J. P., Current Protocols in Cytometry.
19. Beck, J.; Horikawa, I.; Harris, C., Cellular Senescence: Mechanisms, Morphology, and Mouse Models. *Vet Pathol* **2020,** 57, (6), 747-757.
20. Seale, P.; Sabourin, L. A.; Girgis-Gabardo, A.; Mansouri, A.; Gruss, P.; Rudnicki, M. A., Pax7 is required for the specification of myogenic satellite cells. *Cell* **2000,** 102, (6), 777-86.
21. Hernández-Hernández, J. M.; García-González, E. G.; Brun, C. E.; Rudnicki, M. A., The myogenic regulatory factors, determinants of muscle development, cell identity and regeneration. *Semin Cell Dev Biol* **2017,** 72, 10-18.

22. Sinanan, A. C.; Hunt, N. P.; Lewis, M. P., Human adult craniofacial muscle-derived cells: neural-cell adhesion-molecule (NCAM; CD56)-expressing cells appear to contain multipotential stem cells. *Biotechnol Appl Biochem* **2004,** 40, (Pt 1), 25-34.
23. Capkovic, K. L.; Stevenson, S.; Johnson, M. C.; Thelen, J. J.; Cornelison, D. D., Neural cell adhesion molecule (NCAM) marks adult myogenic cells committed to differentiation. *Exp Cell Res* **2008,** 314, (7), 1553-65.
24. Pisani, D. F.; Clement, N.; Loubat, A.; Plaisant, M.; Sacconi, S.; Kurzenne, J. Y.; Desnuelle, C.; Dani, C.; Dechesne, C. A., Hierarchization of myogenic and adipogenic progenitors within human skeletal muscle. *Stem Cells* **2010,** 28, (12), 2182-94.
25. Capetanaki, Y.; Milner, D. J.; Weitzer, G., Desmin in muscle formation and maintenance: knockouts and consequences. *Cell Struct Funct* **1997,** 22, (1), 103-16.
26. Hnia, K.; Ramspacher, C.; Vermot, J.; Laporte, J., Desmin in muscle and associated diseases: beyond the structural function. *Cell Tissue Res* **2015,** 360, (3), 591-608.
27. Schmidt, M.; Schüler, S. C.; Hüttner, S. S.; von Eyss, B.; von Maltzahn, J., Adult stem cells at work: regenerating skeletal muscle. *Cell Mol Life Sci* **2019,** 76, (13), 2559-2570.
28. Pajalunga, D.; Crescenzi, M., Restoring the Cell Cycle and Proliferation Competence in Terminally Differentiated Skeletal Muscle Myotubes. *Cells* **2021,** 10, (10), 2753.
29. Hart, M. L.; Izeta, A.; Herrera-Imbroda, B.; Amend, B.; Brinchmann, J. E., Cell Therapy for Stress Urinary Incontinence. *Tissue Eng Part B Rev* **2015,** 21, (4), 365-76.
30. Herrera-Imbroda, B.; Lara, M. F.; Izeta, A.; Sievert, K. D.; Hart, M. L., Stress urinary incontinence animal models as a tool to study cell-based regenerative therapies targeting the urethral sphincter. *Adv Drug Deliv Rev* **2015,** 82-83, 106-16.
31. Kelp, A.; Albrecht, A.; Amend, B.; Klunder, M.; Rapp, P.; Sawodny, O.; Stenzl, A.; Aicher, W. K., Establishing and monitoring of urethral sphincter deficiency in a large animal model. *World J Urol* **2017,** 35, (12), 1977-1986.
32. Blaganje, M.; Lukanovic‡ , A., Intrasphincteric autologous myoblast injections with electrical stimulation for stress urinary incontinence. *Int J Gynaecol Obstet* **2012,** 117, (2), 164-7.
33. Peters, K. M.; Dmochowski, R. R.; Carr, L. K.; Robert, M.; Kaufman, M. R.; Sirls, L. T.; Herschorn, S.; Birch, C.; Kultgen, P. L.; Chancellor, M. B., Autologous Muscle Derived Cells for Treatment of Stress Urinary Incontinence in Women. *Journal of Urology* **2014,** 192, (2), 469-476.
34. Mitterberger, M.; Pinggera, G. M.; Marksteiner, R.; Margreiter, E.; Plattner, R.; Klima, G.; Strasser, H., Functional and histological changes after myoblast injections in the porcine rhabdosphincter. *Eur Urol* **2007,** 52, (6), 1736-43.
35. Burdzinska, A.; Crayton, R.; Dybowski, B.; Idziak, M.; Gala, K.; Radziszewski, P.; Paczek, L., The effect of endoscopic administration of autologous porcine muscle-derived cells into the urethral sphincter. *Urology* **2013,** 82, (3), 743 e1-8.
36. Burdzinska, A.; Dybowski, B.; Zarychta-Wisniewska, W.; Kulesza, A.; Zagozdzon, R.; Gajewski, Z.; Paczek, L., The Anatomy of Caprine Female Urethra and Characteristics of Muscle and Bone Marrow Derived Caprine Cells for Autologous Cell Therapy Testing. *Anat Rec (Hoboken)* **2017,** 300, (3), 577-588.

37. Burdzinska, A.; Dybowski, B.; Zarychta-Wisniewska, W.; Kulesza, A.; Butrym, M.; Zagozdzon, R.; Graczyk-Jarzynka, A.; Radziszewski, P.; Gajewski, Z.; Paczek, L., Intraurethral co-transplantation of bone marrow mesenchymal stem cells and muscle-derived cells improves the urethral closure. *Stem Cell Res Ther* **2018,** 9, (1), 239.
38. Jankowski, R. J.; Deasy, B. M.; Huard, J., Muscle-derived stem cells. *Gene Therapy* **2002,** 9, (10), 642-647.
39. Mau, M.; Oksbjerg, N.; Rehfeldt, C., Establishment and conditions for growth and differentiation of a myoblast cell line derived from the semimembranosus muscle of newborn piglets. *In Vitro Cellular & Developmental Biology-Animal* 2008, 44, (1), 1-5.
40. Dezawa, M.; Ishikawa, H.; Itokazu, Y.; Yoshihara, T.; Hoshino, M.; Takeda, S.; Ide, C.; Nabeshima, Y., Bone marrow stromal cells generate muscle cells and repair muscle degeneration. *Science* **2005,** 309, (5732), 314-7.
41. Yoshida, N.; Yoshida, S.; Koishi, K.; Masuda, K.; Nabeshima, Y., Cell heterogeneity upon myogenic differentiation: down-regulation of MyoD and Myf-5 generates 'reserve cells'. *J Cell Sci* **1998,** 111 (Pt 6), 769-79.
42. Hannon, K.; Kudla, A. J.; McAvoy, M. J.; Clase, K. L.; Olwin, B. B., Differentially expressed fibroblast growth factors regulate skeletal muscle development through autocrine and paracrine mechanisms. *J Cell Biol* **1996,** 132, (6), 1151-9.
43. Foster, A. A.; Marquardt, L. M.; Heilshorn, S. C., The Diverse Roles of Hydrogel Mechanics in Injectable Stem Cell Transplantation. *Curr Opin Chem Eng* **2017,** 15, 15-23.
44. Amend, B.; Kelp, A.; Vaegler, M.; Klunder, M.; Frajs, V.; Klein, G.; Sievert, K. D.; Sawodny, O.; Stenzl, A.; Aicher, W. K., Precise injection of human mesenchymal stromal cells in the urethral sphincter complex of Gottingen minipigs without unspecific bulking effects. *Neurourol Urodyn* **2017,** 36, (7), 1723-1733.
45. Sasca, D.; Szybinski, J.; Schuler, A.; Shah, V.; Heidelberger, J.; Haehnel, P. S.; Dolnik, A.; Kriege, O.; Fehr, E. M.; Gebhardt, W. H.; Reid, G.; Scholl, C.; Theobald, M.; Bullinger, L.; Beli, P.; Kindler, T., NCAM1 (CD56) promotes leukemogenesis and confers drug resistance in AML. *Blood* **2019,** 133, (21), 2305-2319.
46. Gunasekara, C. J.; Scott, C. A.; Laritsky, E.; Baker, M. S.; MacKay, H.; Duryea, J. D.; Kessler, N. J.; Hellenthal, G.; Wood, A. C.; Hodges, K. R.; Gandhi, M.; Hair, A. B.; Silver, M. J.; Moore, S. E.; Prentice, A. M.; Li, Y.; Chen, R.; Coarfa, C.; Waterland, R. A., A genomic atlas of systemic interindividual epigenetic variation in humans. *Genome Biology* **2019,** 20, (1), 105.
47. Kalbe, C.; Mau, M.; Rehfeldt, C., Developmental changes and the impact of isoflavones on mRNA expression of IGF-I receptor, EGF receptor and related growth factors in porcine skeletal muscle cell cultures. *Growth Horm IGF Res* **2008,** 18, (5), 424-433.
48. Zhang, S.; Chen, X.; Huang, Z.; Chen, D.; Yu, B.; Chen, H.; Luo, J.; He, J.; Zheng, P.; Yu, J., Leucine promotes differentiation of porcine myoblasts through the protein kinase B (Akt)/Forkhead box O1 signalling pathway. *British Journal of Nutrition* **2018,** 119, (7), 727-733.
49. Geng, R.; Knoll, J.; Harland, N.; Amend, B.; Enderle, M. D.; Linzenbold, W.; Abruzzese, T.; Kalbe, C.; Kemter, E.; Wolf, E.; Schenk, M.; Stenzl, A.; Aicher, W.

K., Replacing Needle Injection by a Novel Waterjet Technology Grants Improved Muscle Cell Delivery in Target Tissues. *Cell Transplant* **2022,** 31, 9636897221080943.

50. Maak, S.; Wicke, M.; Swalve, H. H., Analysis of gene expression in specific muscle of swine and turkey. *Arch Tierzucht* **2005,** 48, 135 - 140.

13. Publication 4

Göttingen minipigs present with significant regeneration kinetics after sphincter injury when compared to German landrace gilts

Jasmin Knoll[1#], Niklas Harland[2#], Bastian Amend[2], Arnulf Stenzl[2], Wilhelm K. Aicher[1*]

[1] Centre of Medical Research, Department of Urology at UKT, Eberhard-Karls-University, 72072 Tuebingen, Germany
[2] Department of Urology, University of Tuebingen Hospital, 72076 Tuebingen, Germany

[#] Both, J.K. and N.H., contributed equally to the study and therefore deserve shared first authorship

* Correspondence author

BMC Veterinary Research

Year 2023

BioMed Central (BMC), part of Springer Nature

Submitted: 24 March 2023

Abstract

Background Animals serve as important models for exploring the pathology, diagnosis, and therapy of different diseases and injuries. While smaller animals are preferred for bulk cohort studies, larger animals offer opportunities to investigate surgical procedures at proportions close to the human situation. We therefore investigated urethral sphincter deficiency in pigs to develop a preclinical model of urinary incontinence. German landrace gilts and Göttingen minipigs were included in this study. Urethral sphincter deficiency was induced surgically by transurethral electrocautery and balloon dilatation, and the deficiency was determined by urodynamics after injury and during follow-up. In cryosections, sphincter injury was visualized by histochemistry.

Results In two cohorts of female Göttingen minipigs (total n = 20) sphincter deficiency was induced. One cohort of minipigs showed an initially significant urethral sphincter deficiency (n =16, $p<0.001$). However, spontaneous regeneration was observed within one to two weeks. The other cohort of minipigs (n=4) displayed a not significant reduction of urethral sphincter pressure and an increase in muscle strength over time as well. In contrast, German landrace gilts presented immediately after treatment with significant sphincter deficiency (n =6, 21%, $p<0.001$) and suffered from significant loss of sphincter function for at least five weeks (67%, $p<0.01$).

Conclusion Göttingen minipigs inherit significantly superior sphincter regeneration capacities compared to landrace pigs. This difference may bias preclinical studies in urology and other fields and explain in part seemingly contradictory results from different animal studies.

Keywords

Wound healing animal model, urinary incontinence, sphincter deficiency, Göttingen minipigs, landrace pigs

Background

Urinary incontinence (UI) is a significant personal, social, and medical challenge. A recent meta-analysis reported a mean UI prevalence of 41% (range 9% – 75%), and 26% of women reported daily loss of urine (1). In women, UI is associated with pregnancy, vaginal delivery, and hormonal changes in menopause (2, 3), while in men injuries after prostate cancer surgery predominate (4). In some cases, physical exercise of lower pelvic floor muscles may improve the situation, sometimes complemented by electrophysiological stimulation, bio-feedback devices, or chemicals (5). If these therapies fail to yield improvement, surgical therapies including cell therapies can be considered (6). However, studies reporting on cell therapy of UI grant a quite diverse picture. In several preclinical animal studies, advantages of cell therapies were reported but cohort sizes were often small, follow-up times were short, or studies did not yield an overall significant outcome (7-10). Some clinical studies suffered from similar problems (11-13), other studies were retracted (not cited) or not published nor reported to the authorities (compare e.g., EMA registry on SUI cell therapy). However, some recent papers rated the efficacy of UI cell therapies over other treatments (14, 15), while others reported little benefit (16). Robust and relevant large animal models of human diseases or deficiencies investigating the efficacies and kinetics of different UI therapies are essential to solve these issues (17-23).

A variety of UI animal models were introduced in the field, ranging from rodents (24, 25) to farm animals (8, 17), and non-human primates (26, 27). Rodents facilitate studies with larger cohorts and grant statistical advantages for regimen with small molecules (chemicals, proteins) but come with an entirely different anatomical situation compared to human patients. For instance, precise needle injections of active components in a rodent's urethra require excellent surgical skills. Moreover, in rodents transurethral application of medication and transurethral follow-up seem impossible. In contrast, the anatomy and build of Macaca fascicularis, a non-human primate, comes closer to the human situation and studies in cynomolgus monkeys provided results in favor of UI cell therapy (28). However, this animal model is too small to develop working prototypes of surgical instruments intended for later clinical use. We therefore extended our experimental work with gilts as UI models, as they provide size and metabolism suitable for preclinical studies with standard-size surgical instruments (17, 20, 21, 23). However, rapid growth of young

landrace pigs may cause technical difficulties for long-term follow-up of UI therapy. Hence we investigated if a combination of transurethral injury of the sphincter complex plus urethral dilatation produced a significant and lasting sphincter deficiency in Göttingen minipigs (GM). The GM were selected based on their slow growth kinetics leveling off at a mean weight of 45 ± 15 kg at about 20 months of age, thus facilitating long-term studies (19). Female German landrace gilts (GL) served as control cohort (17). Prior to experimental induction of sphincter deficiency, the sphincter muscle complex was localized under visual control by cystoscope and transurethral determination of the urethral wall pressure. To do so, standard urethral pressure profilometry (s-UPP) and high-definition urethral pressure profilometry (HD-UPP) were employed (17). Immediately after injury and during follow-up, the spontaneous functional recovery of the urethral closure complex was also determined by s-UPP and HD-UPP.

In GM, a robust and durable model of urinary incontinence was not established by electrocautery of the sphincter muscle in combination with urethral balloon dilatation. Sphincter closing pressure was reduced in GM but was no longer significantly different from pretreatment values as early as one or two weeks after treatment due to spontaneous tissue regeneration without active therapy. Even enhanced muscle injury by enforced electrocautery failed to establish a lasting UI model in gilts of this breed. In contrast, moderate sphincter injury followed by urethral dilatation in GL generated a significant sphincter deficiency lasting for five weeks. This leads to the conclusion that GL seem a better model to study cell therapies after sphincter injury. This breed difference may also apply to therapy studies of other muscles or tissues.

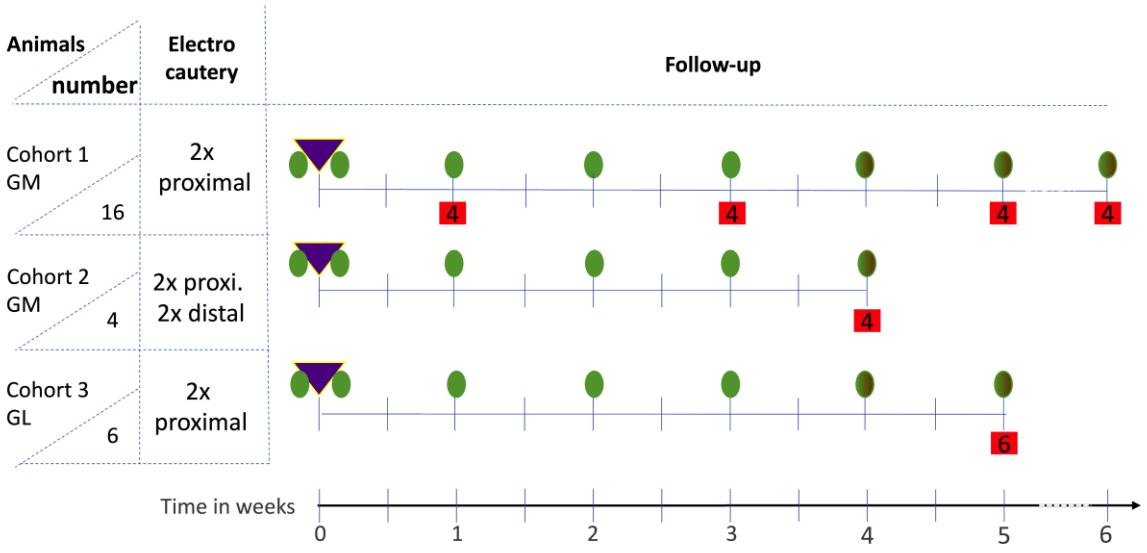

Figure 1: Schematic overview of animal experiments. Timelines of surgically induced urethral sphincter deficiency were investigated in three animal cohorts. Sphincter deficiency was induced in cohort 1 (16 GM gilts) by two proximal electrocauteries and balloon dilatation. The overall follow-up lasted for six weeks. After 1, 3, 5, and 6 weeks 4 GM each were taken out of the study to prepare sphincter samples for histology as indicated by numbers in red boxes. Cohort 2 (four GM gilts) was treated by two proximal and two distal electrocauteries and balloon dilatation. The overall follow-up lasted for four weeks. After sacrifice, urethral sphincter tissue was analyzed by histology. Cohort 3 (six GL) were treated by two proximal electrocauteries and balloon dilatation as cohort 1 animals. The overall follow-up lasted for five weeks. After sacrifice, urethral sphincter tissue was analysed by histology. Urodynamics (green ovals) were performed on day 0 immediately before and immediately after induction of sphincter deficiency (violet triangles) and weekly thereafter as indicated.

Results

Sphincter regeneration after moderate injury in Göttingen minipigs

Sphincter deficiency was induced in 16 GM of cohort 1 in the area of maximal urethral wall pressure by proximal electrocautery followed by balloon dilatation (17) (Figure 1). The degree of muscle deficiency was enumerated by s-UPP immediately after induction of sphincter deficiency and during follow-up for a total of six weeks (Figure 2). When computing the sphincter insufficiency for the four animals completing the study in cohort 1, significant differences were recorded between sphincter function before induction of deficiency and immediately after surgery (Figure 2A; 60.5% ±26.6%; n=4; $p<0.01$). However, as early as one week after surgery and during follow-up, significant differences were not recorded anymore (Figure 2A). Nevertheless, sixteen gilts entered the study in cohort 1 but one, three, and five weeks after surgery four animals each were taken out of the study for histology (Figure 1). We therefore imputed the missing data to maintain a virtual cohort size of 16 GM. In the imputed total population a significant loss of sphincter function was recorded immediately after induction of incontinence (56.9% ±19.7%; n=16; $p<0.001$) and after one week of follow-up (68.8% ± 26.8%; n=16; $p<0.001$) when compared to the same animal prior surgery (Figure 2B). Still, no significant difference was calculated for two weeks of follow-up (Figure 2B; 93% ± 34.6%). Virtually significant differences were computed between the urethral wall pressure before induction of incontinence compared to three to six weeks after surgery (Fig. 2B). Urinary infection, white and red blood cell counts, as well as urine chemistry (pH, glucose, etc.) were monitored throughout the study, and pathological abnormalities were not recorded in 14/16 animals of cohort 1. However, 2/16 animals suffered from urethral infection after induction of sphincter deficiency.

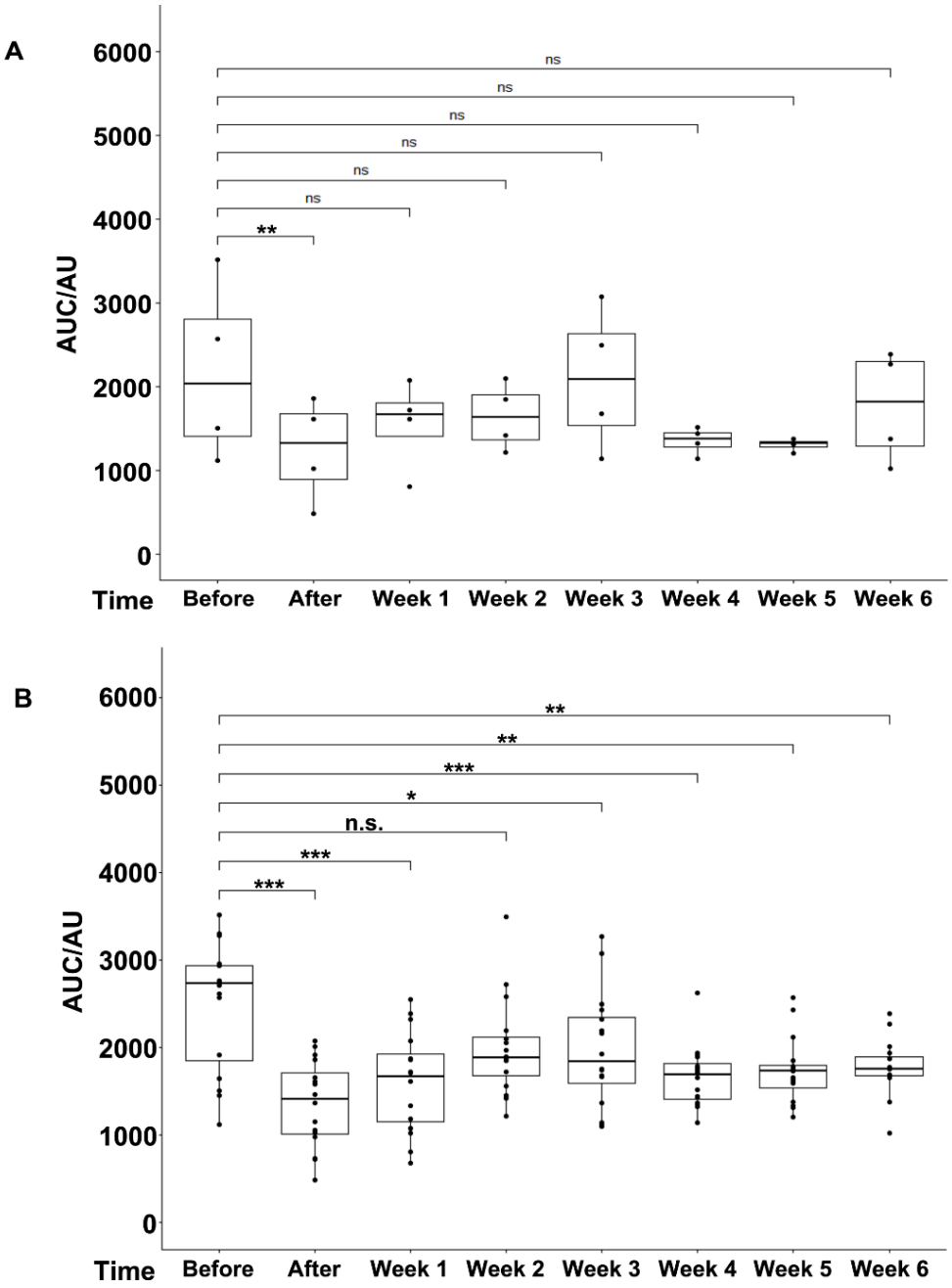

Figure 2: Boxplots of urodynamic measurements of cohort 1 determined with standard urethral pressure profilometry (s-UPP). A: Boxplots and p-values were calculated, and nonparametric analyses are reported for the four GM which completed six weeks of follow-up period. The areas under the curve (AUCs) were obtained from the original measurements. In these analyses, a significant result is computed only between "Before" and "After" surgery ($p<0.01$; **). All other comparisons were not significant (n.s.). **B:** Urodynamic measurements were performed immediately before (Before) and immediately after (After) induction of sphincter deficiency, and weekly during follow-up (Week 1-6). The areas under the curve (AUCs) were obtained from the original measurements. Since after 1, 3, and 5 weeks, four GM each were taken out, the missing data were imputed, averages were built, and p-values were calculated from these averages via nonparametric analyses to maintain an artificial/virtual cohort size of sixteen animals throughout the study. Highly significant results (***) were computed for the AUC median pairs "Before" to "After" and "Before" to "Week 1" ($p<0.001$), respectively. "Before" to "Week 2" was not significant, but "Before" to weeks three to six were significant again, as indicated by asterisks. The x-axes present the time points of urodynamic measurements, the y-axes the urethral wall pressure as AUC in arbitrary units (AU).

From cohort 1, four animals each were sacrificed one, three, and five weeks after induction of incontinence to investigate the sphincter tissue by histology (Figure 1, 3). Tissue injury was noted one week after electrocautery and balloon dilatation (Figure 3A, 3D). In the mucosa no blebs were visible. Signs of infiltration of mononuclear cells were not observed (Figure 3A). After three weeks of follow-up, tissue regeneration was visible by histochemistry in cohort 1 animals. Blebbing of the mucosa was observed (Figure 3B, 3E). Structural changes and muscular abnormalities in the rhabdosphincter were evident in three of four animals investigated in detail (Figure 3E). One of the four animals showed no muscular irregularities (data not shown). After five weeks of follow-up, the muscular layer and the mucosa appeared almost normal in cohort 1 animals (data not shown), except for two animals in which each one suggested electrocautery location with still interrupted muscular layer was recorded (Figure 3C, 3D). These histological analyses of tissue samples (Figure 3) corroborated the results of the urodynamics indicating a rapid functional sphincter regeneration in GM (Figure 2B).

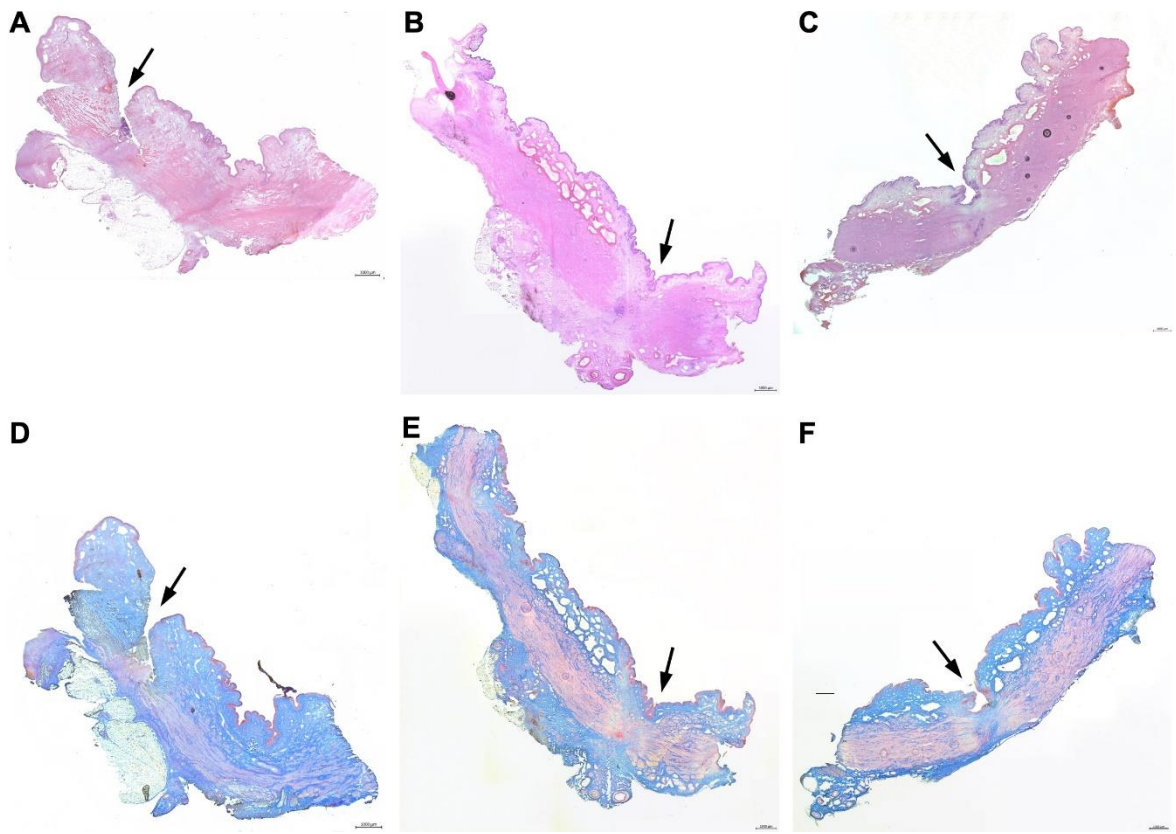

Figure 3: Histological analyses of representative animals of cohort 1 at weeks 1, 3, and 5 after induction of sphincter insufficiency. HE (A-C) and Azan (D-F) staining of consecutive 20 µm-cryosections of one representative animal per time point of cohort 1. **A,D:** One week after surgery, histochemistry shows serious injury of the urothelial layer, incision in the mucosa (arrow), and interrupted muscle structures. Mucosal blebs were not found. **B, E:** Three weeks after surgery, incisions are not observed anymore, the urethral layer is intact, in the mucosa blebs are found, but the sphincter muscle shows structural irregularities (arrow). **C, F:** Five weeks after surgery, the urethral layer is intact, in the mucosa blebs are visible, and the sphincter muscle layer is slightly interrupted in one animal (arrow). Scale bars indicate 1000 µm.

Sphincter regeneration after enhanced injury in Göttingen minipigs

In contrast to our recent study employing GL (17), a functional sphincter recovery in cohort 1 GM was observed as early as one to two weeks after surgery (Figure 2). We hypothesized that two proximal electrocauteries were not sufficient to establish a robust SUI model in GM. In a small feasibility study, four GM were treated by four electrocauteries, placing two injuries just distal and two just proximal outside the zone of maximal urethral wall pressure, and complementing the electrocauteries by balloon dilatation (Figure 1). Significant differences in the urethral wall pressure were not recorded after enhanced induction of sphincter deficiency compared to the wall pressure before

surgery (Figure 4). To confirm the results obtained by s-UPP, urethral wall pressure was also measured by HD-UPP (Figure 5). The HD-UPP prototype recorded the urethral wall pressure by eight sensors positioned on the catheter in a spiral-shaped distribution (29-31). The HD-UPP facilitated a high-resolution measurement as function of the urethral stretch s (in mm) from bladder neck and the angular position Θ (in deg) of an individual measuring point. Pressure levels are indicated by colors in two-dimensional (2D) blots (Figure 5A - F). The green zone of elevated wall pressure with a width of approximately 30 mm indicated the wall pressure maximum and did not disappear nor change color after surgery. However, a narrowing of the ("green") zone of maximal urethral wall pressure was noted immediately after surgery and during follow-up. The HD-UPP prototype also allows to present the urethral pressure profiles as histograms using the same colors as in the 2D blots (Figure 5G – L). A difference in the maximal urethral wall pressure was not recorded in animals before surgery and during follow-up up to four weeks, and pressure levels of approximately 100 cm H_2O were measured (Figure 5G – L). The data generated by s-UPP to compute mean differences and statistics (Figure 4) were utilized to generate pressure histograms as well. The s-UPP histograms confirmed the narrowing of the zone of maximal urethral wall pressure after surgery and during follow-up compared to animals before treatments (Figures 5G – L). Utilizing s-UPP, slightly higher pressure levels of approx. 150 mm H_2O were determined (Figure 5M – R) when compared to HD-UPP histograms (Figure 5G – L). Both sensor types failed to determine significant differences between animals before versus after induction of sphincter deficiency. Therefore, this study was terminated after four weeks to comply with animal welfare regulations. As a prototype sensor was employed for HD-UPP in these experiments, differences observed between HD-UPP and s-UPP can be explained by a different calibration of the device. Urinary infection, white and red blood cell counts, as well as urine chemistry (pH, glucose, etc.) were monitored throughout the study, and pathological abnormalities were not recorded.

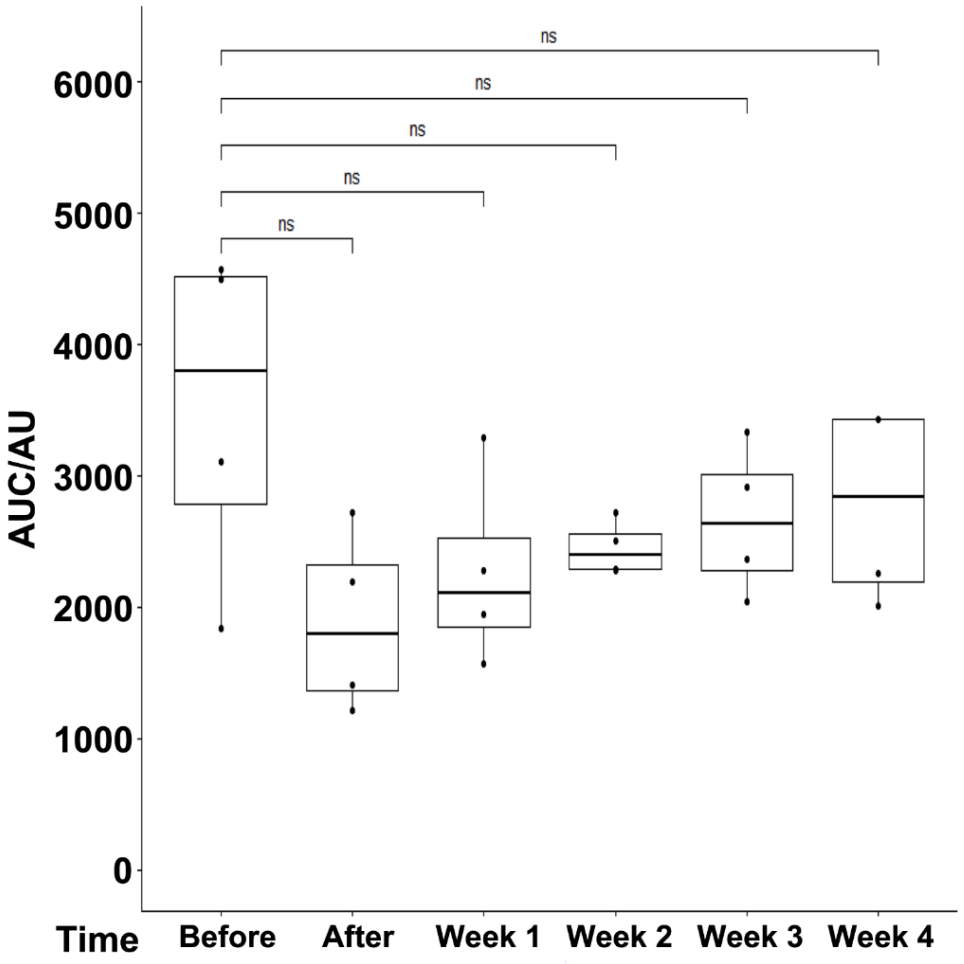

Figure 4: Boxplots of urodynamic measurements of cohort 2 determined with standard urethral pressure profilometry (s-UPP). Urodynamic measurements were performed with standard urethral pressure profilometry (s-UPP) with four cohort 2 animals as described in Figure 2B. Areas under the curve (AUCs) were calculated from the original measurements. No significant p-values were obtained for any of the comparisons. The x-axis presents the time points of urodynamic measurements, the y-axis the urethral wall pressure as AUC in arbitrary units (AU).

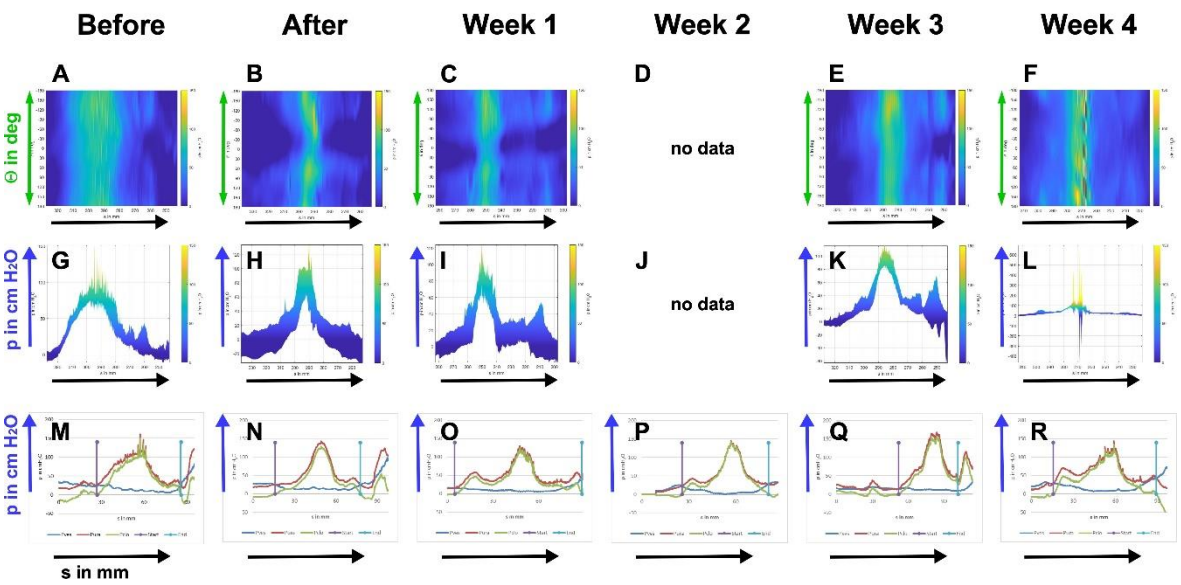

Figure 5: Urethral wall pressure analyses of cohort 2 monitored over four weeks after incontinence induction with two distinct devices. A – L: Urodynamic measurements were performed with a high-definition urethral pressure profilometry (HD-UPP) prototype immediately before incontinence induction ("Before"), immediately after incontinence induction ("After"), and weekly during follow-up (Week 1-4). One representative animal is depicted. In week 2, no data were measured with the HD-UPP due to technical failure of the prototype. The results of HD-UPP measurements are displayed in two versions. Mode 1 (A-F) displays the urethral wall pressure as three-dimensional graph (stretch "s" in mm on the x-axis, angular position θ = clockwise angle in degrees on the y-axis, and urethral wall pressure "p" in cm H_2O as a color range from blue (=0 cm H_2O) to yellow (=150 cm H_2O). Mode 2 (G-L) displays a two-dimensional view of the data produced by HD-UPP. On the x-axis, the stretch in mm is shown, while on the y-axis the urethral wall pressure is displayed in cm H_2O. Note the different dimensions on the y-axis of the graphs. The color code in modes 1 and 2 did not show any difference over time in the height of urethral wall pressure but indicate a smaller width of maximal wall pressure for "After" and "Week 1", respectively. **M - R:** In addition, urodynamic measurements were performed in all animals by standard urethral pressure profilometry (s-UPP). The graphs show data of the same animal and time points as in A – L. The colored curves represent the vesical pressure Pves (blue) and urethral pressure Pura (red) measured with sensors, and the calculated urethral closure pressure Pclo (green). This data set was used to compute the AUC for Figure 4. The upright violet start- and the turquoise end- lines indicate the range selected for AUC calculations. The graphs supported the results of A-L.

Histochemistry of sphincter samples from cohort 2 animals of the proximal electrocauteries was performed after animals' sacrifice after four weeks of follow-up corresponding to cohort 1 animals. Infiltration of mononuclear cells was not observed. At that time point, apparent signs of tissue injury were not recorded in the urothelial, mucosal, and submucosal layers of the urethra. The sphincter muscle stained with regular patterns (Figure 6). The results corroborated that GM recovered from induction of sphincter deficiency by balloon dilatation plus fourfold electrocautery quite fast (Figures 5, 6). Considering GM as SUI models, reliable differences in sphincter recovery were not

observed after moderate versus enhanced electrocautery and balloon dilatation (Figures 2 – 6).

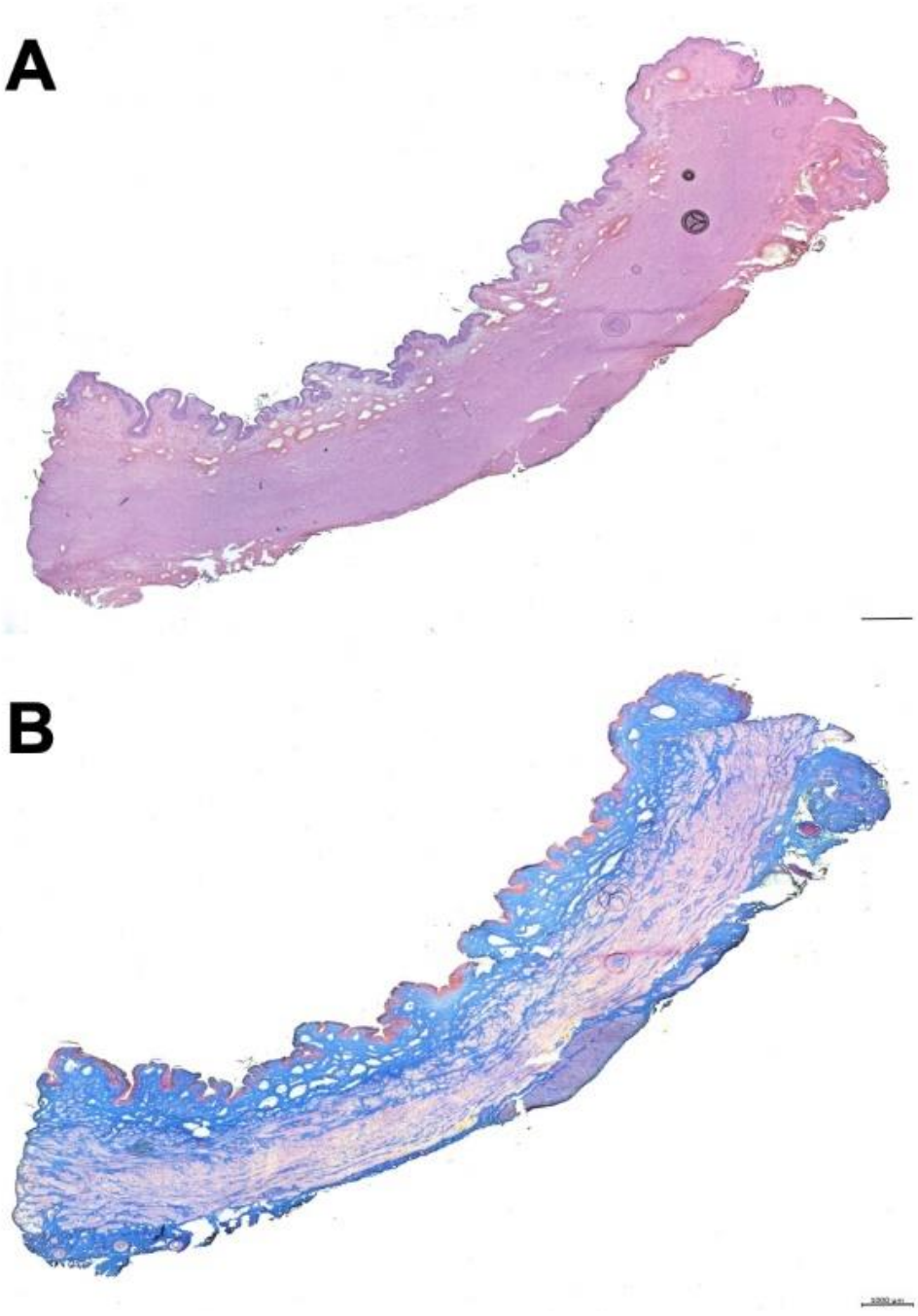

Figure 6: Histological analysis of representative animal of cohort 2. Representative HE (A) and Azan (B) staining of consecutive 20 µm-cryosections of one representative animal of cohort 2 after four weeks of follow-up. Staining provided no evidence for interrupted muscle structures and no interruption of the urothelial structure resulting from the electrocautery was observed. Small blebs in the mucosa were visible. Scale bars indicate 1000 µm.

Sphincter regeneration after moderate injury in German landrace gilts

To verify the improved sphincter regeneration in GM included in this study, sphincter insufficiency was induced in six GL applying the moderate procedure comparable to cohort 1 animals distally in the zone of maximal urethral wall pressure. The animals were observed for five weeks of follow-up (Figure 1). In contrast to GM, a significant and lasting sphincter muscle deficiency was observed in GL after moderate injury using a double electrocautery plus balloon dilatation. This was evident immediately after surgery and during follow-up (Figure 7). The mean urethral wall pressure dropped immediately after surgery to 20.8% ± 12.2% ($p<0.001$). Spontaneous tissue regeneration and wound healing during follow-up elevated the wall pressure to 71.7% ± 19.4% three weeks after surgery. Nevertheless, it remained significantly below levels determined in untreated animals throughout the follow-up of five weeks ($p<0.01$ to $p<0.001$; Figure 7). To corroborate the results obtained by s-UPP after moderate induction of sphincter deficiency, HD-UPP was performed in cohort 3 animals as well (Figure 8). As explained above, green and yellow colors indicate elevated urethral wall pressure in 2D blots (Figure 8A – G). Immediately after induction of sphincter deficiency and during follow-up, sphincter muscle activity or urethral wall pressure remained at ("blue") base levels (Figure 8B – G). The histogram mode of the HD-UPP determined about 80 cm H_20 urethral wall pressure prior to surgery (Figure 8H), a reduction to about 20 cm H_20 (Figure 8I – K) immediately after surgery and during early follow-up, reaching a peak three weeks after surgery (50 cm H_2O; Figure 8L), and leveling off at about 40 cm H_2O, after four and five weeks, respectively (Figure 8M, N). The data generated by s-UPP to compute mean differences and statistics (Figure 7) were utilized to generate pressure histograms as well (Figure 8O - U). By s-UPP, a urethral wall pressure maximum of 100 cm H_2O was recorded in animals prior to induction of sphincter deficiency (Figure 8O). After surgery, the wall pressure dropped below 50 cm H_2O and remained below this level during follow-up (Figure 8P – U). Urinary infection, white and red blood cell counts, as well as urine chemistry (pH, glucose, etc.) were monitored throughout the study, and pathological abnormalities were not recorded.

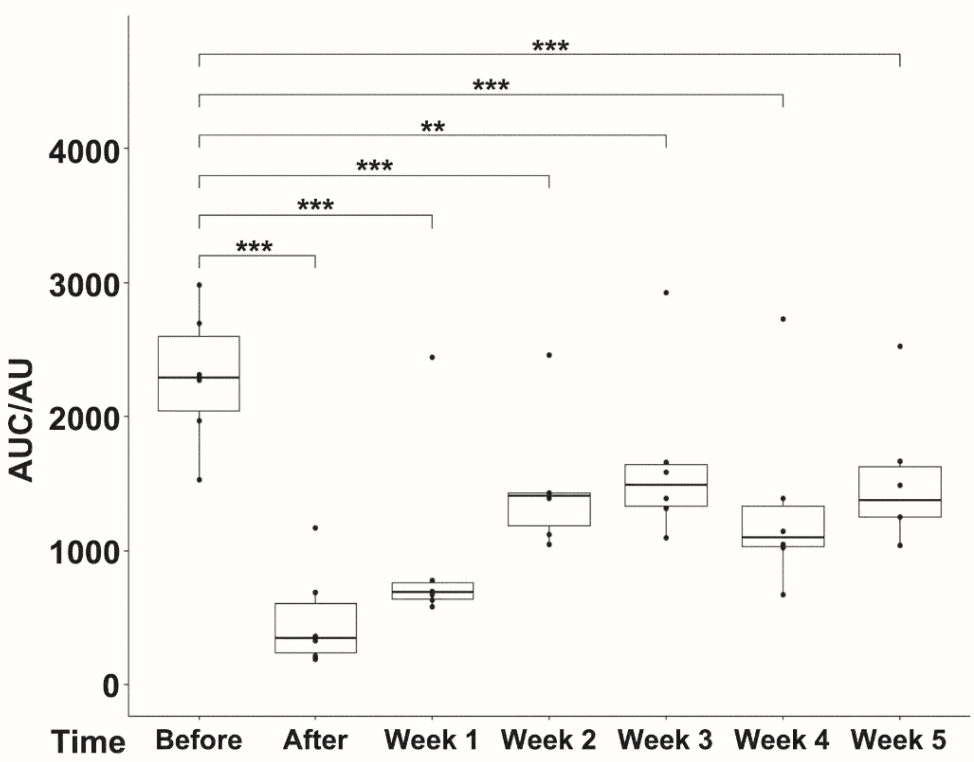

Figure 7: Boxplots of urodynamic measurements of cohort 3 determined with standard urethral pressure profilometry (s-UPP). Urodynamic measurements were performed with standard urethral pressure profilometry (s-UPP) immediately before incontinence induction ("Before"), immediately after incontinence induction ("After"), and weekly during follow-up (Week 1-5). The areas under the curve (AUC) indicating urethral sphincter function were calculated from the original measurements. Significant and highly significant p-values were computed for all comparisons as indicated (**, ***) using "Before" as control. The x-axis presents the time points of urodynamic measurements, the y-axis the urethral wall pressure as AUC in arbitrary units (AU).

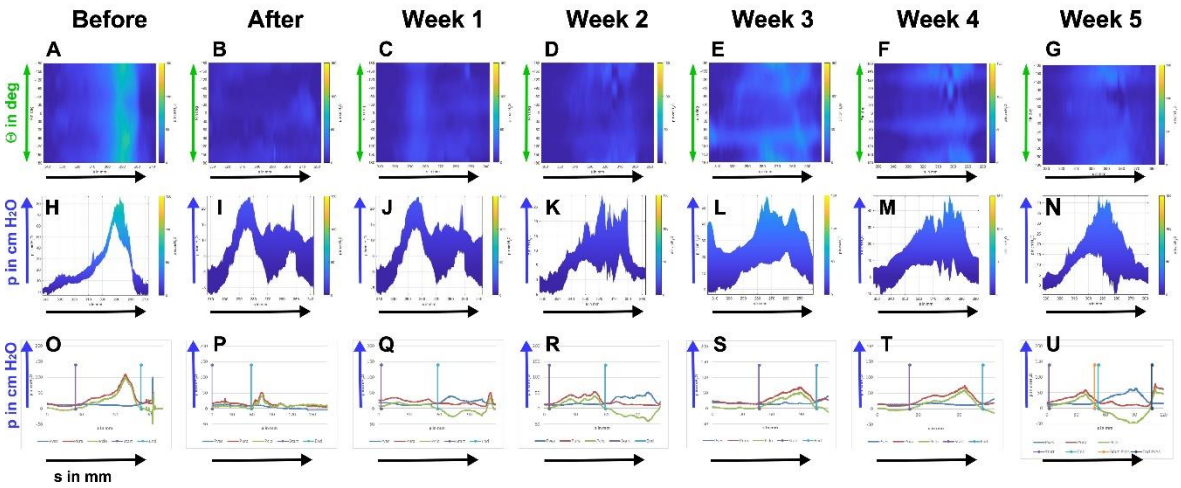

Figure 8: Urethral wall pressures of cohort 3 monitored over five weeks after incontinence induction with two distinct devices. A – N: Measurements of urethral wall pressure were performed with a high-definition urethral pressure profilometry (HD-UPP) in cohort 3 pigs as described in figure 5. One representative animal is shown. Urodynamics with HD-UPP in mode 1 (A-G) display the urethral wall pressures as three-dimensional graphs and in mode 2 (H-N) as two-dimensional histograms. The color code (A – G) and histograms (H - N) depicted normal sphincter function only before (A, H) but not after surgical treatment nor during follow-up (B – G, I – N). **O-U:** In addition, urodynamic measurements were performed in all animals by standard urethral pressure profilometry (s-UPP) as well. The graphs show data of the same animal as in A – N. Details are explained in the legend to figure 5. The graphs also support the results of A-N.

After follow-up and animals' sacrifice, cryosections of urethral sphincter samples were analyzed by histochemistry (Figure 9). Infiltration of mononuclear cells was not observed by HE staining, but the tissue integrity presented with irregularities (Figure 9A). By AZAN staining disruption of the muscular layer and replacement by connective tissue was recorded. Moreover, in the mucosa no blebs were found suggesting compression of the tissue by balloon dilatation. (Figure 9A, 9B). These findings are in line with the results obtained by s-UPP and HD-UPP (Figures 7, 8). Moreover, it confirmed that moderate induction of sphincter deficiency by double electrocautery followed by balloon dilatation persisted in GL significantly during follow-up of five weeks. Thus, GL have proven as robust large animal model of stress urinary incontinence.

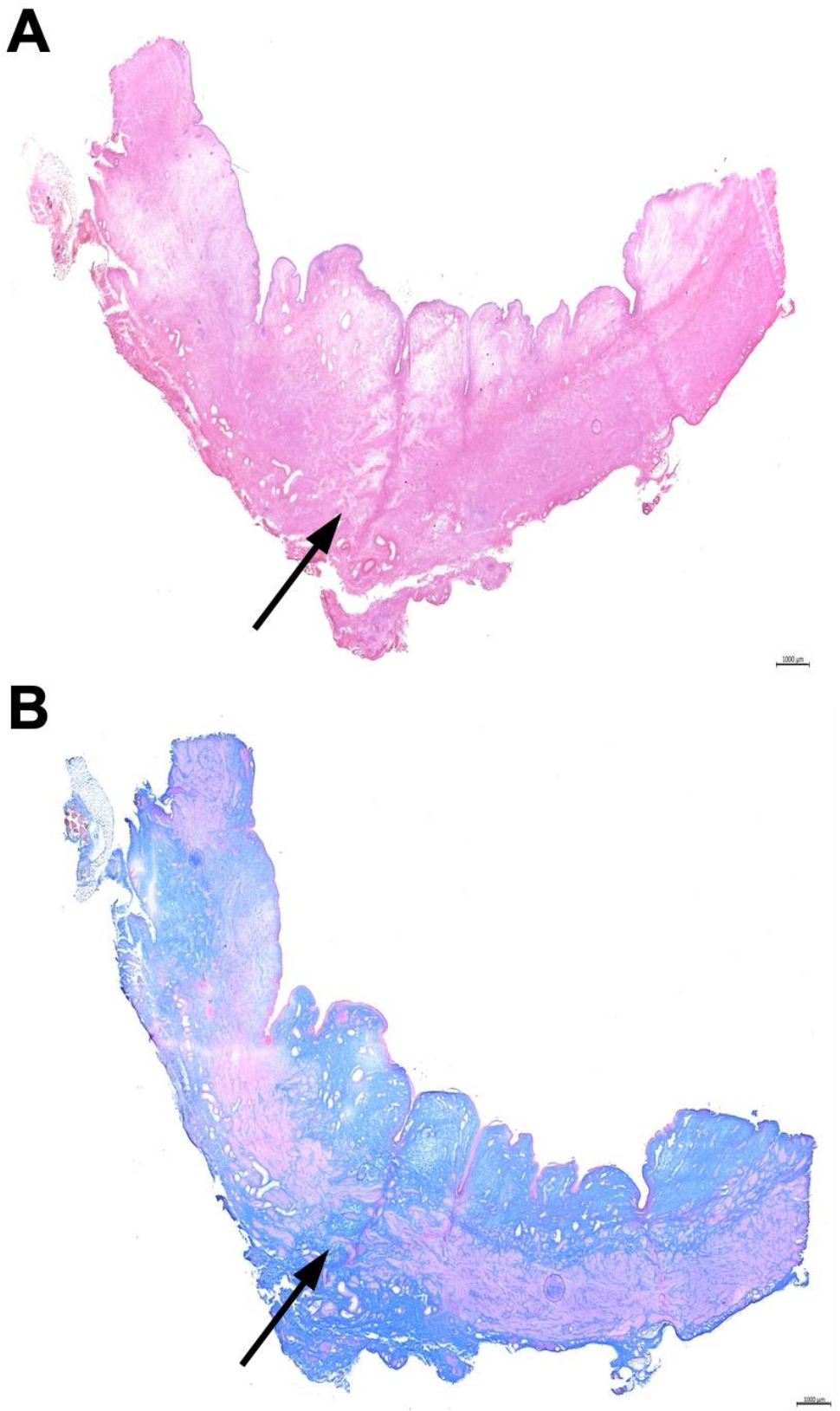

Figure 9: Histological analysis of representative animal of cohort 3. Representative HE (A) and Azan (D) staining of consecutive 20 µm-cryosections of one animal of cohort 3 five weeks after induction of sphincter deficiency. Interruption of muscular structures and connective tissue in the zone of the urethral rhabdosphioncter muscle were seen by HE and AZAN staining (arrows). Alterations in the mucosa or urothelial layer were not noted. Scale bars indicate 1000 µm.

Discussion

Porcine models of diseases gained interest recently upon completion of the sequencing of the porcine genome, generation of mutant lines by recombinant technologies, and based on the fact that e.g., size of organs, omnivore metabolism, genetics, and other characteristic are more closely related to humans when compared, for instance, to rodents (32, 33). Among different porcine breeds, smaller ones such as GM are preferred through their limited growth and weight even after extended follow-up (34). We therefore hypothesized that GM may provide a large animal model of UI to facilitate studies on effects of cell therapy with an extended follow-up but without biasing anatomic changes due to the growth of the animals (19). However, in contrast to recent studies employing landrace gilts (17, 35), significant sphincter deficiency was recorded in GM only up to one to two weeks after induction of urethral muscle injury. Even enhanced electrocautery followed by balloon dilatation failed to induce a significant sphincter deficiency in GM. In contrast, moderate surgical intervention employing only two lateral electrocauteries of the urethral sphincter yielded a significant, robust, and lasting sphincter deficiency in GL. Moreover, the level of reduction of urethral wall pressure immediately after electrocautery and dilatation was only about 40 – 45% in cohort 1 and cohort 2 compared to about 80% in cohort 3 animals. This difference could indicate that the tissue elasticity of the sphincter complex, the mechanical resistance to dilatation, vascularization, and other specificities differ in GM in relevant ways from GL. Such characteristics of the breeds may at least in part contribute to the significant difference in SUI induction observed between cohort 1 and 2 animals when compared to cohort 3 animals. Therefore, we suggested that differences in the outcome of this preclinical study were most likely associated with the breed of the animals, including the anatomy of the sphincter.

Differences in the regeneration of the critical contractile compound in our model, the muscle tissues of the urethral sphincter, must be considered when discussing the differences in sphincter regeneration measured. Growth patterns of smooth muscle cells isolated from GM compared to GL provided evidence that cells of GL proliferated faster and seeded scaffolds better than those isolated from GM (36). Moreover, a higher content of smooth muscle cells was reported in GL arteries compared to GM vessels (37). In one model for muscular ventricular septal defect therapy, GL presented with good results (38), while other authors claimed Yucatan minipigs as preferable model for the same

therapy (39). In a surgical model for cardiomyoplasty, GM and GL performed comparably (40). However, GM granted a superior model for studies of post-myocardial infarction heart failure (41). This finding would align with our results: better muscle regeneration of GM compared to landrace breeds. In previous studies, left ventricular ejection after myocardial infarction was slightly higher in GM (i.e., 11.3%) when compared to Yorkshire swine (42). Again, these findings corroborate our study as GM regenerated the sphincter complex faster than GL. Moreover, significant differences between cartilage and chondrocytes were observed between hybrid pigs and GL, respectively (43). Nevertheless, GM were characteristic of limited repair capacity of osteochondral defects (44). This indicates that GM do not inherit better tissue regeneration capacities in general compared to other breeds. These studies support the hypothesis that the differences in muscle regeneration in GM and GL explain at least in part the significant differences observed in spontaneous sphincter regeneration.

Another aspect merits discussion as well. Our recent study provided evidence that in GL the maximal urethral wall pressure is localized approximately in the middle of the urethra, about 5 cm distal of the bladder (17). In GM, the urethral wall pressure maximum was localized somewhat more proximal (Figure 5). Additionally, the two breeds display different urodynamics profiles in untreated conditions as reported recently and confirmed by our results (45) (Figure 5M, Figure 8O). While GL display a smaller peak in maximal closure pressure, GM represents more with a wider plateau of maximal closure pressure. As electrocautery is a rather pointed injury, it may not harm the wider plateau of the maximal sphincter strength in GM efficiently which might result in a higher loss of wall pressure obtained in GL compared to GM Therefore, this difference in sphincter injury could contribute to the different outcomes of our incontinence induction and seems essential for the SUI model.

In this study, the sphincter injury by electrocautery targeted the zone of the urethral wall pressure maximum. Here the urethral sphincter complex is predominated by smooth muscle tissue in GL as well as in GM, while striated muscle tissue is found only in the very distal parts of the porcine urethra (17, 46). The composition of the contractile tissue of the urethral sphincter does not discriminate between the two breeds included.

Age of the animals could also contribute to the differences observed. However, at least in the human situation, an elevated risk for extended urinary incontinence after mechanical stress by pregnancy or lower pelvic floor muscle trauma upon vaginal delivery is known to

correlate with increased age of the mother (47, 48). Therefore, the older female GM were expected to suffer from more severe sphincter deficiency when compared to the younger GL. So, the age of the animals seems not a key factor contributing to the shorter and not significant incontinence in GM. The health status of all animals was monitored throughout the study by expert veterinarians. The urine status, body temperature, animal behaviour, increase of weight during follow-up of all animals included provided no evidence for differences of illness nor malady between the breeds (data not shown).

However, differences in urethral vascularization and blood supply could contribute to improved sphincter regeneration in GM. Improved blood supply could also activate local satellite cells or other progenitor cells to facilitate tissue regeneration (49). To the best of our knowledge, this has not been investigated in detail in GM versus GL, but in GM hepatic blood flow and perfusion were significantly lower than in landrace hybrids (50). If vascularization is critical in the context of this study, we would expect that sphincter regeneration in GL should not lag significantly behind the functional recovery observed in GM. Nevertheless, detailed studies on urethral vasculature and blood supply are beyond the focus of this study. The composition of the extracellular matrix of the porcine urethra should not be disregarded when investigating differences in sphincter deficiency and regeneration (51). In human tissue samples of the elderly, collagen content increases and muscle tissue reduction were reported (52). The sphincter tissue of older GM could therefore be more resistant to tissue injury generated by electrocautery. This hypothesis is also supported by our finding that fourfold electrocautery applied in cohort 2 animals did not cause a significant sphincter deficiency when compared to the twofold electrocautery used in cohort 1 animals. But again, a detailed investigation of the differences in sphincter histology and regeneration in GM on molecular levels is beyond the focus of this study.

Conclusion

Göttingen minipigs inherit an elevated potential for rapid sphincter muscle regeneration and therefore failed to serve as robust animal model of urinary incontinence. This enhanced potential for muscle regeneration may influence the outcome of animal studies performed with this breed and should be taken into account when comparing studies performed in different breeds.

Material and Methods

Animal model of urinary incontinence and wound healing

Female Göttingen minipigs (GM; n = 20, mean weight approx. 25 kg, 12 months of age) were obtained with excellent health status and reports directly from the breeder (Ellegaard, Dalmose, Denmark). They were housed prior to surgery under specific conditions in the animal facility in cohorts of four to six gilts in separate pens for two weeks. German landrace gilts (GL; n = 6, mean weight approx. 30 kg, 3 months of age) were obtained with excellent health status directly from the breeder (Benz GbR, Bingen, Germany) and housed in the animal facility in one pen for two weeks prior to surgery. Before induction of sphincter deficiency, animals were sedated by pre-medication (atropin: 0.05 mg/kg body weight (bw) i.m. and azaperon: 4.0 mg/kg bw i.m.), followed by midazolam: 1.0 mg/kg bw i.m. and ketamin (14 mg/kg bw i.m.). The localization and muscular strength of the urethral sphincter complex were determined by cystoscopy under visual control measuring the urethral wall pressure using s-UPP (also known as urodynamics) in sedation (Aquarius TT, Laborie, Portsmouth, NH, USA) as described recently (17). Then, the animals were anesthetized (propofol: 5 mg/kg bw i.v. under controlled respiration with 0.6 - 1.6 Vol% isoflurane, complemented if needed by fentanyl: 5µg/kg bw i.v.). To establish the animal model of urinary incontinence, sphincter deficiency was induced in deep anesthesia. In cohort 1, GM (n = 16) were treated by two lateral electrocauteries (Erbe Hybridknife, mode monopolar cut, effect 4, power 100 W max.; ERBE Elektromedizin, Tuebingen, Germany) just proximal of the wall pressure maximum followed by balloon dilatation as described (17). In cohort 2, GM (n = 4), sphincter deficiency was established by two lateral electrocauteries proximal and two additional lateral electrocauteries distal of the urethral wall pressure maximum, followed by balloon dilatation as described above. Cohort 3 GL (n = 6) were treated as cohort 1 GM. Of note, maximum wall pressure was located more distally in the urethra. Immediately after induction of sphincter deficiency and thereafter during follow-up, sphincter function was monitored weekly by s-UPP for up to six weeks. The urine status was determined weekly to monitor, e.g., bleeding, protein, or alike (Combur 10 test, Roche, Pentzberg, Germany). In animals of cohort 2 and 3, a high-definition prototype device with improved local resolution was used (i.e., high-definition urethral pressure profilometry (HD-UPP) in addition to s-UPP monitoring (17, 30). From cohort 1 GM, four animals each were

sacrificed after 1, 3, 5, and 6 weeks of follow-up to prepare urethral tissue samples for histological analyses. GM of cohort 2 and GL of cohort 3 were sacrificed after 4 and 5 weeks of follow-up, respectively, to prepare urethral tissue samples as well (Figure 1).

During husbandry in the animal facility, animals were observed daily, and the health status was monitored by trained personnel. Depending on the breed, animals were given specific food and water ad libitum. The cohort sizes were calculated based on the assumption that induction of sphincter deficiency generated a drop in urethral wall pressure (i.e., sphincter muscle strength measured by urodynamics) of 60% below control levels. Randomization, blinding, or masking were not included in this feasibility study. The animal study was approved by the State of Baden-Württemberg Animal Welfare Authorities under file number 35/9185.81-2 / CU01-20G, and performed in full compliance with the ARRIVE 2.0. standards.

Generation of cryosections and histochemistry

After follow-up, gilts were sacrificed (phenobarbital, lethal). The urethral sphincter was prepared, cut open dorsally, suspicious tissue samples were embedded in freezing compound (Tissue Freezing Medium, Leica, Richmond, USA), frozen in liquid nitrogen, and stored at -80 °C. Cryosections were generated (20 µm, Leica CM1860 UV, Leitz, Wetzlar) and mounted on super frost slides. To visualize the urethral tissue, histochemistry was performed using AZAN trichrome- and HE-staining protocols (17). The samples were evaluated and recorded by microscopy (Zeiss Axio Vert.A1, Zeiss, Oberkochen). Overview pictures were generated by ‘Image Composite Editor’ software (Microsoft, Redmond,WA, USA).

Statistics

Raw data were used for statistical analyses. All statistical analyses were performed with R Statistical Software (v4.2.2) (53), and the nparLD R package (v2.2) (54) was used for calculations of ANOVA-type statistics reported in the figures. Nonparametric analyses were chosen due to small sample sizes and not normal data distributions. P-values < 0.05 were determined as significant and marked in the figures by asterisks ($p<0.001$ ***; $p<0.01$ **, $p<0.05$ *). For the evaluation of data of cohort 1, multiple imputation was performed using the amelia R package (v1.8.1) (55). 100 imputed data sets were created with a linear time effect, lower bound set to zero, and lags and leads defined as the

y-variable “area under the curve (AUC)”. To analyze the results with the nparLD R package, averages of the imputed data sets were built. For better comparison, raw data were normalized to the time point “Before” incontinence induction as 100% for each animal.

List of abbreviations

bw	body weight
GL	German landrace gilts
GM	Göttingen minipigs
HD-UPP	high-definition urethral (wall-) pressure profilometry
s-UPP	standard urethral (wall-) pressure profilometry, alias urodynamics
SUI	stress urinary incontinence
UI	urinary incontinence

Ethics approval, consent to participate and consent for publication

Ø not applicable, no human materials used.

Animal Welfare Statement

The animal study was approved by the State of Baden-Württemberg Authorities under file number 35/9185.81-2 / CU01-20G and performed according to the ARRIVE 2.0 standards.

Availability of data and materials

Data and materials will be disclosed to colleagues in academia upon written, justified, and comprehendible request to the corresponding author.

Competing interests

The authors declare no conflict of interest for this study.

Funding

The study was supported in part by the DFG project PoTuS #429049495 granted to B.A., A.S., and W.K.A. and by institutional funds.

Authors' contributions

J.K. animal experiments, histology, data evaluation, statistics, preparation of manuscript; N.H. animal surgery, urodynamics during follow-up, data evaluation; B.A. grant support, data evaluation; A.S. study design, grant support; W.K.A. study design, grant support, animal experiments incl. follow-up, data evaluation, preparation of manuscript. All authors contributed to the preparation and revision of the manuscript.

Acknowledgements

The authors express their gratitude to Mrs. Tanja Abruzzese MTA and Mrs. Conny Bock LTA for excellent technical support, especially for preparation and serial analyses of the tissue samples, the staining, and recording of the cryosections. We thank Prof. Dr. Oliver Sawodny and Dr. Mario Klünder (ISYS at Stuttgart University) for providing us with the HD-UPP prototype and for excellent training with the corresponding software programs. The authors thank Mrs. Lina Maria Serna Higuita for her support in statistical evaluations, and Mr. Chaim Goziga for expert technical help in preparation of the artwork.

References

1. Moossdorff-Steinhauser HFA, Berghmans BCM, Spaanderman MEA, Bols EMJ. Prevalence, incidence and bothersomeness of urinary incontinence in pregnancy: a systematic review and meta-analysis. International Urogynecology Journal. 2021;32(7):1633-52.
2. Minassian VA, Stewart WF, Wood GC. Urinary incontinence in women: variation in prevalence estimates and risk factors. Obstet Gynecol. 2008;111(2 Pt 1):324-31.
3. Lukacz ES, Santiago-Lastra Y, Albo ME, Brubaker L. Urinary Incontinence in Women: A Review. JAMA. 2017;318(16):1592-604.
4. Nam RK, Herschorn S, Loblaw DA, Liu Y, Klotz LH, Carr LK, et al. Population Based Study of Long-Term Rates of Surgery for Urinary Incontinence After Radical Prostatectomy for Prostate Cancer. Journal of Urology. 2012;188(2):502-6.
5. Berghmans LCM, Hendriks HJM, BØ K, Hay-Smith EJ, De Bie RA, Van Waalwijk van Doorn ESC. Conservative treatment of stress urinary incontinence in women: a systematic review of randomized clinical trials. British Journal of Urology. 1998;82(2):181-91.
6. Aicher WK, Hart ML, Stallkamp J, Klünder M, Ederer M, Sawodny O, et al. Towards a Treatment of Stress Urinary Incontinence: Application of Mesenchymal Stromal Cells for Regeneration of the Sphincter Muscle. J Clin Med. 2014;3(1):197-215.
7. Eberli D, Aboushwareb T, Soker S, Yoo JJ, Atala A. Muscle precursor cells for the restoration of irreversibly damaged sphincter function. Cell Transplant. 2012;21(9):2089-98.

8. Burdzinska A, Crayton R, Dybowski B, Idziak M, Gala K, Radziszewski P, et al. The effect of endoscopic administration of autologous porcine muscle-derived cells into the urethral sphincter. Urology. 2013;82(3):743 e1-8.
9. Williams JK, Eckman D, Dean A, Moradi M, Allickson J, Cline JM, et al. The Dose-Effect Safety Profile of Skeletal Muscle Precursor Cell Therapy in a Dog Model of Intrinsic Urinary Sphincter Deficiency. Stem Cells Translational Medicine. 2015;4(3):286-94.
10. Burdzinska A, Dybowski B, Zarychta-Wisniewska W, Kulesza A, Butrym M, Zagozdzon R, et al. Intraurethral co-transplantation of bone marrow mesenchymal stem cells and muscle-derived cells improves the urethral closure. Stem Cell Res Ther. 2018;9(1):239.
11. Yiou R, Hogrel JY, Loche CM, Authier FJ, Lecorvoisier P, Jouany P, et al. Periurethral skeletal myofibre implantation in patients with urinary incontinence and intrinsic sphincter deficiency: a phase I clinical trial. BJU Int. 2013;111(7):1105-16.
12. Blaganje M, Lukanovic A. Ultrasound-guided autologous myoblast injections into the extrinsic urethral sphincter: tissue engineering for the treatment of stress urinary incontinence. Int Urogynecol J. 2013;24(4):533-5.
13. Gotoh M, Yamamoto T, Shimizu S, Matsukawa Y, Kato M, Majima T, et al. Treatment of male stress urinary incontinence using autologous adipose-derived regenerative cells: Long-term efficacy and safety. International Journal of Urology. 2019;26(3):400-5.
14. Aragón IM, Imbroda BH, Lara MF. Cell Therapy Clinical Trials for Stress Urinary Incontinence: Current Status and Perspectives. Int J Med Sci. 2018;15(3):195-204.
15. Vilsbøll AW, Mouritsen JM, Jensen LP, Bødker N, Holst AW, Pennisi CP, et al. Cell-based therapy for the treatment of female stress urinary incontinence: an early cost–effectiveness analysis. Regenerative Medicine. 2018;13(3):321-30.
16. Pokrywczynska M, Adamowicz J, Czapiewska M, Balcerczyk D, Jundzill A, Nowacki M, et al. Targeted therapy for stress urinary incontinence: a systematic review based on clinical trials. Expert Opinion on Biological Therapy. 2016;16(2):233-42.
17. Kelp A, Albrecht A, Amend B, Klunder M, Rapp P, Sawodny O, et al. Establishing and monitoring of urethral sphincter deficiency in a large animal model. World J Urol. 2017;35(12):1977-86.
18. Burdzinska A, Dybowski B, Zarychta-Wisniewska W, Kulesza A, Hawryluk J, Graczyk-Jarzynka A, et al. Limited accuracy of transurethral and periurethral intrasphincteric injections of cellular suspension. Neurourol Urodyn. 2018;37(5):1612-22.
19. Amend B, Kelp A, Vaegler M, Klunder M, Frajs V, Klein G, et al. Precise injection of human mesenchymal stromal cells in the urethral sphincter complex of Gottingen minipigs without unspecific bulking effects. Neurourol Urodyn. 2017;36(7):1723-33.
20. Jager L, Linzenbold W, Fech A, Enderle M, Abruzzese T, Stenzl A, et al. A novel waterjet technology for transurethral cystoscopic injection of viable cells in the urethral sphincter complex. Neurourol Urodyn. 2020;39(2):594-602.
21. Linzenbold W, Jager L, Stoll H, Abruzzese T, Harland N, Beziere N, et al. Rapid and precise delivery of cells in the urethral sphincter complex by a novel needle-free waterjet technology. BJU Int. 2021;127(4):463-72.

22. Linzenbold W, Fech A, Hofmann M, Aicher WK, Enderle MD. Novel Techniques to Improve Precise Cell Injection. Int J Mol Sci. 2021;22(12).
23. Geng R, Knoll J, Harland N, Amend B, Enderle MD, Linzenbold W, et al. Replacing Needle Injection by a Novel Waterjet Technology Grants Improved Muscle Cell Delivery in Target Tissues. Cell Transplant. 2022;31:9636897221080943.
24. Damaser MS, Kim FJ, Minetti GM. Methods of testing urethral resistance in the female rat. Adv Exp Med Biol. 2003;539(Pt B):831-9.
25. Hijaz A, Daneshgari F, Sievert K-D, Damaser MS. Animal Models of Female Stress Urinary Incontinence. The Journal of Urology. 2008;179(6):2103-10.
26. Badra S, Andersson KE, Dean A, Mourad S, Williams JK. A nonhuman primate model of stable urinary sphincter deficiency. J Urol. 2013;189(5):1967-74.
27. Herrera-Imbroda B, Lara MF, Izeta A, Sievert K-D, Hart ML. Stress urinary incontinence animal models as a tool to study cell-based regenerative therapies targeting the urethral sphincter. Advanced Drug Delivery Reviews. 2015;82-83:106-16.
28. Badra S, Andersson KE, Dean A, Mourad S, Williams JK. Long-term structural and functional effects of autologous muscle precursor cell therapy in a nonhuman primate model of urinary sphincter deficiency. J Urol. 2013;190(5):1938-45.
29. Klunder M, Amend B, Sawodny O, Stenzl A, Ederer M, Kelp A, et al. Assessing the reproducibility of high definition urethral pressure profilometry and its correlation with an air-charged system. Neurourol Urodyn. 2017;36(5):1292-300.
30. Klunder M, Amend B, Vaegler M, Kelp A, Feuer R, Sievert KD, et al. High definition urethral pressure profilometry: Evaluating a novel microtip catheter. Neurourol Urodyn. 2016;35(8):888-94.
31. Klunder M, Sawodny O, Amend B, Ederer M, Kelp A, Sievert KD, et al. Signal processing in urodynamics: towards high definition urethral pressure profilometry. Biomed Eng Online. 2016;15:31.
32. Schook LB, Collares TV, Darfour-Oduro KA, De AK, Rund LA, Schachtschneider KM, et al. Unraveling the swine genome: implications for human health. Annu Rev Anim Biosci. 2015;3:219-44.
33. Perleberg C, Kind A, Schnieke A. Genetically engineered pigs as models for human disease. Dis Model Mech. 2018;11(1).
34. Simianer H, Kohn F. Genetic management of the Gottingen Minipig population. J Pharmacol Toxicol Methods. 2010;62(3):221-6.
35. Burdzinska A, Crayton R, Dybowski B, Koperski L, Idziak M, Fabisiak M, et al. Urethral distension as a novel method to simulate sphincter insufficiency in the porcine animal model. Int J Urol. 2012;19(7):676-82.
36. Leonhauser D, Vogt M, Tolba RH, Grosse JO. Potential in two types of collagen scaffolds for urological tissue engineering applications - Are there differences in growth behaviour of juvenile and adult vesical cells? J Biomater Appl. 2016;30(7):961-73.
37. Nies A, Proft L, Nehring ME, Gruber C, Sievers H, Hunigen H, et al. Growth-related micromorphological characteristics of the porcine femoral artery. Clin Hemorheol Microcirc. 2019;73(1):195-201.

38. Lang N, Merkel E, Fuchs F, Schumann D, Klemm D, Kramer F, et al. Bacterial nanocellulose as a new patch material for closure of ventricular septal defects in a pig model. Eur J Cardiothorac Surg. 2015;47(6):1013-21.
39. Phillips AB, Green J, Bergdall V, Yu J, Monreal G, Gerhardt M, et al. Teaching the "hybrid approach": a novel swine model of muscular ventricular septal defect. Pediatr Cardiol. 2009;30(2):114-8.
40. Hansen SB, Nielsen SL, Christensen TD, Gravergaard AE, Baandrup U, Bille S, et al. Latissimus dorsi cardiomyoplasty: a chronic experimental porcine model. Feasibility study of cardiomyoplasty in Danish Landrace pigs and Gottingen minipigs. Lab Anim Sci. 1998;48(5):483-9.
41. Brenner GB, Giricz Z, Garamvolgyi R, Makkos A, Onodi Z, Sayour NV, et al. Post-Myocardial Infarction Heart Failure in Closed-chest Coronary Occlusion/Reperfusion Model in Gottingen Minipigs and Landrace Pigs. J Vis Exp. 2021(170).
42. Schuleri KH, Boyle AJ, Centola M, Amado LC, Evers R, Zimmet JM, et al. The adult Gottingen minipig as a model for chronic heart failure after myocardial infarction: focus on cardiovascular imaging and regenerative therapies. Comp Med. 2008;58(6):568-79.
43. Muller C, Marzahn U, Kohl B, El Sayed K, Lohan A, Meier C, et al. Hybrid pig versus Gottingen minipig-derived cartilage and chondrocytes show pig line-dependent differences. Exp Biol Med (Maywood). 2013;238(11):1210-22.
44. Gotterbarm T, Breusch SJ, Schneider U, Jung M. The minipig model for experimental chondral and osteochondral defect repair in tissue engineering: retrospective analysis of 180 defects. Lab Anim. 2008;42(1):71-82.
45. Amend B, Harland N, Knoll J, Stenzl A, Aicher WK. Large Animal Models for Investigating Cell Therapies of Stress Urinary Incontinence. Int J Mol Sci. 2021;22(11).
46. Zini L, Lecoeur C, Swieb S, Combrisson H, Delmas V, Ghérardi R, et al. The striated urethral sphincter of the pig shows morphological and functional characteristics essential for the evaluation of treatments for sphincter insufficiency. J Urol. 2006;176(6 Pt 1):2729-35.
47. Peyrat L, Haillot O, Bruyere F, Boutin JM, Bertrand P, Lanson Y. Prevalence and risk factors of urinary incontinence in young and middle-aged women. BJU International. 2002;89(1):61-6.
48. Reynolds WS, Dmochowski RR, Penson DF. Epidemiology of Stress Urinary Incontinence in Women. Current Urology Reports. 2011;12(5):370.
49. Yiou R, Lefaucheur JP, Atala A. The regeneration process of the striated urethral sphincter involves activation of intrinsic satellite cells. Anat Embryol (Berl). 2003;206(6):429-35.
50. Kjaergaard K, Sorensen M, Mortensen FV, Alstrup AKO. Hepatic blood flow in adult Gottingen minipigs and pre-pubertal Danish Landrace x Yorkshire pigs. Lab Anim. 2021;55(4):350-7.
51. Seeger T, Hart M, Patarroyo M, Rolauffs B, Aicher WK, Klein G. Mesenchymal Stromal Cells for Sphincter Regeneration: Role of Laminin Isoforms upon Myogenic Differentiation. PLoS One. 2015;10(9):e0137419.
52. Strasser H, Tiefenthaler M, Steinlechner M, Eder I, Bartsch G, Konwalinka G. Age dependent apoptosis and loss of rhabdosphincter cells. J Urol. 2000;164(5):1781-5.

53. Team RC. R: A language and environment for statistical computing. . In: Computing RFfS, editor. v4.2.2 ed. Vienna, Austria2022.
54. Noguchi K, Gel YR, Brunner E, Konietschke F. nparLD: An R Software Package for the Nonparametric Analysis of Longitudinal Data in Factorial Experiments. Journal of Statistical Software. 2012;50(12):1 - 23.
55. Honaker J, King G, Blackwell M. Amelia II: A Program for Missing Data. Journal of Statistical Software,. 2011;45(7):1-47.

14. Publication 5

Cell therapy by mesenchymal stromal cells versus myoblasts in a pig model of urinary incontinence

Jasmin Knoll[1], Bastian Amend[2], Niklas Harland[2], Simon Isser[3], Nicolas Bézière[3,4], Udo Kraushaar[5], Arnulf Stenzl[2], and Wilhelm K. Aicher[1*]

[1] Centre for Medical Research, Department of Urology at UKT, Eberhard-Karls-University, 72072 Tuebingen, Germany

[2] Department of Urology, University of Tuebingen Hospital, 72076 Tuebingen, Germany

[3] Werner Siemens Imaging Center, Department of Preclinical Imaging and Radiopharmacy, Eberhard-Karls-University of Tübingen, Germany

[4] Cluster of Excellence CMFI (EXC 2124) "Controlling Microbes to Fight Infections", Eberhard-Karls-University Tübingen, Germany

[5] Naturwissenschaftlich-Medizinisches Institut, 72770 Reutlingen, Germany

* Correspondence author

Tissue Engineering: Part A

Year 2023

Mary Ann Liebert, Inc.

Submitted: 8 May 2023

Abstract

The leading cause of stress urinary incontinence in women is the urethral sphincter muscle deficiency caused by mechanical stress during pregnancy and vaginal delivery. In men, prostate cancer surgery and injury of local nerves and muscles are associated with incontinence. Current treatment often fails to satisfy the patient's needs. Cell therapy may improve the situation. We therefore investigated the regeneration potential of cells in ameliorating sphincter muscle deficiency and urinary incontinence in a large animal model. Urethral sphincter deficiency was induced surgically in gilts by electrocautery and balloon dilatation. Adipose tissue-derived stromal cells and myoblasts from *Musculus semitendinosus* were isolated from male littermates, expanded, characterized in depth for expression of marker genes and *in vitro* differentiation, and labelled. The cells were injected into the deficient sphincter complex of the incontinent female littermates. Incontinent gilts receiving no cell therapy served as controls. Sphincter deficiency and functional regeneration were recorded by monitoring the urethral wall pressure during follow-up by two independent methods. Cells injected were detected *in vivo* during follow-up by transurethral fluorimetry, *ex vivo* by fluorescence imaging, and in cryosections of tissues targeted by immunofluorescence and by PCR of the SRY gene. Partial spontaneous regeneration of sphincter muscle function was recorded in control gilts, but the sphincter function remained significantly below levels measured prior to induction of incontinence (67.03±14.00%, n=6, $p<0.05$). Injection of myoblasts yielded an improved sphincter regeneration within five weeks of follow-up but did not reach significance compared to control gilts (81.54±25.40%, n=5). A significant and full recovery of the urethral sphincter function was observed upon injection of adipose tissue-derived mesenchymal stromal cells within five weeks of follow-up (100.4±23.13%, n=6, $p<0.05$). Injection of stromal cells provoked slightly stronger infiltration of $CD45^{pos}$ leukocytes compared to myoblasts injections and controls. The data of this exploratory study indicate that adipose tissue-derived mesenchymal stromal cells inherit a significant potential to regenerate the function of the urethral sphincter muscle.

Impact statement

Urinary incontinence is a significant medical challenge and current therapies often do not satisfy patients' needs. This study investigates the potential of two different types of cells, stromal cells versus myoblasts, head-to-head in a robust animal model of incontinence. The stromal cells outperformed the myoblasts. Autologous stromal cells can be isolated from adipose tissue of patients without intolerable side effects in sufficient amounts and produced with much less efforts under GMP-compliant conditions. Our results suggest confirmatory preclinical studies to verify the efficacy of stromal cell-mediated sphincter regeneration and recommend such cells for future clinical trials.

Keywords

Stress urinary incontinence; cell therapy; adipose tissue-derived mesenchymal stromal cells; myoblasts; large animal model of incontinence

Introduction

Therapy of stress urinary incontinence (SUI) is a significant medical challenge as increasing parts of the ageing population worldwide present with involuntary loss of urine. For women, a prevalence of urinary incontinence (UI) of 45% and higher was estimated, for men about 25% are reported. Many incontinent patients suffer from SUI [1-5]. Chronic UI contributes to dermal irritations, local inflammations, urinary infections, and other comorbidities [6,7].

SUI is caused by an insufficiency or a loss of the urethral sphincter muscle function [8]. In women, SUI is mainly associated with pregnancy, vaginal delivery, and hormonal changes in menopause [9], while in men sequela of prostate surgery predominate [10]. Mild forms of SUI can be managed by adapting the daily routine, drug treatment, and lower pelvic floor muscle training, sometimes complemented with electrophysiology or biofeedback [11,12]. If such regimen fails to satisfy the patient's needs or expectations, different surgical treatment options are available [13,14]. However, they all inherit side effects that must be considered.

Loss of muscle cells of the urethral sphincter apparatus and displacement of striated muscle tissue by collagen fibres were reported in the elderly [15]. This supported the hypothesis that surgical application of muscle fibres [16] or injection of myogenic progenitor cells (MPCs) could strengthen the urethral muscle [17-22]. Application of active components, including cell culture supernatants and exosomes, were explored as well [23-25]. Others investigated if mesenchymal stromal cells (MSCs), including adipose tissue-derived stromal cells (ADSCs), could restore urethral sphincter function [26-30]. However, some clinical studies did not yield convincing outcome [31], some included small cohorts only, and some had to be retracted (not cited). Moreover, mechanisms contributing to cell-based sphincter regeneration are not understood in detail. As study designs of the preclinical and clinical studies published differed considerably, the regenerative potential of the two main active compounds investigated so far, MSC-like cells such as ADSCs versus myoblasts or MPCs, cannot be compared directly [28,32]. We therefore set out to investigate head-to-head if ADSCs or MPCs perform better in sphincter regeneration. To this end, we employed our porcine large animal model of SUI [33] and injected ADSCs or MPCs from a male littermate together with fluorescent-labelled microparticles to facilitate the detection of the cells

applied in tissues targeted *in vivo* and *ex vivo*. In addition, we searched for injected male cells by PCR of the sex-determining region Y (SRY) gene in cryosections of treated gilts.

Methods

Establishing a preclinical model of stress urinary incontinence

German landrace gilts (n = 18) were obtained directly from the breeder (Benz GbR) with excellent health status. Before surgery, animals were sedated. Prior to induction of sphincter insufficiency, the urethral sphincter muscle was localized by transurethral urodynamics, also known as urethral pressure profilometry (UPP) as described recently [33,34]. The sphincter muscle was injured by two lateral electrocauteries just distal of the wall pressure maximum followed by balloon dilatation in deep anaesthesia [33]. Immediately after surgery, efficacy of sphincter deficiency was confirmed by UPP. After SUI induction, the health and urine status were monitored by trained personnel. In addition, the regeneration of the sphincter muscle was monitored weekly by UPP [33]. The study was approved by the State of Baden Württemberg Animal Welfare Authorities under file number 35/9185.81-2 / CU01-20G and performed in full compliance with the ARRIVE 2.0. standards and all other relevant regulations.

Production of myoblasts (MPCs) from *Musculus semitendinosus*

Tissue samples from *Musculus (M.) semitendinosus* were aseptically prepared from young male littermates of the gilts included in the study. In the laboratory, MPCs were isolated and expanded employing a slightly modified protocol [35] based on recent papers [36,37]. For MPC characterization, expression of desmin and CD56 were explored by immunofluorescence (IF) and flow cytometry (FC), respectively (Table 1) [35,36,38]. Expression of myogenic transcripts were determined by RT-qPCR. Differentiation of MPCs was induced as described [36]. Syncytia and multi-nuclear myotubes were recorded by IF using anti-desmin antibodies and DAPI counterstaining. To investigate the functional competence of the porcine myotubes, electrophysiology was employed. In brief, MPCs and myotubes were either stimulated electrically or by caffeine to prove the release of calcium from intracellular compartments [39,40]. Before injection, MPCs were labelled by CMFDA as requested by the supplier (ThermoFisher).

Table 1: Antigens and antibodies

Antigen	Use	Host	Reactivity	Clone	Label	Dilution	Source
CD14	FC	mouse	human	TÜK4	directly FITC	1:10	BioRad
CD45	FC	mouse	pig	K252.1E4	directly FITC	1:10	BioRad
CD29	FC	mouse	pig	NaM160-1A3	directly AF647	1:10	BD Pharmingen
CD44	FC	rat	mouse/ human	IM7	directly PE	1:10	BioLegend
CD90	FC	mouse	human	5E10 (RUO)	directly FITC	1:5	BD Pharmingen
MHC class I	FC	mouse	pig	JM1E3	directly FITC	1:10	BioRad
CD56	FC	mouse	human	MEM-188	directly PE	1:10	BioLegend
CD45	IF	mouse	pig	K252.1E4	unlabelled	1:200	Invitrogen
Desmin	IF	rabbit	mouse/ rat/ human	polyclonal	unlabelled	1:200	Abcam
Anti-ms	IF	goat	mouse	polyclonal	AF555	1:200	Invitrogen
Anti-rbt	IF	donkey	rabbit		FITC	1:200	Jackson-Dianova
DAPI	IF	ø	ø	ø	ø	1:1000	Sigma

Antibodies employed for flow cytometry (FC) and immunofluorescence (IF) stainings.

Production of adipose tissue-derived mesenchymal stroma cells (ADSCs)

Subcutaneous fat tissue was also aseptically prepared from male littermates of the female gilts in the study. The ADSCs were isolated and expanded as described recently [41,42]. In brief, fat was minced and further degraded by proteolysis. Cells were washed, counted, seeded, and expanded in expansion media [41]. For characterization, ADSCs were analysed for expression of cell surface markers by FC (Table 1). In addition, *in vitro* differentiation along the adipogenic and osteogenic lineages was induced [41], and confirmed as described respectively [43]. Expression of cytokines was determined by RT-qPCR. Prior to injection, ADSCs were labelled by CMFDA as requested by the supplier (ThermoFisher).

Transurethral cell therapy and follow-up

Three days after its induction, sphincter deficiency was confirmed by UPP. Two aliquots (250 μl each, $6x10^5$ CMFDA-labelled cells plus $6x10^5$ FITC-labelled microparticles) were injected by transurethral route using a cystoscope under visual control in the urethral

sphincter complex as described [44]. During follow-up of five weeks, animals were monitored weekly by transurethral fluorimetry to localize the fluorescent cells and microparticles. Furthermore, weekly UPP was performed to determine the sphincter muscle regeneration. In addition, the urine was monitored to reveal abnormalities.

Analyses of urethral tissues targeted

After five weeks of follow-up, the final transurethral fluorimetry and UPP were performed and the gilts were sacrificed. The bladder and the urethral sphincter were prepared. The area of injection of fluorescent cells and microparticles was localized using a fluorescence imaging system. The region of interest was cut out, embedded in freezing compound, frozen, and stored at -80°C. Cryosections were generated (20 µm) and mounted on slides. Cryosections containing fluorescent microparticles were considered to represent injection sites. To visualize the urethral tissue, HE- and AZAN-trichrome staining was performed [33]. Muscle tissue was detected by a phalloidin-iFluor594 conjugate (1:1000). Infiltration of inflammatory cells was visualized immunofluorescence (IF) with a cross-reactive anti-CD45 antibody (Table 1). The samples were recorded by microscopy.

PCR was employed to detect male SRY-DNA in cryosections as described [34,45]. Tissue was scratched off from 8 consecutive cryosections and DNA was extracted (DNeasy extraction kit). The product identity was confirmed by melting point analysis of the products and agarose DNA electrophoresis.

Data processing and statistics

Statistical analyses were conducted with the nparLD R package (v2.2) in R Statistical Software (v4.2.2) (Fig.4A, 4B) and an One-Way-ANOVA in IBM SPSS Statistics for Windows (v.29.0) (Fig.4D) [46,47]. P-values were reported as $p<0.001$ ***, $p<0.01$ **, $p<0.05$ *, and $p>0.05$ ns. To be able to compare the results, normalization of raw data to "Before" incontinence for each animal was performed (Fig.4C).

Detailed descriptions of methods and materials employed are presented online (www…)

Experiments

Quality measures of cells produced prior to cell therapy applications

Porcine MPCs were isolated and expanded as described [35]. The cells proliferated as adherent population (Fig. 1A). A uniformly distributed population was recorded by FC of forward and side scatters (not shown), and a prominent expression of CD56 was observed (Fig. 1B) [36]. The cells expressed Pax7, a marker for satellite cells, as well as other myogenic markers such as MyoD, Myf5, myogenin, Myf6, and desmin (Figs. 1C, os1A) [48]. Immunofluorescence with anti-desmin antibodies provided evidence of efficient generation of extended myotubes. By DAPI counterstaining several nuclei per myotube were detected in individual myofibers (Fig. 1D). In addition, MPCs and terminally differentiated myotubes were stimulated by electrodes and caffeine to explore electrophysiological responses. While myoblasts failed to respond to stimulation (Figs. os2A, os2B), myotubes responded well to electrophysiological stimulation and caffeine (Figs. 1E, 1F, os2C). Taken together, the experimental results suggested that *bona fide* porcine MPCs were generated [36].

Porcine ADSCs were isolated and expanded as described recently [41,42] and presented as adherent fibroblast-like (Fig. 2A). Expression of monocyte marker CD14 and leukocyte marker CD45 was not observed (Fig. 2B), but CD29 and CD44 were expressed at high mean fluorescence intensities (MFI), while CD90 and MHC class I were detected on moderate levels (Fig. 2C). The adipogenic and osteogenic differentiation potential of the ADSCs was confirmed by Oil Red O staining and von Kossa staining, upon differentiation (Figs. 2D, 2E). The expression of cytokines associated with tissue regeneration was explored by RT-qPCR, and a prominent expression of VEGF was enumerated, bFGF, IGF1, TGFβ1, and HGF were moderate, BDNF, GDNF, and CXcl12 were somewhat lower, while IGF2 remained at detection levels (Figs. 2F, os1B). Taken together, the data suggested that *bona fide* ADSCs were generated [49].

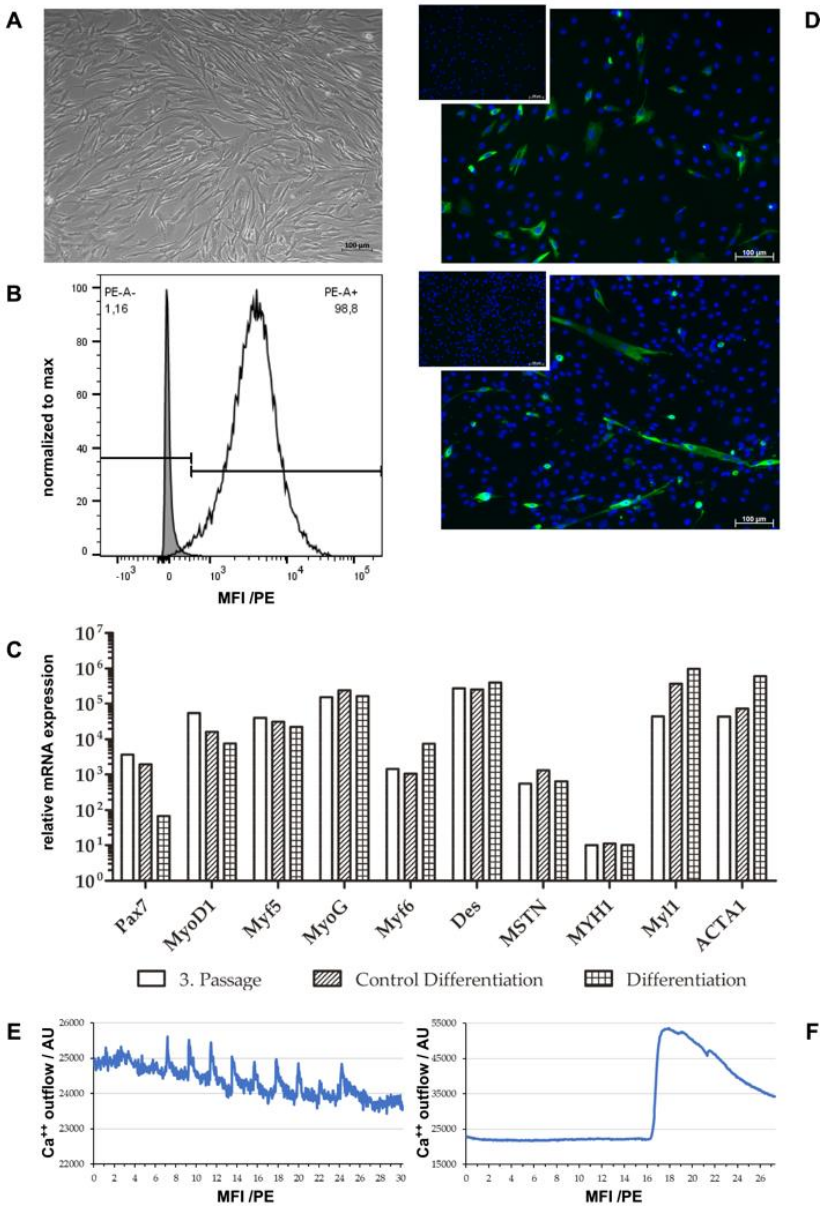

Figure 1: Characterization of porcine MPCs. A: Morphological picture displaying adherent, monocultural growth of MPCs. Scale bar indicates 100 µm. **B:** Uniform expression of myoblast marker CD56 in MPCs determined by flow cytometry with PE-labelled anti-CD56 antibody. Cells omitting staining were used as controls (grey-shaded curve). Gating of CD56-negative cells helped determine the prominent expression of 98.8% CD56-positive cells. **C:** Relative mRNA expression pattern of myogenic markers of normally expanded MPCs (3. Passage) and differentiated MPCs (Differentiation) with their corresponding control (Control Differentiation), indicating bona fide MPCs capable of differentiation into myotubes as indicated by elevated expressions of Myf6, Myl1, and ACTA1, as well as decreased levels of Pax7, MyoD1, and Myf5. **D:** Immunofluorescence staining for desmin in MPCs (upper panel) and after differentiation in myotubes (lower panel). Generation of myotubes is shown by elongation in desmin staining. Counterstaining of nuclei with DAPI confirms multi-nucleated myotubes. Inserted images display control stainings without primary antibody. Scale bars indicate 100 µm. **E:** Electrophysiological measurement of electrode-stimulated myotubes with 4 V for 50 ms every two seconds. Outflow of Ca^{2+} was determined, resulting in peak outflows every two seconds after stimulation. **F:** Electrophysiological measurement of electrode-stimulated myotubes after addition of 30 mM caffeine. Outflow of Ca^{2+} was determined, resulting in highly increased outflow after caffeine-addition diminishing with time.

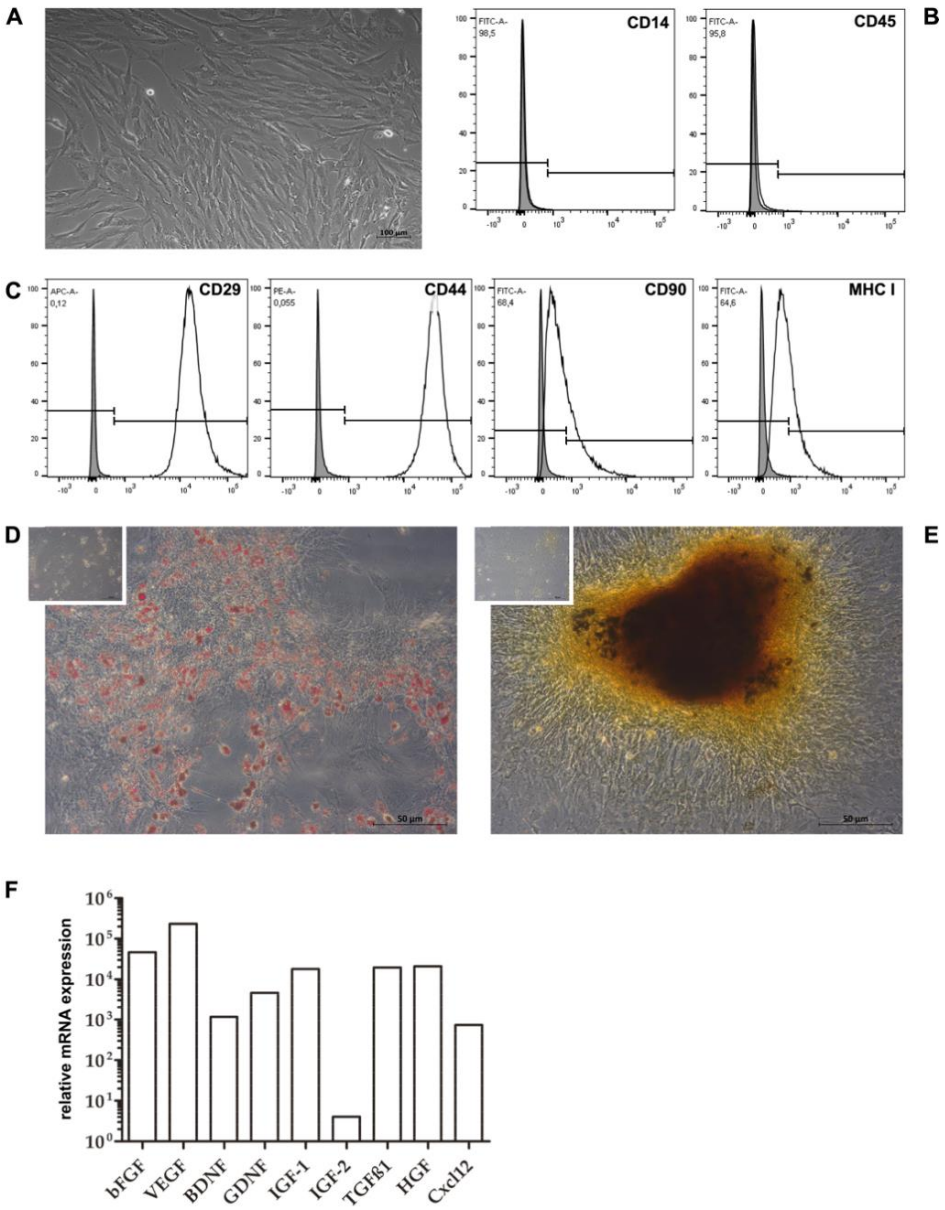

Figure 2: Characterization of porcine ADSCs. A: Morphology of ADSCs showing plastic-adherent, fibroblast-like growth of cells. Scale bar indicates 100 µm. **B, C:** Expression of surface markers of ADSCs. Cells without staining were used as controls (grey-shaded curves). Gating aided in determination of enumeration of positive cells. Monocyte (CD14) and leucocyte (CD45) markers were not expressed on ADSCs (B). CD90 and MHC I were moderately expressed, and CD29 and CD44 were prominently expressed on ADSCs (C). **D:** Successful adipogenic differentiation of ADSCs determined after staining with Oil Red O. **E:** Successful osteogenic differentiation of ADSCs stained by von Kossa. **F:** Relative mRNA expression pattern of cytokines produced by ADSCs displaying a prominent expression of VEGF, followed by moderate expression levels of bFGF, IGF-1, TGFβ1, and HGF, while IGF-2 stayed at baseline level.

Functional follow-up of sphincter recovery by fluorimetry and urodynamics

To confirm injections and to localize the fluorescent cells and particles in the urethral sphincter complex *in vivo*, transurethral fluorimetry was applied. Fluorescence was recorded in the urethra approximately 5 - 7 cm distal of the bladder neck (Fig. 3). Overall, significant differences in fluorescence densities or particle frequencies were not observed between MPC- or ADSC-treated gilts during the follow-up of five weeks (Figs. 3, os3). This suggested that neither cells nor particles migrated or difused over noticeable distances *in situ*. But in some individuals prominent fluorescence was recorded while in others less signal was observed during follow-up. However, this procedure is not a quantitative method and can only qualitatively report on the presence and location of the fluorophores in tissue.

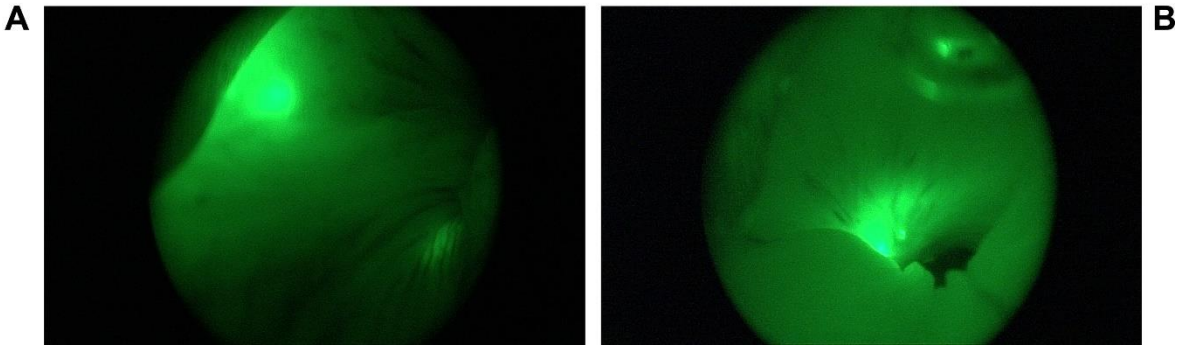

Figure 3: In vivo fluorimetry of labelled cells and microparticles. Representative pictures of in vivo fluorimetry of green labelled cells and microparticles in the urethra of pigs. Strong fluorescent signals are visible. No difference between the two different cell types was detected (**A:** MPCs, **B:** ADSCs)

The urethral sphincter complex of the gilts was injured by electrocautery and dilatation, and the sphincter deficiency was determined by UPP [33]. A highly significant drop of urethral sphincter muscle strength (USMS), also referred to as urethral wall pressure, was recorded by UPP immediately after induction of sphincter deficiency in the controls (20.8±12.2%, n=6, $p<0.001$) when compared to the USMS prior to surgery (Fig. 4A). The same highly significant drop in USMS was recorded immediately after induction of sphincter deficiency in gilts to be treated on day three with MPCs (= cohort 2; 19.64±15.99%, n=5, $p<0.001$) or ADSCs (= cohort 3; 24.32±18.1%, n=6, $p<0.001$) (Fig. 4A). One week after SUI surgery, corresponding to day four after cell injection, sphincter deficiency remained significant in controls, (40.5±21.4%, n=6, $p<0.001$), cohort 2 (47.06±14.63%, n=5, $p<0.001$) and 3 (58.53±23.51%, n=6, $p<0.01$) animals

compared to starting levels (Fig. 4A). During weekly follow-up, regeneration of USMS was observed in all cohorts. But differences between controls and cell-treated gilts were noted. While the USMS remained significantly below starting levels in controls, animals treated with MPCs yielded significance in USMS two, three, and five weeks after surgery compared to starting levels (Fig. 4A). In animals treated with ADSCs significant USMS differences were not recorded three and five weeks after surgery (Fig. 4A). We therefore investigated the functional sphincter regeneration relative to the induced SUI (Fig. 4B). In control animals a significant gain of sphincter function was not observed one week after surgery, while in both, MPC- and ADSC-treated gilts a significant USMS elevation was recorded ($p<0.001$; Fig. 4B). In all cohorts the sphincter recovery was significant after two weeks when compared to the levels determined after SUI induction ($p<0.001$; Fig. 4B). This confirmed that cell therapy facilitates an early sphincter regeneration.

To compare the kinetic of sphincter recovery directly, the UPP data were normalized to the USMS of the starting levels. As early as one week after surgery a trend of elevated sphincter function was noted in cell-treated gilts (Fig. 4C). The ADSC-treated animals tended to increase the USMS better compared to MPC-treated gilts or controls. Only two weeks after surgery, MPC-treated animals showed a higher median USMS when compared to the ADSC-treated cohort (Fig. 4C).

In addition, the normalized overall functional sphincter regeneration was evaluated as well (Fig. 4D). The controls regenerated the USMS spontaneously to a mean level of 67.03±14.00% compared to the same animals prior to SUI induction (= 100%). This level was a significant increase in comparison to the USMS recorded immediately after SUI induction ($p<0.001$; 4B), but it also remained significantly below levels prior to surgery ($p<0.001$; Fig. 4A). This confirmed that electrocautery plus balloon dilatation of the urethral sphincter complex yielded a robust pig model of SUI.

Gilts of cohort 2 received MPCs and increased the normalized USMS within five weeks of follow-up to 81.54±25.40% (Fig. 4D). This was a significant elevation in USMS in comparison to the UPP levels immediately after SUI induction ($p<0.001$; Fig. 4B). Nevertheless, this level of regeneration was not significantly different from the USMS prior to SUI induction (Fig. 4A). Additionally, an elevated but not significant sphincter regeneration was measured compared to controls (Fig.4D). We conclude that MPCs facilitated an accelerated regeneration of the sphincter deficiency as induced in our SUI model.

Gilts of cohort 3 received ADSCs and regenerated the USMS in full within five weeks of follow-up to 100.4±23.13% recovery (Fig. 4D). This was a significant increase in USMS in comparison to the levels measured by UPP immediately after SUI induction ($p<0.001$; Fig. 4B) but not different at all compared to USMS starting levels (Fig. 4A). This amount of regeneration by ADSCs was significantly higher compared to controls ($p<0.05$) and superior but not significant compared to the regeneration by MPCs (Fig. 4D).

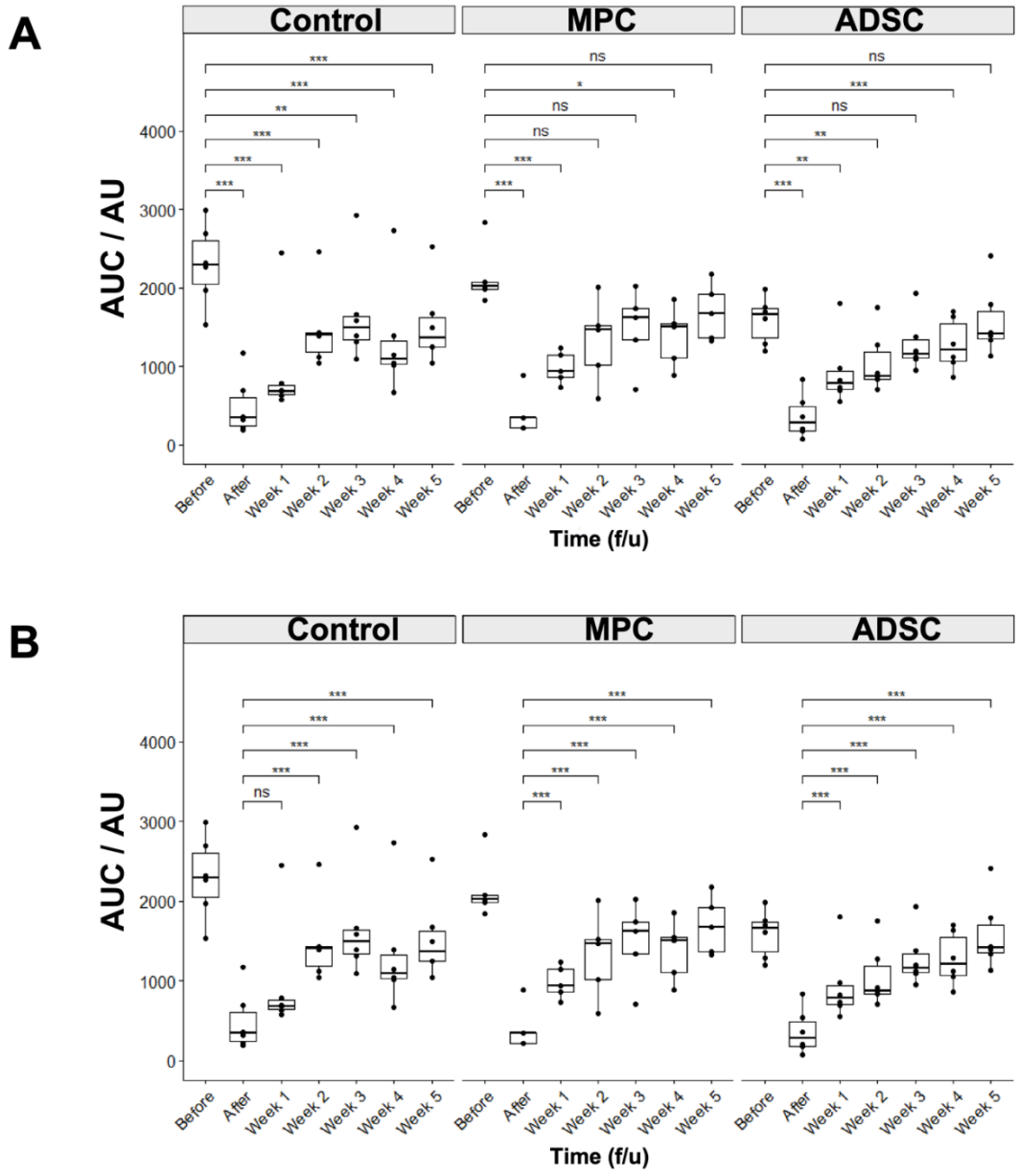

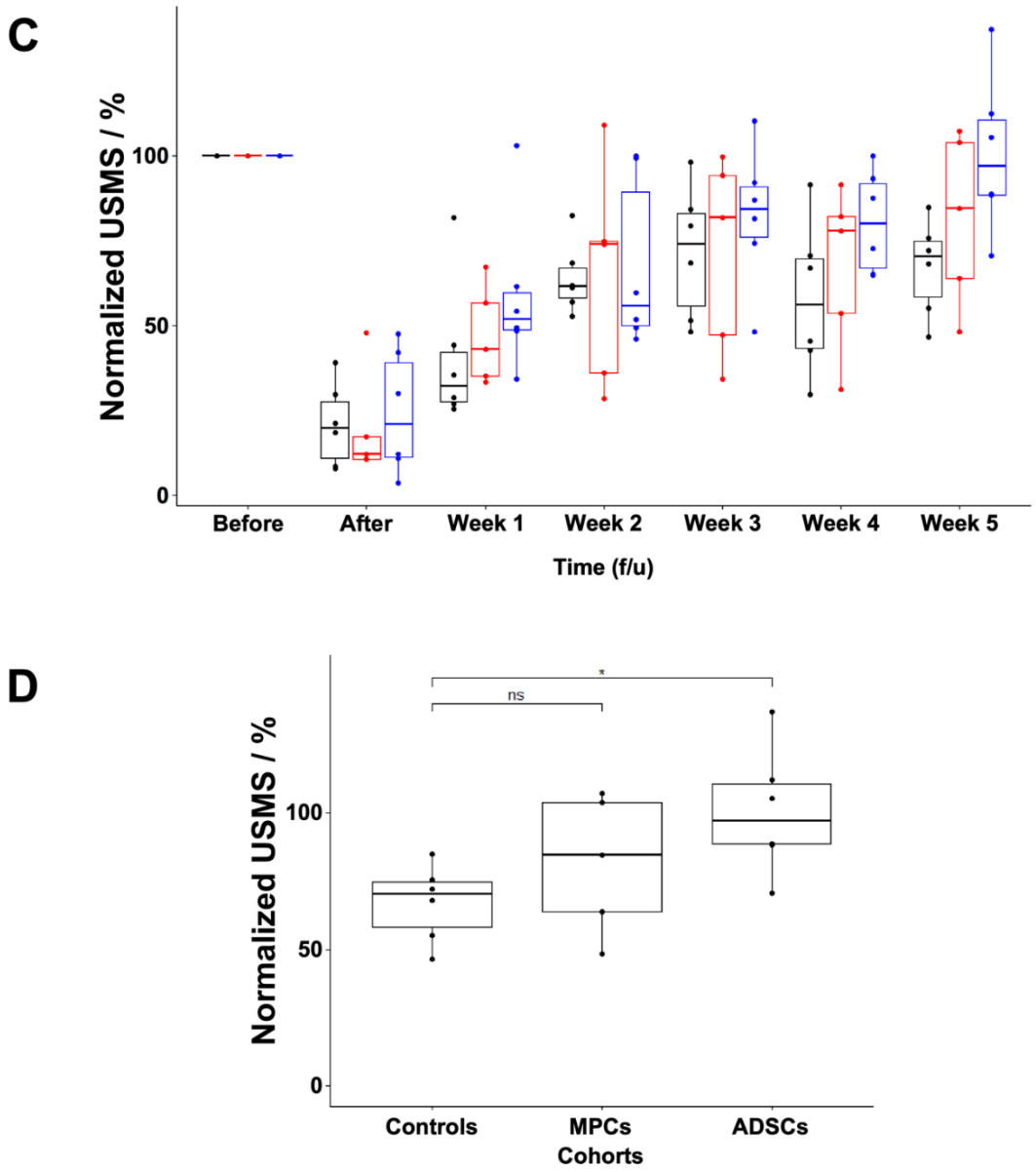

Figure 4: Boxplots of urodynamic data measured with urethral pressure profilometry over five weeks. Urodynamic measurements were conducted using urethral pressure profilometry. Over five weeks, animals of each group (Control n = 6; MPC n = 5; ADSC n = 6) were measured before and directly after incontinence induction, as well as weekly thereafter. Areas under the curve (AUCs) were calculated and statistical tests performed. **A, B:** Measured AUC values in arbitrary units (y-axis) for each group are separately displayed. On the x-axis the time points of measurements are plotted. Significances were calculated between each time point and the value before incontinence induction (A). Controls remained significantly different over the whole follow-up, while the MPC-injected group displayed no durable significance after 2 weeks and the ADSC-injected group after 3 weeks. Additionally, significances were calculated between each time point and the value after incontinence induction (B). Only in controls, the difference between the time points after and week 1 were not significant. All other comparisons showed highly significant differences. **C, D:** Urethral sphincter muscle strength (USMS) was determined by AUC values, normalized to the measured values of before incontinence induction. Cell-treated animals displayed a better improvement compared to controls starting after 1 week (C). At the last time point of week 5, statistical analyses were performed (D), resulting in significant improvement of ADSC-treated animals compared to controls. MPC-treated animals also displayed higher levels but remained not significantly different.

Ex vivo localization of injected cells in the tissue targeted

As animals in cohort 3 fully recovered after five weeks, this exploratory preclinical animal study was terminated to comply with the animal welfare regulations. The bladders and urethras were harvested. Identification of the distribution of the labelled cell and particles injected on day 1 was achieved by fluorescence imaging (Fig. 5). Fluorescent signals were obtained in almost all urethras of cell-treated gilts. In some samples, even the two lateral injections could be still seen (Fig. 5). This result is in line with the *in vivo* fluorimetry (Figs. 3, os3) and the UPP analyses during follow-up (Fig. 4).

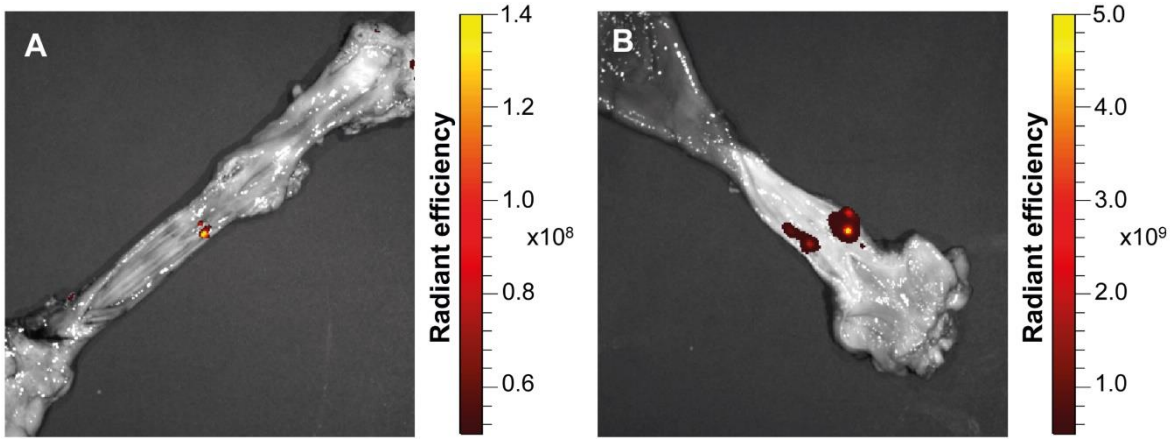

Figure 5: Fluorescence imaging of FITC-labelled microparticles and CMFDA-labelled cells distribution in prepared, dorsally opened urethrae. Representative images of urethrae of pigs injected with microparticles and ADSCs (A) or with MPCs (B) obtained 5 weeks after injection. The areas presenting the most intense fluorescence signal represented the site of injection and were excised and prepared for cryosectioning.

Investigation of inflammatory responses upon cell injection

Fluorescent signal obtained *ex vivo* (Fig. 5) was used to guide tissue resection for cryosection preparation [34]. Representative examples of tissues of control animals, MPC-treated, and ADSC-treated animals are presented (Figs. 6 – 8, os4). These figures document a representative animal with better (top panels) and another one with worse outcome (bottom panels). In controls with better spontaneous tissue regeneration (Fig. 6A - 6D), HE-staining did not indicate a noticeable infiltration of mononuclear cells five weeks after SUI induction (Fig. 6A). AZAN-staining confirmed irregularities of the urethral sphincter muscle (Fig. 6B). In this sample, $CD45^{pos}$ leucocytes were not found (Fig. 6C). Phalloidin-staining corroborated the results (Fig. D). Comparable results were obtained in a control animal with worse regeneration (Figs. 6E – 6H). A few $CD45^{pos}$

leucocytes were detected along the interruption sites but they remined only slightly visible (Fig. 6G).

Tissue samples from MPC-treated gilts are presented in figure 7. HE-staining revealed no evidence for massive infiltration of mononuclear cells in the animal with good recovery. Tissue stretching and injury were not observed (Fig. 7A). By AZAN-staining only minor irregularities of the muscular were recorded (Fig. 7B). Green fluorescence was observed in this animal with better regeneration. Almost no $CD45^{pos}$ leukocytes were recorded (Fig. 7C). Continuous phalloidin-staining confirmed that the omega-shaped sphincter muscle was not interrupted and fluorescence war recorded within the muscle layer (Fig. 7D). In a MPC-treated animal of worse recovery, infiltration of mononuclear cells was also not observed (Fig. 7E), but AZAN-staining indicated interrupted muscle tissue and an irregular submucosal layer (Fig. 7F). Green fluorescence was not observed, indicating that the MPCs were possibly misplaced or lost during follow-up. Infiltration of $CD45^{pos}$ leukocytes was not recorded (Fig. 7G). By phalloidin-staining an interruption of the sphincter muscle was corroborated (Fig. 7H). These results indicate that the efficacy of SUI cell therapy depends at least in part on exact injection of the active component.

Two examples of ADSC-treated gilts are presented in Figure 8. An example each with better (Fig. 8A – 8D) and worse (Fig. 8e – 8H) regeneration is shown. Again, HE-staining revealed no evidence for massive infiltration of mononuclear cells (Fig. 8A). AZAN-staining showed muscular tissue throughout the sample (Fig. 7B). A distinct green fluorescence was observed in the muscle of this animal with better regeneration and the two lateral sites of cell injection were seen (Fig. 8C). This correlated well with the IVIS results (Fig. 5B). Some $CD45^{pos}$ cells were recorded (Fig. 8C). Continuous phalloidin-staining confirmed that the omega-shaped sphincter muscle was not interrupted (Fig. 8D). In an ADSC-treated animal of worse recovery, massive infiltration of mononuclear cells was not observed (Fig. 8E), and AZAN-staining did not indicate muscle tissue injury (Fig. 8F). By fluorescence microscopy, slight green fluorescence behind the muscle layer was observed in consecutive cryosections, indicating that few cells in the injured sphincter correlated with worse outcome. Little infiltration of $CD45^{pos}$ leukocytes was recorded (Fig. 8G). Phalloidin-staining corroborated a continuous muscle layer (Fig. 8H). Overall, the ADSC injections corroborated that efficacy of SUI cell therapy depends at least in part on exact injection of the active component.

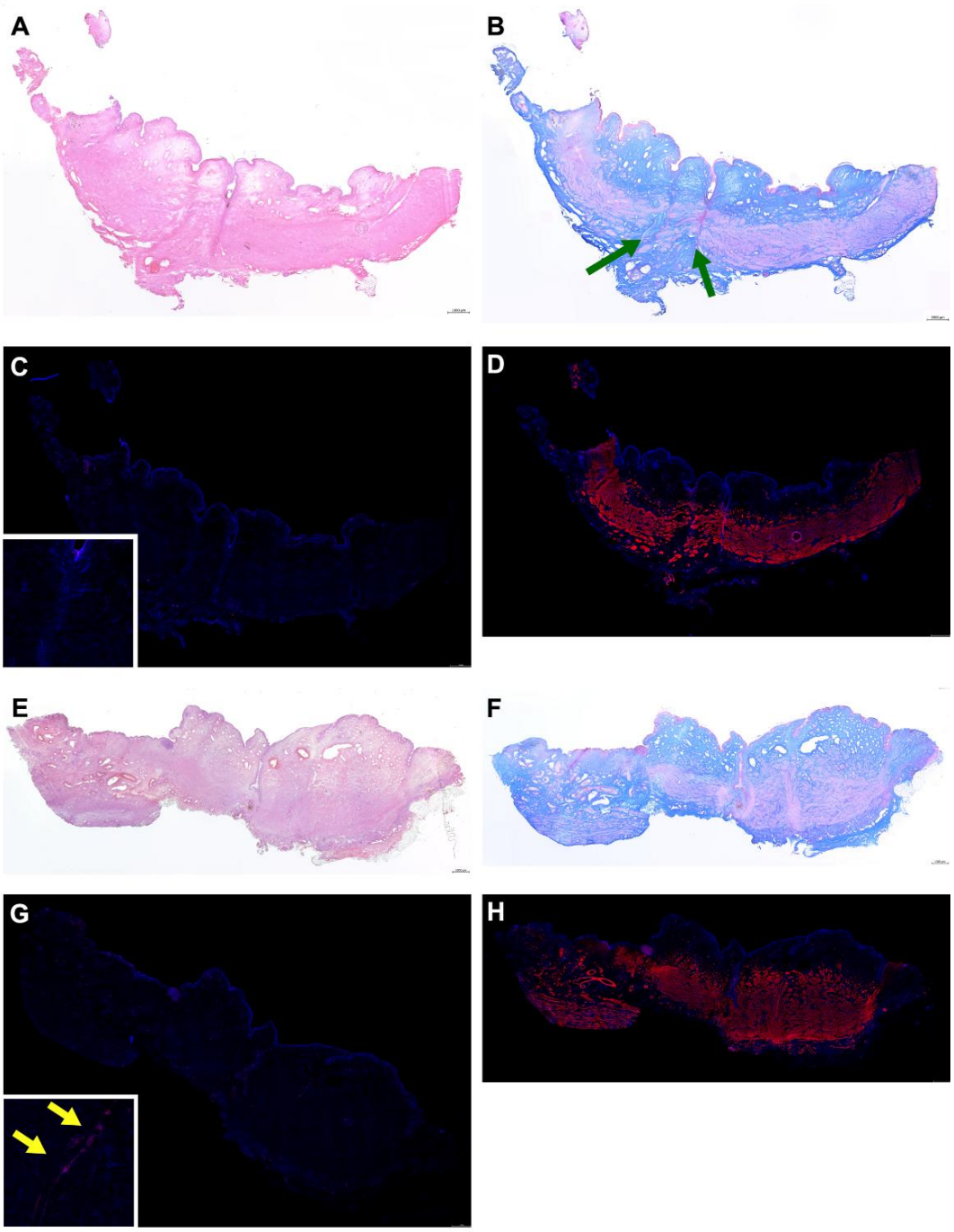

Figure 6: Histological and immunofluorescent analyses of representative animals of controls after 5 weeks of follow-up. Consecutive 20-µm cryosections were stained. Scale bar represents 1000 µm. A - D represent an animal with better tissue regeneration; E - H represent an animal with worse tissue regeneration. **A, E:** HE stainings showed no evidence of infiltration of mononuclear cells. **B, F:** AZAN stainings displayed some irregularities in the muscle structure (green arrows). **C, G:** Immunofluorescence staining for CD45-positive cells. Counterstaining with DAPI for nuclei was performed. Inserts show magnified regions of interest. In the animal with better regeneration no signs of inflammation were seen (C), while in the animal with worse regeneration slight accumulation of CD45-positive cells along the injection site were visible (D, yellow arrows). **D, H:** Phalloidin staining (red) documented the striated muscle and corroborated the results of AZAN stainings.

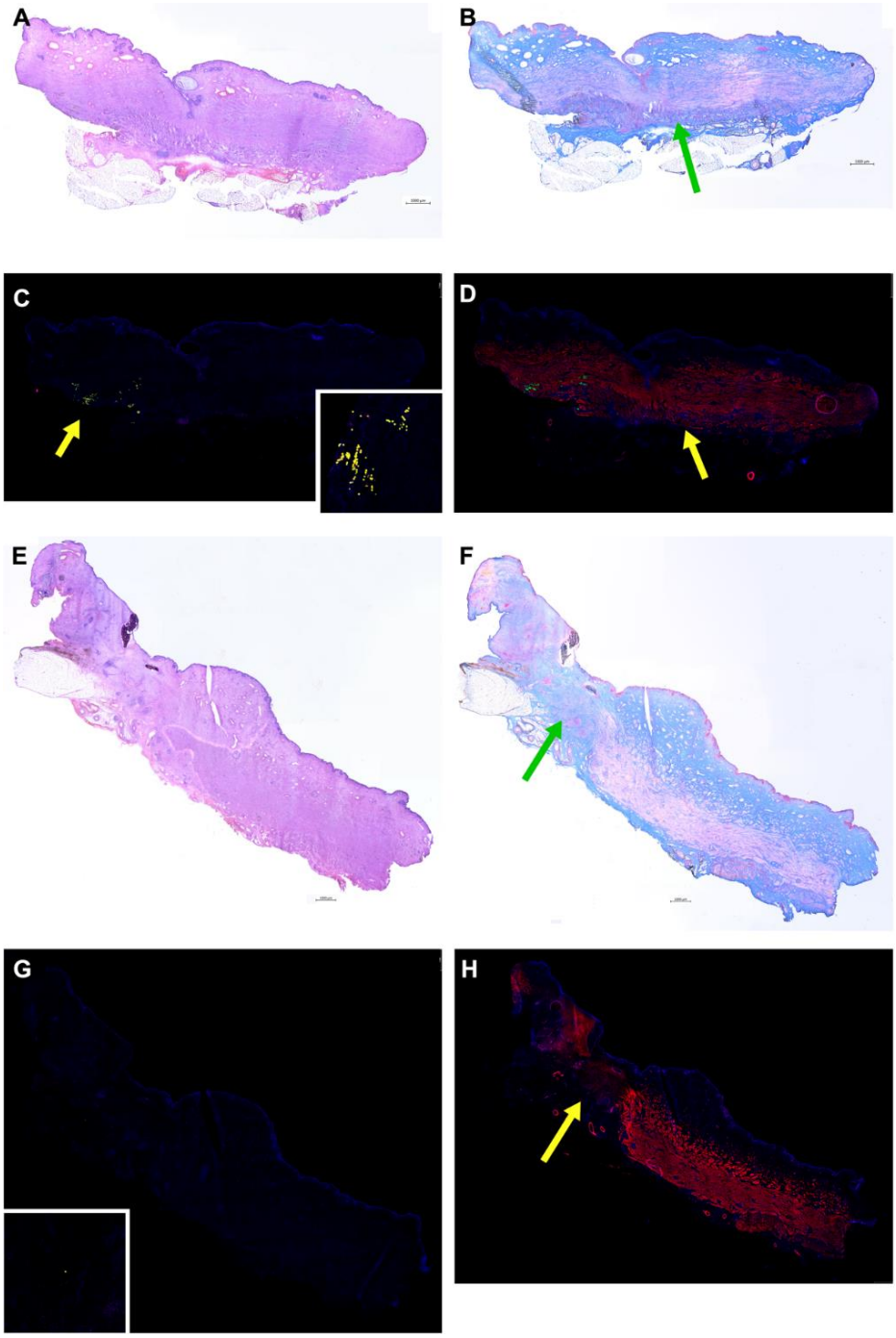

Figure 7: Histological and immunofluorescent analyses of representative MPC-treated animals after 5 weeks of follow-up. Consecutive 20-µm cryosections were stained. Scale bar represents 1000 µm. A - D represent an animal with better tissue regeneration; E - H represent an animal with worse tissue regeneration. **A, E:** HE stainings showed no evidence of infiltration of mononuclear cells. **B, F:** AZAN stainings displayed only minor irregularities in the muscle structure of the better-regenerated animal (B, green arrow), while in the animal with worse regeneration, the muscle structure was interrupted (F, green arrow). **C, G:** Immunofluorescence staining for CD45-positive cells. Counterstaining with DAPI for nuclei was performed. Inserts show magnified regions of interest. In both animals, almost no signs of inflammation were seen. The arrow indicates the injection site of fluorescent microparticles and MPCs (C, yellow arrow). However, in the animal with worse regeneration also almost no microparticles were found. **D, H:** Phalloidin staining (red) shows the striated muscle and corroborates the results of AZAN stainings with some irregularities (D, yellow arrow) and interruption (H, yellow arrow).

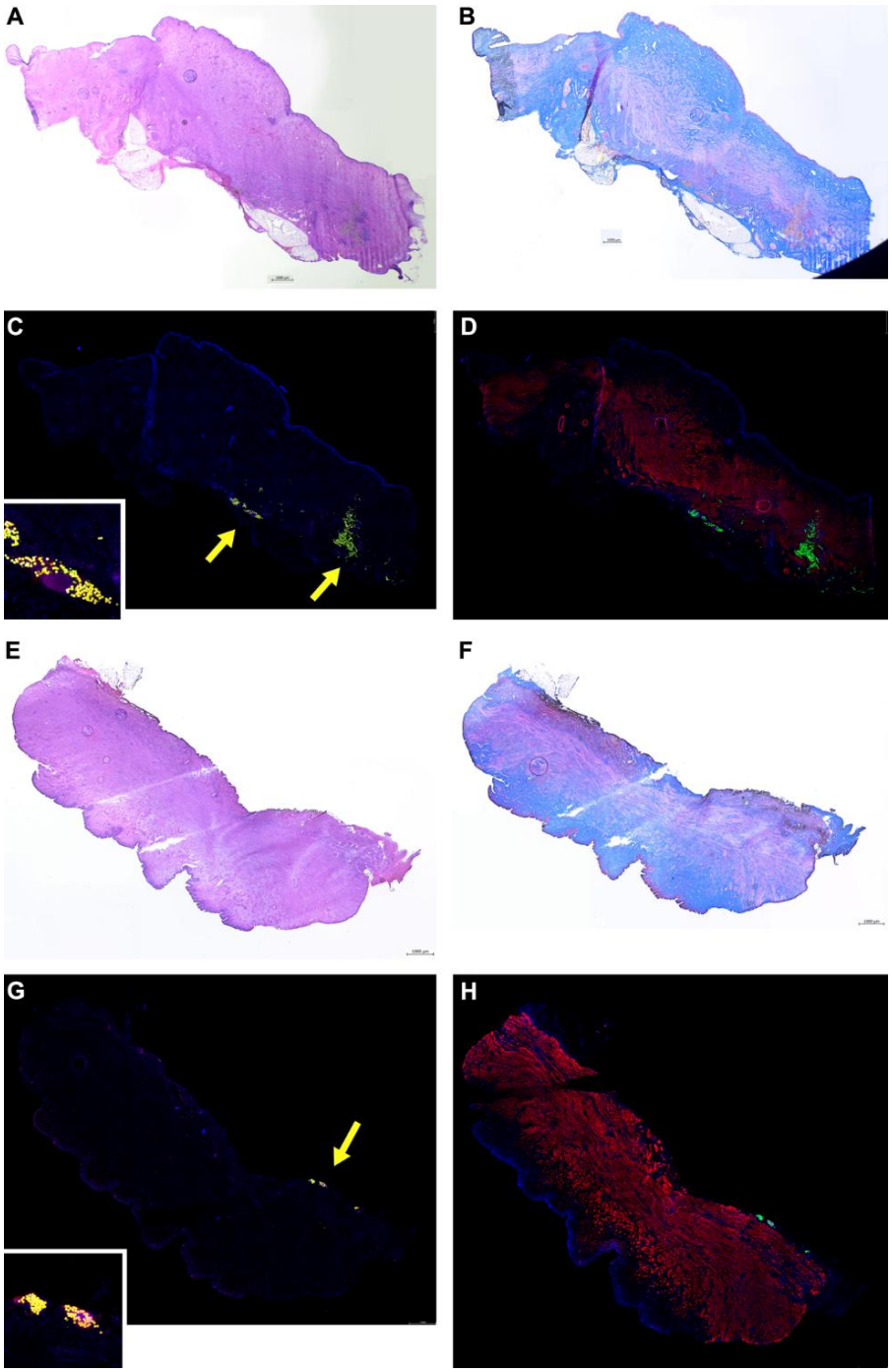

Figure 8: Histological and immunofluorescent analyses of representative ADSC-treated animals after 5 weeks of follow-up. Consecutive 20-µm cryosections were stained. Scale bar represents 1000 µm. A - D represent an animal with better tissue regeneration; E - H represent an animal with worse tissue regeneration. **A, E:** HE stainings showed no evidence of infiltration of mononuclear cells. **B, F:** AZAN stainings displayed no interruptions or irregularities of the urethral muscle layer in both animals. **C, G:** Immunofluorescence staining for CD45-positive cells. Counterstaining with DAPI for nuclei was performed. Inserts show magnified regions of interest. In both animals, slight and local infiltration of CD45-positive cells are visible. Yellow arrows indicate the injection sites of fluorescent microparticles and ADSCs found in both animals. The animal with better regeneration showed two injection sites and more distributed particles in the muscle layer (C). In the animal with worse regeneration only one injection site was detected, and particles were found mostly behind the muscular layer (G). **D, H:** Phalloidin staining (red) displays the striated muscle and corroborates the results of AZAN stainings showing a complete muscular structure.

Amplification of male DNA by PCR from cryosections of tissues targeted

To investigate if the male cells injected were detectable in tissue samples after five weeks of follow-up, PCR of DNA extracted from cryosections was performed in samples from all three cohorts (Fig. 9). By agarose gel electrophoresis false-positive PCR products were seen in the same samples running slightly above the expected SRY PCR product (Fig. 3A). This slightly larger PCR product was observed in samples from 1/2 MPC-treated and 1/2 ADSC-treated samples, but also in 1/2 control animals which did not receive any male cells (Fig. 9A). Therefore, melting point analyses of the PCR samples were performed (Fig. 9B). These analyses proved correct SRY-PCR products only in amplifications of DNA extracted directly from male cells in culture or from cryosections prepared immediately after cell injections, but not in any of the cryosections from cohort 1 – 3 animals (Fig. 9B). We conclude that the urethral samples from cell-treated gilts did not contain the numbers of male cells sufficient for detection by PCR after five weeks of follow-up.

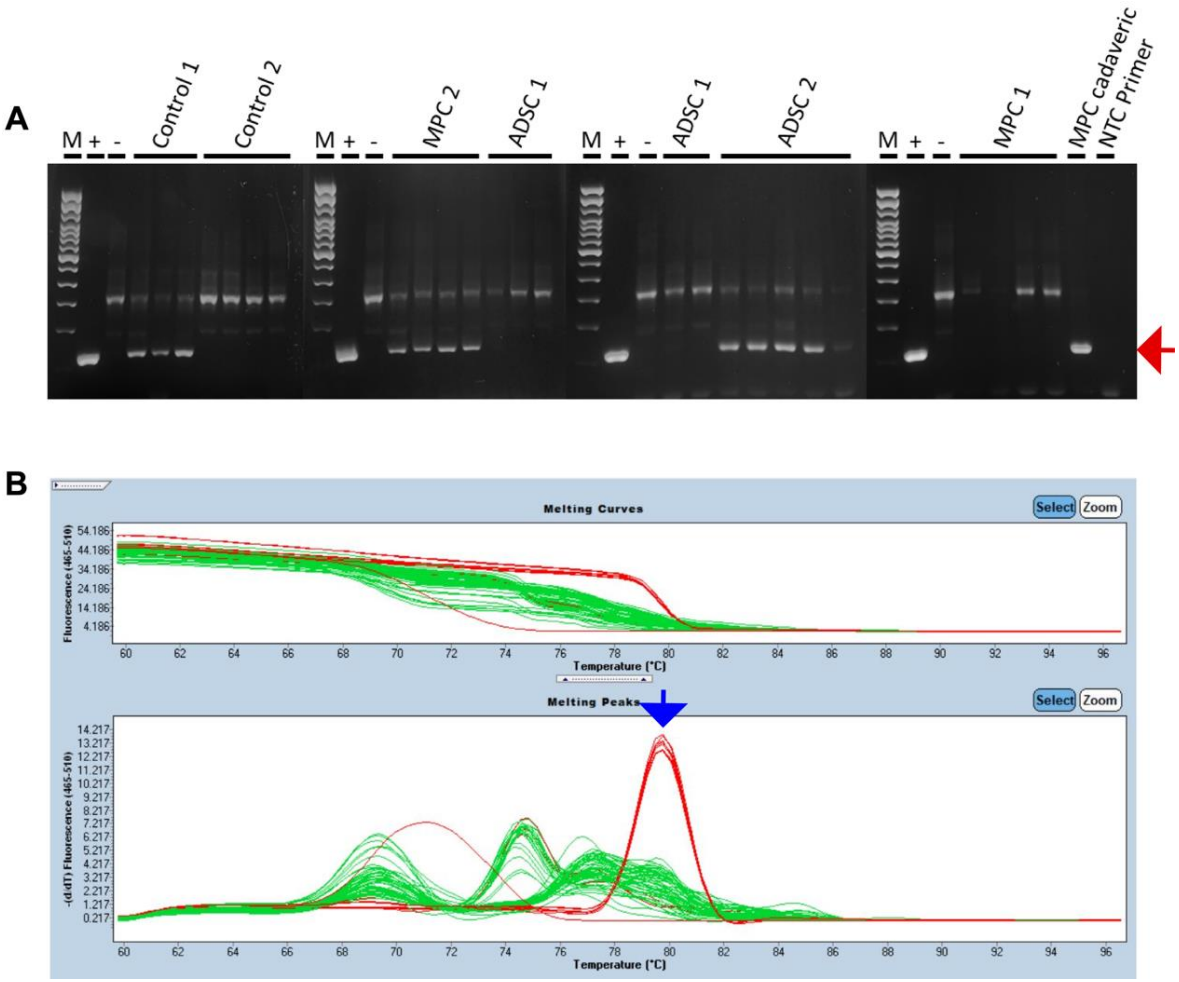

Figure 9: Detection of SRY-Gene in cryosections of controls and cell-treated animals. DNA of injected male cells was detected after five weeks of follow-up by PCR. **A:** Agarose gel of PCR products from randomly distributed cryosections from urethral tissue samples of the two representative animals (compare Figs. 6 – 8) of controls, MPC-, and ADSC-treated gilts. Positive control (+, male cells only) and negative control (-, female cells only) were analysed as well. Additionally, an injection of male MPCs into cadaveric tissue and direct isolation was investigated (MPC cadaveric). The expected PCR product of 133bp was seen in the positive controls and the MPC cadaveric injection (red arrow). A slightly larger PCR product was detected in the half of the samples. **B:** Melting curve analyses of PCR products. Only the positive controls and the MPC cadaveric probe resulted in specific melting curves (blue arrow), while the others displayed no specificity.

Discussion

Many preclinical and clinical SUI cell therapy studies built on the hypothesis that injection of cells facilitates a functional sphincter regeneration [19-21,30,50]. Some of these studies reported success, while others remained less optimistic [31,51,52]. We therefore compared the efficacy of MPCs and ADSCs SUI therapy in a porcine SUI model. Among others, several aspects merit discussion in the context of SUI cell therapy.

Isolation of autologous myoblasts causes more challenges when compared to the isolation of ADSCs from subcutaneous fat. The production of differentiation-competent MPCs under GMP-compliant conditions seems more complex compared to production of ADSCs [53,54]. There is evidence that activation of satellite cells in the sphincter muscle is important for a therapeutic effect [16]. Therefore, advanced myoblast therapies of SUI include injection of MPCs plus electrophysiological stimulation [19,21]. However, our results suggest that application of ADSCs yielded a superior sphincter regeneration compared to myoblasts. The kinetics of early USMS increase is comparable between MPC and ADSC application, suggesting that time-consuming differentiation of myoblasts to myotubes is not contributing to the SUI regeneration. Moreover, efficient regeneration of striated muscles requires more than adding additional myotubes. Myoblasts alone may not be capable of regenerating the vasculature, enervation, and extracellular matrix needed for satisfactory function of the sphincter [53,55]. The different secretome of ADSCs compared to MPCs may contribute to the sphincter regeneration observed. The distinct expression of VEGF in combination with IGF-1 by ADSCs may contribute to improved muscular regeneration, to the regeneration of peripheral nerves, and to angiogenesis [56]. However, this was not explored in this study in detail. A transient bulking effect of the cell injection itself cannot be excluded in the first phase after cell therapy [44]. The quality of injected cells may influence the outcome as well. For production of MPCs we recently optimized the protocol and such MPCs were employed here [35]. However, MPCs from other muscles may yield better regeneration to comply with the composition of the urethral sphincter muscle regarding fast- and slow-twitch fibers [36,57]. Experiments along these lines are ongoing.

Muscle injury and regeneration go along a pattern of inflammatory responses up to three weeks, followed by a non-inflammatory phase of tissue remodeling [58]. We detected $CD45^{pos}$ leukocytes in cell-treated gilts. Our data suggest that the paracrine action of injected cells is driving the regenerative processes [55,59]. This hypothesis is supported by the

correlation between the numbers the fluorescent particles (as surrogate for injected cells) detected by macroscopic *ex vivo* fluorescence and fluorescence microscopy after five weeks of follow-up and clinical outcome. As mechanism of action we propose the local of activation satellite cells [16,17] and general processes of muscle repair by ADSCs [60,61]. Dose-response analyses of cell application could not be performed yet but are part of current and future studies. Overall our results emphasized that precise cell injection is critical component for therapy success [34,42,44]. This is especially critical for MPC injections, as their terminal differentiation in myotubes and functional integration in the rhabdosphincter is required. This process works efficiently only, when the MPCs are placed in a healthy muscular environment [51,62].

Long-term survival of injected cells *in situ* seems not to contribute to therapy success, as clear differences in the slope of sphincter regeneration were observed early on. This was especially evident after MPC injection, while after ADSC injections a trend of further elevation of USMS was noted three to five weeks after cell application. This is in line with recent reports employing stromal cells and wound-healing models [63,64]. Moreover, DNA of male cells was not detected after five weeks of follow-up, indicating that neither ADSCs nor MPCs survived. Evidence indicating that MPCs differentiated in situ to myotubes or integrated in the rhabdosphincter was not found. In contrast, in our recent study injected cells were detected early after application [34]. We conclude that early processes are critical for overall sphincter regeneration.

Our experiments have explicit limitations. The cohort size was optimized to an exploratory study. Consequently, the standard deviations are remarkable and inter-individual outcome depends on a few single animals. Significance of MPC therapy over spontaneous regeneration may be achieved in larger cohorts, and the kinetics of cell therapy versus spontaneous regeneration may stand out more clearly. Our analyses focused on the efficacy of MPC versus ADSC in SUI therapy. The involvement of inflammation, vascularization, and the contribution of cells located in the tissue targeted were not investigated in great detail. The characteristics of the animal's breed and age may also influence the outcome and in part explain the differences reported by other studies [51,65,66]. Nevertheless, a systematic comparison between animal breeds, age, donor muscles as sources for MPCs, the role of inflammatory processes, and the contribution of other cells *in situ* are beyond this exploratory study.

Here, young gilts provided the SUI model and young boars served as cell source. Typical SUI patients are older. In women, SUI is associated with sphincter injury by pregnancy and vaginal delivery, but sequela develops decades later [2,5,9,10]. Still, success of cell therapy was reported in young and elderly patients [18,20-22]. As mesenchymal stromal cells such as MSCs, ADSCs, or placenta-derived MSCs express very little MHC class I [67-69], SUI therapy with homologous juvenile mesenchymal stromal cells may be envisioned for elderly human patients [70]. However, this again, is beyond the focus of this study.

To conclude, ADSCs regenerated the sphincter deficiency in our SUI model within five weeks in total and achieved better regeneration than MPC-treated gilts and a significant outcome compared to mock-treated controls. ADSCs might therefore be suitable candidates for further feasibility studies [30].

Abbreviations

ADSCs	adipose tissue-derived mesenchymal stromal cells
FC	flow cytometry
IF	immunofluorescence
IHC	immunohistochemistry
MPCs	myogenic progenitor cells, also referred to as myoblasts
(q)PCR	(quantitative) polymerase chain reaction
RT	Real Time
SRY	sex determining region Y
SUI	stress urinary incontinence
UI	urinary incontinence
USMS	urethral sphincter muscle strength
UPP	urethral pressure profilometry, alias urodynamics

Acknowledgments

The authors owe the team of animal wardens, the colleagues in the animal surgery unit, and the veterinarians at the University a great depth of gratitude for expert help in ethics, husbandry and surgery of animals. We thank Mrs. Tanja Abruzzese and Mrs. Conny Bock for excellent technical assistance and Mr. Chaim Goziga for help in preparation of the artwork of this study.

Author Contributions

Experiments: JK, BA, NH, SI, NB, WKA; resources: BA, AS, WKA; writing: all authors; All authors have read and agreed to the published version of the manuscript.

Conflicts of interest

The authors declare no conflict of interest.

Funding

The project was supported in part by the DFG grants PoTuS (# 429049495) to BA, AS, WKA and MyoRepair (# 468616715) to WKA, the Werner Siemens Foundation to SI and NB, and in part by institutional funds.

Institutional Review Board Statement

The animal study was approved by the State of Baden-Württemberg Animal Welfare under file # 35/9185.81-2 / CU01-20G.

Informed Consent Statement

ø, not applicable

References

1. Broome BA. The impact of urinary incontinence on self-efficacy and quality of life. Health Qual Life Outcomes 2003;1(35, doi:10.1186/1477-7525-1-35
2. Luber KM. The definition, prevalence, and risk factors for stress urinary incontinence. Rev Urol 2004;6 Suppl 3(Suppl 3):S3-9
3. Shamliyan TA, Wyman JF, Ping R, et al. Male urinary incontinence: prevalence, risk factors, and preventive interventions. Rev Urol 2009;11(3):145-65
4. Abrams P, Andersson KE, Birder L, et al. Fourth International Consultation on Incontinence Recommendations of the International Scientific Committee: Evaluation and treatment of urinary incontinence, pelvic organ prolapse, and fecal incontinence. Neurourol Urodyn 2010;29(1):213-40, doi:10.1002/nau.20870
5. Milsom I, Gyhagen M. The prevalence of urinary incontinence. Climacteric 2019;22(3):217-222, doi:10.1080/13697137.2018.1543263
6. Coyne KS, Wein A, Nicholson S, et al. Comorbidities and personal burden of urgency urinary incontinence: a systematic review. International Journal of Clinical Practice 2013;67(10):1015-1033, doi:https://doi.org/10.1111/ijcp.12164
7. Chapple CR, Osman NI. Current issues in managing men with lower urinary tract symptoms in primary care. International Journal of Clinical Practice 2013;67(10):931-933, doi:https://doi.org/10.1111/ijcp.12170
8. Patel PD, Amrute KV, Badlani GH. Pelvic organ prolapse and stress urinary incontinence: A review of etiological factors. Indian J Urol 2007;23(2):135-41, doi:10.4103/0970-1591.32064
9. Gonzales AL, Barnes KL, Qualls CR, et al. Prevalence and Treatment of Postpartum Stress Urinary Incontinence: A Systematic Review. Urogynecology 2021;27(1):e139-e145, doi:10.1097/spv.0000000000000866
10. Buckley BS, Lapitan MCM. Prevalence of Urinary Incontinence in Men, Women, and Children—Current Evidence: Findings of the Fourth International Consultation on

Incontinence. Urology 2010;76(2):265-270, doi:https://doi.org/10.1016/j.urology.2009.11.078
11. Richter HE, Burgio KL, Goode PS, et al. Non-surgical management of stress urinary incontinence: ambulatory treatments for leakage associated with stress (ATLAS) trial. Clinical Trials 2007;4(1):92-101, doi:10.1177/1740774506075237
12. Lucas MG, Bosch RJL, Burkhard FC, et al. European Association of Urology guidelines on assessment and nonsurgical management of urinary incontinence. Actas Urológicas Españolas (English Edition) 2013;37(4):199-213, doi:https://doi.org/10.1016/j.acuroe.2012.12.002
13. Walters MD, Daneshgari F. Surgical Management of Stress Urinary Incontinence. Clinical Obstetrics and Gynecology 2004;47(1):93-103
14. Harland N, Aicher WK, Stenzl A, et al. Stress urinary incontinence. An unsolved clinical challenge. BJS Open 2022;submitted(
15. Strasser H, Tiefenthaler M, Steinlechner M, et al. Urinary incontinence in the elderly and age-dependent apoptosis of rhabdosphincter cells. Lancet 1999;354(9182):918-9, doi:10.1016/s0140-6736(99)02588-x
16. Yiou R, Lefaucheur JP, Atala A. The regeneration process of the striated urethral sphincter involves activation of intrinsic satellite cells. Anat Embryol (Berl) 2003;206(6):429-35, doi:10.1007/s00429-003-0313-x
17. Yiou R, Dreyfus P, Chopin DK, et al. Muscle precursor cell autografting in a murine model of urethral sphincter injury. BJU International 2002;89(3):298-302, doi:https://doi.org/10.1046/j.1464-4096.2001.01618.x
18. Mitterberger M, Pinggera G-M, Marksteiner R, et al. Adult Stem Cell Therapy of Female Stress Urinary Incontinence. European Urology 2008;53(1):169-175, doi:https://doi.org/10.1016/j.eururo.2007.07.026
19. Eberli D, Aboushwareb T, Soker S, et al. Muscle Precursor Cells for the Restoration of Irreversibly Damaged Sphincter Function. Cell Transplantation 2012;21(9):2089-2098, doi:10.3727/096368911x623835
20. Peters KM, Dmochowski RR, Carr LK, et al. Autologous Muscle Derived Cells for Treatment of Stress Urinary Incontinence in Women. Journal of Urology 2014;192(2):469-476, doi:doi:10.1016/j.juro.2014.02.047
21. Schmid FA, Williams JK, Kessler TM, et al. Treatment of Stress Urinary Incontinence with Muscle Stem Cells and Stem Cell Components: Chances, Challenges and Future Prospects. International Journal of Molecular Sciences 2021;22(8):3981
22. Blaganje M, Lukanović A. The effect of skeletal muscle-derived cells implantation on stress urinary incontinence and functional urethral properties in female patients. International Journal of Gynecology & Obstetrics 2022;157(2):444-451, doi:https://doi.org/10.1002/ijgo.13853
23. Dissaranan C, Cruz MA, Kiedrowski MJ, et al. Rat mesenchymal stem cell secretome promotes elastogenesis and facilitates recovery from simulated childbirth injury. Cell Transplant 2014;23(11):1395-406, doi:10.3727/096368913x670921
24. Wu R, Huang C, Wu Q, et al. Exosomes secreted by urine-derived stem cells improve stress urinary incontinence by promoting repair of pubococcygeus muscle injury in rats. Stem Cell Research & Therapy 2019;10(1):80, doi:10.1186/s13287-019-1182-4

25. Rolland TJ, Peterson TE, Singh RD, et al. Exosome biopotentiated hydrogel restores damaged skeletal muscle in a porcine model of stress urinary incontinence. npj Regenerative Medicine 2022;7(1):58, doi:10.1038/s41536-022-00240-9
26. Corcos J, Loutochin O, Campeau L, et al. Bone marrow mesenchymal stromal cell therapy for external urethral sphincter restoration in a rat model of stress urinary incontinence. Neurourology and Urodynamics 2011;30(3):447-455, doi:https://doi.org/10.1002/nau.20998
27. Deng K, Lin DL, Hanzlicek B, et al. Mesenchymal stem cells and their secretome partially restore nerve and urethral function in a dual muscle and nerve injury stress urinary incontinence model. American Journal of Physiology-Renal Physiology 2015;308(2):F92-F100, doi:10.1152/ajprenal.00510.2014
28. Hart ML, Izeta A, Herrera-Imbroda B, et al. Cell Therapy for Stress Urinary Incontinence. Tissue Eng Part B Rev 2015;21(4):365-76, doi:10.1089/ten.TEB.2014.0627
29. Aragón IM, Imbroda BH, Lara MF. Cell Therapy Clinical Trials for Stress Urinary Incontinence: Current Status and Perspectives. Int J Med Sci 2018;15(3):195-204, doi:10.7150/ijms.22130
30. Gotoh M, Yamamoto T, Shimizu S, et al. Treatment of male stress urinary incontinence using autologous adipose-derived regenerative cells: Long-term efficacy and safety. International Journal of Urology 2019;26(3):400-405, doi:https://doi.org/10.1111/iju.13886
31. Garcia-Arranz M, Alonso-Gregorio S, Fontana-Portella P, et al. Two phase I/II clinical trials for the treatment of urinary incontinence with autologous mesenchymal stem cells. Stem Cells Translational Medicine 2020;9(12):1500-1508, doi:10.1002/sctm.19-0431
32. Herrera-Imbroda B, Lara MF, Izeta A, et al. Stress urinary incontinence animal models as a tool to study cell-based regenerative therapies targeting the urethral sphincter. Adv Drug Deliv Rev 2015;82-83(106-16, doi:10.1016/j.addr.2014.10.018
33. Kelp A, Albrecht A, Amend B, et al. Establishing and monitoring of urethral sphincter deficiency in a large animal model. World J Urol 2017;35(12):1977-1986, doi:10.1007/s00345-017-2088-3
34. Geng R, Knoll J, Harland N, et al. Replacing Needle Injection by a Novel Waterjet Technology Grants Improved Muscle Cell Delivery in Target Tissues. Cell Transplant 2022;31(9636897221080943, doi:10.1177/09636897221080943
35. Knoll J, Amend B, Abruzzese T, et al. Improved production of proliferation- and differentiation-competent porcine striated muscle-derived myoblasts. submitted;
36. Ding S, Wang F, Liu Y, et al. Characterization and isolation of highly purified porcine satellite cells. Cell Death Discovery 2017;3(1):17003, doi:10.1038/cddiscovery.2017.3
37. Metzger K, Tuchscherer A, Palin MF, et al. Establishment and validation of cell pools using primary muscle cells derived from satellite cells of pig skeletal muscle. In Vitro Cell Dev Biol Anim 2020;56(3):193-199, doi:10.1007/s11626-019-00428-2
38. Pilz GA, Braun J, Ulrich C, et al. Human mesenchymal stromal cells express CD14 cross-reactive epitopes. Cytometry A 2011;79(8):635-45, doi:10.1002/cyto.a.21073

39. Lock JT, Parker I, Smith IF. A comparison of fluorescent Ca(2)(+) indicators for imaging local Ca(2)(+) signals in cultured cells. Cell Calcium 2015;58(6):638-48, doi:10.1016/j.ceca.2015.10.003
40. Reggiani C. Caffeine as a tool to investigate sarcoplasmic reticulum and intracellular calcium dynamics in human skeletal muscles. Journal of Muscle Research and Cell Motility 2021;42(2):281-289, doi:10.1007/s10974-020-09574-7
41. Chen YJ, Liu HY, Chang YT, et al. Isolation and Differentiation of Adipose-Derived Stem Cells from Porcine Subcutaneous Adipose Tissues. J Vis Exp 2016;109):e53886, doi:10.3791/53886
42. Linzenbold W, Jager L, Stoll H, et al. Rapid and precise delivery of cells in the urethral sphincter complex by a novel needle-free waterjet technology. BJU Int 2021;127(4):463-472, doi:10.1111/bju.15249
43. Pilz GA, Ulrich C, Ruh M, et al. Human term placenta-derived mesenchymal stromal cells are less prone to osteogenic differentiation than bone marrow-derived mesenchymal stromal cells. Stem Cells Dev 2011;20(4):635-46, doi:10.1089/scd.2010.0308
44. Amend B, Kelp A, Vaegler M, et al. Precise injection of human mesenchymal stromal cells in the urethral sphincter complex of Gottingen minipigs without unspecific bulking effects. Neurourol Urodyn 2017;36(7):1723-1733, doi:10.1002/nau.23182
45. Jaillard S, Holder-Espinasse M, Hubert T, et al. Tracheal replacement by allogenic aorta in the pig. Chest 2006;130(5):1397-404, doi:10.1378/chest.130.5.1397
46. Noguchi K, Gel YR, Brunner E, et al. nparLD: An R Software Package for the Nonparametric Analysis of Longitudinal Data in Factorial Experiments. Journal of Statistical Software 2012;50(1 - 23
47. RC T. R: A language and environment for statistical computing. Computing RFfS, editor 2022;
48. Jankowski RJ, Deasy BM, Huard J. Muscle-derived stem cells. Gene Ther 2002;9(10):642-7, doi:10.1038/sj.gt.3301719
49. Mitchell JB, McIntosh K, Zvonic S, et al. Immunophenotype of human adipose-derived cells: temporal changes in stromal-associated and stem cell-associated markers. Stem Cells 2006;24(2):376-85
50. Jankowski RJ, Tu LM, Carlson C, et al. A double-blind, randomized, placebo-controlled clinical trial evaluating the safety and efficacy of autologous muscle derived cells in female subjects with stress urinary incontinence. Int Urol Nephrol 2018;50(12):2153-2165, doi:10.1007/s11255-018-2005-8
51. Burdzinska A, Crayton R, Dybowski B, et al. The effect of endoscopic administration of autologous porcine muscle-derived cells into the urethral sphincter. Urology 2013;82(3):743 e1-8, doi:10.1016/j.urology.2013.03.030
52. Pokrywczynska M, Adamowicz J, Czapiewska M, et al. Targeted therapy for stress urinary incontinence: a systematic review based on clinical trials. Expert Opin Biol Ther 2016;16(2):233-42, doi:10.1517/14712598.2016.1118459
53. Roche R, Festy F, Fritel X. Stem cells for stress urinary incontinence: the adipose promise. J Cell Mol Med 2010;14(1-2):135-42, doi:10.1111/j.1582-4934.2009.00915.x

54. Saury C, Lardenois A, Schleder C, et al. Human serum and platelet lysate are appropriate xeno-free alternatives for clinical-grade production of human MuStem cell batches. Stem Cell Res Ther 2018;9(1):128, doi:10.1186/s13287-018-0852-y
55. Delo DM, Eberli D, Williams JK, et al. Angiogenic gene modification of skeletal muscle cells to compensate for ageing-induced decline in bioengineered functional muscle tissue. BJU International 2008;102(7):878-884, doi:https://doi.org/10.1111/j.1464-410X.2008.07750.x
56. Borselli C, Storrie H, Benesch-Lee F, et al. Functional muscle regeneration with combined delivery of angiogenesis and myogenesis factors. Proc Natl Acad Sci U S A 2010;107(8):3287-92, doi:10.1073/pnas.0903875106
57. Bazeed MA, Thuroff JW, Schmidt RA, et al. Effect of chronic electrostimulation of the sacral roots on the striated urethral sphincter. J Urol 1982;128(6):1357-62, doi:10.1016/s0022-5347(17)53507-7
58. Smith C, Kruger MJ, Smith RM, et al. The inflammatory response to skeletal muscle injury: illuminating complexities. Sports Med 2008;38(11):947-69, doi:10.2165/00007256-200838110-00005
59. Gill BC, Sun DZ, Damaser MS. Stem Cells for Urinary Incontinence: Functional Differentiation or Cytokine Effects? Urology 2018;117(9-17, doi:10.1016/j.urology.2018.01.002
60. Miyoshi N, Fujino S, Takahashi Y, et al. Implantation of human adipose-derived stromal cells for the functional recovery of a murine heat-damaged muscle model. Surg Today 2020;50(12):1699-1706, doi:10.1007/s00595-020-02026-2
61. Bunnell BA. Adipose Tissue-Derived Mesenchymal Stem Cells. Cells-Basel 2021;10(12), doi:ARTN 3433 10.3390/cells10123433
62. Peyromaure M, Sebe P, Praud C, et al. Fate of implanted syngenic muscle precursor cells in striated urethral sphincter of female rats: perspectives for treatment of urinary incontinence. Urology 2004;64(5):1037-41, doi:10.1016/j.urology.2004.06.058
63. Gorodetsky R, Aicher WK. Allogenic Use of Human Placenta-Derived Stromal Cells as a Highly Active Subtype of Mesenchymal Stromal Cells for Cell-Based Therapies. Int J Mol Sci 2021;22(10), doi:10.3390/ijms22105302
64. Santos AdL, Silva CGD, Barreto LSDS, et al. Treatment of Muscle Injury with Stem Cells – Experimental Study in Rabbits. Rev Bras, Ortop 2022;57(5):788 - 794
65. Amend B, Harland N, Knoll J, et al. Large Animal Models for Investigating Cell Therapies of Stress Urinary Incontinence. International Journal of Molecular Sciences 2021;22(11), doi:ARTN 6092 10.3390/ijms22116092
66. Knoll J, Harland N, Amend B, et al. Göttingen minipigs present with significant regeneration kinetics after sphincter injury compared to German landrace gilts. submitted.
67. Dominici M, Le Blanc K, Mueller I, et al. Minimal criteria for defining multipotent mesenchymal stromal cells. The International Society for Cellular Therapy position statement. Cytotherapy 2006;8(4):315-7, doi:10.1080/14653240600855905
68. McIntosh K, Zvonic S, Garrett S, et al. The Immunogenicity of Human Adipose-Derived Cells: Temporal Changes In Vitro. Stem Cells 2006;24(5):1246-1253, doi:10.1634/stemcells.2005-0235
69. Kim MJ, Shin KS, Jeon JH, et al. Human chorionic-plate-derived mesenchymal stem cells and Wharton's jelly-derived mesenchymal stem cells: a comparative analysis of

their potential as placenta-derived stem cells. Cell Tissue Res 2011;346(1):53-64, doi:10.1007/s00441-011-1249-8
70. Winkler T, Perka C, von Roth P, et al. Immunomodulatory placental-expanded, mesenchymal stromal cells improve muscle function following hip arthroplasty. J Cachexia Sarcopenia Muscle 2018;9(5):880-897, doi:10.1002/jcsm.12316
71. Kalbe C, Mau M, Rehfeldt C. Developmental changes and the impact of isoflavones on mRNA expression of IGF-I receptor, EGF receptor and related growth factors in porcine skeletal muscle cell cultures. Growth Horm IGF Res 2008;18(5):424-433, doi:10.1016/j.ghir.2008.03.002
72. Zhang S, Chen X, Huang Z, et al. Leucine promotes differentiation of porcine myoblasts through the protein kinase B (Akt)/Forkhead box O1 signalling pathway. British Journal of Nutrition 2018;119(7):727-733, doi:10.1017/S0007114518000181
73. Maak S, Wicke M, Swalve HH. Analysis of gene expression in specific muscle of swine and turkey. Arch Tierzucht 2005;48(135 - 140

Supplementary Materials

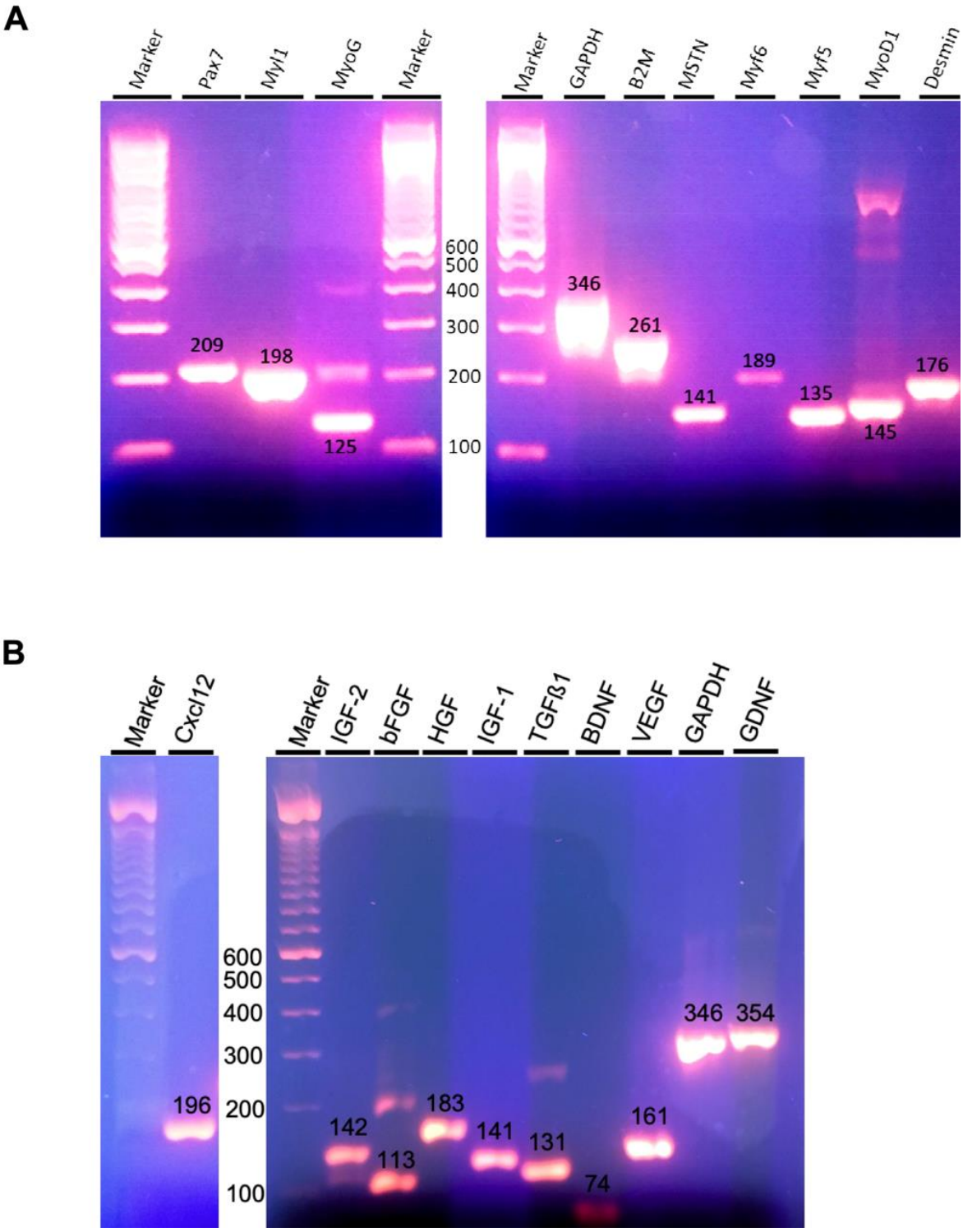

Figure os1: Agarose gels of specific primers. A: Specific primers of myogenic factors showing expected product sizes. **B:** Specific primers of cytokines of ADSCs showing expected product sizes.

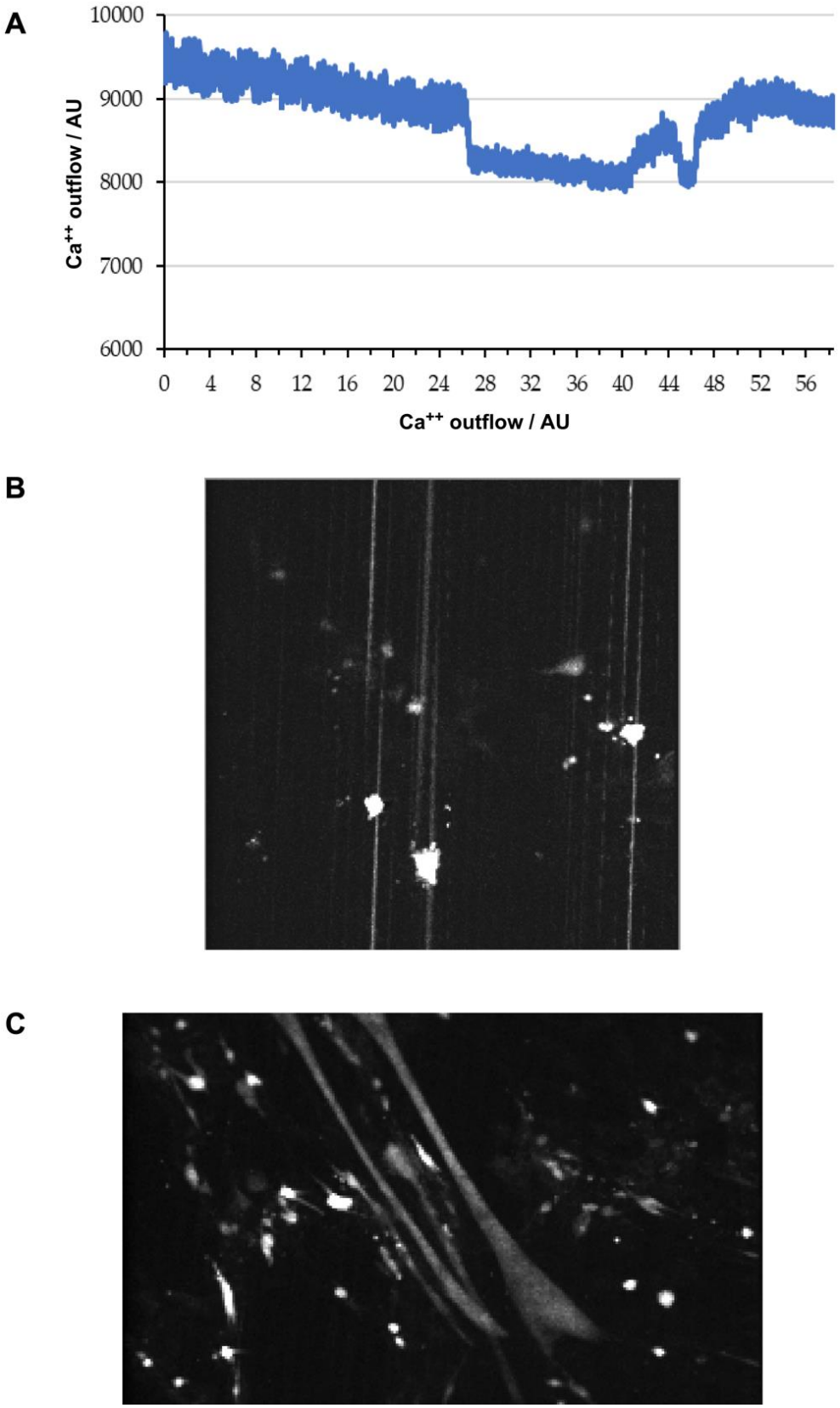

Figure os2: Electrophysiological measurements of MPCs. A: Electrophysiological measurement of electrode- and caffeine-stimulated MPCs. Outflow of Ca^{2+} was determined. However, no reaction of cells was visible to stimulation. **B:** Image of Cal-520 AM-stained myoblasts under stimulation. **C:** Image of Cal-520 AM-stained myotubes under stimulation.

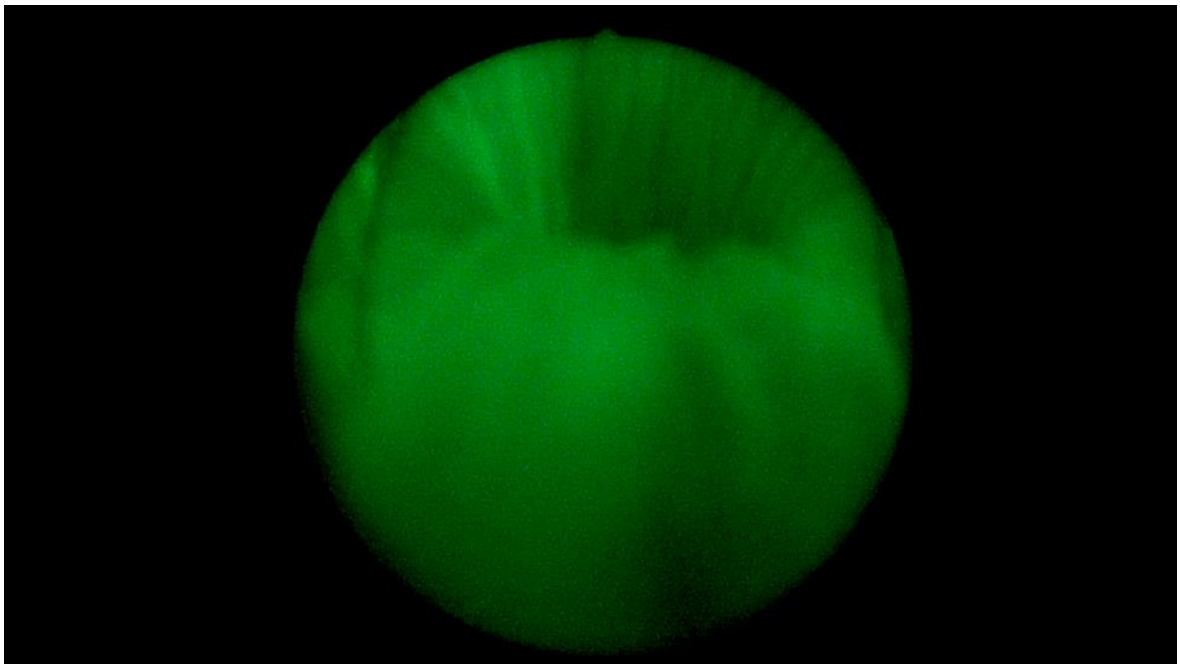

Figure os3: Video of in vivo fluorimetry of labelled cells and microparticles. Representative video of in vivo fluorimetry of green labelled cells and microparticles in the urethra of a pig. Clear fluorescence signals are visible throughout the porcine urethra.

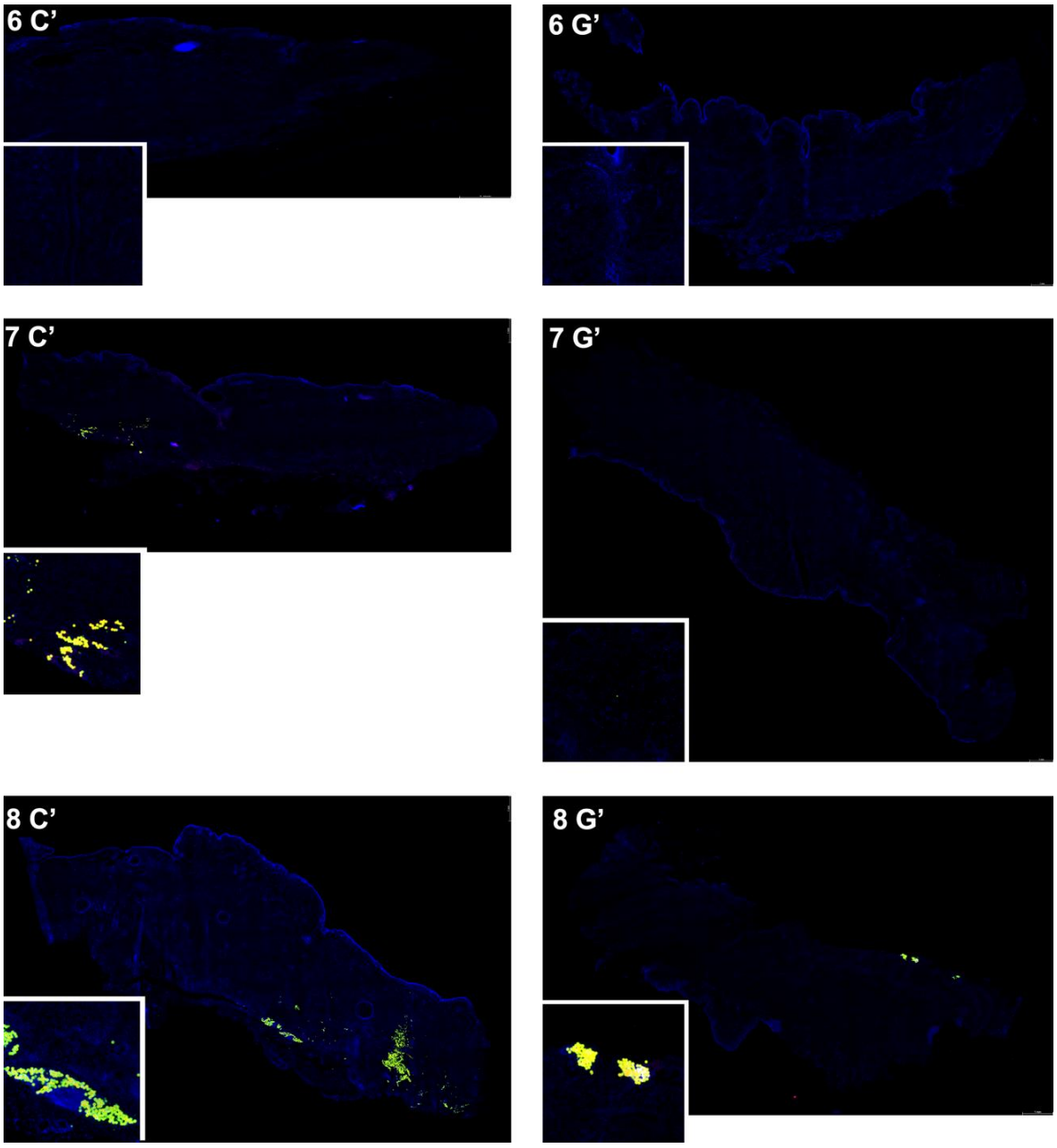

Figure os4: Controls to immunofluorescence stainings of CD45. Corresponding controls to the stainings of CD45 in consecutive 20 µm-cryosections presented in figures 6 - 8. Controls were stained with secondary antibody only. No unspecific reactions were detected.

Supplementary Extended Methods

Establishing a preclinical model of stress urinary incontinence

German landrace gilts (n= 18; body weight approx. 30 kg, 3 months of age) were obtained directly from the breeder (Benz GbR) with excellent health status. The gilts were housed in the animal facility in one pen prior to surgery for two weeks. During husbandry, animals were observed, fed with specific food, given water ad libitum every day, and the health status was monitored by trained personnel. Prior to induction of sphincter deficiency, animals were sedated by pre-medication (atropin: 0.05 mg/kg body weight (bw) i.m. and azaperon: 4.0 mg/kg bw i.m.), followed by midazolam: 1.0 mg/kg bw i.m. and ketamin (14 mg/kg bw i.m.). Prior to induction of sphincter insufficiency, the urethral sphincter muscle was localized in sedation by transurethral urodynamics under visual control using an air-charged dual sensor catheter (Aquarius TT, Laborie) as described recently [1,2]. Urethral pressure profilometry (UPP), sometimes called urodynamics, was performed to monitor sphincter function. To induce sphincter deficiency as model of SUI, the sphincter muscle was injured by two lateral electrocauteries (ERBE Hybridknife, mode monopolar cut, effect 4, power 100 W max.; ERBE Elektromedizin) just distal of the wall pressure maximum followed by balloon dilatation (2 way balloon catheter, 20 mL filling, approx. 37 mm diameter ≈ 110 Fr; Teleflex Medical) in deep anaesthesia (propofol: 5 mg/kg bw i.v. under controlled respiration with 0.6 - 1.6 Vol% isofluran, complemented if needed by fentanyl: 5µg/kg bw i.v.) [1]. Immediately after surgery, efficacy of sphincter deficiency was confirmed by UPP. The animals were observed during follow-up daily and fed with a specific diet and water *ad libitum*. After induction of sphincter deficiency, the health status (body weight, body temperature) and urine status (Combur 10 test, Roche) were monitored by trained personnel. In addition, the regeneration of the sphincter muscle was monitored weekly by UPP [1]. The study was approved by the State of Baden Württemberg Animal Welfare Authorities under file number 35/9185.81-2 / CU01-20G and performed in full compliance with the ARRIVE 2.0. standards and all other relevant regulations.

Production of myoblasts (MPCs) from *Musculus semitendinosus*

Tissue samples from *Musculus (M.) semitendinosus* were aseptically prepared from young male littermates of the gilts included in the study. To this end, boars were sedated by pre-medication as described above and sacrificed by a lethal dose of phenobarbital. The

dermis was cleaned and disinfected. By scalpel and scissors a small incision was made and parts of the *M. semitendinosus* were removed aseptically. The muscle samples were submerged in pre-cooled medium and transported on wet ice to the laboratory. There, MPCs were isolated and expanded employing a slightly modified protocol [3] based on recent papers [4,5]. In brief, muscle tissue was minced mechanically and further degraded by aid of collagenase I, DNase I and trypsin from bovine pancreas [5]. Erythrocytes were lysed and debris was removed. The yield and viability of MPCs were determined. MPCs were seeded and expanded on gelatine-coated flasks and expanded in F10 medium complemented with 15% FBS, 5 ng/mL bFGF, and antibiotics [4]. For MPC characterization, expression of desmin and CD56 were explored by immunofluorescence (IF) and flow cytometry (FC), respectively (Table 1) [3,4,6]. Expression of myogenic transcripts including skeletal muscle actin alpha 1 (ACTA1), myogenin (MyoG), desmin (Des), myostatin (MSTN), myogenic factor (Myf5), myogenic factor (Myf6), myosin heavy chain 1 (MYH1), myosin light chain 1 (Myl1), myogenic differentiation 1(MyoD1), myogenin (MyoG), paired box 7 (Pax7) were determined by RT-qPCR (online supplement Fig. os1A). Differentiation of MPCs was induced by medium enriched with 2% horse serum [4]. Syncytia and multi-nuclear myotubes were recorded by IF using anti-desmin antibodies and DAPI counterstaining. To investigate the functional competence of the porcine myotubes, electrophysiology was employed. In brief, MPCs and myotubes were expanded on cover glasses and plates were loaded with 2 µmol Cal520-AM (AAT Bioquest) for 45 min at 37°C. Cells were placed in a Zeiss Cell Observer system equipped with a Yokogawa spinning disk confocal imaging under environmental control. Allowing to record at 37°C and nominal 5% CO_2 electrophysiologic stimulation was induced with platinum electrodes in close vicinity to the cells. Stimulation pulses were applied as rectangular biphasic pulses of +/- 4 V for 50 ms every two seconds. After a baseline recording 300 mM caffeine was added to a final concentration of 30 mM and stimulation was continued. In both cases, release of calcium from intracellular compartments was recorded as described [7,8]. Evaluation was conducted with FIJI. Prior to injection, MPCs were labelled by CMFDA as requested by the supplier (ThermoFisher).

Production of adipose tissue-derived mesenchymal stroma cells (ADSCs)

Subcutaneous fat tissue was aseptically prepared from the same boars utilized for preparation of MPCs (see above). Subcutaneous adipose tissue was harvested aseptically,

tissue samples were submerged in pre-cooled medium, and transported on wet ice to the laboratory. There, ADSCs were isolated and expanded as described recently [9,10]. In brief, fat was minced by blades and further degraded by proteolysis. Cells were washed, counted, seeded, and expanded in DMEM low glucose complemented by 10% FBS and antibiotics [9]. For characterization, ADSCs were detached by mild proteolysis (Accutase, Sigma), washed and analysed for expression of cell surface markers by FC (Table 1). Detection of CD14 and CD45 facilitates the exclusion of monocytic cells or leukocytes. Staining of CD29, CD44, and CD90 indicated mesenchymal lineage of the cells. Low expression of MHC class I was important in the context of homologous injection of male cells in littermate gilts. In addition, in vitro differentiation along the adipogenic and osteogenic lineages was induced [9], and detected by Oil Red O staining and von Kossa staining, respectively [11]. Moreover, the cytokine expression of produced ADSCs was analysed via RT-qPCR using specific primers (Table 2) regarding their potential to secrete paracrine factors. Insulin-like growth factor 1 and 2 (IGF-1, IGF-2), basic fibroblast growth factor (bFGF), hepatocyte growth factor (HGF), transforming growth factor ß 1 (TGFß1), brain-derived neurotrophic (BDNF), glia cell line-derived neurotrophic factor (GDNF), C-X-C motif chemokine 12 (Cxcl12), and vascular endothelial growth factor (VEGF) expression patterns were determined (online supplement Fig. os1B). Prior to injection, ADSCs were labelled by CMFDA as requested by the supplier (ThermoFisher).

Analysis of marker gene expression by RT-qPCR, flow cytometry, and immunofluorescence

The expression of a panel of marker genes was investigated by reverse transcription of mRNA followed by real time quantitative polymerase chain reaction (RT-qPCR), flow cytometry, and immunofluorescence. For RT-qPCR cells were harvested, RNA was isolated (RNeasy kit, Qiagen) [12], cDNA was generated (PrimeScript, TaKaRa) and gene expression was investigated by PCR using specific oligonucleotides (Table 2; LightCycler 480, Roche) at optimized cycling protocols [2,3]. Amplification of swine GAPDH and β2 microglobulin served as housekeeping controls [13]. Melting curves were checked after each PCR run and expected product sizes were confirmed by agarose gel electrophoresis.

For detection of cell surface markers FC and IF were employed. For FC cells were washed twice with cold PBS, detached by mild proteolysis (Accutase, Sigma), counted by trypan

blue dye exclusion, and $5x10^5$ cells were blocked with pre-immune serum and then reacted in 50 μL FC buffer with labelled primary antibody (Table 1) for 20 min. on ice [6,11]. Unbound antibodies were washed off and cells were investigated by flow cytometry (LSR II, BD Bioscience). Unlabelled cells and compensation beads served as controls. Data were evaluated by FACS Diva and FlowJo (both BD Bioscience) software programs [6,11]. For IF, cells seeded in chamber slides and expanded to reach 70% of confluence. The cells were washed twice with cold PBS, fixed by 4% paraformaldehyde, blocked by 5% milk powder in PBS-Tween (30 min, room temperature, humidified chamber), and incubated with anti-desmin antibody for 90 min at 37°C in a humidified chamber. After three washing steps with PBS-Tween, the cells were incubated with the secondary antibody anti-rbt (45 min, 37°C, humidified chamber). Thereafter, cell nuclei were counterstained by DAPI and images were obtained with AxioVert200M (Table 1).

Table 2: Pig-specific oligonucleotides for qPCR

Gene	Forward Sequence	Reverse Sequence	Accession No.	Reference	Size
GAPDH	CCATCACCATCTTCCAGGAG	ACAGTCTTCTGGGTGGCAGT	NM_001206359.1	(Kobayashi-Kinoshita et al. 2016)	346
B2MG	ACGGAAAGCCAAATTACCTGAACTG	TCTGTGATGCCGGTTAGTGGTCT	NM_213978.1[#]	(71)	261
MyoG	CGCCATCCAGTACATCGAG	TGTGGGAACTGCATTCACTG	NM_001012406.1	(72)	125
Pax7	AGATCGCAGCAGGGGTAAAG	GACCCCACCAAGCTGATTGA	XM_021095458.1	Primerblast	209
Myl1	CTCTCAAGATCAAGCACTGCG	GCAGACACTTGGTTTGTGTGG	NM_214374.2	(34)	198
Myf5	GCTGCTGAGGGAACAGGTGGA	CTGCTGTTCTTTCGGGACCAGAC	NM_001278775.1	(73)	135
MSTN	CCCGTCAAGACTCCTACAACA	CACATCAATGCTCTGCCAA	NM_005259.3	(73)	141
MYH1	CCAGGGAGAGATGGAGGACA	TCAAGTTCACGTACCCTGGC	NM_001104951.2	Primerblast	258
Des	ACACCTCAAGGATGAGATGGC	CAGGGCTTGTTTCTCGGAAG	NM _001001535.1	(34)	176
Myf6	AGTGGCCAAGTGTTTCGGATC	CGCGAGTTATTTCTCCCCCA	NM_001244672.1	Primerblast	179
ACTA1	ACCCGACGCCATGTGTGA	GTCGCCCACGTAGGAATCTT	NM_001167795.1	Primerblast	184
MyoD1	CACTACAGCGGTGACTCAGACGCA	GACCGGGGTCGCTGGGCGCCTCGCT	NM_001002824.1	(73)	145
BDNF	TGTATACGTCCCGAGTCATGCT	GTATTCCTCCAGCAGAAAGAGAA GAG	NM 214259	(Hausman, Barb et al. 2008)	74
GDNF	ATGCCCGAGGAGTATCCTGA	CACCAGCCGTCTGTTTTTGG	AB675653.1	Primerblast	354
bFGF	GCGACCCTCACATCAAACTAC	AGCCAGTAATCTTCCATCTTCC	AJ577089.1; XM_021100546.1	(Liu, Ji et al. 2012)	113
IGF-1	GACGCTCTTCAGTTCGTGTG	CTCCAGCCTCCTCAGATCAC	NM-214256	(Casado, Gomez-Mauricio et al. 2012)	141
IGF-2	TCAGGCTAGTCTCTCCTCGG	GTGGTTGAGGGGTTCAATTTTTGG	NM-213883	(Casado, Gomez-Mauricio et al. 2012), Primerblast	142
HGF	ATGGTACTTGGTGTCATTGTTCCT	TTGATGTAAAGAGAGTTGTGTTAA TGG	CU656003	(Tetzlaff, Murani et al. 2009)	183
TGFß1	GCCTGCTGAGGCTCAAGTTA	ATCAAAGGACAGCCACTCCG	NM_214015	(Kobayashi-Kinoshita et al. 2016)	131
VEGF	GACGAAGGTCTGGAGTGTGTG	GGATTTTCTTGCCTCGCTCTATCTT	AF318502	(Tetzlaff, Murani et al. 2009); Primerblast	161
Cxcl12	GTCAGCCTGAGCTACAGATGC	TGTTTAAAGCTTTCTCCAGGTATTC	NM_001009580.1	(Han, Jeong et al. 2018)	196

Oligonucleotides employed for quantitative reverse-transcription polymerase chain reaction of swine cDNAs in 5'-3' orientation, including gene bank access, reference, and expected DNA product size in base pairs. Primers also amplify alternative transcripts for sB2M: [#] XM_021096362.1.

Transurethral cell therapy and follow-up

Three days after its induction, sphincter deficiency was confirmed by UPP. Then two aliquots 250 μl each containing $6x10^5$ CMFDA-labelled cells plus $6x10^5$ FITC-labelled microbeads (ø 20 μm, ρ = 1.05 g/mL, microParticles) were injected (Williams cystoscopic injection needle; Cook Medical) by transurethral route using a cystoscope under visual control. Cells and particles were injected in the urethral sphincter complex as described [14]. During follow-up of five weeks, animals were sedated for transurethral fluorimetry weekly to localize the fluorescent cells and microparticles (modified D-light-P, Image-1S-connect, Image-S1-H3-link, Karl Storz). Then weekly UPP was performed to determine the sphincter muscle regeneration as described above (Aquarius TT). In addition, the urine was monitored to monitor pathological abnormalities (Combur 10 test).

Analyses of urethral tissues targeted

After five weeks of follow-up, the final transurethral fluorimetry and UPP were performed and the gilts were sacrificed (phenobarbital, lethal). The bladder and the urethral sphincter were prepared. The area of injection of the CMFDA-labelled fluorescent cells and FITC labelled microparticles was localized using a planar fluorescence imaging system (IVIS Spectrum In Vivo Imaging System, Perkin Elmer) using a filter pair with λex = 500 nm and λem = 540 nm, f2, a binning of 8, an exposure time of 1s and displayed with a smoothing of 3x3 pixels after fluorescent background correction. Images were analysed using the Living Image software (Perkin Elmer). Areas presenting a fluorescent signal above background fluorescence were excised, embedded in freezing compound (Tissue Freezing Medium, Leitz), frozen in liquid nitrogen, and stored at -80 °C. Cryosections were generated (20 µm, Leica CM1860 UV, Leitz) and mounted on super frost slides. Cryosections containing fluorescent microparticles were considered to represent the area of injection. To visualize the urethral tissue, histochemistry was performed using HE- and AZAN-trichrome protocols via Axio Ver.A1 (Zeiss) and stitched together by aid of Image Composite Editor (Microsoft) [1]. Muscle tissue was detected in cryosections by a phalloidin-iFluor 594 conjugate as requested by the supplier (1:1000, Biomol). To detect infiltration of inflammatory cells, immune fluorescene (IF) was performed with a cross-reactive anti CD45 antibody and the secondary AF555-labeled anti-ms-antibody (Table 1). Stained samples were recorded by microscopy (Leica DMi8, LASX software), and exported as TIFF files for evaluation.

Polymerase chain reaction was employed to detect male SRY-DNA in cryosections. Tissue was scratched of from 8 consecutive cryosections and DNA was extracted as requested by the supplier (DNeasy extraction kit, Qiagen). The SYR gene was amplified by PCR (LightCycler 480, Roche) using a hot start step (5‘‘ 95°C), 40 amplification cycles (30‘‘ 60°C, 60‘‘72°C, 10‘‘ 94°C) and pig-specific oligonucleotides (5’ GACAATCATAGCTCAAACGATG / 5‘ TCTCTAGAGCCACTTTTCTCC; gene bank access number NC_010462.3, product size 133 bp) as described [2,15]. The product identity was confirmed by melting point analysis of the products and agarose DNA electrophoresis.

Data processing and statistics

Statistical analyses were conducted with the raw data in the nparLD R package (v2.2) in R Statistical Software (v4.2.2) (Fig.4A, 4B) and the ANOVA-like type statistics was calculated and reported [16,17]. To be able to compare the results, normalization of raw data to “Before” incontinence for each animal was performed (Fig.4C). For normalized data, after testing for normality distribution, a One-Way-ANOVA in IBM SPSS Statistics for Windows (v.29.0) (Fig.4D) was performed. P-values were reported as asterisks ($p<0.001$ ***, $p<0.01$ **, $p<0.05$ *, and $p>0.05$ ns).

References

1. Kelp A, Albrecht A, Amend B, et al. Establishing and monitoring of urethral sphincter deficiency in a large animal model. World J Urol 2017;35(12):1977-1986, doi:10.1007/s00345-017-2088-3
2. Geng R, Knoll J, Harland N, et al. Replacing Needle Injection by a Novel Waterjet Technology Grants Improved Muscle Cell Delivery in Target Tissues. Cell Transplant 2022;31(9636897221080943, doi:10.1177/09636897221080943
3. Knoll J, Amend B, Abruzzese T, et al. Improved production of proliferation- and differentiation-competent porcine striated muscle-derived myoblasts. submitted;
4. Ding S, Wang F, Liu Y, et al. Characterization and isolation of highly purified porcine satellite cells. Cell Death Discovery 2017;3(1):17003, doi:10.1038/cddiscovery.2017.3
5. Metzger K, Tuchscherer A, Palin MF, et al. Establishment and validation of cell pools using primary muscle cells derived from satellite cells of pig skeletal muscle. In Vitro Cell Dev Biol Anim 2020;56(3):193-199, doi:10.1007/s11626-019-00428-2
6. Pilz GA, Braun J, Ulrich C, et al. Human mesenchymal stromal cells express CD14 cross-reactive epitopes. Cytometry A 2011;79(8):635-45, doi:10.1002/cyto.a.21073

7. Reggiani C. Caffeine as a tool to investigate sarcoplasmic reticulum and intracellular calcium dynamics in human skeletal muscles. Journal of Muscle Research and Cell Motility 2021;42(2):281-289, doi:10.1007/s10974-020-09574-7
8. Lock JT, Parker I, Smith IF. A comparison of fluorescent Ca(2)(+) indicators for imaging local Ca(2)(+) signals in cultured cells. Cell Calcium 2015;58(6):638-48, doi:10.1016/j.ceca.2015.10.003
9. Chen YJ, Liu HY, Chang YT, et al. Isolation and Differentiation of Adipose-Derived Stem Cells from Porcine Subcutaneous Adipose Tissues. J Vis Exp 2016;109):e53886, doi:10.3791/53886
10. Linzenbold W, Jager L, Stoll H, et al. Rapid and precise delivery of cells in the urethral sphincter complex by a novel needle-free waterjet technology. BJU Int 2021;127(4):463-472, doi:10.1111/bju.15249
11. Pilz GA, Ulrich C, Ruh M, et al. Human term placenta-derived mesenchymal stromal cells are less prone to osteogenic differentiation than bone marrow-derived mesenchymal stromal cells. Stem Cells Dev 2011;20(4):635-46, doi:10.1089/scd.2010.0308
12. Brun J, Lutz KA, Neumayer KM, et al. Smooth Muscle-Like Cells Generated from Human Mesenchymal Stromal Cells Display Marker Gene Expression and Electrophysiological Competence Comparable to Bladder Smooth Muscle Cells. PLoS One 2015;10(12):e0145153, doi:10.1371/journal.pone.0145153
13. Rasmussen R, Morrison T, Herrmann M, et al. Quantitative PCR by continuous fluorescence monitoring of a double strand dna specific binding dye. Biochemica 1998;2(8 - 11
14. Amend B, Kelp A, Vaegler M, et al. Precise injection of human mesenchymal stromal cells in the urethral sphincter complex of Gottingen minipigs without unspecific bulking effects. Neurourol Urodyn 2017;36(7):1723-1733, doi:10.1002/nau.23182
15. Jaillard S, Holder-Espinasse M, Hubert T, et al. Tracheal replacement by allogenic aorta in the pig. Chest 2006;130(5):1397-404, doi:10.1378/chest.130.5.1397
16. Noguchi K, Gel YR, Brunner E, et al. nparLD: An R Software Package for the Nonparametric Analysis of Longitudinal Data in Factorial Experiments. Journal of Statistical Software 2012;50(1 - 23
17. RC T. R: A language and environment for statistical computing. Computing RFfS, editor 2022;

VII. Discussion and Outlook

Urethral sphincter insufficiency is one of the leading causes of SUI [1,2]. Since current standard treatments do not provide satisfactory results [1,3-6], improved techniques for SUI cell therapy are being explored as they tackle the underlying pathology and etiology [7]. This thesis investigated the injection of progenitor cells from adipose and muscle tissue for the therapy of urethral sphincter insufficiency in a large animal model. It included the examination of a novel cell injection technique (Publication 1, Publication 2), the optimization of cell production and cell quality management (Publication 3), the validation and possible transfer of the urethral sphincter insufficiency in the large animal model of pigs (Publication 4), and the determination of the regeneration potential of two different cell types in the incontinence model of the large animal pig (Publication 5). Detailed discussions are provided in the publications.

Publication 1 and Publication 2 showed that the waterjet technology is suitable for cell therapies. Both studies reported rapid injections of cells without a clinically significant decrease in viability. Viability was determined by cell counting after injection into fluids and cadaveric samples (Publication 1) and by assessing intact DNA seven days after injection into living animals (Publication 2). Publication 1 demonstrated that a cell injection by the waterjet does not alter the characteristics of the cells except for their biomechanical elasticity. However, it remains to be clarified whether these changes in cell morphology are helpful, as they are associated with increased migration potential, or whether the waterjet device needs to be optimized [8]. Combining the data of the two publications with the existing data [9-11], the waterjet technology outperforms the needle injections in terms of reproducibility, precision, and cell distribution in situ. The viability of waterjet-injected cells is constantly above 80% [9, Publication 1], and the application process is not dependent on the surgeon regarding the pressure and speed applied on the syringe. In needle injections, only about 67–73% of injected cells are located in the urethral wall [12,13], while the waterjet improved the precision of cell injection to above 95% (Publication 2). Additionally, Publication 2 demonstrated wider cell distribution in the tissue supporting the data of an earlier study [11]. Moreover, the waterjet provides the capability to adapt the injection depth of the cells by modifying the applied pressures at the waterjet device [9,11]. This ability might be crucial for future studies. As the muscle mass in the rhabdosphincter decreases with age, a risk factor for UI, the need to adjust the penetration depth of the cells

may arise [14,15]. Current studies were performed only in healthy pigs [11, Publication 2], therefore requiring the investigation of cell injection in incontinent pigs to determine and optimize the pressure profiles of the waterjet device. Additionally, larger cohort studies are needed to provide safety and performance requirements for the CE certification.

Publication 3 and Publication 4 were prerequisites for conducting the experiments in Publication 5. Publication 3 established an optimized protocol for the isolation, production, and characterization of porcine MPCs. Nevertheless, interindividual differences in batches isolated from different piglets were observed. Publication 4 validated the urethral sphincter incontinence model established before and extended the follow-up to five weeks [16]. However, the transfer of the incontinence induction via balloon dilatation and electrocautery from landrace gilts to female Göttingen minipigs was not successful. Göttingen minipigs showed improved regeneration of the urethral sphincter muscle even after more severe incontinence treatment. Therefore, long-term follow-up studies must be deferred because they are challenging to perform in landrace pigs due to the growth curve.

Nevertheless, in Publication 5, MPCs produced by the optimized protocol could be compared to ADSCs in the validated sphincter insufficiency model of landrace pigs regarding their regeneration potential. This study confirmed the promising results of cell therapy efficacy reported in other preclinical and clinical studies [4,7]. However, because this study (Publication 5) was also conducted in a small cohort, future studies must be conducted as preclinical confirmatory studies to provide more reliable data in terms of statistics as well. In our SUI model, ADSCs displayed better regeneration compared to MPCs in a follow-up of five weeks. MPCs showed an improvement but were not significantly different from the controls. Therefore, optimization is still required in the isolation and production of MPCs since they are currently not exploiting their full potential. These further investigations are still pending. Various muscle sources are currently being explored for their potential to regenerate the sphincter deficiency. Different muscle sources are reported to have different amounts of Pax7 expressions related to the presence of more differentiable progenitor cells in these muscles [17]. Furthermore, the precise injection of the cells has to be addressed in future studies. Especially for MPCs, the precise injection into the muscle layer is critical because they are reported to not differentiate outside this structure, limiting their regeneration potential [18,19]. In Publication 5, the state-of-the-art injection method of needle injection was used. In future animal studies of SUI therapy, the waterjet technology will be employed due to its more

precise and wider distribution of cells (Publication 2), granting a better comparison of the different cell types applied.

In conclusion, this thesis provides insights into the regeneration potential of two cell types. MPCs and ADSCs both show the potential of regenerating a sphincter deficiency in pigs, with ADSCs being the more promising cell type. However, the precise injection seems to be critical as well. Additionally, new data were generated to support the medical product approval of the waterjet device for cell therapy. This technique might provide better results in cell therapy and might help generate more reliable data in treating SUI with cell therapy. Overall, still several studies are necessary before cell therapy is applicable in humans.

15. References

1 Aoki, Y. *et al.* Urinary incontinence in women. *Nat Rev Dis Primers* **3**, 17042 (2017). https://doi.org:10.1038/nrdp.2017.42

2 Irwin, G. M. Urinary Incontinence. *Primary Care: Clinics in Office Practice* **46**, 233-242 (2019). https://doi.org:https://doi.org/10.1016/j.pop.2019.02.004

3 Abrams, P., Cardozo, L., Wagg, A. & Wein, A. *Incontinence 6th Edition*. (ICI-ICS. International Continence Society 2017).

4 Aragón, I. M., Imbroda, B. H. & Lara, M. F. Cell Therapy Clinical Trials for Stress Urinary Incontinence: Current Status and Perspectives. *Int J Med Sci* **15**, 195-204 (2018). https://doi.org:10.7150/ijms.22130

5 de Vries, A. M. & Heesakkers, J. Contemporary diagnostics and treatment options for female stress urinary incontinence. *Asian J Urol* **5**, 141-148 (2018). https://doi.org:10.1016/j.ajur.2017.09.001

6 Vilsbøll, A. W. *et al.* Cell-based therapy for the treatment of female stress urinary incontinence: an early cost–effectiveness analysis. *Regenerative Medicine* **13**, 321-330 (2018). https://doi.org:10.2217/rme-2017-0124

7 Hart, M. L., Izeta, A., Herrera-Imbroda, B., Amend, B. & Brinchmann, J. E. Cell Therapy for Stress Urinary Incontinence. *Tissue Engineering Part B: Reviews* **21**, 365-376 (2015). https://doi.org:10.1089/ten.teb.2014.0627

8 Szydlak, R., Majka, M., Lekka, M., Kot, M. & Laidler, P. AFM-based Analysis of Wharton's Jelly Mesenchymal Stem Cells. *Int J Mol Sci* **20** (2019). https://doi.org:10.3390/ijms20184351

9 Jäger, L. *et al.* A novel waterjet technology for transurethral cystoscopic injection of viable cells in the urethral sphincter complex. *Neurourology and Urodynamics* **39**, 594-602 (2020). https://doi.org:https://doi.org/10.1002/nau.24261

10 Linzenbold, W., Fech, A., Hofmann, M., Aicher, W. K. & Enderle, M. D. Novel Techniques to Improve Precise Cell Injection. *Int J Mol Sci* **22** (2021). https://doi.org:10.3390/ijms22126367

11 Linzenbold, W. *et al.* Rapid and precise delivery of cells in the urethral sphincter complex by a novel needle-free waterjet technology. *BJU International* **127**, 463-472 (2021). https://doi.org:https://doi.org/10.1111/bju.15249

12 Amend, B. *et al.* Precise injection of human mesenchymal stromal cells in the urethral sphincter complex of Göttingen minipigs without unspecific bulking effects. *Neurourology and Urodynamics* **36**, 1723-1733 (2017). https://doi.org:https://doi.org/10.1002/nau.23182

13 Burdzinska, A. *et al.* Limited accuracy of transurethral and periurethral intrasphincteric injections of cellular suspension. *Neurourology and Urodynamics* **37**, 1612-1622 (2018). https://doi.org:https://doi.org/10.1002/nau.23522

14 Fry, C. H. *et al.* Animal models and their use in understanding lower urinary tract dysfunction. *Neurourology and Urodynamics* **29**, 603-608 (2010). https://doi.org:https://doi.org/10.1002/nau.20903

15 Strasser, H. *et al.* Age dependent apoptosis and loss of rhabdosphincter cells. *Journal of Urology* **164**, 1781-1785 (2000). https://doi.org:doi:10.1016/S0022-5347(05)67106-6

16 Kelp, A. *et al.* Establishing and monitoring of urethral sphincter deficiency in a large animal model. *World Journal of Urology* **35**, 1977-1986 (2017). https://doi.org:10.1007/s00345-017-2088-3

17 Ding, S. *et al.* Characterization and isolation of highly purified porcine satellite cells. *Cell Death Discovery* **3**, 17003 (2017). https://doi.org:10.1038/cddiscovery.2017.3

18 Burdzińska, A. *et al.* The Effect of Endoscopic Administration of Autologous Porcine Muscle-derived Cells Into the Urethral Sphincter. *Urology* **82**, 743.e741-743.e748 (2013). https://doi.org:https://doi.org/10.1016/j.urology.2013.03.030

19 Peyromaure, M. *et al.* Fate of implanted syngenic muscle precursor cells in striated urethral sphincter of female rats: Perspectives for treatment of urinary incontinence. *Urology* **64**, 1037-1041 (2004). https://doi.org:https://doi.org/10.1016/j.urology.2004.06.058

VIII. Abbreviations

ADSC	adipose-derived stromal cells
AUC	area under the curve
ICS	International Continence Society
ISCT	International Society for Cellular Therapy
MPC	myogenic progenitor cell/myoblast
MRF4/Myf6	myogenic regulatory factor 4/myogenic factor 6
MSC	mesenchymal stromal cells
MUI	mixed urinary incontinence
Myf5	myogenic factor 5
MyoD1	myoblast determination protein 1
MyoG	myogenin
Pax7	paired box protein 7
Pclo	urethral closure pressure
Pura	urethral pressure
Pves	bladder pressure, intravesical pressure
SUI	stress urinary incontinence
UI	urinary incontinence
UUI	urgency urinary incontinence

IX. Acknowledgments

I want to take the opportunity to thank all the people who supported, inspired, and motivated me during my entire doctoral period.

First of all, I want to thank my supervisor Prof. Dr. Wilhelm K. Aicher for giving me the opportunity to realize this thesis. This work would not have been possible without his endless support, enthusiasm, ideas, and discussions about new concepts.

Furthermore, I want to express my gratitude to Prof. Dr. Stefan Laufer for reviewing my thesis and being my second supervisor.

Since this dissertation is part of the PoTuS project granted by DFG, I also want to thank the DFG for the generous support of personnel, investigations, and supplies required to successfully complete the studies.

I also show my appreciation to several people involved in the individual projects:

- Dr. Niklas Harland for his skills during the surgeries of the pigs.
- Dr. Marina Danalache, for her support and teaching in AFM measurements.
- The ERBE Medizintechnik company for providing the waterjet equipment.
- Dr. Nicolas Bézière and Simon Freisinger for their assistance in the IVIS measurements
- Dr. Udo Kraushaar for his time and support during the electrophysiological measurements
- Prof. Dr. Sawodny for providing the prototype of HD-UPP
- Dr. Mario Klünder for his supervision and teaching in the technology of the HD-UDP

My special thanks go to my colleagues. I especially want to thank Tanja Abruzzese and Cornelia Bock. They made me feel at home in the laboratory, shared their excellent technical expertise, and were always ready to listen. Without their methodological training, ongoing support, and patience, these experiments would not have been possible.

Lastly, I want to thank my parents for their continuous support. I also would like to thank my friends, especially my friend Manuel, for their support and motivation during this time.